Matteo Piccardo

Theoretical Models for Vibro-Rotational Spectroscopy Beyond the Harmonic Approximation

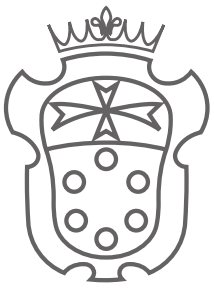

SCUOLA
NORMALE
SUPERIORE

Ph.D. in Chemistry

Supervisor: Prof. Vincenzo Barone

Scuola Normale Superiore
Classe di Scienze
Pisa, 21st May, 2015

Matteo Piccardo: *Theoretical Models for Vibro-Rotational Spectroscopy Beyond the Harmonic Approximation,* Ph.D. in Chemistry, Pisa, 21st May, 2015.

To my family, with intense love.

Contents

Preface

Up to now, the developments that will be discussed in this thesis have led to the following publications:

- M. Piccardo, J. Bloino, V. Barone, Generalized vibrational perturbation theory for roto-vibrational energies of linear, symmetric and asymmetric tops: theory, approximations and automated approaches to deal with medium-to-large molecular systems, *Int. J. Quantum Chem.* just accepted (April 2015);

- M. Piccardo, E. Penocchio, C. Puzzarini, M. Biczysko, V. Barone, Semi-Experimental Equilibrium Structure Determinations by Employing B3LYP/SNSD Anharmonic Force Fields: Validation and Application to Semi-rigid Organic Molecules, *J. Phys. Chem. A* 119, 2058 (2015);

- F. Egidi, T. Giovannini, M. Piccardo, J. Bloino, C. Cappelli, V. Barone, Stereoelectronic, Vibrational, and Environmental Contributions to Polarizabilities of Large Molecular Systems: A Feasible Anharmonic Protocol, *J. Chem. Theory Comput.* 10, 2456 (2014);

- C. Latouche, F. Palazzetti, D. Skouteris, V. Barone, High-Accuracy Vibrational Computations for Transition-Metal Complexes Including Anharmonic Corrections: Ferrocene, Ruthenocene, and Osmocene as Test Cases, *J. Chem. Theory Comput.* 10, 4565 (2014).

We are working now on the following new paper:

- M. Piccardo, E. Penocchio, V. Barone, Semi-Experimental Equilibrium Structures for accurate determinations of organic and biological molecular building blocks, in preparation (April 2015).

These Ph.D. studies have also led to the applications published in:

- A. Lapini, P. Fabbrizzi, M. Piccardo, M. di Donato, L. Lascialfari, P. Foggi, S. Cicchi, M. Biczysko, I. Carnimeo, F. Santoro, C. Cappelli, R. Righini, Ultrafast resonance energy transfer in the umbelliferone-alizarin bichromophore, *Phys. Chem. Chem. Phys.* 16, 10059 (2014).

Introduction

Vibrational and rotational spectroscopies are among the most powerful tools for the study of chemical systems [1, 2]. The investigation of the rotational and roto-vibrational spectra of polyatomic molecules has become of basic importance to determine accurate molecular geometries, as well as to get information on molecular force fields, roto-vibrational interaction parameters and the relations between structure and chemical-physical properties. Nowadays, there is a constant interplay between molecular spectroscopy and computational chemistry. Indeed, computed data have become crucial for the interpretation of experimental results and, conversely, accurate spectroscopic measurements are used as benchmarks to validate theoretical approaches [1–6].

The reliability of the theoretical models to support experimental findings is related to their accuracy. To this end, attention is usually concentrated on the choice of the method used to compute the electronic structure, and the way in which nuclear motions are simulated is often basic, namely the harmonic approximation for vibrations and the rigid-rotor approximation for rotations. However, the neglect of anharmonicity and roto-vibrational couplings can lead to significant errors and may result in incorrect interpretations of experimental data. To overcome such a limitation, various strategies have been devised [7–28].

Among them, the approach based on perturbation theory applied to the expansion of the molecular Hamiltonian in power series of products of vibrational and rotational operators, also referred to as vibrational perturbation theory (VPT), is particularly appealing for its computational efficiency to treat medium-to-large semi-rigid systems [29–43]. Moreover, some formulations of VPT, such as the Van Vleck contact transformation method, completely justify a generalized model (GVPT) [44, 45], coupling the advantages of the perturbative development to deal with weakly coupled terms and those of the variational treatment to handle tight coupled ones. Implementation of VPT approaches in computational programs for chemistry has become common and black-box procedures have been devised to

offer simple yet reliable ways of computing accurate roto-vibrational spectra [3, 31, 46–54].

In this context, two points should be noted:

- taking into account that the majority of chemical systems fall into the asymmetric top category and because of the simpler formulation, most developments in the last years have been focused on this case. As a result, a significant ensemble of molecular systems, ranging from small to large sizes, and of interest in various research fields, has been excluded or approximately treated. Among others, we can mention organic and organometallic compounds as coronene and ferrocene [38, 55–57] or acetylene derivatives [58–69]. The proper and effective introduction of symmetry leads to different developments for linear, symmetric and spherical top systems with respect to the formulation of asymmetric tops. Though the rotational problem is simpler in the first three cases than in the last one, because the rigid rotor problem can be solved analytically, the theory of linear, symmetric or spherical top molecules shows a number of complications due to the presence of degenerate vibrational modes, that makes analytical expressions for the vibrational interaction terms less simple [70, 71].

- several studies have been performed concerning vibrational averaging [22, 72–77] and transition matrix elements [31, 38, 42, 43, 52, 78–96] for molecular properties. Comparatively, less work has been done to compute vibrational transition moments beyond the harmonic approximation, due to the complexity of treating at the same time anharmonicity either of the wavefunction (mechanical anharmonicity) and of the property (electric anharmonicity). The complete treatments are highly demanding due to the large number of terms involved and their complexity. Only recently compact analytical formulas have been presented in the literature to handle transition moments of fundamentals, overtones, and combination bands of different properties (i.e. electric and magnetic dipoles and polarizability tensor) [97, 98]. However, it should be noted that the latter developments were limited to excitations from the vibrational ground state.

Starting from the developments already presented in the literature [29, 32, 47, 99, 100], the main aim of this work is to present a complete framework for the vibrational energies and vibrational averaged properties of asymmetric tops, as well as, linear and symmetric tops. We review and generalize the formalism in order to completely support intrinsic and accidental degeneracies, where the first ones are generated by the molecular symmetry and lead to further terms in VPT developments, and the latter are not imposed by the symmetry of the Hamiltonian and lead to singularities in the perturbative formulation, e.g. the well-known Fermi

resonances [32, 101, 102]. Particular attention is devoted to the latter singularities, presenting their treatment both within the rigorous variational-perturbative coupled GVPT approach, and within approximate methods. Moreover, a full general formulation of the roto-vibrational energies is presented to allow a unified treatment of both minima and first-order saddle points of the molecular potential energy surface (PES). Together with spectroscopic quantities, also thermodynamic functions and reaction rates are considered.

Focusing on the asymmetric top systems, then we present the first development concerning the generalization of the transition matrix elements for vibrational excitations from a generic vibrational states, where the anharmonicity of both the wavefunction and the properties is taken into account.

This document is organized in two parts. The first is dedicated to the presentation of the theoretical framework discussed above. In the second part, first we focus our attention on the issue of determination of accurate molecular geometries, which is essential for a correct development of accurate force fields, as well as, for a deeper understanding of physical-chemical properties and a fruitful interplay of experiment and theory. Then, we discuss the vibrational energies and thermodynamic quantities of different molecular systems in order to validate our developments and show the feasibility and the limitations of the VPT approach.

Because of the large number of acronyms that will be used to name the different developments and approximations presented in the text, an acronyms index has been reported at the end of this document.

Part I

Theory

I think I can safely say that nobody understands quantum mechanics.

Richard Feynman
1918-1988

This first part presents the molecular Hamiltonian and its treatment by perturbation theory to compute roto-vibrational energies, thermodynamic quantities and molecular properties. The formulation is completely generalized and reviewed in order to support both intrinsic and accidental degenerations, where the former are generated by the molecular symmetry present in linear and symmetric top systems.

As a reminder, a symmetric top is defined by two properties: the equilibrium configuration of the nuclei has a symmetry axis of order 3 or higher and, if there is more than one axis satisfying the above condition, these axes are all coincident. If all the above conditions are present, the molecule has two equal moments of inertia. Otherwise, the molecule is either an asymmetric top (first condition not met, all moments of inertia different) or a spherical top (second condition not satisfied, all moments of inertia are equal). Moreover, in a linear top system all the nuclei fall on a straight line and the molecule has one vanishing moment of inertia and two non-null coincident ones. Asymmetric tops have only non-degenerate harmonic vibrational frequencies, linear and symmetric tops both non-degenerate and doubly-degenerate harmonic frequencies, and spherical tops can be affected by degenerations larger than two.

The developments for the molecular Hamiltonian presented in the following consider systems involving at most doubly-degenerate harmonic frequencies, letting aside the case of spherical tops.

Chapter 1

General framework

The theoretical framework presented in this work relies on a number of approximations, in particular the Born-Oppenheimer (BO) approximation and the Eckart-Sayvetz conditions, and assumptions, specifically regarding the molecular and normal modes orientations, which will be presented in this first section.

Afterwards, a short recall of the harmonic vibrational theory is presented to introduce the equation of the molecular Hamiltonian of nuclei and its treatment by perturbation theory.

1.1 The Born-Oppenheimer approximation

The BO approximation allows to separate the total Hamiltonian of a molecule into an electronic and a nuclear component [103, 104]. To briefly recall it, let we start writing down the complete Hamiltonian of a molecular system,

$$\mathcal{H}_{\text{mol}} = T_{\text{nuc}} + T_{\text{el}} + V_{\text{nuc,nuc}} + V_{\text{nuc,el}} + V_{\text{el,el}} \tag{1.1}$$

where the first two terms on the right-hand side are the kinetic energy of the nuclei and the electrons, respectively, and the remaining terms are the potential energies. T_{nuc} contains a sum of terms weighted by the nuclear masses. For this reason, it can be regarded as a small term with respect to the electronic Hamiltonian,

$$\mathcal{H}_{\text{el}} = T_{\text{el}} + V_{\text{nuc,nuc}} + V_{\text{nuc,el}} + V_{\text{el,el}} \tag{1.2}$$

Assuming that the Schrödinger equation for $\mathcal{H}_{el}$ for a given nuclear configuration $\mathbf{R}$ can be exactly solved, each eigenstates $|\, \Psi_i(\mathbf{r}, \mathbf{R}) \,\rangle$ of the total Hamiltonian $\mathcal{H}_{\text{mol}}$ can be expressed in the basis of the eigenstates $|\, \varphi_j(\mathbf{r}; \mathbf{R}) \,\rangle$ of the electronic Hamiltonian $\mathcal{H}_{\text{el}}$ as,

$$|\, \Psi_i(\mathbf{r}, \mathbf{R}) \,\rangle = \sum_j \psi_{ij}(\mathbf{R}) |\, \varphi_j(\mathbf{r}; \mathbf{R}) \,\rangle \tag{1.3}$$

where with ";" we indicate that the electronic state is function of the electronic coordinates $\mathbf{r}$ and parametrically depends on the nuclear coordinates $\mathbf{R}$.
Therefore, introducing the states given by eq. 1.3 into the Schrödinger equation of $\mathcal{H}_{\text{mol}}$, it can be shown that we obtain,

$$\big[T_{\text{nuc}} + E_k(\mathbf{R}) - E_i\big]\psi_{ik}(\mathbf{R}) = \sum_j \big[\mathcal{A}_{ij}(\mathbf{R}) + \mathcal{B}_{ij}(\mathbf{R})\big]\psi_{jk}(\mathbf{R}) \tag{1.4}$$

where $E_k(\mathbf{R})$ and E_i are the eigenvalues of $\mathcal{H}_{\text{el}}$ and $\mathcal{H}_{\text{mol}}$, respectively. $\mathcal{A}_{ij}(\mathbf{R})$ and $\mathcal{B}_{ij}(\mathbf{R})$ are non-adiabatic coupling coefficients, which allow the interaction between the states i and j. Since they depend on the inverse of the nuclear masses, and assuming there is no large coupling between the different electronic states, they are usually small. Then eq. 1.3 can be simplified neglecting the latter terms, leading to the approximate equation,

$$\left[T_{\text{nuc}} + E_k(\mathbf{R})\right]\psi_{ik}(\mathbf{R}) = E_i\psi_{ik}(\mathbf{R}) \tag{1.5}$$

where now the electronic energy $E_i(\mathbf{R})$ plays the role of an external potential in which the nuclei move (i.e. PES). From a classical point of view, this means that the electrons interact and move in a field of fixed nuclei and the nuclei move in an external potential generated by the electrons. Moreover, with the BO approximation the molecular wavefunction can be expressed as a product of an electronic and a nuclear wavefunction.

1.2 The Eckart-Sayvetz conditions

In order to further simplify the problem, the space-fixed coordinates system X, Y, Z can be replaced by new coordinate systems suitable for the description of the individual types of molecular motions, which are the overall translations and rotations and the vibrations of atomic nuclei. This is possible by choosing an appropriate Cartesian axis system x, y, z that moves and rotates with the molecule, hereafter called molecule-fixed system [32, 33]. With respect to X, Y, Z one, a set of N equations holds for the positions of the N nuclei in the x, y, z system,

$$\mathbf{R}_q = \mathbf{R}_0 + \mathbf{B}(\theta, \phi, \chi)(\mathbf{d}_q^0 + \mathbf{d}_q) \qquad (q = 1, 2, \ldots, N) \tag{1.6}$$

where $\mathbf{R}_0$ is the the position vector of the molecule-fixed system origin with respect to the space-fixed one and $\mathbf{B}$ is a 3×3 orthogonal transformation matrix, function of θ, ϕ, χ Euler angles, which give the orientation of X, Y, Z system with respect to x, y, z one. $(\mathbf{d}_q^0 + \mathbf{d}_q)$ is the vector of the x, y, z coordinates for the atom q, defined as the displacement $\mathbf{d}_q$ with respect to a reference position $\mathbf{d}_q^0$. The N position vectors $\mathbf{d}_q^0$ define a reference configuration of nuclei.

It is possible to choose a reference configuration in many different ways. For example, the configuration that corresponds to the minimum of the PES is called "equilibrium configuration of the atomic nuclei". In this work, only rigid reference configurations will be considered, for which $\dot{d}_{q,\tau}[\equiv d(d_{q,\tau})/dt] = 0$ for all $q = 1, 2, \ldots, N; \tau = x, y, z$ with respect to the molecule-fixed frame.
There are $3N$ variables ($\mathrm{R}_{q,\tau}$, $q = 1, 2, \ldots, N$, $\tau = X, Y, Z$) on the left-hand sides of the equations 1.6, while $3N + 6$ variables ($3N + 5$ for linear configurations) on the right-hand sides (3 from $\mathbf{R}_0$, 3 or 2 Euler angles and $3N$ from $d_{q,\tau}$, $q = 1, 2, \ldots, N$, $\tau = x, y, z$). In order to have the same number of independent variables, it is necessary to introduce six constraints for the $3N$ coordinates $(\mathbf{d}_q^0 + \mathbf{d}_q)$. These constraints can be defined in many different ways. Eckart [105], and later Sayvetz [106], demonstrated that the conditions which minimize the interactions between the translational, rotational and vibrational motions are the following:

1. we require the center of mass of the molecule to be fixed on the origin of the x, y, z axis system:
$$\sum_q m_q(\mathbf{d}_q^0 + \mathbf{d}_q) = \mathbf{0} \tag{1.7}$$
Remembering that the molecule is subject to the rotation of the x, y, z system, described by the angular velocity $\boldsymbol{\omega}$, it follows by differentiation with respect to time that $\dot{\mathbf{d}}_q^0 = \boldsymbol{\omega} \times \mathbf{d}_q^0$, $\dot{\mathbf{d}}_q = \boldsymbol{\omega} \times \mathbf{d}_q + \dot{\mathbf{d}}_q$, and,
$$\begin{aligned}\mathbf{0} &= \sum_q m_q \left[\boldsymbol{\omega} \times \left(\mathbf{d}_q^0 + \mathbf{d}_q\right) + \dot{\boldsymbol{d}}_q\right] \\ &= \boldsymbol{\omega} \times \sum_{i=1} m_q \left(\mathbf{d}_q^0 + \mathbf{d}_q\right) + \sum_{i=1}^{N} m_q \dot{\boldsymbol{d}}_d \\ &= \sum_{i=1} m_q \dot{\boldsymbol{d}}_q \end{aligned} \tag{1.8}$$
This means that there is no linear momentum during the out of reference configuration motions, i.e. vibrations. If this relation is met, the translational motion can be totally decoupled from the rotational and vibrational ones;

2. we require that, whenever the out of reference configuration motions produce a rotation of the molecule, the rotating system shifts in order to eliminate this component from the motion:
$$\sum_q m_q \mathbf{d}_q^0 \times (\mathbf{d}_q^0 + \mathbf{d}_q) = \mathbf{0} \tag{1.9}$$

It follows by differentiation with respect to time,

$$\begin{aligned}\mathbf{0} &= \sum_q m_q(\boldsymbol{\omega} \times \mathbf{d}_q^0) \times (\mathbf{d}_q^0 + \mathbf{d}_q) \\ &\quad + \sum_q m_q \mathbf{d}_q^0 \times \left[\boldsymbol{\omega} \times (\mathbf{d}_q^0 + \mathbf{d}_q)\right] + \sum_q m_q \mathbf{d}_q^0 \times \dot{\mathbf{d}}_q \\ &= \sum_q m_q \mathbf{d}_q^0 \times \dot{\mathbf{d}}_q \end{aligned} \tag{1.10}$$

This means that there is no zero-order angular momentum during the vibrational motions. This condition minimizes the rotational-vibrational interaction, usually called Coriolis coupling.

Under these two constraints, called Eckart-Sayvetz conditions, the term related to translational motions is completely separated from the nuclear Hamiltonian and the interaction between rotations and vibrations is minimized.

1.3 The harmonic oscillator model

Let us first consider the pure vibrational Hamiltonian of a molecular system in a harmonic potential [32, 33],

$$\mathcal{H}_{\text{vib}} = -\frac{1}{2} \sum_{i,\gamma} \left(\frac{\partial^2}{\partial Q_{i_\gamma}^2} - \lambda_i Q_{i_\gamma}^2 \right) \tag{1.11}$$

where $\lambda_i = {\omega_i}^2$, with ω the classical vibrational frequency, and we denote a mass-weighted normal coordinate by Q_{i_γ}, where the first subscript i (or j, k, l) indicates the vibrational frequency associated to the coordinate, and the second subscript γ (or ϵ, θ, ι) takes the values 1 and 1, 2 for non-degenerate and two-fold degenerate frequencies, respectively. The set of the normal coordinates Q_{i_γ} is related to the Cartesian coordinates $d_{q,\tau}$ by the relation,

$$d_{q,\tau} = m_q^{-1/2} \sum_{i,\gamma} l_{i_\gamma q,\tau} Q_{i_\gamma} \tag{1.12}$$

If all frequencies are non-degenerate, the eigenfunctions of the Hamiltonian 1.11 will be written as the product of $3N-6$ ($3N-5$ for linear systems) independent eigenfunctions $\phi_m(Q_m; n_m)$,

$$-\frac{1}{2} \left(\frac{\partial^2}{\partial Q_m^2} - \lambda_i Q_m^2 \right) \phi_m(Q_m; n_m) = E_m(n_m) \phi_i(Q_i; n_m) \tag{1.13}$$

and the vibrational energy as the sum of $3N-6$[5] eigenvalues $E_m(n_m)$, where hereafter we reserve the subscript m, n, o, p to non-degenerate vibrations (omitting the second subscript 1).

Eq. 1.13 is the well-known Schrödinger equation for one-dimensional harmonic oscillators. The solutions were obtained by Schrödinger in terms of the dimensionless normal coordinates q_i and the conjugate momenta p_i,

$$q_i = \gamma_i^{1/2} Q_i \qquad\qquad p_i = P_i/(\gamma_i^{1/2}\hbar) \tag{1.14}$$

where $P_i = -i\hbar\partial/\partial Q_i$ and $\gamma_i = \lambda_i^{1/2}/\hbar$. The introduction of the above terms in eq. 1.13 leads to the solutions,

$$\phi_m(q_m; n_m) = \mathcal{N}_m(n_m) H_m(q_m; n_m) e^{-q_m^2/2} \qquad E_m(n_m) = \hbar\omega_m \left(n_m + \frac{1}{2}\right) \tag{1.15}$$

where $n_m = 0, 1, 2, \ldots$ is a parameter, called vibrational quantum number, $\mathcal{N}_m$ is a normalization factor and H_m is an Hermite polynomial of degree n_m.

If two normal coordinates are associated to the same frequency ω_s, the functions $\phi_s(Q_{s_1}, Q_{s_2}; n_s, l_s)$ will be the solutions of,

$$-\frac{1}{2}\left[\frac{\partial^2}{\partial Q_{s_1}^2} + \frac{\partial^2}{\partial Q_{s_2}^2} - \lambda_s\left(Q_{s_1}^2 + Q_{s_2}^2\right)\right]\phi_s(Q_{s_1}, Q_{s_2}; n_s, l_s) = E_s(n_s, l_s)\phi_s(Q_{s_1}, Q_{s_2}; n_s, l_s) \tag{1.16}$$

where hereafter we use the subscript s, t, u, v to indicate doubly-degenerate vibrations. The solutions of eq. 1.16 is found introducing the reduced normal coordinates q_{s_1} and q_{s_2} and then the set of polar coordinates ϱ ($0 \leqslant \varrho < +\infty$) and φ ($0 \leqslant \varphi < 2\pi$), defined as,

$$q_{s_1} = \varrho\cos\varphi \qquad\qquad q_{s_2} = \varrho\sin\varphi \tag{1.17}$$

The eigenfunctions of eq. 1.16 can be written as the product of a radial ϱ-dependent and an angular φ-dependent functions,

$$\phi_s(q_{s_1}, q_{s_2}; n_s, l_s) = \mathcal{N}_s(n_s, l_s)\left[e^{-\varrho/2}\varrho^{|l_s|} L_s(\varrho; n_s, l_s)\right]\left[e^{il_s\varphi}\right] \tag{1.18}$$

where $\mathcal{N}_s$ is a normalization factor, L_s is the associated Laguerre polynomial and n_s and l_s are two parameters, which can be assume the following values,

$$n_s = 0, 1, 2, \ldots \tag{1.19}$$

$$l_s = \pm n_s, \pm(n_s - 2), \pm(n_s - 4), \ldots, \pm 1 \text{ or } 0 \tag{1.20}$$

The presence of $e^{il_s\varphi}$ in eq. 1.18 indicates the existence of a vibrational angular momentum. For this reason, l_s is called vibrational angular momentum quantum number. Finally, the expression for the energy levels of the two-dimensional isotropic harmonic oscillator is,

$$E_s(n_s) = \hbar\,\omega_s\,(n_s + 1) \tag{1.21}$$

It is noteworthy that E_s is independent of l_s and then $(n_s + 1)$-fold degenerate.

1.4 Normal modes orientation

Since all combinations of the normal coordinates related to a degenerate frequency are again normal coordinates, standard rules can be used to orient them [70, 71].

As first point, the principal symmetry axis of the molecule is superimposed with the z axis of moving reference frame. The N-fold order of the z axis is then equal to the order of the symmetry operation R used for the definition of the non-degenerate (A, B) and degenerate $(E_1, E_2, E_3, \ldots)$ symmetry species.
The standard orientation chosen for the degenerate normal coordinates will be defined by two rules:

1. the relative signs of all Q_{s_1} and Q_{s_2} are chosen such that they transform under the operation R according to,

$$\begin{bmatrix} RQ_{s_1} \\ RQ_{s_2} \end{bmatrix} = \begin{bmatrix} \cos\alpha & \sin\alpha \\ -\sin\alpha & \cos\alpha \end{bmatrix} \begin{bmatrix} Q_{s_1} \\ Q_{s_2} \end{bmatrix} \tag{1.22}$$

   where $\alpha = 2\pi m/N$ and $m = 1, 2, 3, \ldots$ is the integer corresponding to the subscripts of the symmetry species label $E_1, E_2, E_3, \ldots$ $(1 \leqslant m < N/2)$. It is noteworthy that when $m = 1$, Q_{s_1} and Q_{s_2} transform exactly like the x and y components of a vector in a two-dimensional plane.

2. the orientation of every couple of coordinates Q_{s_1} and Q_{s_2} is chosen so that every Q_{s_1} is symmetric and every Q_{s_2} is antisymmetric with respect to the operation R',

$$\begin{bmatrix} R'Q_{s_1} \\ R'Q_{s_2} \end{bmatrix} = \begin{bmatrix} +1 & 0 \\ 0 & -1 \end{bmatrix} \begin{bmatrix} Q_{s_1} \\ Q_{s_2} \end{bmatrix} \tag{1.23}$$

   where R' is a rotation about a two-fold axis perpendicular to z when the group is D_n, D_{nh}, D_{Nd} (N odd), $D_{(N/2)d}$ ($N/2$ even) and a reflexion with respect to a plane σ_v (through the z axis) when the group is C_{nv}.

Using these rules, the non-vanishing PES derivatives and Coriolis coupling constants can be classified by their symmetry relations.

1.5 Nuclear Hamiltonian and perturbation theory

Within the BO approximation and the Eckart-Sayvetz conditions, the roto-vibrational quantum mechanical Hamiltonian for the equilibrium configuration of the atomic nuclei in a given electronic state can be written as [32, 102, 107],

$$\mathcal{H}_{\text{nuc}} = \frac{\hbar^2}{2} \sum_{\tau,\eta} \mu_{\tau\eta} \left(J_\tau - \pi_\tau\right) \left(J_\eta - \pi_\eta\right) + \frac{1}{2} \sum_{i,\gamma} P_{i_\gamma}^2 + V + U \tag{1.24}$$

where $\mu_{\tau\eta}$ is an element of the effective inverse molecular inertia tensor $\boldsymbol{\mu}$ and $\hbar J_\tau$ and $\hbar\pi_\tau$ are, respectively, the components of the total and vibrational angular momentum operators along the molecule-fixed Cartesian axes τ, η or ϱ [30, 32, 102, 108]. The explicit form of the latter is,

$$\hbar\pi_\tau = \sum_{i,\gamma} \sum_{j,\epsilon} \zeta_{i_\gamma j_\epsilon,\tau} Q_{i_\gamma} P_{j_\epsilon} \tag{1.25}$$

where $\zeta_{i_\gamma j_\epsilon,\tau}$ is the Coriolis constant, which couples Q_{i_γ} to Q_{j_ϵ} vibrational modes through the τ axis rotation:

$$\begin{aligned} \zeta_{i_\gamma j_\epsilon,\tau} &= -\zeta_{j_\epsilon i_\gamma,\tau} \\ &= \sum_{k,\theta} \left(l_{k_\theta i_\gamma,\eta} l_{k_\theta j_\epsilon,\varrho} - l_{i_\gamma j_\epsilon,\varrho} l_{k_\theta i_\gamma,\eta} \right) \end{aligned} \tag{1.26}$$

$l_{k_\theta,i}$ is from eq. 1.12. V is the PES in which nuclei move and U is a mass-dependent contribution, which vanishes for linear systems [102, 108],

$$U = -\frac{\hbar^2}{8} \sum_{\tau} \mu_{\tau\tau} \tag{1.27}$$

In eq. 1.24 both $\boldsymbol{\mu}$ and V can be expanded as Taylor series of the mass-weighted normal coordinates $\boldsymbol{Q}$ about the equilibrium geometry[32, 102],

$$\begin{aligned} \mu_{\tau\eta} = \mu^e_{\tau\eta} &- \sum_{i,\gamma} \mu^e_{\tau\tau} a_{i_\gamma,\tau\eta} \mu^e_{\eta\eta} Q_{i_\gamma} \\ &+ \frac{3}{4} \sum_{\varsigma} \sum_{i,\gamma} \sum_{j,\epsilon} \mu^e_{\tau\tau} a_{i_\gamma,\tau\varsigma} \mu^e_{\varsigma\varsigma} a_{j_\epsilon,\varsigma\eta} \mu^e_{\eta\eta} Q_{i_\gamma} Q_{j_\epsilon} + \dots \end{aligned} \tag{1.28}$$

$$\begin{aligned} V = \frac{1}{2} \sum_{i,\gamma} \lambda_i Q_{i_\gamma}^2 &+ \frac{1}{6} \sum_{i,\gamma} \sum_{j,\epsilon} \sum_{k,\theta} K_{i_\gamma j_\epsilon k_\theta} Q_{i_\gamma} Q_{j_\epsilon} Q_{k_\theta} \\ &+ \frac{1}{24} \sum_{i,\gamma} \sum_{j,\epsilon} \sum_{k,\theta} \sum_{l,\iota} K_{i_\gamma j_\epsilon k_\theta l_\iota} Q_{i_\gamma} Q_{j_\epsilon} Q_{k_\theta} Q_{l_\iota} + \dots \end{aligned} \tag{1.29}$$

where $\mu^e_{\tau\eta} = \{[\mathbf{I}^e]^{-1}\}_{\tau\eta}$ is an element of the inverse of the equilibrium inertia moment of the molecule,

$$\mathbf{I}^e = \sum_q m_q \left(|\mathbf{d}_q|^2 \mathbf{1} - \mathbf{d}_q \cdot \mathbf{d}_q^{\mathrm{T}} \right) \tag{1.30}$$

and $a_{i_\gamma,\tau\eta} = (\partial I^e_{\tau\eta}/\partial Q_{i_\gamma})$[3, 32, 108]. $K_{i_\gamma j_\epsilon k_\theta}$ and $K_{i_\gamma j_\epsilon k_\theta l_\iota}$ are respectively the third and fourth derivatives of the potential energy with respect to the normal modes, also referred to as the cubic and quartic force constants[32, 33, 102],

$$K_{i_\gamma j_\epsilon k_\theta} = \frac{\partial^3 V}{\partial Q_{i_\gamma} \partial Q_{j_\epsilon} \partial Q_{k_\theta}} \qquad \text{and} \qquad K_{i_\gamma j_\epsilon k_\theta l_\iota} = \frac{\partial^4 V}{\partial Q_{i_\gamma} \partial Q_{j_\epsilon} \partial Q_{k_\theta} \partial Q_{l_\iota}} \tag{1.31}$$

After substitution of $\boldsymbol{\mu}$ and V in eq. 1.24 by their respective definitions in eqs. 1.28 and 1.29, the terms in $\mathcal{H}_{\mathrm{nuc}}$ can be written as,

$$\begin{aligned} \mathcal{H}_{\mathrm{nuc}} =& \mathcal{H}_{20} + \mathcal{H}_{30} + \mathcal{H}_{40} + \dots \\ &+ \mathcal{H}_{21} + \mathcal{H}_{31} + \mathcal{H}_{41} + \dots \\ &+ \mathcal{H}_{02} + \mathcal{H}_{12} + \mathcal{H}_{22} + \dots \end{aligned} \tag{1.32}$$

where $\mathcal{H}_{fg}$ represents all the terms with a degree f in the vibrational operators (Q_i or P_i) and degree g in the rotational operators (J_τ). Hence, $\mathcal{H}_{f0}$ collect purely vibrational terms,

$$\mathcal{H}_{20} = \frac{1}{2} \sum_{i,\gamma} \left(P^2_{i_\gamma} + \lambda_i Q^2_{i_\gamma} \right) \tag{1.33}$$

$$\mathcal{H}_{30} = \frac{1}{6} \sum_{i,\gamma} \sum_{j,\epsilon} \sum_{k,\theta} K_{i_\gamma j_\epsilon k_\theta} Q_{i_\gamma} Q_{j_\epsilon} Q_{k_\theta} \tag{1.34}$$

$$\mathcal{H}_{40} = \frac{1}{24} \sum_{i,\gamma} \sum_{j,\epsilon} \sum_{k,\theta} \sum_{l,\iota} K_{i_\gamma j_\epsilon k_\theta l_\iota} Q_{i_\gamma} Q_{j_\epsilon} Q_{k_\theta} Q_{l_\iota} + \frac{\hbar^2}{2} \sum_\tau \mu^e_{\tau\tau} \pi^2_\tau \tag{1.35}$$

where,

$$\frac{\hbar^2 \mu^e_{\tau\tau} \pi^2_\tau}{2} = B^e_\tau \sum_{i,\gamma} \sum_{j,\epsilon} \sum_{k,\theta} \sum_{l,\iota} \zeta_{i_\gamma j_\epsilon,\tau} \zeta_{k_\theta l_\iota,\tau} Q_{i_\gamma} P_{j_\epsilon} Q_{k_\theta} P_{l_\iota} \tag{1.36}$$

are the terms of the expanded Hamiltonian corresponding to the zeroth-order development of $\boldsymbol{\mu}$ written in term of the equilibrium molecular rotation constant $B^e_\tau = \hbar^2/(2I^e_\tau)$. Note that all the constants in eqs. 1.33-1.35 are given by slightly non standard expressions based on mass-weighted vibrational normal coordinates, rather than on their reduced counterparts, since this allows a cleaner treatment when dealing with transition states (TSs), rather than energy minima, avoiding complex force constants [36, 40, 109–111].

$\mathcal{H}_{f1}$ and $\mathcal{H}_{f2}$ collect the Coriolis ($J_\tau \cdot \pi_\eta$) and roto-vibrational ($J_\tau \cdot J_\eta$) terms, respectively. More complete expressions have been reported by Aliev and Watson (see Table I in ref. [108]). Here, we reproduce only the lower-order terms,

$$\mathcal{H}_{02} = \sum_\tau B^e_\tau J^2_\tau \tag{1.37}$$

$$\mathcal{H}_{21} = -2 \sum_\tau B^e_\tau J_\tau \sum_{i,\gamma} \sum_{j,\epsilon} \zeta_{i_\gamma j_\epsilon, \tau} Q_{i_\gamma} P_{j_\epsilon} \tag{1.38}$$

$$\mathcal{H}_{12} = -\frac{\hbar^2}{2} \sum_{\tau,\eta} J_\tau J_\eta \sum_{i,\gamma} Q_{i_\gamma} \frac{a_{i_\gamma,\tau\eta}}{I^e_\tau I^e_\eta} \tag{1.39}$$

This way, $\mathcal{H}_{\rm mol}$ can be treated perturbatively, taking as zeroth-order contribution the harmonic oscillator Hamiltonian, $\mathcal{H}_{20}$. The separation in perturbative orders of $\mathcal{H}_{fg}$ terms has been widely discussed in the literature, and different classification schemes have been proposed[3, 6, 29, 30, 32, 108]. A detailed assignment was proposed by Aliev and Watson (see Table II of ref. [108]). It is noteworthy that the rigid-rotor term, $\mathcal{H}_{02}$, is usually treated as part of the perturbation to avoid rotational energy differences in the denominators of the perturbation development.

Various formulations of perturbation theory have been devised, such as the Rayleigh-Schrödinger (RS) method [112, 113], the Bloch projector formalism [114, 115], or the Van Vleck contact transformation (CT) method [44, 45]. We recall here the main features of the CT method. Differences with the RS development, also commonly used in the literature, will be highlighted. The CT formalism is based on the transformation of the Schrödinger equation [3, 30, 32, 108, 116],

$$\mathcal{H}\psi = E\psi \qquad \text{to} \qquad \tilde{\mathcal{H}}\phi = E\phi \tag{1.40}$$

where the original Hamiltonian $\mathcal{H}$ and wavefunction ψ are transformed as,

$$\tilde{\mathcal{H}} = e^{i\mathcal{S}} \mathcal{H} e^{-i\mathcal{S}} \qquad \text{and} \qquad \phi = e^{i\mathcal{S}}\psi \tag{1.41}$$

$\mathcal{S}$ is an Hermitian operator so that $e^{i\mathcal{S}}$ is unitary. It is chosen to obtain an effective block-diagonal Hamiltonian $\tilde{\mathcal{H}}$ in a given basis ϕ, in order to separate each vibrational level or block of degenerate or near-degenerate vibrational levels, with the property that the eigenvalues of these blocks are the same as for $\mathcal{H}$. The operator $e^{i\mathcal{S}}$ can be written as a product of successive contact transformations,

$$e^{i\mathcal{S}} = e^{i\lambda\mathcal{S}^{(1)}} e^{i\lambda^2\mathcal{S}^{(2)}} \dots \tag{1.42}$$

where $\mathcal{S}^{(n)}$ is chosen in order to diagonalize $\mathcal{H}$ up to the n-th order. Up to the

second-order, eq. 1.41 for $\tilde{\mathcal{H}}$ corresponds to,

$$\tilde{\mathcal{H}}^{(0)} = \mathcal{H}^{(0)} \tag{1.43}$$

$$\tilde{\mathcal{H}}^{(1)} = \mathcal{H}^{(1)} + i\,[\mathcal{S}^{(1)}, \mathcal{H}^{(0)}] \tag{1.44}$$

$$\tilde{\mathcal{H}}^{(2)} = \mathcal{H}^{(2)} + i\,[\mathcal{S}^{(1)}, \mathcal{H}^{(1)}] - \frac{1}{2}\,[\mathcal{S}^{(1)}, [\mathcal{S}^{(1)}, \mathcal{H}^{(0)}]] + i\,[\mathcal{S}^{(2)}, \mathcal{H}^{(0)}] \tag{1.45}$$

where $[X, Y]$ represents a commutator. Taking matrix elements in the basis of eigenfunctions of $\mathcal{H}^{(0)}$, let us first consider the terms $\langle\, \phi^{(0)}_{A_a} \mid \tilde{\mathcal{H}}^{(1)} \mid \phi^{(0)}_{B_b} \,\rangle$ to illustrate the choice of $\mathcal{S}^{(n)}$,

$$\langle\, \phi^{(0)}_{A_a} \mid \tilde{\mathcal{H}}^{(1)} \mid \phi^{(0)}_{B_b} \,\rangle = \langle\, \phi^{(0)}_{A_a} \mid \mathcal{H}^{(1)} \mid \phi^{(0)}_{B_b} \,\rangle - i\left[E^{(0)}_A - E^{(0)}_B\right] \langle\, \phi^{(0)}_{A_a} \mid \mathcal{S}^{(1)} \mid \phi^{(0)}_{B_b} \,\rangle \tag{1.46}$$

where the uppercase subscript represents states with different energies and the lowercase one differentiates degenerate states. This means that $E^{(0)}_A$ is the eigenvalue for all eigenstates $|\, \phi^{(0)}_{A_x} \,\rangle$ of the zeroth-order Hamiltonian $\mathcal{H}^{(0)}$. For the case $|\, \phi^{(0)}_{B_b} \,\rangle = |\, \phi^{(0)}_{A_a} \,\rangle$, which is also referred to as a diagonal matrix element of $\tilde{\mathcal{H}}^{(1)}$, the second term in the right-hand side of eq. 1.46 vanishes, that is,

$$\langle\, \phi^{(0)}_{A_a} \mid \tilde{\mathcal{H}}^{(1)} \mid \phi^{(0)}_{A_a} \,\rangle = \langle\, \phi^{(0)}_{A_a} \mid \mathcal{H}^{(1)} \mid \phi^{(0)}_{A_a} \,\rangle \tag{1.47}$$

which is identical to the result derived via RS first-order perturbation theory[112, 113]. For the off-diagonal elements with $E^{(0)}_B \neq E^{(0)}_A$, the first-order interaction term $\langle\, \phi^{(0)}_{A_a} \mid \tilde{\mathcal{H}}^{(1)} \mid \phi^{(0)}_{B_b} \,\rangle$ will vanish if we choose $\mathcal{S}^{(1)}$ satisfying the following equation,

$$\langle\, \phi^{(0)}_{A_a} \mid \mathcal{S}^{(1)} \mid \phi^{(0)}_{B_b} \,\rangle = -\frac{i\langle\, \phi^{(0)}_{A_a} \mid \mathcal{H}^{(1)} \mid \phi^{(0)}_{B_b} \,\rangle}{E^{(0)}_A - E^{(0)}_B} \qquad (E^{(0)}_B \neq E^{(0)}_A) \tag{1.48}$$

In this case, $\mathcal{S}^{(1)}$ will only contribute to the effective Hamiltonian for perturbation orders higher than the first one. If $E^{(0)}_B \approx E^{(0)}_A$, the value of $\langle\, \phi^{(0)}_{A_a} \mid \mathcal{S}^{(1)} \mid \phi^{(0)}_{B_b} \,\rangle$ as defined in eq. 1.48 will be excessively large. In this case, $|\, \phi^{(0)}_{A_a} \,\rangle$ and $|\, \phi^{(0)}_{B_b} \,\rangle$ are said to be in resonance and $\langle\, \phi^{(0)}_{A_a} \mid \mathcal{S}^{(1)} \mid \phi^{(0)}_{B_b} \,\rangle$ is set to be null, so that,

$$\langle\, \phi^{(0)}_{A_a} \mid \tilde{\mathcal{H}}^{(1)} \mid \phi^{(0)}_{B_b} \,\rangle = \langle\, \phi^{(0)}_{A_a} \mid \mathcal{H}^{(1)} \mid \phi^{(0)}_{B_b} \,\rangle \qquad (E^{(0)}_B \approx E^{(0)}_A) \tag{1.49}$$

The case of degenerate states, where $E^{(0)}_B = E^{(0)}_A$, is treated in the same way as for states of near-equal energies, with the term $\langle\, \phi^{(0)}_{A_a} \mid \mathcal{S}^{(1)} \mid \phi^{(0)}_{A_b} \,\rangle$ set to be null, so we have,

$$\langle\, \phi^{(0)}_{A_a} \mid \tilde{\mathcal{H}}^{(1)} \mid \phi^{(0)}_{A_b} \,\rangle = \langle\, \phi^{(0)}_{A_a} \mid \mathcal{H}^{(1)} \mid \phi^{(0)}_{A_b} \,\rangle \tag{1.50}$$

It is noteworthy that this off-diagonal term can result in the lifting, also called doubling, of the zeroth-order energy degeneracy.

The same considerations apply for the choice of $\mathcal{S}^{(2)}$ in eq. 1.45, with the difference

that, now, we impose that the terms $\langle\, \phi^{(0)}_{A_a} \mid \tilde{\mathcal{H}}^{(2)} \mid \phi^{(0)}_{B_b} \,\rangle$ vanish and $i\,[\mathcal{S}^{(1)}, \mathcal{H}^{(1)}] - [\mathcal{S}^{(1)}, [\mathcal{S}^{(1)}, \mathcal{H}^{(0)}]]\,/2$ is the perturbation correction to $\mathcal{H}^{(2)}$ that derives from the cancellation of the off-diagonal terms of $\mathcal{H}^{(1)}$. It can be shown that the general matrix element of $\tilde{\mathcal{H}}^{(2)}$ is given by the expression [116],

$$\begin{aligned}\langle\, \phi^{(0)}_{A_a} \mid \tilde{\mathcal{H}}^{(2)} \mid \phi^{(0)}_{B_b} \,\rangle &= \langle\, \phi^{(0)}_{A_a} \mid \mathcal{H}^{(2)} \mid \phi^{(0)}_{B_b} \,\rangle \\ &- \frac{1}{2} \sum_{C\neq A,B}^{*} \left[\frac{1}{E^{(0)}_C - E^{(0)}_A} + \frac{1}{E^{(0)}_C - E^{(0)}_B} \right] \sum_c \langle\, \phi^{(0)}_{A_a} \mid \mathcal{H}^{(1)} \mid \phi^{(0)}_{C_c} \,\rangle \langle\, \phi^{(0)}_{C_c} \mid \mathcal{H}^{(1)} \mid \phi^{(0)}_{B_b} \,\rangle \end{aligned} \tag{1.51}$$

where the first summation, with the $*$ symbol, is only carried out over the non-resonant states. It is noteworthy that for the elements $\langle\, \phi^{(0)}_{A_a} \mid \tilde{\mathcal{H}}^{(1)} \mid \phi^{(0)}_{A_b} \,\rangle$, be it $b = a$ and $b \neq a$, the above equation reduces to,

$$\begin{aligned}\langle\, \phi^{(0)}_{A_a} \mid \tilde{\mathcal{H}}^{(2)} \mid \phi^{(0)}_{A_b} \,\rangle &= \langle\, \phi^{(0)}_{A_a} \mid \mathcal{H}^{(2)} \mid \phi^{(0)}_{A_b} \,\rangle \\ &- \sum_{C\neq A}^{*} \sum_c \frac{\langle\, \phi^{(0)}_{A_a} \mid \mathcal{H}^{(1)} \mid \phi^{(0)}_{C_c} \,\rangle \langle\, \phi^{(0)}_{C_c} \mid \mathcal{H}^{(1)} \mid \phi^{(0)}_{A_b} \,\rangle}{E^{(0)}_C - E^{(0)}_A} \end{aligned} \tag{1.52}$$

which is identical to the matrix element derived via RS second-order perturbation theory[112, 113]. Conversely, the derivation of the off-diagonal elements of $\tilde{\mathcal{H}}^{(2)}$ with $B \neq A$ from the Rayleigh-Schrödinger development is less rigorous. For this reason, an alternative form with respect to eq. 1.51 has been often used for the treatment of the latter [117–119],

$$\begin{aligned}\langle\, \phi^{(0)}_{A_a} \mid \tilde{\mathcal{H}}^{(2)} \mid \phi^{(0)}_{B_b} \,\rangle &= \langle\, \phi^{(0)}_{A_a} \mid \mathcal{H}^{(2)} \mid \phi^{(0)}_{B_b} \,\rangle \\ &- \sum_{C} \sum_c \frac{\langle\, \phi^{(0)}_{A_a} \mid \mathcal{H}^{(1)} \mid \phi^{(0)}_{C_c} \,\rangle \langle\, \phi^{(0)}_{C_c} \mid \mathcal{H}^{(1)} \mid \phi^{(0)}_{B_b} \,\rangle}{E^{(0)}_C - E^{(0)}_{AB}} \end{aligned} \tag{1.53}$$

where $E^{(0)}_{AB} = (E^{(0)}_A + E^{(0)}_B)/2$.

Chapter 2

Vibrational Hamiltonian

In this chapter, we focus our attention on the pure vibrational Hamiltonian $\tilde{\mathcal{H}}_{\text{vib}} = \mathcal{H}_{20}+\tilde{\mathcal{H}}_{30}+\tilde{\mathcal{H}}_{40}$, which is obtained by correcting $\mathcal{H}^{(0)} = \mathcal{H}_{20}$ with $\mathcal{H}^{(1)} = \mathcal{H}_{30}$ and $\mathcal{H}^{(2)} = \mathcal{H}_{40}$ [32, 108]. An additional term is usually included to account for the zeroth-order expansion of U (see eqs. 1.27 and 1.28) [30, 32, 102, 108],

$$U^{(0)} = -\Gamma \sum_{\tau} \frac{\hbar^2}{8I_\tau^e} = -\Gamma \sum_{\tau} \frac{B_\tau^e}{4} \tag{2.1}$$

where $\Gamma = 1$ for asymmetric and symmetric top systems, and $\Gamma = 0$ for linear systems. It should be noted that, due to its small contribution, this term is generally neglected.

After the presentation of the developments for the second-order VPT (VPT2) energies, a particular attention is devoted to the treatments of the perturbative equations in the presence of resonances, showing the formal developments as well as possible approximations.

2.1 Vibrational energies

If no resonance occurs, the first-order effect of $\mathcal{H}_{30}$ does not contribute to the energy of any vibrational state, since both diagonal (eq. 1.47), and off-diagonal (eq. 1.50), terms are null. Hence, the perturbative corrections to the energy up to the second order are all due to $\tilde{\mathcal{H}}_{40}$, with the largest contribution related to the diagonal elements $\langle\, \phi_{A_a}^{(0)} \mid \tilde{\mathcal{H}}_{40} \mid \phi_{A_a}^{(0)} \,\rangle$.

Nielsen first derived the solution for the latter [29], which was subsequently refined with more general formulas [29, 30]. Later, Plíva fixed omissions for symmetric tops with a principal axis of order higher than three [99], mainly due to missing force constants. His formulas were in turn corrected by Willetts and Handy [100].

Following those works, we present here a new derivation, taking advantage of the framework built previously for asymmetric tops [47, 53], done with an *ad hoc* tool, based on a symbolic algebra program [120].

By applying the rules presented in section 1.4 to orient the degenerate normal vibrations, simple symmetry relations can be established between sets of related cubic and quartic force constants, as well as Coriolis constants. A first detailed classification was done by Henry and Amat in refs. [60, 121], for the first, and refs. [70] and [71] for the latter. For the force constants, at variance with eqs. 1.34 and 1.35, restricted sums were used in the potential energy expansions. Remembering that $[Q_{i_1}, Q_{i_2}] = 0$, the non-vanishing cubic and quartic force constants with at least one degenerate normal mode for the case of unrestricted summations have been reordered and reported in Tables A.2-A.8 of Appendix A. The notation adopted in those Tables is similar to the one used by Plíva [99]. The symmetry relations affecting the Coriolis terms has been reported in Appendix B. For transition states, the transition vector (i.e. the normal mode with the non-degenerate imaginary frequency) is labeled by the subscript F.

In this framework, the vibrational second-order perturbation theory leads to the following expression for the energies,

$$\begin{aligned} E(\boldsymbol{n},\boldsymbol{l}) =& E_0 + \sum_{i\neq F} \hbar\sqrt{\lambda_i}\, n_i \\ &+ \sum_i \sum_{j\geq i} \delta_{ij}^F \chi_{ij} \left(n_i n_j + n_i \frac{d_j}{2} + n_j \frac{d_i}{2} \right) + \sum_s \sum_{t\geq s} g_{st} l_s l_t \end{aligned} \tag{2.2}$$

with,

$$\delta_{ij}^F = (1-\delta_{iF})(1-\delta_{jF}) + \delta_{iF}\delta_{jF} \tag{2.3}$$

δ_{ij} is the Kronecker's delta, $\boldsymbol{n}$ and $\boldsymbol{l}$ are respectively the principal and angular vibrational quantum numbers, and d_i is the degeneracy of mode i. In the above expression, all $\boldsymbol{n}$- and $\boldsymbol{l}$-independent terms are collected in E_0, a term which can be written in a form devoid of resonances,

$$\begin{aligned} E_0 =& \frac{\hbar}{2} \sum_{i\neq F} \sqrt{\lambda_i} d_i + \frac{\hbar^2}{32} \sum_m \sum_n \frac{\delta_{mn}^F K_{mmnn}}{\sqrt{\lambda_m \lambda_n}} \\ &+ \frac{\hbar^2}{12} \sum_s \sum_{\sigma\leq III} \frac{\delta_\sigma K_{ssss}^{(\sigma)}}{\lambda_s} + \frac{\hbar^2}{8} \sum_{m\neq F} \sum_s \frac{K_{mmss}}{\sqrt{\lambda_m \lambda_s}} + \frac{\hbar^2}{8} \sum_s \sum_{t\neq s} \sum_{\sigma\leq VII} \frac{\delta'_\sigma K_{sstt}^{(\sigma)}}{\sqrt{\lambda_s \lambda_t}} \end{aligned}$$

$$
\begin{aligned}
&- \hbar^2 \sum_m \sum_n \sum_o \left[\frac{\delta^F_{mn} K_{mmo} K_{nno}}{32\lambda_o \sqrt{\lambda_m \lambda_n}} + \frac{\delta^F_{mno} {K_{mno}}^2}{48\sqrt{\lambda_m \lambda_n \lambda_o}(\sqrt{\lambda_m} + \sqrt{\lambda_n} + \sqrt{\lambda_o})} \right] \\
&- \frac{\hbar^2}{36} \sum_s \sum_\sigma \frac{\left\{K^{(\sigma)}_{sss}\right\}^2}{{\lambda_s}^2} - \hbar^2 \sum_m \sum_s \Bigg\{ \frac{\delta^F_m \left\{K^{(I)}_{mss}\right\}^2 (\sqrt{\lambda_m} + \sqrt{\lambda_s})}{4\lambda_m \lambda_s (2\sqrt{\lambda_s} + \sqrt{\lambda_m})} \\
&\quad + \frac{\delta^F_m \left\{K^{(III)}_{mss}\right\}^2 + \delta^F_m \left\{K^{(IV)}_{mss}\right\}^2}{8\lambda_s \sqrt{\lambda_m}(2\sqrt{\lambda_s} + \sqrt{\lambda_m})} + \frac{1}{8} \sum_n \frac{\delta^F_m K_{mmn} K^{(I)}_{nss}}{\lambda_n \sqrt{\lambda_m \lambda_s}} \\
&\quad + \frac{1}{4} \sum_{t>s} \left[\frac{K^{(I)}_{mss} K^{(I)}_{mtt}}{\lambda_m \sqrt{\lambda_s \lambda_t}} + \sum_\sigma \frac{\delta^F_m \left\{K^{(\sigma)}_{mst}\right\}^2}{\sqrt{\lambda_m \lambda_s \lambda_t}(\sqrt{\lambda_m} + \sqrt{\lambda_s} + \sqrt{\lambda_t})} \right] \Bigg\} \\
&- \frac{\hbar^2}{4} \sum_s \sum_{t \neq s} \sum_\sigma \frac{\left\{K^{(\sigma)}_{sst}\right\}^2}{\lambda_s \sqrt{\lambda_t}(2\sqrt{\lambda_s} + \sqrt{\lambda_t})} \\
&- \frac{\hbar^2}{2} \sum_s \sum_{t>s} \sum_{u>t} \sum_\sigma \frac{\left\{K^{(\sigma)}_{stu}\right\}^2}{\sqrt{\lambda_s \lambda_t \lambda_u}(\sqrt{\lambda_s} + \sqrt{\lambda_t} + \sqrt{\lambda_u})} \\
&- \frac{\Gamma}{4} \sum_\tau B^e_\tau + \frac{1}{4} \sum_\tau B^e_\tau \sum_m \sum_{n>m} \left\{\zeta_{mn,\tau}\right\}^2 \left[\frac{\delta^F_{mn}(\lambda_m + \lambda_n)}{\sqrt{\lambda_m \lambda_n}} - 2 \right] \\
&+ \frac{B^e_x}{2} \sum_m \sum_s \left[\left\{\zeta^{(I)}_{ms}\right\}^2 + \left\{\zeta^{(II)}_{ms}\right\}^2 \right] \left[\frac{\delta^F_m(\lambda_m + \lambda_s)}{\sqrt{\lambda_m \lambda_s}} - 2 \right] \\
&+ \sum_s \sum_{t>s} \Bigg\{ \frac{B^e_z}{2} \left[\left\{\zeta^{(I)}_{st}\right\}^2 + \left\{\zeta^{(II)}_{st}\right\}^2 \right] \\
&\quad + B^e_x \left[\left\{\zeta^{(III)}_{st}\right\}^2 + \left\{\zeta^{(IV)}_{st}\right\}^2 \right] \Bigg\} \left[\frac{\lambda_s + \lambda_t}{\sqrt{\lambda_s \lambda_t}} - 2 \right]
\end{aligned}
\tag{2.4}
$$

with,

$$\delta^F_i = (1 - \delta_{iF}) \tag{2.5}$$

$$\delta^F_{ijk} = (1 - \delta_{iF})(1 - \delta_{jF})(1 - \delta_{kF}) + \delta_{iF}\delta_{jF}\delta_{kF} \tag{2.6}$$

and (see Appendix A),

$$\delta_\sigma = \begin{cases} 1 & \text{if } \sigma = I \\ 3/4 & \text{if } \sigma > I \end{cases} \qquad \text{and} \qquad \delta'_\sigma = \begin{cases} 1 & \text{if } \sigma = I \\ 1/2 & \text{if } \sigma \in \{I, VII\} \end{cases} \tag{2.7}$$

The elements of the anharmonic matrices $\boldsymbol{\chi}$ and $\boldsymbol{g}$ are given by,

$$B_m\chi_{mm} = K_{mmmm} - \frac{5}{3}\frac{{K_{mmm}}^2}{\lambda_m} - \sum_{n\neq m}\frac{{K_{mmn}}^2(8\lambda_m - 3\lambda_n)}{\lambda_n(4\lambda_m - \lambda_n)} \tag{2.8}$$

$$\begin{aligned} C_{mn}\chi_{mn} =& K_{mmnn} - \frac{K_{mmm}K_{mnn}}{\lambda_m} - \frac{K_{mmn}K_{nnn}}{\lambda_n} - 2\frac{{K_{mmn}}^2}{(4\lambda_m - \lambda_n)} \\ & - 2\frac{{K_{mnn}}^2}{(4\lambda_n - \lambda_m)} + \sum_{o\neq m,n}\left[\frac{2{K_{mno}}^2(\lambda_m + \lambda_n - \lambda_o)}{\Delta_{mno}} - \frac{K_{mmo}K_{nno}}{\lambda_o}\right] \\ & + \frac{4}{\hbar^2}\sum_\tau B_\tau^e\{\zeta_{mn,\tau}\}^2(\lambda_m + \lambda_n) \end{aligned} \tag{2.9}$$

$$\begin{aligned} C_{ms}\chi_{ms} =& K_{mmss} - \frac{K_{mmm}K^{(I)}_{mss}}{\lambda_m} - 2\sum_\sigma\frac{\left\{K^{(\sigma)}_{mss}\right\}^2}{(4\lambda_s - \lambda_m)} \\ & - \sum_{n\neq m}\frac{K_{mmn}K^{(I)}_{nss}}{\lambda_n} + 2\sum_{t\neq s}\sum_\sigma\frac{\left\{K^{(\sigma)}_{mst}\right\}^2(\lambda_m + \lambda_s - \lambda_t)}{\Delta_{mst}} \\ & + \frac{4B_x^e}{\hbar^2}\left[\left\{\zeta^{(I)}_{ms}\right\}^2 + \left\{\zeta^{(II)}_{ms}\right\}^2\right](\lambda_m + \lambda_s) \end{aligned} \tag{2.10}$$

$$\begin{aligned} B_s\chi_{ss} =& \sum_{\sigma\leq III}\delta_\sigma K^{(\sigma)}_{ssss} - \frac{5}{3}\sum_\sigma\frac{\left\{K^{(\sigma)}_{sss}\right\}^2}{\lambda_s} \\ & - \sum_m\sum_\sigma\frac{\delta'_\sigma\left\{K^{(\sigma)}_{mss}\right\}^2(8\lambda_s - 3\lambda_m)}{\lambda_m(4\lambda_s - \lambda_m)} - \sum_{t\neq s}\sum_\sigma\frac{\left\{K^{(\sigma)}_{sst}\right\}^2(8\lambda_s - 3\lambda_t)}{\lambda_t(4\lambda_s - \lambda_t)} \end{aligned} \tag{2.11}$$

$$\begin{aligned} C_{st}\chi_{st} =& \sum_{\sigma\leq VII}\delta'_\sigma K^{(\sigma)}_{sstt} - 2\sum_\sigma\frac{\left\{K^{(\sigma)}_{sst}\right\}^2}{4\lambda_s - \lambda_t} - 2\sum_\sigma\frac{\left\{K^{(\sigma)}_{stt}\right\}^2}{4\lambda_t - \lambda_s} \\ & + \sum_m\left[\sum_\sigma\frac{\left\{K^{(\sigma)}_{mst}\right\}^2(\lambda_s + \lambda_t - \lambda_m)}{\Delta_{mst}} - \frac{K^{(I)}_{mss}K^{(I)}_{mtt}}{\lambda_m}\right] \\ & + 2\sum_{u\neq s,t}\sum_\sigma\frac{\left\{K^{(\sigma)}_{stu}\right\}^2(\lambda_s + \lambda_t - \lambda_u)}{\Delta_{stu}} \\ & + \frac{4}{\hbar^2}\left(\frac{1}{2}B_z^e\left[\left\{\zeta^{(I)}_{st}\right\}^2 + \left\{\zeta^{(II)}_{st}\right\}^2\right] + B_x^e\left[\left\{\zeta^{(III)}_{st}\right\}^2 + \left\{\zeta^{(IV)}_{st}\right\}^2\right]\right)(\lambda_s + \lambda_t) \end{aligned} \tag{2.12}$$

$$
\begin{aligned}
B_s g_{ss} =& -\frac{1}{3}\sum_{\sigma\le III}\delta_\sigma K^{(\sigma)}_{ssss} + \frac{7}{3}\sum_{\sigma}\frac{\left\{K^{(\sigma)}_{sss}\right\}^2}{\lambda_s} \\
&+ \sum_m\left[-\frac{\left\{K^{(I)}_{mss}\right\}^2}{(4\lambda_s-\lambda_m)} + \frac{\left[\left\{K^{(III)}_{mss}\right\}^2+\left\{K^{(IV)}_{mss}\right\}^2\right](8\lambda_s-\lambda_m)}{2\lambda_m(4\lambda_s-\lambda_m)}\right] \\
&+ \sum_{t\neq s}\sum_{\sigma}\frac{\left\{K^{(\sigma)}_{sst}\right\}^2(8\lambda_s-\lambda_t)}{\lambda_t(4\lambda_s-\lambda_t)} + B_s B^e_z\left\{\zeta^{(I)}_{ss}\right\}^2 \qquad (2.13)\\
g_{st} =& \hbar^2\sum_m\sum_\sigma\frac{\delta''_\sigma\left\{K^{(\sigma)}_{mst}\right\}^2}{2\Delta_{mst}} - \hbar^2\sum_{u\neq s,t}\sum_\sigma\frac{\left\{K^{(\sigma)}_{stu}\right\}^2}{\Delta_{stu}} \\
&+ \hbar^2\sum_\sigma\left[\frac{\delta''_\sigma\left\{K^{(\sigma)}_{sst}\right\}^2}{\lambda_t(4\lambda_s-\lambda_t)} + \frac{\delta''_\sigma\left\{K^{(\sigma)}_{stt}\right\}^2}{\lambda_s(4\lambda_t-\lambda_s)}\right] \\
&+ B^e_x\Big[\big(s_x\cdot 1 - s'_y\cdot 1\big)\{\zeta^{(III)}_{st}\}^2 + \big(s_y\cdot 1 - s'_x\cdot 1\big)\{\zeta^{(IV)}_{st}\}^2\Big] \\
&+ B^e_z\Big[\left\{\zeta^{(I)}_{st}\right\}^2 + \left\{\zeta^{(II)}_{st}\right\}^2 + 2\zeta^{(I)}_{ss}\zeta^{(I)}_{tt}\Big] \qquad (2.14)\\
\Delta_{ijk} =& \lambda_i^2+\lambda_j^2+\lambda_k^2 - 2(\lambda_i\lambda_j+\lambda_i\lambda_k+\lambda_j\lambda_k) \qquad (2.15)
\end{aligned}
$$

with $B_i = 16\lambda_i/\hbar^2$, $C_{ij} = 4\sqrt{\lambda_i\lambda_j}/\hbar^2$, $s_\tau = \mathrm{sign}(\zeta_{s_1t_1,\tau}\zeta_{s_2t_2,\tau})$, $s'_\tau = \mathrm{sign}(\zeta_{s_1t_2,\tau}\zeta_{s_2t_1,\tau})$ and (see Appendix A),

$$
\delta''_\sigma = \begin{cases} 1 & \text{if } \sigma\in\{I,II\} \\ -1 & \text{if } \sigma\in\{III,IV\}\end{cases} \qquad (2.16)
$$

In the formulation adopted here, it is easy to see from eqs. 2.8 to 2.14 that the matrix elements χ_{Fi}, with $i \neq F$, are imaginary. They are excluded from the vibrational energy, which contains only real terms, and enter, together with the imaginary frequency ω_F, in the expression providing tunneling and non classical reflection contributions to reaction rates [53].

It is noteworthy that, at variance with eq. 2.2, the anharmonic contribution to the vibrational energy is usually expressed in the literature as the sum of $\chi_{ij}(n_i + d_i/2)(n_j + d_j/2)$ and χ_0 (or G_0) terms. In the specific case of symmetric and linear tops, the χ_0 term was omitted by Plíva, Willetts and Handy in their respective works [99, 100]. It was included in the derivation proposed by Truhlar and coworkers [39] but it was based on a less general treatment than the one proposed by Plíva, which led to discrepancies with respect to the formulas given by Willetts and Handy and obtained in the present work. The explicit form of χ_0 is

shown in Appendix B. To the best of our knowledge, this is the first time that all terms needed to compute the vibrational energy as given in eq. 2.2 for symmetric, asymmetric and linear tops are gathered in a single work.

From eq. 2.2, it is possible to calculate the energy of any vibrational state. The energy of the vibrational ground state, i.e. the zero-point vibrational energy (ZPVE), is $E(\mathbf{0},\mathbf{0}) = E_0$. It is straightforward to determine transition energies governing vibrational spectra (i.e. at constant n_F) with the relation,

$$\begin{aligned}\nu(\Delta\boldsymbol{n},\Delta\boldsymbol{l};\boldsymbol{n},\boldsymbol{l}) &= E(\boldsymbol{n}+\Delta\boldsymbol{n},\boldsymbol{l}+\Delta\boldsymbol{l}) - E(\boldsymbol{n},\boldsymbol{l}) \\ &= \sum_i \hbar\omega_i\,\Delta n_i + \sum_i \chi_{ii}\Delta n_i\Big(\Delta n_i + 2n_i + d_i\Big) \\ &\quad + \frac{1}{2}\sum_i\sum_{j\neq i}\chi_{ij}\left[\Delta n_i\Big(n_j + d_j\Big) + n_i\,\Delta n_j + \Delta n_i\Delta n_j\right] \\ &\quad + \sum_s g_{ss}\Delta l_s\Big(2l_s + \Delta l_s\Big) + \frac{1}{2}\sum_s\sum_{t\neq s} g_{st}\Delta l_s\Big(2l_t + \Delta l_t\Big) \qquad (2.17)\end{aligned}$$

For excitations from the vibrational ground state, the fundamental bands are given by [33],

$$\nu(1_i, \pm 1_i \text{ or } 0_i) = \hbar\omega_i + \chi_{ii}(1 + d_i) + \frac{1}{2}\sum_{j\neq i}\chi_{ij}d_j + g_{ii} \qquad (2.18)$$

where, between parentheses, $\boldsymbol{n} = \mathbf{0}$ and $\boldsymbol{l} = \mathbf{0}$ in eq. 2.17 are omitted, as well as all null quantum numbers related to the normal modes not involved in the excitation. If i is a non-degenerate mode, g_{ii} vanishes and, since $l_i = 0$, it is usually omitted and only the principal quantum number n_i is specified. The expressions for the first overtones are,

$$\begin{aligned}\nu(2_i, 0_i) &= 2\hbar\omega_i + 2\chi_{ii}(2 + d_i) + \sum_{j\neq i}\chi_{ij}d_j \\ &= 2\nu(1_i, \pm 1_i \text{ or } 0_i) + 2\chi_{ii} - 2g_{ii} \qquad (2.19) \\ \nu(2_i, \pm 2_i) &= 2\hbar\omega_i + 2\chi_{ii}(2 + d_i) + \sum_{j\neq i}\chi_{ij}d_j + 4g_{ii} \\ &= 2\nu(1_i, \pm 1_i \text{ or } 0_i) + 2\chi_{ii} + 2g_{ii} \qquad (2.20)\end{aligned}$$

Finally, the first combination bands are given by,

$$\begin{aligned}\nu(1_i1_j, \pm 1_i \text{ or } 0_i \pm 1_j \text{ or } 0_j) =& \hbar\omega_i + \hbar\omega_j + \chi_{ii}(1+d_i) + \chi_{jj}(1+d_j) \\ &+ \chi_{ij}\left(1 + \frac{d_i}{2} + \frac{d_j}{2}\right) + \frac{1}{2}\sum_{k\neq i,j}\left(\chi_{ik}d_k + \chi_{jk}d_k\right) \\ &+ g_{ii} + g_{jj} + g_{ij} \\ =& \nu(1_i, \pm 1_i \text{ or } 0_i) + \nu(1_j, \pm 1_j \text{ or } 0_j) + \chi_{ij} + g_{ij}\end{aligned} \tag{2.21}$$

$$\begin{aligned}\nu(1_i1_j, \pm 1_i \mp 1_j) =& \hbar\omega_i + \hbar\omega_j + \chi_{ii}(1+d_i) + \chi_{jj}(1+d_j) \\ &+ \chi_{ij}\left(1 + \frac{d_i}{2} + \frac{d_j}{2}\right) + \frac{1}{2}\sum_{k\neq i,j}\left(\chi_{ik}d_k + \chi_{jk}d_k\right) \\ &+ g_{ii} + g_{jj} - g_{ij} \\ =& \nu(1_i, \pm 1_i) + \nu(1_j, \pm 1_j) + \chi_{ij} - g_{ij}\end{aligned} \tag{2.22}$$

The fundamental band for a degenerate mode is degenerate with respect to l, while the first overtone shows a partial lifting of the degeneracy resulting in one non-degenerate and one doubly-degenerate levels. Combination bands of two degenerate modes are split into two doubly-degenerate levels.

Finally, , the tunnelling probability P, of interest in chemical rate constants computations, can be evaluated using the microcanonical ensamble with the semiclassical TS theory of Miller and co-workers [122, 123]. They used the definitions,

$$\omega_F = i|\omega_F| \equiv i\bar{\omega}_F \tag{2.23}$$

$$n_F + \frac{1}{2} \equiv \frac{i\theta}{\pi} \tag{2.24}$$

$$\chi_{iF} \equiv -i\bar{\chi}_{iF} \tag{2.25}$$

to invert the relation $E = E(\boldsymbol{n}, \boldsymbol{l}, \theta)$, where,

$$E(\boldsymbol{n}, \boldsymbol{l}, \theta) = E(\boldsymbol{n}, \boldsymbol{l}) + i\left[\hbar\bar{\omega}_F - \sum_i \bar{\chi}_{iF}\left(n_i + \frac{1}{2}\right)\left(n_F + \frac{1}{2}\right)\right] \tag{2.26}$$

and obtain the generalized barrier penetration integral $\theta(\boldsymbol{n}, \boldsymbol{l}, E)$ in terms of the n_i and l_i quantum numbers of the activated system, with $i \neq F$, and the total energy E,

$$\theta(\boldsymbol{n}, \boldsymbol{l}, E) = \frac{\pi\Delta E}{\hbar\Omega_F}\frac{1}{1 + \sqrt{1 + 4\chi_{FF}\Delta E/(\hbar\Omega_F)^2}} \tag{2.27}$$

where,

$$\Delta E = E(\boldsymbol{n}, \boldsymbol{l}) - E \tag{2.28}$$

$$\hbar\Omega_F = \hbar\bar{\omega}_F - \sum_i \bar{\chi}_{iF}(n_i + \frac{1}{2}) \tag{2.29}$$

In this framework, the semi-classical tunneling probability P for a one-dimensional barrier is given by,

$$P(\boldsymbol{n}, \boldsymbol{l}, E) = \frac{1}{1 + e^{2\theta(\boldsymbol{n},\boldsymbol{l},E)}} \tag{2.30}$$

2.2 Vibrational l-type doubling and l-type resonance

Vibrational energies of non-degenerate states can be determined directly from eq. 2.2. For degenerate zeroth-order states, as seen above, the interaction terms $\langle\, \phi^{(0)}_{A_a} \mid \tilde{\mathcal{H}}_{40} \mid \phi^{(0)}_{A_b} \,\rangle$ cannot be canceled out with $\mathcal{S}^{(2)}$ and must be treated variationally. The presence of those off-diagonal elements in the variational matrix will result in a further lifting of the degeneracy of the vibrational energies, initiated with the application of the second-order correction. This splitting is called l-type doubling or l-type resonance, depending if the diagonal energies involved have equal or different values, respectively. Using symmetry considerations, Amat derived a general rule to identify *a priori* the possible non-null off-diagonal matrix elements [32, 124]. It depends on the N-fold principal symmetry axis and the difference of quanta in the principal (Δn_i) and angular (Δl_i) vibrational quantum numbers between the states involved in the interaction term. The ensemble of non-zero l-type off-diagonal terms is obtained from the following relations,

$$\begin{aligned}
&\langle\, n_s, l_s \mid \tilde{\mathcal{H}}_{40} \mid n_s, (l_s \pm 4)_s \,\rangle = \\
&\qquad U^{\pm}_s \sqrt{(n_s \pm l_s + 4)(n_s + l_s \pm 2)(n_s - l_s \mp 2)(n_s \mp l_s)}
\end{aligned} \tag{2.31}$$

$$\begin{aligned}
&\langle\, n_s n_t, l_s l_t \mid \tilde{\mathcal{H}}_{40} \mid n_s n_t, (l_s \pm 2)_s (l_t \mp 2)_t \,\rangle = \\
&\qquad R^{\pm}_{st} \sqrt{(n_s \pm l_s + 2)(n_t \mp l_t + 2)(n_s \mp l_s)(n_t \pm l_t)}
\end{aligned} \tag{2.32}$$

$$\begin{aligned}
&\langle\, n_s n_t, l_s l_t \mid \tilde{\mathcal{H}}_{40} \mid n_s n_t, (l_s \pm 2)_s (l_t \pm 2)_t \,\rangle = \\
&\qquad S^{\pm}_{st} \sqrt{(n_s \pm l_s + 2)(n_t \pm l_t + 2)(n_s \mp l_s)(n_t \mp l_t)}
\end{aligned} \tag{2.33}$$

where, as usual, only the modes undergoing a change in their quantum numbers between the two states involved in the matrix elements are shown. The off-diagonal elements given in eq. 2.31 are non-null if N is a multiple of 4, those given in eq. 2.32 for any symmetric top molecule and the elements of eq. 2.33 if N is even.

The first expressions of U, R and S for the various point groups have been given by Grenier-Besson [125, 126]. The formulas have been re-derived here, with the notation introduced in this work, and validated with respect to those obtained by Grenier-Besson. They are gathered in the Appendix C.

2.3 Vibrational first-order resonances

It has been shown that if two states are in resonance it is not possible to make their off-diagonal terms vanish. A resonance can connect two or several vibrational levels and, moreover, multiple resonances can connect a network of levels. The sub-matrices where the resonances are involved are called polyads [108, 119].

Since $\tilde{\mathcal{H}}^{(0)}$ has only diagonal elements, all off-diagonal terms are null. The presence of an off-diagonal first-order correction due to $\tilde{\mathcal{H}}_{30}$ is related to the so-called Fermi resonances. The latter are characterized by a strong interaction between two states that differ by one quantum in one mode and two quanta in either one (type I) or two different (type II) modes[32, 33, 101]. Due to the creation of one vibrational quantum and the annihilation of two others, or conversely, these singularities are also called vibrational 1-2 resonances[119]. They can appear when $\langle \phi^{(0)}_{A_a} \mid \mathcal{H}^{(1)} \mid \phi^{(0)}_{B_b} \rangle$ in eq. 1.48 is excessively large or $E^{(0)}_A \approx E^{(0)}_B$ in eq. 1.46, condition which can occur in two cases: $2\omega_i \approx \omega_j$ (type I) or $\omega_i \approx \omega_j + \omega_k$ (type II).

Different methods have been developed to overcome the problem of Fermi resonances. The most common approach, called deperturbed VPT2 (DVPT2), consists in simply removing from the perturbative treatment the resonant terms after their identification. The explicit expressions of the potentially resonant terms in eqs. 2.8-2.14 are given in Appendix D. However, this treatment is incomplete due to the neglect of the resonant terms. An improvement can be obtained by treating variationally the levels involved in the resonance, reintroducing the removed terms as off-diagonal interaction elements. This method has been called generalized VPT2 (GVPT2) [29, 30, 32, 47] or, more recently, CVPT2+K [116] or CVPT2+WK [127]. The list of possible off-diagonal first-order interaction terms generalized to linear, symmetric and asymmetric tops is given in Table 2.1.

Although those methods have been widely discussed in the literature, less attention has been devoted to the identification of a general strategy to determine when an interaction term has to be considered in resonance. Indeed, all the methods presented above rely directly on the identification of the resonant terms. The definition of a singularity giving rise to unphysical contributions is far from straightforward, and different schemes have been proposed. The simplest approach is to check the magnitude of the denominator (i.e. $|2\omega_i - \omega_j|$ and $|\omega_i - \omega_j - \omega_k|$) with respect to a fixed threshold. If the value is below this limit, the term is considered resonant. Such a scheme does not account for the magnitude of the numerator,

Table 2.1: Non-zero off-diagonal variational elements involved in the first order vibrational (Fermi) resonances.

Type I Fermi resonances
$\langle\, n_m n_n \mid \tilde{\mathcal{H}}^{(1)} \mid (n_m+2)(n_n-1)\,\rangle = G_{mmn} K_{mmn} \sqrt{(n_m+1)(n_m+2)n_n}/(4\sqrt{2})$
$\langle\, n_m n_s, l_s \mid \tilde{\mathcal{H}}^{(1)} \mid (n_m+1)(n_s-2), l_s\,\rangle = -G_{mss} K^{(I)}_{mss} \sqrt{(n_m+1)(n_s+l_s)(n_s-l_s)}/(4\sqrt{2})$
$\langle\, n_m n_s, l_s \mid \tilde{\mathcal{H}}^{(1)} \mid (n_m+1)(n_s-2), (l_s\pm 2)\,\rangle = G_{mss}\left(K^{(III)}_{mss} \pm i K^{(IV)}_{mss}\right) \sqrt{(n_m+1)(n_s\mp l_s)(n_s\mp l_s-2)}/(8\sqrt{2})$
$\langle\, n_s n_t, l_s l_t \mid \tilde{\mathcal{H}}^{(1)} \mid (n_s+2)(n_t-1), (l_s\pm 2)(l_t\pm 1)\,\rangle = G_{sst}\left(\pm K^{(I)}_{sst} + i K^{(II)}_{sst}\right) \sqrt{n_s\pm l_s+2)(n_s\pm l_s+4)(n_t\mp l_t)}/(8\sqrt{2})$
$\langle\, n_s n_t, l_s l_t \mid \tilde{\mathcal{H}}^{(1)} \mid (n_s+2)(n_t-1), (l_s\pm 2)(l_t\mp 1)\,\rangle = G_{sst}\left(\mp K^{(III)}_{sst} + i K^{(IV)}_{sst}\right) \sqrt{(n_s\pm l_s+2)(n_s\pm l_s+4)(n_t\pm l_t)}/(8\sqrt{2})$
Type II Fermi resonances
$\langle\, n_m n_n n_o \mid \tilde{\mathcal{H}}^{(1)} \mid (n_m+1)(n_n-1)(n_o-1)\,\rangle = G_{mno} K_{mno} \sqrt{(n_m+1)n_n n_o}/(2\sqrt{2})$
$\langle\, n_m n_s n_t, l_s l_t \mid \tilde{\mathcal{H}}^{(1)} \mid (n_m+1)(n_s-1)(n_t-1), (l_s\pm 1)(l_t\mp 1)\,\rangle = G_{mst}\left(-K^{(I)}_{mst} \pm i K^{(II)}_{mst}\right) \sqrt{(n_m+1)(n_s\mp l_s)(n_t\pm l_t)}/(4\sqrt{2})$
$\langle\, n_m n_s n_t, l_s l_t \mid \tilde{\mathcal{H}}^{(1)} \mid (n_m+1)(n_s-1)(n_t-1), (l_s\pm 1)(l_t\pm 1)\,\rangle = G_{mst}\left(K^{(III)}_{mst} \pm i K^{(IV)}_{mst}\right) \sqrt{(n_m+1)(n_s\mp l_s)(n_t\mp l_t)}/(4\sqrt{2})$
$\langle\, n_m n_s n_t, l_s l_t \mid \tilde{\mathcal{H}}^{(1)} \mid (n_m-1)(n_s+1)(n_t-1), (l_s\pm 1)(l_t\mp 1)\,\rangle = G_{mst}\left(K^{(I)}_{mst} \mp i K^{(II)}_{mst}\right) \sqrt{n_m(n_s\pm l_s+2)(n_t\pm l_t)}/(4\sqrt{2})$
$\langle\, n_m n_s n_t, l_s l_t \mid \tilde{\mathcal{H}}^{(1)} \mid (n_m-1)(n_s+1)(n_t-1), (l_s\pm 1)(l_t\pm 1)\,\rangle = G_{mst}\left(-K^{(III)}_{mst} \mp i K^{(IV)}_{mst}\right) \sqrt{n_m(n_s\pm l_s+2)(n_t\mp l_t)}/(4\sqrt{2})$
$\langle\, n_s n_t n_u, l_s l_t l_u \mid \tilde{\mathcal{H}}^{(1)} \mid (n_s+1)(n_t-1)(n_u-1), (l_s\pm 1)(l_t\pm 1)(l_u\pm 1)\,\rangle = G_{stu}\left(\mp K^{(I)}_{stu} - i K^{(II)}_{stu}\right) \sqrt{(n_s\pm l_s+2)(n_t\mp l_t)(n_u\mp l_u)}/(4\sqrt{2})$
$\langle\, n_s n_t n_u, l_s l_t l_u \mid \tilde{\mathcal{H}}^{(1)} \mid (n_s+1)(n_t-1)(n_u-1), (l_s\pm 1)(l_t\pm 1)(l_u\mp 1)\,\rangle = G_{stu}\left(\pm K^{(III)}_{stu} - i K^{(IV)}_{stu}\right) \sqrt{(n_s\pm l_s+2)(n_t\mp l_t)(n_u\pm l_u)}/(4\sqrt{2})$

$G_{ijk} = \hbar^{-3/2}/\sqrt{\omega_i\omega_j\omega_k}$

which makes difficult the definition of a reliable threshold adapted to a wide range of molecular systems. A more robust solution to this problem has been suggested by Martin and co-workers[128]. Considering two resonant states $|\,\phi^{(0)}_{A_a}\,\rangle$ and $|\,\phi^{(0)}_{B_b}\,\rangle$, we can write down the interaction between the two states as a variational matrix,

$$\begin{pmatrix} \langle\,\phi^{(0)}_{A_a}\mid \mathcal{H}^{(0)}+\mathcal{H}^{(1)}\mid \phi^{(0)}_{A_a}\,\rangle & \langle\,\phi^{(0)}_{B_b}\mid \mathcal{H}^{(0)}+\mathcal{H}^{(1)}\mid \phi^{(0)}_{A_a}\,\rangle \\ \langle\,\phi^{(0)}_{A_a}\mid \mathcal{H}^{(0)}+\mathcal{H}^{(1)}\mid \phi^{(0)}_{B_b}\,\rangle & \langle\,\phi^{(0)}_{B_b}\mid \mathcal{H}^{(0)}+\mathcal{H}^{(1)}\mid \phi^{(0)}_{B_b}\,\rangle \end{pmatrix} = \begin{pmatrix} E^{(0)}_A & \rho^\dagger \\ \rho & E^{(0)}_B \end{pmatrix} \tag{2.34}$$

where $\rho = \langle\,\phi^{(0)}_{A_a}\mid \mathcal{H}^{(0)}+\mathcal{H}^{(1)}\mid \phi^{(0)}_{B_b}\,\rangle = \langle\,\phi^{(0)}_{A_a}\mid \mathcal{H}^{(1)}\mid \phi^{(0)}_{B_b}\,\rangle$ and $\rho^\dagger$ is the complex conjugate of ρ. If ρ tends to zero, the eigenvalues $E^\pm$ of the matrix in eq. 2.34 can be written as the following Taylor series,

$$\begin{aligned} E^\pm &= \frac{E^{(0)}_A + E^{(0)}_B}{2} \pm \sqrt{\frac{\Delta^2}{4}+|\rho|^2} \\ &\xrightarrow[\rho\to 0]{} \frac{E^{(0)}_A + E^{(0)}_B}{2} \pm \left[\frac{\Delta}{2} + \frac{|\rho|^2}{\Delta} - \frac{(|\rho|^2)^2}{\Delta^3} + \circ(\rho^4)\right] \end{aligned} \tag{2.35}$$

where $\Delta = |E^{(0)}_A - E^{(0)}_B|$ and must be non-null. Up to the second-order, $E^\pm$ coincides with the vibrational energies $E^{(0)}_A$ or $E^{(0)}_B$ corrected with a second-order perturbation term, which arises from the interaction between $|\,\phi^{(0)}_{A_a}\,\rangle$ and $|\,\phi^{(0)}_{B_b}\,\rangle$ (here the case $|E^{(0)}_A - E^{(0)}_B| = E^{(0)}_A - E^{(0)}_B$) [129],

$$E^+ = E^{(0)}_A + \frac{|\rho|^2}{\Delta} \qquad \text{and} \qquad E^- = E^{(0)}_B - \frac{|\rho|^2}{\Delta} \tag{2.36}$$

where $|\rho|^2/\Delta$ is precisely the possible resonant term in the VPT2 equations, i.e. one of the terms in the summation in the right-hand side of eq. 1.52. Based on those considerations, the importance of the higher-order perturbative terms can be estimated from the fourth-order expansion term in eq. 2.35,

$$\Xi = \frac{(|\rho|^2)^2}{\Delta^3} \tag{2.37}$$

where $\Delta = \hbar|2\omega_i - \omega_j|$ for type I Fermi resonances and $\Delta = \hbar|\omega_i - \omega_j - \omega_k|$ for type II Fermi resonances. Consequently, a threshold on the term can be a good marker to evaluate the importance of higher order effects and then if the second-order term has to be treated as resonant. Moreover, this term accounts not only for the energy difference but also for the magnitude of ρ. In a slightly different formulation, the threshold used to evaluate the presence of first-order resonances is calculated taking into account all high-order expansion terms, obtained subtracting the first two expansion terms from the square root of eq. 2.35 [127],

$$\Xi' = \sqrt{\frac{\Delta^2}{4}+|\rho|^2} - \frac{\Delta}{2} - \frac{|\rho|^2}{\Delta} \tag{2.38}$$

A general approach can be derived from the development presented above, which is to apply to all potentially resonant terms in the VPT2 formulas the transformation described previously,

$$\frac{|\rho|^2}{\Delta} \approx \sqrt{\frac{\Delta^2}{4} + |\rho|^2} - \frac{\Delta}{2} \tag{2.39}$$

An interesting feature of this approach is that there is no need for an identification of the resonant terms, which can be inconsistent whenever one has to consider a series of force fields for a given system, or a series of geometries along a reaction path. Indeed, variations in the set of resonant terms can make difficult any comparison of the VPT2 results between two or more simulations. This scheme is similar to the degeneracy-corrected PT2 (DCPT2) introduced by Kuhler and coworkers[130], which will be discussed afterwards. The interest is to prevent the appearance of singularities in the calculation of anharmonic contributions using a simplified variational approach, since the right-hand side of eq. 2.39 cannot diverge if Δ becomes small. Far from resonance, the substitution still accounts for the interaction between the vibrational states $|\,\phi^{(0)}_{A_a}\,\rangle$ and $|\,\phi^{(0)}_{B_b}\,\rangle$. At variance with what has been done in refs. [53] and [130], this time we apply the transformation of eq. 2.39 directly on the possibly resonant terms in the effective Hamiltonian, that are all terms in the summation in the right-hand side of eq. 1.52, which have frequencies differences (i.e. $2\omega_i - \omega_j$ or $\omega_i - \omega_j - \omega_k$) in the denominator. For this reason, we will refer to this approach as degeneracy smeared PT2 (DSPT2). After the complete development of eq. 1.52, the possibly resonant terms can be grouped in sets of 2 or 4 components having the same definition of Δ. For the two terms with the same Δ the substitution given in eq. 2.39 leads to,

$$\begin{aligned}\frac{\left|\langle\, \phi^{(0)}_{A_a} \mid \mathcal{H}^{(1)} \mid \phi^{(0)}_{B_b}\,\rangle\right|^2}{E^{(0)}_A - E^{(0)}_B} + \frac{\left|\langle\, \phi^{(0)}_{A_a} \mid \mathcal{H}^{(1)} \mid \phi^{(0)}_{C_c}\,\rangle\right|^2}{E^{(0)}_A - E^{(0)}_C} &= \mathrm{S}_1\frac{|\rho_1|^2}{\Delta} + \mathrm{S}_2\frac{|\rho_2|^2}{\Delta} \\ \rightarrow \mathrm{S}_1\sqrt{\frac{\Delta^2}{4} + |\rho_1|^2} + \mathrm{S}_2\sqrt{\frac{\Delta^2}{4} + |\rho_2|^2} &- (\mathrm{S}_1 + \mathrm{S}_2)\frac{\Delta}{2}\end{aligned} \tag{2.40}$$

with $\Delta = |E^{(0)}_A - E^{(0)}_B| = |E^{(0)}_A - E^{(0)}_C|$, $\mathrm{S}_1 = \mathrm{sign}(E^{(0)}_A - E^{(0)}_B)$ and $\mathrm{S}_2 = \mathrm{sign}(E^{(0)}_A - E^{(0)}_C)$. Since S_1 and S_2 are opposite, the last term of the transformation disappears. As an example, let us consider the terms involving $\Delta = \hbar|2\omega_m - \omega_n|$,

$$\begin{aligned}\frac{|\langle\, n_m n_n \mid \mathcal{H}^{(1)} \mid (n_m+2)_m(n_n+1)_n\,\rangle|^2}{\hbar(2\omega_m - \omega_n)} + \frac{|\langle\, n_m n_n \mid \mathcal{H}^{(1)} \mid (n_m+2)_m(n_n-1)_n\,\rangle|^2}{\hbar(2\omega_m - \omega_n)} \\ = \frac{\hbar^3 {K_{mmn}}^2 n_m(n_m-1)(n_n+1)}{32\lambda_m\omega_n\hbar(2\omega_m - \omega_n)} - \frac{\hbar^3 {K_{mmn}}^2 (n_m+1)(n_m+2)n_n}{32\lambda_m\omega_n\hbar(2\omega_m - \omega_n)}\end{aligned} \tag{2.41}$$

The substitution given in eq. 2.40 can be carried out with the following definitions,

$$\Delta = \hbar|2\omega_m - \omega_n| \tag{2.42}$$

$$|\rho_1|^2 = \hbar^3 {K_{mmn}}^2 n_m(n_m - 1)(n_n + 1)/(32\lambda_m\omega_s) \tag{2.43}$$

$$|\rho_2|^2 = \hbar^3 {K_{mmn}}^2 (n_m + 1)(n_m + 2)n_n/(32\lambda_m\omega_n) \tag{2.44}$$

$$\mathrm{S}_1 = -\mathrm{S}_2 = \mathrm{sign}(2\omega_m - \omega_n) \tag{2.45}$$

The transformation to be applied in the case of 4 terms having the same Δ is straightforwardly derived,

$$\begin{aligned}
&\frac{\left|\langle\, \phi^{(0)}_{A_a} \mid \mathcal{H}^{(1)} \mid \phi^{(0)}_{B_b} \,\rangle\right|^2}{E^{(0)}_A - E^{(0)}_B} + \frac{\left|\langle\, \phi^{(0)}_{A_a} \mid \mathcal{H}^{(1)} \mid \phi^{(0)}_{C_c} \,\rangle\right|^2}{E^{(0)}_A - E^{(0)}_C} + \frac{\left|\langle\, \phi^{(0)}_{A_a} \mid \mathcal{H}^{(1)} \mid \phi^{(0)}_{D_d} \,\rangle\right|^2}{E^{(0)}_A - E^{(0)}_D} \\
&\quad + \frac{\left|\langle\, \phi^{(0)}_{A_a} \mid \mathcal{H}^{(1)} \mid \phi^{(0)}_{E_e} \,\rangle\right|^2}{E^{(0)}_A - E^{(0)}_E} = \mathrm{S}_1\frac{|\rho_1|^2}{\Delta} + \mathrm{S}_2\frac{|\rho_2|^2}{\Delta} + \mathrm{S}_3\frac{|\rho_3|^2}{\Delta} + \mathrm{S}_4\frac{|\rho_4|^2}{\Delta} \\
&\rightarrow \mathrm{S}_1\sqrt{\frac{\Delta^2}{4} + |\rho_1|^2} + \mathrm{S}_2\sqrt{\frac{\Delta^2}{4} + |\rho_2|^2} + \mathrm{S}_3\sqrt{\frac{\Delta^2}{4} + |\rho_3|^2} + \mathrm{S}_4\sqrt{\frac{\Delta^2}{4} + |\rho_4|^2} \\
&\qquad - (\mathrm{S}_1 + \mathrm{S}_2 + \mathrm{S}_3 + \mathrm{S}_4)\frac{\Delta}{2}
\end{aligned} \tag{2.46}$$

with $\Delta = |E^{(0)}_A - E^{(0)}_B| = |E^{(0)}_A - E^{(0)}_C| = |E^{(0)}_A - E^{(0)}_D| = |E^{(0)}_A - E^{(0)}_E|$. As before, the previous transformation can be further simplified since the term $(\mathrm{S}_1 + \mathrm{S}_2 + \mathrm{S}_3 + \mathrm{S}_4)$ is null. All potentially resonant terms and the definition required to apply the transformation given above are gathered in Table 2.2.

The extension of the DSPT2 treatment to the off-diagonal elements $\langle\, \phi^{(0)}_{A_a} \mid \tilde{\mathcal{H}}_{40} \mid \phi^{(0)}_{A_b} \,\rangle$ requires further discussion. Let us consider one of the terms in the summation in the right-hand side of eq. 1.52 with $a \neq b$. This contribution can be related to the eigenvalues of the following matrix,

$$\begin{pmatrix} E^{(0)}_A & \rho_2 \\ \rho_1 & E^{(0)}_C \end{pmatrix} \tag{2.47}$$

where $\rho_1 = \langle\, \phi^{(0)}_{A_a} \mid \mathcal{H}^{(1)} \mid \phi^{(0)}_{C_c} \,\rangle$ and $\rho_2 = \langle\, \phi^{(0)}_{C_c} \mid \mathcal{H}^{(1)} \mid \phi^{(0)}_{A_b} \,\rangle$, with associated eigenvalues,

$$E^{\pm} = \frac{E^{(0)}_A + E^{(0)}_C}{2} \pm \sqrt{\frac{\Delta^2}{4} + \bar{\rho}} \xrightarrow[\bar{\rho}\to 0]{} \frac{E^{(0)}_A + E^{(0)}_C}{2} \pm \left[\frac{\Delta}{2} + \frac{\bar{\rho}}{\Delta} - \frac{\bar{\rho}^2}{\Delta^3} + \circ(\bar{\rho}^4)\right] \tag{2.48}$$

$\bar{\rho} = \rho_1\rho_2$ and $\Delta = |E^{(0)}_A - E^{(0)}_C|$. This matrix differs slightly from the one obtained with the proper variational description, which has the form,

$$\begin{pmatrix} \langle\, \phi^{(0)}_{A_a} \mid \mathcal{H}^{(0)} + \mathcal{H}^{(1)} \mid \phi^{(0)}_{A_b} \,\rangle & \langle\, \phi^{(0)}_{C_c} \mid \mathcal{H}^{(0)} + \mathcal{H}^{(1)} \mid \phi^{(0)}_{A_b} \,\rangle \\ \langle\, \phi^{(0)}_{A_a} \mid \mathcal{H}^{(0)} + \mathcal{H}^{(1)} \mid \phi^{(0)}_{C_c} \,\rangle & \langle\, \phi^{(0)}_{C_c} \mid \mathcal{H}^{(0)} + \mathcal{H}^{(1)} \mid \phi^{(0)}_{C_c} \,\rangle \end{pmatrix} = \begin{pmatrix} 0 & \rho_2 \\ \rho_1 & E^{(0)}_C \end{pmatrix} \tag{2.49}$$

Table 2.2: Δ and $|\rho|^2$ terms involved in the DSPT2 treatment of $\tilde{\mathcal{H}}_{40}$ diagonal elements.

Type I Fermi resonances	**Type II Fermi resonances**
$\Delta=\hbar\lvert 2\omega_m-\omega_n\rvert$ $\mathrm{S}_1=-\mathrm{S}_2=\mathrm{sign}(2\omega_m-\omega_n)$ $\lvert\rho_1\rvert^2=H_{mmn}{K_{mmn}}^2 n_m(n_m-1)(n_n+1)/32$ $\lvert\rho_2\rvert^2=H_{mmn}{K_{mmn}}^2(n_m+1)(n_m+2)n_n/32$	$\Delta=\hbar\lvert\omega_m-\omega_n-\omega_o\rvert$ $\mathrm{S}_1=-\mathrm{S}_2=\mathrm{sign}(\omega_m-\omega_n-\omega_o)$ $\lvert\rho_1\rvert^2=H_{mno}{K_{mno}}^2 n_m(n_n+1)(n_o+1)/8$ $\lvert\rho_2\rvert^2=H_{mno}{K_{mno}}^2(n_m+1)n_n n_o/8$
$\Delta=\hbar\lvert 2\omega_s-\omega_m\rvert$ $\mathrm{S}_1=-\mathrm{S}_2=\mathrm{sign}(2\omega_s-\omega_m)$ $\lvert\rho_1\rvert^2=H_{mss}\{K^{(I)}_{mss}\}^2(n_m+1)(n_s+l_s)(n_s-l_s)/32$ $\lvert\rho_2\rvert^2=H_{mss}\{K^{(I)}_{mss}\}^2 n_m(n_s+l_s+2)(n_s-l_s+2)/32$	$\Delta=\hbar\lvert\omega_m-\omega_s-\omega_t\rvert$ $\mathrm{S}_1=\mathrm{S}_2=-\mathrm{S}_3=-\mathrm{S}_4=\mathrm{sign}(\omega_m-\omega_s-\omega_t)$ $\lvert\rho_1\rvert^2=H_{mst}\{K^{(I/II)}_{mst}\}^2 n_m(n_s+l_s+2)(n_t-l_t+2)/32$ $\lvert\rho_2\rvert^2=H_{mst}\{K^{(I/II)}_{mst}\}^2 n_m(n_s-l_s+2)(n_t+l_t+2)/32$ $\lvert\rho_3\rvert^2=H_{mst}\{K^{(I/II)}_{mst}\}^2(n_m+1)(n_s+l_s)(n_t-l_t)/32$ $\lvert\rho_4\rvert^2=H_{mst}\{K^{(I/II)}_{mst}\}^2(n_m+1)(n_s-l_s)(n_t+l_t)/32$
$\Delta=\hbar\lvert 2\omega_s-\omega_m\rvert$ $\mathrm{S}_1=\mathrm{S}_2=-\mathrm{S}_3=-\mathrm{S}_4=\mathrm{sign}(2\omega_s-\omega_m)$ $\lvert\rho_1\rvert^2=H_{mss}\{K^{(III/IV)}_{mss}\}^2(n_m+1)(n_s+l_s-2)(n_s+l_s)/128$ $\lvert\rho_2\rvert^2=H_{mss}\{K^{(III/IV)}_{mss}\}^2(n_m+1)(n_s-l_s-2)(n_s-l_s)/128$ $\lvert\rho_3\rvert^2=H_{mss}\{K^{(III/IV)}_{mss}\}^2 n_m(n_s+l_s+2)(n_s+l_s+4)/128$ $\lvert\rho_4\rvert^2=H_{mss}\{K^{(III/IV)}_{mss}\}^2 n_m(n_s-l_s+2)(n_s-l_s+4)/128$	$\Delta=\hbar\lvert\omega_m-\omega_s-\omega_t\rvert$ $\mathrm{S}_1=\mathrm{S}_2=-\mathrm{S}_3=-\mathrm{S}_4=\mathrm{sign}(\omega_m-\omega_s-\omega_t)$ $\lvert\rho_1\rvert^2=H_{mst}\{K^{(III/IV)}_{mst}\}^2 n_m(n_s+l_s+2)(n_t+l_t+2)/32$ $\lvert\rho_2\rvert^2=H_{mst}\{K^{(III/IV)}_{mst}\}^2 n_m(n_s-l_s+2)(n_t-l_t+2)/32$ $\lvert\rho_3\rvert^2=H_{mst}\{K^{(III/IV)}_{mst}\}^2(n_m+1)(n_s+l_s)(n_t+l_t)/32$ $\lvert\rho_4\rvert^2=H_{mst}\{K^{(III/IV)}_{mst}\}^2(n_m+1)(n_s-l_s)(n_t-l_t)/32$
$\Delta=\hbar\lvert 2\omega_s-\omega_t\rvert$ $\mathrm{S}_1=\mathrm{S}_2=-\mathrm{S}_3=-\mathrm{S}_4=\mathrm{sign}(2\omega_s-\omega_t)$ $\lvert\rho_1\rvert^2=H_{sst}\{K^{(I/II)}_{sst}\}^2(n_s+l_s)(n_s+l_s-2)(n_t-l_t+2)/128$ $\lvert\rho_2\rvert^2=H_{sst}\{K^{(I/II)}_{sst}\}^2(n_s-l_s)(n_s-l_s-2)(n_t+l_t+2)/128$ $\lvert\rho_3\rvert^2=H_{sst}\{K^{(I/II)}_{sst}\}^2(n_s+l_s+2)(n_s+l_s+4)(n_t-l_t)/128$ $\lvert\rho_4\rvert^2=H_{sst}\{K^{(I/II)}_{sst}\}^2(n_s-l_s+2)(n_s-l_s+4)(n_t+l_t)/128$	$\Delta=\hbar\lvert\omega_s-\omega_m-\omega_t\rvert$ $\mathrm{S}_1=\mathrm{S}_2=-\mathrm{S}_3=-\mathrm{S}_4=\mathrm{sign}(\omega_s-\omega_m-\omega_t)$ $\lvert\rho_1\rvert^2=H_{mst}\{K^{(I/II)}_{mst}\}^2(n_m+1)(n_s+l_s)(n_t+l_t+2)/32$ $\lvert\rho_2\rvert^2=H_{mst}\{K^{(I/II)}_{mst}\}^2(n_m+1)(n_s-l_s)(n_t-l_t+2)/32$ $\lvert\rho_3\rvert^2=H_{mst}\{K^{(I/II)}_{mst}\}^2 n_m(n_s+l_s+2)(n_t+l_t)/32$ $\lvert\rho_4\rvert^2=H_{mst}\{K^{(I/II)}_{mst}\}^2 n_m(n_s-l_s+2)(n_t-l_t)/32$
$\Delta=\hbar\lvert 2\omega_s-\omega_t\rvert$ $\mathrm{S}_1=\mathrm{S}_2=-\mathrm{S}_3=-\mathrm{S}_4=\mathrm{sign}(2\omega_s-\omega_t)$ $\lvert\rho_1\rvert^2=H_{sst}\{K^{(III/IV)}_{sst}\}^2(n_s+l_s)(n_s+l_s-2)(n_t+l_t+2)/128$ $\lvert\rho_2\rvert^2=H_{sst}\{K^{(III/IV)}_{sst}\}^2(n_s-l_s)(n_s-l_s-2)(n_t-l_t+2)/128$ $\lvert\rho_3\rvert^2=H_{sst}\{K^{(III/IV)}_{sst}\}^2(n_s+l_s+2)(n_s+l_s+4)(n_t+l_t)/128$ $\lvert\rho_4\rvert^2=H_{sst}\{K^{(III/IV)}_{sst}\}^2(n_s-l_s+2)(n_s-l_s+4)(n_t-l_t)/128$	$\Delta=\hbar\lvert\omega_s-\omega_m-\omega_t\rvert$ $\mathrm{S}_1=\mathrm{S}_2=-\mathrm{S}_3=-\mathrm{S}_4=\mathrm{sign}(\omega_s-\omega_m-\omega_t)$ $\lvert\rho_1\rvert^2=H_{mst}\{K^{(III/IV)}_{mst}\}^2(n_m+1)(n_s+l_s)(n_t-l_t+2)/32$ $\lvert\rho_2\rvert^2=H_{mst}\{K^{(III/IV)}_{mst}\}^2(n_m+1)(n_s-l_s)(n_t+l_t+2)/32$ $\lvert\rho_3\rvert^2=H_{mst}\{K^{(III/IV)}_{mst}\}^2 n_m(n_s+l_s+2)(n_t-l_t)/32$ $\lvert\rho_4\rvert^2=H_{mst}\{K^{(III/IV)}_{mst}\}^2 n_m(n_s-l_s+2)(n_t+l_t)/32$
	$\Delta=\hbar\lvert\omega_s-\omega_t-\omega_u\rvert$ $\mathrm{S}_1=\mathrm{S}_2=-\mathrm{S}_3=-\mathrm{S}_4=\mathrm{sign}(\omega_s-\omega_t-\omega_u)$ $\lvert\rho_1\rvert^2=H_{stu}\{K^{(I/II)}_{stu}\}^2(n_s+l_s)(n_t-l_t+2)(n_u-l_u+2)/32$ $\lvert\rho_2\rvert^2=H_{stu}\{K^{(I/II)}_{stu}\}^2(n_s-l_s)(n_t+l_t+2)(n_u+l_u+2)/32$ $\lvert\rho_3\rvert^2=H_{stu}\{K^{(I/II)}_{stu}\}^2(n_s+l_s+2)(n_t-l_t)(n_u-l_u)/32$ $\lvert\rho_4\rvert^2=H_{stu}\{K^{(I/II)}_{stu}\}^2(n_s-l_s+2)(n_t+l_t)(n_u+l_u)/32$
	$\Delta=\hbar\lvert\omega_s-\omega_t-\omega_u\rvert$ $\mathrm{S}_1=\mathrm{S}_2=-\mathrm{S}_3=-\mathrm{S}_4=\mathrm{sign}(\omega_s-\omega_t-\omega_u)$ $\lvert\rho_1\rvert^2=H_{stu}\{K^{(III/IV)}_{stu}\}^2(n_s+l_s)(n_t-l_t+2)(n_u+l_u+2)/32$ $\lvert\rho_2\rvert^2=H_{stu}\{K^{(III/IV)}_{stu}\}^2(n_s-l_s)(n_t+l_t+2)(n_u-l_u+2)/32$ $\lvert\rho_3\rvert^2=H_{stu}\{K^{(III/IV)}_{stu}\}^2(n_s+l_s+2)(n_t-l_t)(n_u+l_u)/32$ $\lvert\rho_4\rvert^2=H_{stu}\{K^{(III/IV)}_{stu}\}^2(n_s-l_s+2)(n_t+l_t)(n_u-l_u)/32$

$H_{ijk}=\hbar^3/\omega_i\omega_j\omega_k$ and the slash symbol ("/") between latin numbers is used as a separator between the possible force constants for which the relation stands.

Table 2.3: Δ, s and $\bar{\rho}$ terms involved in the DSPT2 treatment of $\tilde{\mathcal{H}}_{40}$ l-doubling off-diagonal elements.

U l-type doubling
$\Delta = \hbar\lvert 2\omega_s - \omega_m\rvert$ $\bar{\mathrm{S}} = \mathrm{sign}(2\omega_s - \omega_m)$ $\bar{\rho} = H_{mss}\left\{K_{mss}^{(III/IV)}\right\}^2\sqrt{(n_s \pm l_s + 4)(n_s + l_s \pm 2)(n_s - l_s \mp 2)(n_s \mp l_s)}/128$
R l-type doubling
$\Delta = \hbar\lvert \omega_m - \omega_s - \omega_t\rvert$ $\bar{\mathrm{S}} = -\mathrm{sign}(\omega_m - \omega_s - \omega_t)$ $\bar{\rho} = H_{mst}\left\{K_{mst}^{(I)}\right\}^2\sqrt{(n_s \pm l_s + 2)(n_t \mp l_t + 2)(n_s \mp l_s)(n_t \pm l_t)}/32$
$\Delta = \hbar\lvert \omega_s - \omega_m - \omega_t\rvert$ $\bar{\mathrm{S}} = \mathrm{sign}(\omega_s - \omega_m - \omega_t)$ $\bar{\rho} = H_{mst}\left\{K_{mst}^{(I)}\right\}^2\sqrt{(n_s \pm l_s + 2)(n_t \mp l_t + 2)(n_s \mp l_s)(n_t \pm l_t)}/32$
$\Delta = \hbar\lvert \omega_m - \omega_s - \omega_t\rvert$ $\bar{\mathrm{S}} = \mathrm{sign}(\omega_m - \omega_s - \omega_t)$ $\bar{\rho} = H_{mst}\left\{K_{mst}^{(II)}\right\}^2\sqrt{(n_s \pm l_s + 2)(n_t \mp l_t + 2)(n_s \mp l_s)(n_t \pm l_t)}/32$
$\Delta = \hbar\lvert \omega_s - \omega_m - \omega_t\rvert$ $\bar{\mathrm{S}} = -\mathrm{sign}(\omega_s - \omega_m - \omega_t)$ $\bar{\rho} = H_{mst}\left\{K_{mst}^{(II)}\right\}^2\sqrt{(n_s \pm l_s + 2)(n_t \mp l_t + 2)(n_s \mp l_s)(n_t \pm l_t)}/32$
S l-type doubling
$\Delta = \hbar\lvert \omega_m - \omega_s - \omega_t\rvert$ $\bar{\mathrm{S}} = -\mathrm{sign}(\omega_m - \omega_s - \omega_t)$ $\bar{\rho} = H_{mst}\left\{K_{mst}^{(III)}\right\}^2\sqrt{(n_s \pm l_s + 2)(n_t \pm l_t + 2)(n_s \mp l_s)(n_t \mp l_t)}/32$
$\Delta = \hbar\lvert \omega_s - \omega_m - \omega_t\rvert$ $\bar{\mathrm{S}} = \mathrm{sign}(\omega_s - \omega_m - \omega_t)$ $\bar{\rho} = H_{mst}\left\{K_{mst}^{(III)}\right\}^2\sqrt{(n_s \pm l_s + 2)(n_t \pm l_t + 2)(n_s \mp l_s)(n_t \mp l_t)}/32$
$\Delta = \hbar\lvert \omega_m - \omega_s - \omega_t\rvert$ $\bar{\mathrm{S}} = \mathrm{sign}(\omega_m - \omega_s - \omega_t)$ $\bar{\rho} = H_{mst}\left\{K_{mst}^{(IV)}\right\}^2\sqrt{(n_s \pm l_s + 2)(n_t \pm l_t + 2)(n_s \mp l_s)(n_t \mp l_t)}/32$
$\Delta = \hbar\lvert \omega_s - \omega_m - \omega_t\rvert$ $\bar{\mathrm{S}} = -\mathrm{sign}(\omega_s - \omega_m - \omega_t)$ $\bar{\rho} = H_{mst}\left\{K_{mst}^{(IV)}\right\}^2\sqrt{(n_s \pm l_s + 2)(n_t \pm l_t + 2)(n_s \mp l_s)(n_t \mp l_t)}/32$

$H_{ijk} = \hbar^3/\omega_i\omega_j\omega_k$ and the slash symbol ("/") between latin numbers is used as a separator between the possible force constants for which the relation stands.

Nevertheless, the matrix given in eq. 2.47 is more convenient for the mathematical derivation of the possible resonant terms, on which the previous substitution is applied,

$$\bar{\mathrm{S}}\,\frac{\bar{\rho}}{\Delta} \approx \bar{\mathrm{S}}\left(\sqrt{\frac{\Delta^2}{4}+\bar{\rho}}-\frac{\Delta}{2}\right) \tag{2.50}$$

where $\bar{\mathrm{S}}$ accounts for the signs of both $(E_A^{(0)} - E_C^{(0)})$ and $\bar{\rho}$.
To illustrate this point, let us consider the resonant term with $2\omega_s \approx \omega_m$ in $U^{\pm}$,

$$\begin{aligned}\frac{\langle\, n_m n_s, l_s \mid \mathcal{H}^{(1)} \mid (n_m-1)_m(n_s+2)_s, (l_s\pm 2)_s \,\rangle}{\hbar(2\omega_s-\omega_m)} \\ \times \langle\, (n_m-1)_m(n_s+2)_s, (l_s\pm 2)_s \mid \mathcal{H}^{(1)} \mid n_m n_s, (l_s\pm 4)_s \,\rangle = \\ \frac{\hbar^3\left\{K_{mss}^{(III/IV)}\right\}^2\sqrt{(n_s\pm l_s+4)(n_s+l_s\pm 2)(n_s-l_s\mp 2)(n_s\mp l_s)}}{128\omega_m\lambda_s\hbar(2\omega_s-\omega_m)}\end{aligned} \tag{2.51}$$

We then apply the relation given in eq. 2.50 after the proper identification of the terms involved in the transformation,

$$\Delta = \hbar|2\omega_s - \omega_m| \tag{2.52}$$

$$\bar{\mathrm{S}} = \mathrm{sign}\,(2\omega_s - \omega_m) \tag{2.53}$$

$$\bar{\rho} = \frac{\hbar^3\left\{K_{mss}^{(III/IV)}\right\}^2\sqrt{(n_s\pm l_s+4)(n_s+l_s\pm 2)(n_s-l_s\mp 2)(n_s\mp l_s)}}{128\omega_m\lambda_s} \tag{2.54}$$

The other identification sets to be used in the transformations of the possibly resonant terms in U, R and S are gathered in Table 2.3. An alternative way to treat resonances was proposed by Kuhler and co-workers in 1995 and slightly modified by some of us. The difference with the DSPT2 development lies in the terms on which the substitution given in eq. 2.39 is applied. Indeed, in DCPT2, the elements of the $\boldsymbol{\chi}$ matrix are derived first and the possibly resonant terms are identified within the elements of χ_{ij} (eqs. 2.8–2.12) and transformed. Further details can be found in refs. [53] and [130]. For degenerate modes, not treated in those previous work, we use the same transformation as for non-degenerate modes. To illustrate this point, let us consider the last term in the right-hand side of eq. 2.11, developed in partial fractions,

$$-\frac{\hbar^2\left\{K_{sst}^{(\sigma)}\right\}^2(8\lambda_s-3\lambda_t)}{16\lambda_s\lambda_t(4\lambda_s-\lambda_t)} = -\frac{\hbar^2\left\{K_{sst}^{(\sigma)}\right\}^2}{32\lambda_s\omega_t}\left(\frac{4}{\omega_t}+\frac{1}{2\omega_s+\omega_t}-\frac{1}{2\omega_s-\omega_t}\right) \tag{2.55}$$

By setting $\Delta = \hbar|2\omega_s - \omega_t|$ and $|\rho|^2 = \hbar^3\left\{K_{sst}^{(\sigma)}\right\}^2/(32\lambda_s\omega_t)$, we obtain the

following transformation,

$$\frac{\hbar^3\left\{K_{sst}^{(\sigma)}\right\}^2}{32\lambda_s\omega_t\hbar(2\omega_s-\omega_t)} \rightarrow \mathrm{sign}(2\omega_s-\omega_t)\left[\sqrt{\frac{\hbar|2\omega_s-\omega_t|^2}{4}+\frac{\hbar^3\left\{K_{sst}^{(\sigma)}\right\}^2}{32\lambda_s\omega_t}}-\frac{\hbar|2\omega_s-\omega_t|}{2}\right] \quad (2.56)$$

The new $\boldsymbol{\chi}$ matrix obtained by replacing possibly resonant terms in non-resonant ones is then used in the calculations of the vibrational energies.

However, both DSPT2 and DCPT2 transformations can give poor results far from resonance when both numerator and denominator become large. Indeed, when ρ is large, the equivalence of eq. 2.35 is not true and, while the VPT2 term $|\rho|^2/\Delta$ can be still valid due to a large Δ, the DSPT2 and DCPT2 transformations are incorrect. To cope with this shortcoming, an hybrid scheme (HDCPT2) has been proposed by some of us. In this method, a switch function, Λ, is used to mix the results from the original VPT2 and the DCPT2 approaches for all possibly resonant terms in $\boldsymbol{\chi}$ as follows[53],

$$f_{\mathrm{HDCPT2}} = \Lambda f_{\mathrm{VPT2}} + (1-\Lambda) f_{\mathrm{DCPT2}} \quad (2.57)$$

where f_{VPT2} represents the value of a possibly resonant term calculated with the original VPT2 formulation (left-hand side term in eq. 2.56), and f_{DCPT2} its counterpart calculated by mean of DCPT2 (right-hand side term in eq. 2.56). Λ is defined as,

$$\Lambda = \frac{\tanh\left[\alpha\left(\sqrt{\frac{|\rho|^2\Delta^2}{4}}-\beta\right)\right]+1}{2} \quad (2.58)$$

where β controls the transition threshold between DCPT2 and VPT2, and α the "smoothness" of the transition. The same scheme applies for the hybrid DSPT2 (HDSPT2),

$$f_{\mathrm{HDSPT2}} = \Lambda f_{\mathrm{VPT2}} + (1-\Lambda) f_{\mathrm{DSPT2}} \quad (2.59)$$

where f_{VPT2} is the true VPT2 term (e.g. $\mathrm{S}_1|\rho_1|^2/\Delta$ in eq. 2.40 or 2.46) and f_{DSPT2} is its DSPT2 counterpart (i.e. $\mathrm{S}_1\sqrt{(\Delta^2/4)+|\rho_1|^2}$).

2.4 Vibrational second-order resonances

In analogy with first-order resonances, when two zeroth-order states involved in the contact transformation given by $\mathcal{S}^{(2)}$ are close to each other, the off-diagonal

elements $\langle \phi^{(0)}_{A_a} \mid \tilde{\mathcal{H}}^{(2)} \mid \phi^{(0)}_{B_b} \rangle$ cannot be canceled out and have to be treated variaton-ally. Many types of resonances lead to off-diagonal second order energy corrections. According to the classification of the total change of quanta, there are 1-1, 2-2 and 1-3 second-order resonances. For asymmetric tops, a detailed description of all these off-diagonal terms has been recently given by Rosnik and Polik [116]. The total number of non-zero second-order off-diagonal elements becomes very large when doubly-degenerate normal modes are also taken into account, because of the large number of combinations of non-degenerate/doubly-degenerate normal modes that can be obtained when considering all states involved in the matrix elements. In this work, we have generalized the expression for the 2-2 vibrational second-order resonances to support also doubly degenerate states, in the specific case of the annihilation of two quanta in one mode and the creation of two quanta in another one. Known also as Darling-Dennison resonances [131], the non-zero off-diagonal elements for this situation are given by,

$$\langle\, n_m n_n \mid \tilde{\mathcal{H}}^{(2)} \mid (n_m+2)_m (n_n-2)_n \,\rangle = \frac{\kappa_{mn}}{16}\sqrt{(n_m+1)(n_m+2)n_n(n_n-1)} \tag{2.60}$$

$$\langle\, n_m n_s, l_s \mid \tilde{\mathcal{H}}^{(2)} \mid (n_m+2)_m (n_s-2)_s, l_s \,\rangle = \frac{\kappa_{ms}}{16}\sqrt{(n_m+1)(n_m+2)(n_s-l_s)(n_s+l_s)} \tag{2.61}$$

$$\langle\, n_s n_t, l_s l_t \mid \tilde{\mathcal{H}}^{(2)} \mid (n_s+2)_s (n_t-2)_t, l_s l_t \,\rangle = \frac{\kappa^{(I)}_{st}}{16}\sqrt{(n_s-l_s+2)(n_s+l_s+2)(n_t-l_t)(n_t+l_t)} \tag{2.62}$$

$$\langle\, n_s n_t, l_s l_t \mid \tilde{\mathcal{H}}^{(2)} \mid (n_s+2)_s (n_t-2)_t, (l_s\pm 2)_s (l_t\pm 2)_t \,\rangle = \frac{\kappa^{\pm(II)}_{st}}{64}\sqrt{(n_s\pm l_s+2)(n_s\pm l_s+4)(n_t\mp l_t-2)(n_t\mp l_t)} \tag{2.63}$$

$$\langle\, n_s n_t, l_s l_t \mid \tilde{\mathcal{H}}^{(2)} \mid (n_s+2)_s (n_t-2)_t, (l_s\pm 2)_s (l_t\mp 2)_t \,\rangle = \frac{\kappa^{\pm(III)}_{st}}{64}\sqrt{(n_s\pm l_s+2)(n_s\pm l_s+4)(n_t\pm l_t-2)(n_t\pm l_t)} \tag{2.64}$$

The definition of the κ terms is reported in Appendix E. The second-order off-diagonal elements are then used within the GVPT2 approach in the variational treatment of the polyads.

Therefore, each polyad contains the deperturbed vibrational energies of the resonances interacting states in the diagonal elements, the first- and second-order resonances off-diagonal elements, as well as the possibly l-doubling and l-resonance, also off-diagonal terms. Note that, up to the second-order, we will never have $\langle\, \phi^{(0)}_{A_a} \mid \tilde{\mathcal{H}}^{(1)} + \tilde{\mathcal{H}}^{(2)} \mid \phi^{(0)}_{B_b} \,\rangle$, with both $\langle\, \phi^{(0)}_{A_a} \mid \tilde{\mathcal{H}}^{(1)} \mid \phi^{(0)}_{B_b} \,\rangle$ and $\langle\, \phi^{(0)}_{A_a} \mid \tilde{\mathcal{H}}^{(2)} \mid \phi^{(0)}_{B_b} \,\rangle$ non-null, because the couples of states interacting within first-order resonances are

always different from the couples interacting by second-order resonances.

2.5 Vibrational partition function

The partition function of a system is the sum of the Boltzmann factors of the energy levels E_σ each weighted by its degeneracy D_σ[132],

$$Q(T) = \sum_\sigma e^{-\beta E_\sigma} D_\sigma \tag{2.65}$$

where $\beta = 1/(k_B T)$, k_B and T are the Boltzmann constant and the temperature, respectively, and the summation is on all possibly states σ. We treat here the vibrational molecular partition function Q_{vib}, for which E_σ and D_σ are the energies and degeneracies of vibrational levels. Starting from eq. 2.65 and focusing on at most doubly degenerate vibrational modes, the harmonic vibrational partition function $Q_{\text{vib}}^{(H)}$ is obtained by,

$$Q_{\text{vib}}^{(H)} = \sum_{n_m=0}^{\infty} \sum_{n_n=0}^{\infty} \dots \sum_{n_s=0}^{\infty} \sum_{n_t=0}^{\infty} \dots e^{-\beta E(\boldsymbol{n})} (n_s+1)(n_t+1)\dots \tag{2.66}$$

where $E(\boldsymbol{n}) = \sum_i \hbar\omega_i (n_i + d_i/2)$ is the harmonic formulation of the vibrational energy and (n_s+1) is the degeneracy due to the degenerate mode s. Developing the previous expression,

$$\begin{aligned}
Q_{\text{vib}}^{(H)} =& e^{-\beta E_0^{(H)}} \sum_{n_m=0}^{\infty} \sum_{n_n=0}^{\infty} \dots \sum_{n_s=0}^{\infty} \sum_{n_t=0}^{\infty} \dots \prod_i e^{-\beta\hbar\omega_i n_i} (n_s+1)(n_t+1)\dots \\
=& e^{-\beta E_0^{(H)}} \sum_{n_m=0}^{\infty} e^{-\beta\hbar\omega_m n_m} \dots \sum_{n_s=0}^{\infty} e^{-\beta\hbar\omega_s n_s} (n_s+1)\dots \\
=& e^{-\beta E_0^{(H)}} \frac{1}{(1-e^{-\beta\hbar\omega_m})} \dots \frac{1}{(1-e^{-\beta\hbar\omega_s})^2} \dots \\
=& \frac{e^{-\beta E_0^{(H)}}}{\prod_i (1-e^{-\beta\hbar\omega_i})^{d_i}}
\end{aligned} \tag{2.67}$$

where $E_0^{(H)} = \sum_i \hbar\omega_i d_i/2$ is the harmonic ZPVE and we have used the relations $\sum_{n=0}^{\infty} q^n = 1/(1-q)$ and $\sum_{n=0}^{\infty}(n+1)q^n = 1/(1-q)^2$ when $|q| < 1$.

Unfortunately, an analytical development of Q_{vib} is not available beyond the harmonic level. Truhlar and Isaacson proposed a method, called simple perturbation theory (SPT), in which the formal expression of the harmonic partition

function is retained, but the ZPVE and ω_i terms are replaced with their anharmonic counterparts [35, 130, 133],

$$Q_{\text{vib}}^{(SPT)} = \frac{e^{-\beta E_0}}{\prod_i \left(1 - e^{-\beta \nu(1,\pm 1 \text{ or } 0)_i}\right)^{d_i}} \tag{2.68}$$

where E_0 is the anharmonic ZPVE given in eq. 2.4, and $\nu(1, \pm 1 \text{ or } 0)_i$, defined in eq. 2.18, is reduced to ν_i below for the sake of readability. This approximation leads to analytical expressions for the vibrational contributions to the internal energy U, entropy S, and constant volume specific heat c [113, 132],

$$U = \frac{R}{k_B}\left[E_0 + \sum_i \frac{\nu_i d_i}{e^{\beta\nu_i} - 1}\right] \tag{2.69}$$

$$S = \frac{R}{k_B T}\sum_i d_i \left[\frac{\nu_i}{e^{\beta\nu_i} - 1} - k_B T \ln\left(1 - e^{-\beta\nu_i}\right)\right] \tag{2.70}$$

$$c = \frac{R}{k_B T}\sum_i d_i e^{\beta\nu_i}\left[\frac{\nu_i}{e^{\beta\nu_i} - 1}\right]^2 \tag{2.71}$$

where R is the Boltzmann universal gas constant.

2.6 Vibrational energy at non stationary points

In the previous sections we have analyzed the expression of vibrational energy up to second perturbative order when the nuclei are in their equilibrium configuration, which is a stationary point of the PES ($\boldsymbol{\nabla} V = \mathbf{0}$). In this configuration, the expansion of the potential energy on the normal coordinates is given by eq. 1.29. Some additional terms appear if the configuration of nuclei is not a stationary point and $\boldsymbol{Q}$ is a set of orthonormal coordinates, with Q_i a generic linear combination of nuclei's Cartesian coordinates. The new set $\boldsymbol{Q}$ will not diagonalize the Hessian matrix $\boldsymbol{H}$, but, if the off-diagonal elements H_{ij} are small with respect to the diagonal ones H_{ii}, the latter can be regarded as perturbative terms and included in $\mathcal{H}^{(1)}$. Moreover, $\boldsymbol{\nabla} V \neq \mathbf{0}$ leads to first derivative terms in the expansion of V that can be also treated as part of $\mathcal{H}^{(1)}$.
Focusing on asymmetric top systems, we have,

$$\mathcal{H}^{(1)} = \mathcal{H}_{30} + \sum_m K_m Q_m + \frac{1}{2}\sum_m \sum_{n \neq m} K_{mn} Q_m Q_n \tag{2.72}$$

where $\mathcal{H}_{30}$ is given by eq. 1.34, $K_m = \partial V / \partial Q_m$ and $K_{mn} = \partial^2 V / (\partial Q_m \partial Q_n)$. Into the perturbative treatment, the expression for the vibrational energy up to second

order becomes,

$$\begin{aligned} E'(\boldsymbol{n}) =& E(\boldsymbol{n}) - \sum_m \frac{K_m^2}{2\lambda_m} - \hbar \sum_m \sum_n \frac{K_m K_{mnn}}{2\lambda_m \sqrt{\lambda_n}} \left(n_n + \frac{1}{2} \right) \\ & - \hbar \sum_m \sum_{n \neq m} \frac{K_{mn}^2}{2\sqrt{\lambda_n} \left(\lambda_m^2 - \lambda_n^2 \right)} \left(n_n + \frac{1}{2} \right) \end{aligned} \tag{2.73}$$

where $E(\boldsymbol{n})$ is given by eq. 2.2.

Chapter 3

Rotational Hamiltonian

The rotational energy levels for the zero-point vibrational state are given by the terms $\tilde{\mathcal{H}}_{0g}$ ($g = 2, 4, 6, 8, \ldots$) of the effective Hamiltonian, while the operators $\tilde{\mathcal{H}}_{22}$, $\tilde{\mathcal{H}}_{42}$, $\tilde{\mathcal{H}}_{24}$, ... contain the terms describing the dependence of the rotational and centrifugal constants on the vibrational quantum numbers.
The complete treatment of all these terms has been widely discussed in the literature and we will recall in this chapter only the main aspects of the quartic $\tilde{\mathcal{H}}_{04}$ and sextic $\tilde{\mathcal{H}}_{06}$ centrifugal distortion terms, and the perturbative corrections that can be introduced to describe the dependence of the rotational equilibrium constants on the vibrational quantum numbers [3, 6, 32, 134–139].

3.1 Rotational constants

The quartic centrifugal terms $\tilde{\mathcal{H}}_{04}$ form the simplest second-order contribution to $\tilde{\mathcal{H}}_{\mathrm{rot}}$. Their expression results from the second-order effect of $\mathcal{H}^{(1)} = \mathcal{H}_{12}$,

$$\begin{aligned}\tilde{\mathcal{H}}_{04} =& -\frac{\hbar^2}{4}\sum_{\tau\eta\varsigma\varrho} J_\tau J_\eta J_\varsigma J_\varrho \sum_{i,\gamma} \frac{a_{i_\gamma,\tau\eta} a_{i_\gamma,\varsigma\varrho}}{2\lambda_i I^e_\tau I^e_\eta I^e_\varsigma I^e_\varrho} \\ =& \frac{1}{4}\sum_{\tau\eta\varsigma\varrho} \tau_{\tau\eta\varsigma\varrho} J_\tau J_\eta J_\varsigma J_\varrho \end{aligned} \tag{3.1}$$

where the tensor $\tau_{\tau\eta\varsigma\varrho}$ was originally introduced by Wilson [140, 141]. The sextic centrifugal distortion constants arise from the term $\tilde{\mathcal{H}}_{06}$. The perturbation terms required for their calculation are $\mathcal{H}_{12}\mathcal{H}_{12}\mathcal{H}_{22}$ (harmonic), $\mathcal{H}_{30}\mathcal{H}_{12}\mathcal{H}_{21}\mathcal{H}_{21}$ (anharmonic) and $\mathcal{H}_{12}\mathcal{H}_{12}\mathcal{H}_{21}\mathcal{H}_{21}$, $\mathcal{H}_{12}\mathcal{H}_{12}\mathcal{H}_{21}\mathcal{H}_{02}$, $\mathcal{H}_{12}\mathcal{H}_{12}\mathcal{H}_{02}\mathcal{H}_{02}$ (Coriolis), where the last two Coriolis contributions should be considered even if they have a degree in J greater than six because they can be reduced to sixth degree terms by the

rotational commutators (i.e. $[J_\tau, J_\eta] = -iJ_\varsigma$ (see refs. [32, 134] for further details). With the assignment $\mathcal{H}^{(1)} = \mathcal{H}_{02} + \mathcal{H}_{12} + \mathcal{H}_{21} + \mathcal{H}_{30}$ and $\mathcal{H}^{(2)} = \mathcal{H}_{22}$ all contributions reported above appear in the fourth order perturbative development. The final expression for $\tilde{\mathcal{H}}_{06}$ was obtained by Chung and Parker [142, 143] and collected by Aliev and Watson (see Table III of ref. [139].

The vibrational contact transformation then leads to the rotational Hamiltonian,

$$\tilde{\mathcal{H}}_{\rm rot} = \mathcal{H}_{02} + \tilde{\mathcal{H}}_{04} + \tilde{\mathcal{H}}_{06} \tag{3.2}$$

where now both $\tilde{\mathcal{H}}_{04}$ and $\tilde{\mathcal{H}}_{06}$ contain terms that can be reduced by the use of rotational commutation relations. Taking as an example the explicit form of $\tilde{\mathcal{H}}_{04}$ given in eq. 3.1, there are $3^4 = 81$ terms that can be reduced to,

$$\tilde{\mathcal{H}}'_{04} = \frac{1}{4}\sum_{\tau\eta} \tau'_{\tau\tau\eta\eta} {J_\tau}^2 {J_\eta}^2 \tag{3.3}$$

where

$$\tau'_{\tau\tau\eta\eta} = \tau_{\tau\tau\eta\eta} + 2\tau_{\tau\eta\tau\eta}(1 - \delta_{\tau\eta}) \tag{3.4}$$

As a consequence of this reduction, B^e_τ is corrected by a small contribution from the quartic terms,

$$B^{e\prime}_\tau = B^e_\tau + \frac{1}{4}\left(3\tau_{\eta\varsigma\eta\varsigma} - 2\tau_{\varsigma\tau\varsigma\tau} - 2\tau_{\tau\eta\tau\eta}\right) \tag{3.5}$$

$B^{e\prime}_\eta$ and $B^{e\prime}_\varsigma$ are obtained by cyclic permutation of the indices.

Further contact transformations with purely rotational operators, thus diagonal in the vibrational quantum numbers, are required in order to achieve a complete reduction of $\tilde{\mathcal{H}}_{\rm rot}$. In the completely reduced Hamiltonian, combinations of quartic and sextic distortion parameters are strictly related to the eigenvalues of $\tilde{\mathcal{H}}_{\rm rot}$, and then to physical observables. Different results can be obtained depending on the arbitrary choice applied to fix the reduction's parameters. The general form of the reduced Hamiltonian of an arbitrary molecule has been given by Watson[137, 138, 144]. With the choice called by Watson asymmetric top (A) reduction, the matrix representation of $\tilde{\mathcal{H}}_{\rm rot}$ in the symmetric top basis has the same form as that of a rigid asymmetric top,

$$\begin{aligned}
\tilde{\mathcal{H}}^{(A)}_{\rm rot} =& \sum_\tau B^{(A)}_\tau {\boldsymbol{J}_\tau}^2 - \Delta_J (\boldsymbol{J}^2)^2 - \Delta_{Jk} \boldsymbol{J}^2 {J_z}^2 - \Delta_k {J_z}^4 \\
& - \frac{1}{2}\left[(\delta_J \boldsymbol{J}^2 + \delta_k {J_z}^2), ({J_+}^2 + {J_-}^2)\right]_+ + \Phi_J (\boldsymbol{J}^2)^3 \\
& + \Phi_{Jk} (\boldsymbol{J}^2)^2 J_z^2 + \Phi_{kJ} \boldsymbol{J}^2 {J_z}^4 + \Phi_k {J_z}^6 \\
& + \frac{1}{2}\left[(\varphi_J (\boldsymbol{J}^2)^2 + \varphi_{Jk} \boldsymbol{J}^2 {J_z}^2 + \varphi_k {J_z}^4), ({J_+}^2 + {J_-}^2)\right]
\end{aligned} \tag{3.6}$$

where $\boldsymbol{J}^2$ and $\mathrm{J}_\pm$ are the total angular momentum and the ladder operators, respectively [145] and $[X,Y]_+$ represents an anticommutator. Δ and δ refer to the quartic distortion constants, Φ, and φ to the sextic ones. The latter coefficients are given in refs. [108, 134]. The disadvantage of the asymmetric top reduction is that it fails for both genuine and accidental symmetric tops. For the latter, the symmetric top (S) reduction suggested by Winnewisser and Van Eijck can be used [146, 147],

$$\begin{aligned}\tilde{\mathcal{H}}_{\mathrm{rot}}^{(S)} = &\sum_\tau B_\tau^{(S)} \boldsymbol{J}_\tau{}^2 - D_J(\boldsymbol{J}^2)^2 - D_{Jk}\boldsymbol{J}^2 J_z{}^2 - D_k J_z{}^4 + d_1 \boldsymbol{J}^2(J_+{}^2 + J_-{}^2) \\ &+ d_2(J_+{}^4 + J_-{}^4) + H_J(\boldsymbol{J}^2)^3 + H_{Jk}(\boldsymbol{J}^2)^2 J_z{}^2 + H_{kJ}\boldsymbol{J}^2 J_z{}^4 + H_k J_z{}^6 \\ &+ h_1(\boldsymbol{J}^2)^2(J_+{}^2 + J_-{}^2) + h_2 \boldsymbol{J}^2(J_+{}^4 + J_-{}^4) + h_3(J_+{}^6 + J_-{}^6) \end{aligned} \tag{3.7}$$

where the expression for the quartic (D and d) and sextic (H and h) distortion constants are presented in ref. [134].

For linear molecules, the angular momentum J_z is null. In this case, Watson has shown that the nuclear Hamiltonian in eq. 1.24 becomes[148],

$$\mathcal{H}_{\mathrm{nuc}} = \frac{\hbar^2}{2}\mu\Big[(J_x - \pi_x)^2 + (J_y - \pi_y)^2\Big] + \frac{1}{2}\sum_{i,\gamma} P_{i_\gamma}{}^2 + V \tag{3.8}$$

$\tilde{\mathcal{H}}_{\mathrm{rot}}$ for linear molecules is then given by[30, 102, 108, 134],

$$\tilde{\mathcal{H}}_{\mathrm{rot}} = B^e\left(J_x^2 + J_y^2\right) - D_J\left(J_x^2 + J_y^2\right)^2 + H_J\left(J_x^2 + J_y^2\right)^3 - \ldots \tag{3.9}$$

in which B^e is the equilibrium rotational constant and the explicit formulation of the quartic (D_J) and sextic (H_J) centrifugal distortion constants are given in Refs. [32, 134]. $\tilde{\mathcal{H}}_{\mathrm{rot}}$ is already in a fully reduced form. The rotational energies for linear tops are obtained by replacing $(J_x{}^2 + J_y{}^2)$ with $(\boldsymbol{J}^2 - J_z{}^2)$ and then by their eigenvalues,

$$E_{\mathrm{rot}} = B^e\left[J(J+1) - l^2\right] - D_J\left[J(J+1) - l^2\right]^2 + H_J\left[J(J+1) - l^2\right]^3 \tag{3.10}$$

where J is the total angular momentum quantum number and l the total vibrational angular momentum $l = \sum_s l_s$.

3.2 Vibrational dependence of equilibrium rotational constants

The vibrational dependence of the rotational constants in the quartic approximation is described by,

$$B_\tau^v = B_\tau^e - \sum_i \alpha_{i,\tau}\left(n_i + \frac{d_i}{2}\right) \tag{3.11}$$

where now v indicates a specific vibrational state. The vibrational correction derives from the diagonal matrix elements of $\tilde{\mathcal{H}}_{22}$, specifically by the second-order corrections, considering $\mathcal{H}^{(2)} = \mathcal{H}_{22}$ and $\mathcal{H}^{(1)} = \mathcal{H}_{21} + \mathcal{H}_{30}$. For asymmetric tops, the $\boldsymbol{\alpha}$ constants are given by [30, 32, 108],

$$\alpha_{m,\tau} = -\frac{2\{B_z^e\}^2}{\hbar\omega_m}\left[\sum_\tau \frac{3{a_{m,\eta\varsigma}}^2}{4I_\tau^e} + \sum_n \{\zeta_{mn,\tau}\}^2 \frac{3\lambda_m + \lambda_n}{\lambda_m - \lambda_n} + \sum_n K_{mmn}\frac{a_{n,\tau\tau}}{2\lambda_n}\right] \quad (3.12)$$

Using the symmetry relations for $a_{i,\tau\eta}$ and $\zeta_{i_\gamma j_\epsilon,\tau}$ given in refs.[70, 71] and accounting for the doubly-degenerate normal modes, the α coefficients for linear and symmetric tops are [32],

$$\alpha_{m,z} = -\frac{2\{B_z^e\}^2}{\hbar\omega_m}\left[\frac{3{a_{m,zz}}^2}{4I_z^e} + \sum_n \{\zeta_{mn,z}\}^2 \frac{3\lambda_m + \lambda_n}{\lambda_m - \lambda_n} + \sum_n K_{mmn}\frac{a_{n,zz}}{2\lambda_n}\right] \quad (3.13)$$

$$\alpha_{s,z} = -\frac{2\{B_z^e\}^2}{\hbar\omega_s}\left[\frac{3{a_{s_1,xz}}^2}{4I_x^e} + \sum_t \{\zeta_{st}^{(II)}\}^2 \frac{3\lambda_s + \lambda_t}{\lambda_s - \lambda_t} + \sum_m K_{mss}^{(I)}\frac{a_{m,zz}}{2\lambda_m}\right] \quad (3.14)$$

$$\alpha_{m,x} = -\frac{2\{B_x^e\}^2}{\hbar\omega_m}\left[\frac{3\left({a_{m,xx}}^2 + {a_{m,xy}}^2\right)}{4I_x^e} + \sum_s \left(\{\zeta_{ms}^{(I)}\}^2 + \{\zeta_{ms}^{(II)}\}^2\right)\frac{3\lambda_m + \lambda_s}{\lambda_m - \lambda_s} + \sum_n K_{mmn}\frac{a_{n,xx}}{2\lambda_n}\right] \quad (3.15)$$

$$\alpha_{s,x} = -\frac{2\{B_x^e\}^2}{\hbar\omega_s}\left[\frac{3{a_{s_1,xz}}^2}{8I_e^z} + \frac{3{a_{s_1,xx}}^2}{4I_x^e} + \frac{1}{2}\sum_m \left(\{\zeta_{ms}^{(I)}\}^2 + \{\zeta_{ms}^{(II)}\}^2\right)\frac{3\lambda_s + \lambda_m}{\lambda_s - \lambda_m} + \sum_t \left(\{\zeta_{st}^{(III)}\}^2 + \{\zeta_{st}^{(IV)}\}^2\right)\frac{3\lambda_s + \lambda_t}{\lambda_s - \lambda_t} + \sum_m K_{mss}^{(I)}\frac{a_{m,xx}}{2\lambda_m}\right] \quad (3.16)$$

with $\alpha_{i,x} = \alpha_{i,y}$. The first contribution in eqs. 3.12-3.16 is a corrective term related to the moment of inertia, the second one is due to the Coriolis interactions, and the last is an anharmonic correction. It is noteworthy that the Coriolis coupling term may be affected by resonances. In analogy with vibrational first-order resonance, the strategy that is adopted when a resonance occurs is to expand the Coriolis term and neglect the resonant part, as shown in Appendix D. By contrast, the summed Coriolis coupling term $\sum_i \alpha_{i,\tau} d_i$ is not affected by resonances, as it is possible to write,

$$-\frac{2\{B_\tau^e\}^2}{\omega_i}\sum_j \{\zeta_{ij,\tau}\}^2 \frac{3\lambda_i + \lambda_j}{\lambda_i - \lambda_j} = \frac{\{B_\tau^e\}^2}{\omega_i}\sum_j \frac{\{\zeta_{ij,\tau}\}^2}{\omega_j}\left[\frac{(\omega_i - \omega_j)^2}{\omega_i + \omega_j} - \frac{(\omega_i + \omega_j)^2}{\omega_i - \omega_j}\right] \quad (3.17)$$

Taking as an example the resonance $\omega_m \approx \omega_n$, we have ($d_m = 1$ and $d_n = 1$),

$$\begin{aligned}
\sum_m \alpha_{m,\tau} d_m =& \ldots - 2\{B_\tau^e\}^2 \sum_{m,n} \frac{\{\zeta_{mn,\tau}\}^2}{\omega_m} \frac{3\lambda_m + \lambda_n}{\lambda_m - \lambda_n} \\
& - 2\{B_\tau^e\}^2 \sum_{m,n} \frac{\{\zeta_{nm,\tau}\}^2}{\omega_n} \frac{3\lambda_n + \lambda_m}{\lambda_n - \lambda_m} + \ldots \\
=& \ldots + \{B_\tau^e\}^2 \sum_{m,n} \frac{\{\zeta_{mn,\tau}\}^2}{\omega_m \omega_n} \left[\frac{(\omega_m - \omega_n)^2}{\omega_m + \omega_n} - \frac{(\omega_m + \omega_n)^2}{\omega_m - \omega_n} \right. \\
& \left. + \frac{(\omega_n - \omega_m)^2}{\omega_n + \omega_m} - \frac{(\omega_n + \omega_m)^2}{\omega_n - \omega_m} \right] + \ldots \\
=& \ldots + 2\{B_\tau^e\}^2 \sum_{m,n} \frac{\{\zeta_{mn,\tau}\}^2}{\omega_m \omega_n} \frac{(\omega_m - \omega_n)^2}{\omega_m + \omega_n} + \ldots
\end{aligned} \tag{3.18}$$

Similar simplifications can be applied for $\omega_m \approx \omega_s$ (note that the factor 1/2, which multiplies the Coriolis terms in eq. 3.16, is simplified by $d_s = 2$) and $\omega_s \approx \omega_t$ resonances. Taking these considerations into account, it easy to see that eq. 3.11 for the vibrational ground state is devoid of resonances, i.e. $B_\tau^0 = B_\tau^e - \sum_i \alpha_{i,\tau} d_i/2$.

Chapter 4

Molecular properties

After the presentation of the roto-vibrational energies and rotational constants, we dedicate four sections to the molecular properties.

First, we extend the previous general formalism to the expectation value of an electronic property in a given vibrational state, of interest for the calculation of the vibrational averaged properties for asymmetric tops, as well as, linear and symmetric tops.

Then, focusing on asymmetric top systems, in the second section we treat the molecular polarizability, presenting new equations to deal with the pure vibrational terms, which allow the calculation of the transition probability from any vibrational state. The new formulation is an extension of that present in the literature, which considers only the transition from the vibrational ground state.

In the third section, the new equations are applied to the electric dipole transition moments, of great interest in the calculations of infrared spectrum intensities.

The last section is dedicated to the temperature effects, which can be introduced dealing with both the vibrational averaged properties and the transition moments.

4.1 Vibrational average

As first approximation, a generic electronic property $\boldsymbol{M}$ can be calculated from the electronic wavefunction fixing the nuclei in their equilibrium geometry. However, because of the property change depending on the molecular geometry, to have accurate calculations we can introduce the effect of nuclei vibrations making the vibrational average of the property. It is given by the expectation value of the

property $\boldsymbol{M}$ on the vibrational state $\mid \psi_A \rangle$,

$$\begin{aligned} \langle \boldsymbol{M} \rangle_{A_a} &= \frac{\langle \psi_{A_a} \mid \boldsymbol{M} \mid \psi_{A_a} \rangle}{\langle \psi_{A_a} \mid \psi_{A_a} \rangle} \\ &= \langle \phi^{(0)}_{A_a} \mid \tilde{\boldsymbol{M}} \mid \phi^{(0)}_{A_a} \rangle \end{aligned} \tag{4.1}$$

where $\tilde{\boldsymbol{M}}$ is the property transformed to the basis $\phi = e^{i\mathcal{S}}\psi$ (see eq. 1.41), with the choice $\phi \equiv \phi^{(0)}$ (we recall that $\langle \phi^{(0)}_{A_a} \mid \phi^{(0)}_{A_a} \rangle = 1$). Also called effective property, $\tilde{\boldsymbol{M}} = e^{i\mathcal{S}}\boldsymbol{M}e^{-i\mathcal{S}}$ is then given by (see eqs. 1.43-1.45),

$$\tilde{\boldsymbol{M}}^{(0)} = \boldsymbol{M}^{(0)} \tag{4.2}$$

$$\tilde{\boldsymbol{M}}^{(1)} = \boldsymbol{M}^{(1)} + i\,[\mathcal{S}^{(1)}, \boldsymbol{M}^{(0)}] \tag{4.3}$$

$$\tilde{\boldsymbol{M}}^{(2)} = \boldsymbol{M}^{(2)} + i\,[\mathcal{S}^{(1)}, \boldsymbol{M}^{(1)}] - \frac{1}{2}\,[\mathcal{S}^{(1)}, [\mathcal{S}^{(1)}, \boldsymbol{M}^{(0)}]] + i\,[\mathcal{S}^{(2)}, \boldsymbol{M}^{(0)}] \tag{4.4}$$

where $\mathcal{S}^{(n)}$ are now known from the treatment of $\mathcal{H}$. Generally, $\boldsymbol{M}$ is a function of the total angular momentum as well as the normal coordinates and momenta. In terms of fg-subscripts notation introduced in Section 1.5, the expansion of $\boldsymbol{M}$ can be written as [108],

$$\boldsymbol{M} = \boldsymbol{M}_{01} + \boldsymbol{M}_{11} + \boldsymbol{M}_{21} + \ldots \tag{4.5}$$

Focusing here on the vibrational part, we can identify as perturbation orders $\mathcal{H}^{(1)} = \mathcal{H}_{30}$, $\mathcal{H}^{(2)} = \mathcal{H}_{40}$ for the Hamiltonian and $\boldsymbol{M}^{(0)} = \boldsymbol{M}_{00}$, $\boldsymbol{M}^{(1)} = \boldsymbol{M}_{10}$ and $\boldsymbol{M}^{(2)} = \boldsymbol{M}_{20}$ for the property, where,

$$\boldsymbol{M}_{00} = \boldsymbol{M}^{e} \tag{4.6}$$

$$\boldsymbol{M}_{10} = \sum_{i}\sum_{\gamma} \boldsymbol{M}_{i_\gamma} Q_{i_\gamma} \tag{4.7}$$

$$\boldsymbol{M}_{20} = \frac{1}{2}\sum_{i,j}\sum_{\gamma,\epsilon} \boldsymbol{M}_{i_\gamma j_\epsilon} Q_{i_\gamma} Q_{j_\epsilon} \tag{4.8}$$

$\boldsymbol{M}^e$ is the property at the equilibrium position of the nuclei,

$$\boldsymbol{M}_{i_\gamma} = \frac{\partial \boldsymbol{M}}{\partial Q_\gamma} \qquad \text{and,} \qquad \boldsymbol{M}_{i_\gamma j_\epsilon} = \frac{\partial^2 \boldsymbol{M}}{\partial Q_{i_\gamma} Q_{j_\epsilon}} \tag{4.9}$$

By eqs. 4.2-4.4, we can find that,

$$\langle \tilde{\boldsymbol{M}}_{00} \rangle_{A_a} = \boldsymbol{M}^e \tag{4.10}$$

$$\langle \tilde{\boldsymbol{M}}_{10} \rangle_{A_a} = 0 \tag{4.11}$$

$$\begin{aligned}\langle \tilde{\boldsymbol{M}}_{20} \rangle_{A_a} =& \frac{1}{2}\sum_m \frac{\boldsymbol{M}_{mm}}{\sqrt{\lambda_m}}\left(n_m+\frac{1}{2}\right)+\frac{1}{2}\sum_s \frac{\boldsymbol{M}_{s_1s_1}+\boldsymbol{M}_{s_2s_2}}{\sqrt{\lambda_s}}\left(n_s+1\right) \\ &-\frac{1}{2}\sum_m\sum_n \frac{K_{mnn}\boldsymbol{M}_m}{\lambda_m\sqrt{\lambda_n}}\left(n_n+\frac{1}{2}\right)-\frac{1}{2}\sum_m\sum_s \frac{K^{(I)}_{mss}\boldsymbol{M}_m}{\lambda_m\sqrt{\lambda_s}}\left(n_s+1\right)\end{aligned} \tag{4.12}$$

where, differently from the cubic and quartic force treatment, we have not introduced any symmetry relation between the property derivatives, with the aim of having fully general expressions. It is noteworthy that, similar to the energy up to second order, both CT and RS formulations lead to the same result (see Appendix F).

If no resonances or doublings occur, the sum of the terms in eqs. 4.10-4.12 is then the expression for the averaged property up to second perturbative order. It is easy to see that eq. 4.12 does not contain possibly resonant terms. Despite this, if $|\,\phi^{(0)}_{A_a}\rangle$ is one of the n states involved in a polyad, within the GVPT2 formulation it will be variationally combined with all the others to originate n new states. The latter states will be the combinations given by the eigenvectors of the polyad having the polyad's eigenvalues as energies [108].
As an example, if the two states $|\phi_{A_a}\rangle$ and $|\phi_{A_b}\rangle$ interact by a l-doubling interaction element (see eqs. 2.31-2.33), they will form a 2-dimensional polyad and, after the variational diagonalization, we will have the two new states $|\,\phi_{A'_a}\,\rangle$ and $|\,\phi_{A'_b}\,\rangle$. Then,

$$\begin{aligned}\langle \tilde{\boldsymbol{M}}_{20} \rangle_{A'_a} =& c_{11}^2\langle\,\phi_{A_a}\mid\tilde{\boldsymbol{M}}_{20}\mid\phi_{A_a}\,\rangle + c_{11}c_{12}\langle\,\phi_{A_a}\mid\tilde{\boldsymbol{M}}_{20}\mid\phi_{A_b}\,\rangle \\ &+ c_{21}c_{11}\langle\,\phi_{A_b}\mid\tilde{\boldsymbol{M}}_{20}\mid\phi_{A_a}\,\rangle + c_{12}^2\langle\,\phi_{A_b}\mid\tilde{\boldsymbol{M}}_{20}\mid\phi_{A_b}\,\rangle\end{aligned} \tag{4.13}$$

with a similar expression for $|\,\phi_{A'_b}\,\rangle$, where c_{ij} are the elements of the polyad's eigenvectors. It is of interest to note that the off-diagonal elements $\langle\, n_s, l_s \mid \tilde{\boldsymbol{M}}_{20} \mid n_s, (l_s+4)\,\rangle$, $\langle\, n_sn_t, l_sl_t \mid \tilde{\boldsymbol{M}}_{20} \mid n_sn_t, (l_s\pm2)_s(l_t\mp2)_t\,\rangle$ and $\langle\, n_sn_t, l_sl_t \mid \tilde{\boldsymbol{M}}_{20} \mid n_sn_t, (l_s\pm2)_s(l_t\pm2)_t\,\rangle$ are all zero, which simplifies the above expression.

4.2 Vibrational polarizability

When a molecule is placed in an static and/or dynamic electric field both electronic and vibrational motions change to allow the redistribution of both the

electrons and the nucleus that gives the smallest field-dependent energy. The molecule exhibits a polarization, and the measure of this polarization is called polarizability.

Within the BO approximation, the molecular polarizability $\boldsymbol{\alpha}$ (both static and frequency-dependent) in a given non-degenerate vibrational state $\mid \psi_A \rangle$ can be written as [89, 90, 96, 149–151]:

$$\boldsymbol{\alpha} = \langle\, \boldsymbol{\alpha} \,\rangle_A + \boldsymbol{\alpha}_A^{\mathrm{pv}} \tag{4.14}$$

where $\langle\, \boldsymbol{\alpha} \,\rangle_A = \boldsymbol{\alpha}^e + \langle\, \tilde{\boldsymbol{\alpha}}_{20} \,\rangle_A$ is the vibrational averaged polarizability up to second perturbative order, with $\boldsymbol{\alpha}^e$ the electronic polarizability of the molecule at the equilibrium geometry and $\langle\, \tilde{\boldsymbol{\alpha}}_{20} \,\rangle_A$ given by eq. 4.12, and $\boldsymbol{\alpha}_A^{\mathrm{pv}}$ is the so-called pure vibrational polarizability. The latter term represents the vibrational response to the external perturbation, and can be expressed as [96, 150],

$$\{\alpha_{\tau,\eta}\}_A^{\mathrm{pv}} = \frac{2}{\hbar} \sum_{B \neq A} \Omega[\Delta] \frac{\langle\, \psi_A \mid \mu_\tau \mid \psi_B \,\rangle \langle\, \psi_B \mid \mu_\eta \mid \psi_A \,\rangle}{\langle\, \psi_A \mid \psi_A \,\rangle \langle\, \psi_B \mid \psi_B \,\rangle} \tag{4.15}$$

where $\Omega[\Delta] = \Delta/(\Delta^2 - \nu_{\mathrm{ext}})$, $\Delta = (E_B - E_A)$ and ν_{ext} is the frequency of the external electric field. μ is the electric dipole moment. It is clear from this expression that, as ν_{ext} increases, the pure vibrational contribution goes to zero. It is therefore expected to be negligible in the case of light in the UV-visible range of the spectrum. This term can instead be significant in the case of the static polarizability (i.e. $\nu_{\mathrm{ext}} = 0$).

Eq. 4.15 can be treated by perturbation theory in a similar way as for the vibrational averaged term, where now the dipole moment is expressed by,

$$\mu_\tau = \mu_\tau^{(0)} + \mu_\tau^{(1)} + \mu_\tau^{(2)} + \dots \tag{4.16}$$

where,

$$\mu_\tau^{(0)} = \mu_\tau^e + \sum_m \mu_{m,\tau} Q_i \tag{4.17}$$

$$\mu_\tau^{(1)} = \frac{1}{2} \sum_{m,n} \mu_{mn,\tau} Q_m Q_n \tag{4.18}$$

$$\mu_\tau^{(2)} = \frac{1}{6} \sum_{m,n,o} \mu_{mno,\tau} Q_m Q_n Q_o \tag{4.19}$$

$\mu_{m,\tau}$, $\mu_{mn,\tau}$, $\mu_{mno,\tau}$ are respectively the first, second and third derivatives of the electric dipole moment with respect to the normal coordinates, and μ_τ^e the dipole moment at the equilibrium geometry. Up to second perturbative order, the total

value of $\alpha^{\rm pv}$ is usually separated into an harmonic term and three anharmonic contributions, which are distinguished according to their degree of mechanical (i.e., contributions from higher-order terms in the wavefunction expansion in RS representation, right index) and electric (i.e. contributions from higher-order terms in the electronic property expansions) anharmonicity,

$$\alpha^{\rm pv} = [\mu^2]^{0,0} + [\mu^2]^{2,0} + [\mu^2]^{1,1} + [\mu^2]^{0,2} \tag{4.20}$$

A formulation for the last terms is present in the literature for the specific case of $|\,\psi_A\,\rangle$ equal to the vibrational ground state [96]. Focusing on asymmetric top systems, we present here the generalization of the previous expressions for a generic vibrational state,

$$[\mu^2]^{0,0}_{\tau,\eta} = \sum_m \frac{\mu_{m,\tau}\mu_{m,\eta}}{\sqrt{\lambda_m}} \left[\Omega[\nu(+1)_m](n_m+1) + \Omega[\nu(-1)_m] n_m \right] \tag{4.21}$$

$$\begin{aligned}
[\mu^2]^{2,0}_{\tau,\eta} =& \hbar \sum_m \Bigg\{ \frac{\mu_{mm,\tau}\mu_{mm,\eta}}{8\lambda_m} \left[\Omega[\nu(+2)_m](n_m+2)(n_m+1) + \Omega[\nu(-2)_m] n_m(n_m-1) \right] \\
& - \frac{(\mu_{mmm,\tau}\mu_{m,\eta} + \mu_{m,\tau}\mu_{mmm,\eta})}{4\lambda_m} \Bigg[\Omega[\nu(+1)_m] n_m(n_m+1) \\
& + \Omega[\nu(-1)_m] n_m(n_m+1) \Bigg] \Bigg\} \\
& + \hbar \sum_{m,n} \Bigg\{ \frac{(\mu_{mnn,\tau}\mu_{m,\eta} + \mu_{m,\tau}\mu_{mnn,\eta})}{4\sqrt{\lambda_m\lambda_n}} \Bigg[\Omega[\nu(+1)_m](n_m+1)(2n_n+1) \\
& + \Omega[\nu(-1)_m] n_m(2n_n+1) \Bigg] \Bigg\} \\
& + \hbar \sum_{m\neq n} \Bigg\{ \frac{\mu_{mn,\tau}\mu_{mn,\eta}}{4\sqrt{\lambda_m\lambda_n}} \Bigg[\Omega[\nu(+1)_m(+1)_n](n_m+1)(n_n+1) \\
& + 2\Omega[\nu(+1)_m(-1)_n](n_m+1)n_n + \Omega[\nu(-1)_m(-1)_n] n_m n_n \Bigg] \Bigg\}
\end{aligned} \tag{4.22}$$

$$
\begin{aligned}
[\mu^2]^{1,1}_{\tau,\eta} =& \hbar \sum_{m,n} \Bigg\{ \frac{(\mu_{mm,\tau}\mu_{n,\eta} + \mu_{n,\tau}\mu_{mm,\eta})\, K_{mmn}}{8\lambda_m(4\lambda_m - \lambda_n)} \Bigg[\Omega[\nu(+2)_m](n_m+2)(n_m+1) \\
& \qquad + \Omega[\nu(-2)_m] n_m(n_m-1) \Bigg] \\
& + \frac{(\mu_{mn,\tau}\mu_{m,\eta} + \mu_{m,\tau}\mu_{mn,\eta})\, K_{mmn}\,(8\lambda_m - 3\lambda_n)}{4\lambda_m\lambda_n(4\lambda_m - \lambda_n)} \Bigg[\Omega[\nu(+1)_m] n_m(n_m+1) \\
& \qquad + \Omega[\nu(-1)_m] n_m(n_m+1) \Bigg] \Bigg\} \\
& + \hbar \sum_{m,n,o} \Bigg\{ \Bigg[\frac{(\mu_{no,\tau}\mu_{m,\eta} + \mu_{m,\tau}\mu_{no,\eta})\, K_{mno}(\lambda_m - \lambda_n + \lambda_o)}{2\sqrt{\lambda_m\lambda_o}\Delta_{mno}} \\
& \qquad - \frac{(\mu_{mn,\tau}\mu_{m,\eta} + \mu_{m,\tau}\mu_{mn,\eta})\, K_{noo}}{4\lambda_n\sqrt{\lambda_m\lambda_o}} \Bigg] \\
& \qquad \times \Big[\Omega[\nu(+1)_m](n_m+1)(2n_o+1) + \Omega[\nu(-1)_m] n_m(2n_o+1) \Big] \Bigg\} \\
& + \hbar \sum_{m\neq n} \sum_{o} \Bigg\{ \frac{(\mu_{mn,\tau}\mu_{o,\eta} + \mu_{o,\tau}\mu_{mn,\eta})\, K_{mno}}{4\sqrt{\lambda_m\lambda_n}(\sqrt{\lambda_m} + \sqrt{\lambda_n} + \sqrt{\lambda_o})(\sqrt{\lambda}_m + \sqrt{\lambda}_n - \sqrt{\lambda}_o)} \\
& \qquad \times \Big[\Omega[\nu(+1)_m(+1)_n](n_m+1)(n_n+1) + \Omega[\nu(-1)_m(-1)_n] n_m n_n \Big] \\
& \qquad + \frac{(\mu_{mn,\tau}\mu_{o,\eta} + \mu_{o,\tau}\mu_{mn,\eta})\, K_{mno}}{2\sqrt{\lambda_m\lambda_n}(\sqrt{\lambda}_m - \sqrt{\lambda}_n - \sqrt{\lambda}_o)(\sqrt{\lambda}_m - \sqrt{\lambda}_n + \sqrt{\lambda}_o)} \\
& \qquad \times \Big[\Omega[\nu(+1)_m(-1)_n](n_m+1) n_n \Big] \Bigg\} \qquad (4.23)
\end{aligned}
$$

$$
\begin{aligned}
[\mu^2]^{0,2}_{\tau,\eta} =& \hbar \sum_m \left\{ -\frac{\mu_{m,\tau}\mu_{m,\eta}K_{mmmm}}{8\lambda_m^2} \left[\Omega[\nu(+1)_m](n_m+1)^2 + \Omega[\nu(-1)_m]n_m^2 \right] \right\} \\
&+ \hbar \sum_{m\neq n} \left\{ -\frac{\mu_{m,\tau}\mu_{m,\eta}K_{mmnn}}{8\lambda_m\sqrt{\lambda_m\lambda_n}} \left[\Omega[\nu(+1)_m](n_m+1)(2n_n+1) \right.\right. \\
&\qquad \left.\left. + \Omega[\nu(-1)_m]n_m(2n_n+1) \right] \right. \\
&\quad \left. - \frac{(\mu_{m,\tau}\mu_{n,\eta}+\mu_{n,\tau}\mu_{m,\eta})\,K_{mmmn}}{4\lambda_m(\lambda_m-\lambda_n)} \left[\Omega[\nu(+1)_m]n_m(n_m+1) \right.\right. \\
&\qquad \left.\left. + \Omega[\nu(-1)_m]n_m(n_m+1) \right] \right\} \\
&+ \hbar \sum_{m\neq n}\sum_o \left\{ \frac{(\mu_{m,\tau}\mu_{n,\eta}+\mu_{n,\tau}\mu_{m,\eta})\,K_{mnoo}}{4\sqrt{\lambda_m\lambda_o}(\lambda_m-\lambda_n)} \left[\Omega[\nu(+1)_m](n_m+1)(2n_o+1) \right.\right. \\
&\qquad \left.\left. + \Omega[\nu(-1)_m]n_m(2n_o+1) \right] \right\} \\
&+ \hbar \sum_{m,n} \left\{ -\frac{\mu_{m,\tau}\mu_{m,\eta}K^2_{mmn}(32\lambda_m^2-24\lambda_m\lambda_n+3\lambda_n^2)}{8\lambda_m^2\lambda_n(4\lambda_m-\lambda_n)^2} \left[\Omega[\nu(+1)_m]n_m(n_m+1) \right.\right. \\
&\qquad \left.\left. + \Omega[\nu(-1)_m]n_m(n_m+1) \right] \right\} \\
&+ \hbar \sum_{m,n,o} \left\{ \frac{(\mu_{n,\tau}\mu_{o,\eta}+\mu_{o,\tau}\mu_{n,\eta})\,K_{mmn}K_{mmo}}{16\lambda_m(4\lambda_m-\lambda_n)(4\lambda_m-\lambda_o)} \left[\Omega[\nu(+2)_m](n_m+2)(n_m+1) \right.\right. \\
&\qquad \left.\left. + \Omega[\nu(-2)_m]n_m(n_m-1) \right] \right. \\
&\quad + \frac{\mu_{m,\tau}\mu_{m,\eta}}{\lambda_m\sqrt{\lambda_m\lambda_o}} \left[\frac{K_{mmn}K_{noo}}{8\lambda_n} - \frac{K^2_{mno}(\lambda_m-\lambda_n)^2(3\lambda_m-\lambda_n)}{4\Delta^2_{mno}} \right. \\
&\qquad \left. + \frac{K^2_{mno}\left[(3\lambda_m^2+2\lambda_m\lambda_n+3\lambda_n^2)\lambda_o^2-(7\lambda_m+3\lambda_n)\lambda_o^2+\lambda_o^3\right]}{4\Delta^2_{mno}} \right] \\
&\qquad \left. \times \left[\Omega[\nu(+1)_m](n_m+1)(2n_o+1) + \Omega[\nu(-1)_m]n_m(2n_o+1) \right] \right\}
\end{aligned}
$$

$$
\begin{aligned}
&+\hbar\sum_{m\neq n}\sum_{o}\Bigg\{\frac{\left(\mu_{m,\tau}\mu_{n,\eta}+\mu_{n,\tau}\mu_{m,\eta}\right)K_{mmo}K_{mno}\left(8\lambda_m-3\lambda_o\right)}{4\lambda_m\lambda_o(\lambda_m-\lambda_n)(4\lambda_m-\lambda_o)}\\
&\qquad\times\left[\Omega[\nu(+1)_m]n_m(n_m+1)+\Omega[\nu(-1)_m]n_m(n_m+1)\right]\Bigg\}\\
&+\hbar\sum_{m\neq n}\sum_{o,p}\Bigg\{\frac{\left(\mu_{m,\tau}\mu_{n,\eta}+\mu_{n,\tau}\mu_{m,\eta}\right)}{\sqrt{\lambda_m\lambda_p}(\lambda_m-\lambda_n)}\left[\frac{K_{mop}K_{nop}\left(\lambda_m-\lambda_o+\lambda_p\right)}{2\Delta_{mop}}-\frac{K_{mno}K_{opp}}{4\lambda_o}\right]\\
&\qquad\times\left[\Omega[\nu(+1)_m](n_m+1)(2n_p+1)+\Omega[\nu(-1)_m]n_m(2n_p+1)\right]\\
&\quad+\frac{\left(\mu_{p,\tau}\mu_{o,\eta}+\mu_{o,\tau}\mu_{p,\eta}\right)K_{mno}K_{mnp}}{8\sqrt{\lambda_m\lambda_n}(\sqrt{\lambda_m}+\sqrt{\lambda_n}+\sqrt{\lambda_o})(\sqrt{\lambda_m}+\sqrt{\lambda_n}-\sqrt{\lambda_o})}\\
&\qquad\times\frac{1}{(\sqrt{\lambda_m}+\sqrt{\lambda_n}+\sqrt{\lambda_p})(\sqrt{\lambda_m}+\sqrt{\lambda_n}-\sqrt{\lambda_p})}\\
&\qquad\times\left[\Omega[\nu(+1)_m(+1)_n](n_m+1)(n_n+1)+\Omega[\nu(-1)_m(-1)_n]n_mn_n\right]\\
&\quad+\frac{\left(\mu_{p,\tau}\mu_{o,\eta}+\mu_{o,\tau}\mu_{p,\eta}\right)K_{mno}K_{mnp}}{4\sqrt{\lambda_m\lambda_n}(\sqrt{\lambda_m}-\sqrt{\lambda_n}+\sqrt{\lambda_o})(\sqrt{\lambda_m}-\sqrt{\lambda_n}-\sqrt{\lambda_o})}\\
&\qquad\times\frac{1}{(\sqrt{\lambda_m}-\sqrt{\lambda_n}+\sqrt{\lambda_p})(\sqrt{\lambda_m}-\sqrt{\lambda_n}-\sqrt{\lambda_p})}\\
&\qquad\times\left[\Omega[\nu(+1)_m(-1)_n](n_m+1)n_n\right]\Bigg\}\\
&+\frac{1}{\hbar}\sum_{\tau}\sum_{m,n,o}\Bigg\{\frac{B^e_\tau(\mu_{m,\tau}\mu_{o,\eta}+\mu_{m,\tau}\mu_{o,\eta})\zeta_{mn,\tau}\zeta_{no,\tau}}{2\sqrt{\lambda_m\lambda_o}}\\
&\qquad\times\Bigg[\sqrt{\frac{\lambda_n}{\sqrt{\lambda_m\lambda_o}}}\left(\frac{1}{\sqrt{\lambda_m}+\sqrt{\lambda_o}}-\frac{1-\delta_{mo}}{\sqrt{\lambda_m}-\sqrt{\lambda_o}}\right)\\
&\qquad\quad-\sqrt{\frac{\sqrt{\lambda_m\lambda_o}}{\lambda_n}}\left(\frac{1}{\sqrt{\lambda_m}+\sqrt{\lambda_o}}+\frac{1-\delta_{mo}}{\sqrt{\lambda_m}-\sqrt{\lambda_o}}\right)\Bigg]\\
&\qquad\times\left[\Omega[\nu(+1)_m](n_m+1)(2n_n+1)+\Omega[\nu(-1)_m]n_m(2n_n+1)\right]\Bigg\}
\end{aligned}
\tag{4.24}
$$

4.3 Electric dipole transition moments

It can be shown that the infra-red (IR) intensity of any vibrational transition from a given non-degenerate vibrational state $\mid \psi_A \rangle$ is proportional to [33, 97],

$$I_A(\nu_{\text{ext}}) \propto \sum_{\tau} \sum_{B \neq A} \Omega[\Delta] \frac{\langle \psi_A \mid \mu_\tau \mid \psi_B \rangle \langle \psi_B \mid \mu_\tau \mid \psi_A \rangle}{\langle \psi_A \mid \psi_A \rangle \langle \psi_B \mid \psi_B \rangle} \tag{4.25}$$

where $\Omega[\Delta] = \Delta/(\Delta^2 - \nu_{\text{ext}})$, $\Delta = (E_B - E_A)$ and ν_{ext} is the frequency of the external electric field. Comparing the previous expression with eq. 4.15, it easy to see that the intensity is proportional to the sum of the terms given by eqs. 4.21-4.24, where now $\eta = \tau$. For example, the harmonic contributions due to the vibrational normal mode m to the absorption and emission intensity are respectively proportional to,

$$\sum_{\tau} \frac{\mu_{m,\tau}^2}{\sqrt{\lambda_m}}(n_m + 1) \qquad \text{and,} \qquad \sum_{\tau} \frac{\mu_{m,\tau}^2}{\sqrt{\lambda_m}} n_m \tag{4.26}$$

where n_m is the vibrational quantum number of the mode m in the $|\psi_A\rangle$ vibrational state.

Observing the terms appearing in eqs. 4.21-4.24, it is noteworthy that handling $[\mu]^2$ up to the second perturbative order means to allow transition simultaneously involving at most two vibrational quanta. There is an alternative way to obtain the VPT2 IR intensities: instead of applying the perturbative development on the complete formulation of the transition property in eq. 4.25, one can first compute the anharmonic transition dipole moment $\langle \psi_A \mid \mu_\tau \mid \psi_B \rangle$ and then square the result to obtain the intensity [97, 98]. This leads to slightly different expressions, because of the inclusion of higher order perturbative terms when the transition property is squared. However, high order perturbative corrections are expected to be small, therefore there should be very little numerical difference between the two methods. In the last approach, the intensities for excitations involving more then two vibrational quanta can be also non null. Such an example, the intensities for excitations involving three vibrational quanta on mode m are proportional to the square of,

$$\begin{aligned} \langle n_m \mid \mu_\tau \mid n_m + 3 \rangle = & \frac{\hbar^{1/2}\sqrt{(n_m+1)(n_m+2)(n_m+3)}}{\lambda_m^{3/2}\sqrt{2}} \\ & \times \left\{ \frac{\mu_{mmm,\tau}}{12} + \sum_n \left[\frac{K_{mmmn}\mu_n}{24(9\lambda_m - \lambda_n)} + \frac{K_{mmn}\mu_{mn,\tau}}{8(4\lambda_m - \lambda_n)} \right.\right. \\ & \left.\left. + \sum_o \frac{K_{mmo}K_{mno}\mu_{n,\tau}}{4(9\lambda_m - \lambda_n)(4\lambda_m - \lambda_o)} \right] \right\} \end{aligned} \tag{4.27}$$

4.4 Temperature effects

Temperature effects can be taken into account for both vibrational averaged and pure vibrational property, as well as for electric dipole transition moments, explicitly by summing the contributions over all vibrational states, each weighted by its Boltzmann population.
Remembering the vibrational partition function in eq. 2.67, we can write down,

$$\frac{\sum_\nu D_\nu e^{-\beta E_\nu(\boldsymbol{n})}}{Q_{\text{vib}}^{(H)}} = 1 \tag{4.28}$$

$$\begin{aligned}\frac{\sum_\nu D_\nu e^{-\beta E_\nu(\boldsymbol{n})}}{Q_{\text{vib}}^{(H)}} n_m &= \frac{\prod_i \left(1-e^{-\beta\omega_i}\right)^{d_i} e^{-\beta\omega_m}}{\prod_{i\neq m}\left(1-e^{-\beta\omega_i}\right)^{d_i}\left(1-e^{-\beta\omega_m}\right)^2} \\ &= \frac{e^{-\beta\omega_m}}{(1-e^{-\beta\omega_m})}\end{aligned} \tag{4.29}$$

$$\begin{aligned}\frac{\sum_\nu D_\nu e^{-\beta E_\nu(\boldsymbol{n})}}{Q_{\text{vib}}^{(H)}} n_s &= -\frac{\prod_i \left(1-e^{-\beta\omega_i}\right)^{d_i} 2e^{-\beta\omega_s}}{\prod_{i\neq s}\left(1-e^{-\beta\omega_i}\right)^{d_i}\left(e^{-\beta\omega_m}-1\right)^3} \\ &= \frac{2e^{-\beta\omega_s}}{(1-e^{-\beta\omega_s})}\end{aligned} \tag{4.30}$$

$$\begin{aligned}\frac{\sum_\nu D_\nu e^{-\beta E_\nu(\boldsymbol{n})}}{Q_{\text{vib}}^{(H)}} n_m^2 &= -\frac{\prod_i \left(1-e^{-\beta\omega_i}\right)^{d_i} e^{-\beta\omega_m}(1+e^{-\beta\omega_m})}{\prod_{i\neq m}\left(1-e^{-\beta\omega_i}\right)^{d_i}\left(e^{-\beta\omega_m}-1\right)^3} \\ &= \frac{e^{-\beta\omega_m}(1+e^{-\beta\omega_m})}{\left(1-e^{-\beta\omega_m}\right)^2}\end{aligned} \tag{4.31}$$

$$\frac{\sum_\nu D_\nu e^{-\beta E_\nu(\boldsymbol{n})}}{Q_{\text{vib}}^{(H)}} n_m n_n = \frac{e^{-\beta\omega_m}}{(1-e^{-\beta\omega_m})}\frac{e^{-\beta\omega_n}}{(1-e^{-\beta\omega_n})} \tag{4.32}$$

where the summations in the left-hand sides is on all possible vibrational states ν, and we have used the relations $\sum_{n=0}^{\infty} nq^n = q/(1-q)^2$, $\sum_{n=0}^{\infty} n(n+1)q^n = -2q/(q-1)^3$ and $\sum_{n=0}^{\infty} n^2 q^n = -q(q+1)/(q-1)^3$ when $|q| < 1$.
These terms can be introduced into the equations 4.12 and 4.21-4.24 in place of the quantum numbers to obtain the temperature-dependent vibrational averages

and transitions. For example, for $[\mu^2]^{2,0}_{\tau,\eta}$ we will have,

$$\begin{aligned}[\mu^2]^{0,0}_{\tau,\eta}(T) &= \sum_m \frac{\mu_{m,\tau}\mu_{m,\eta}}{\sqrt{\lambda_m}}\left[\Omega[\nu(+1)_m]\left(\frac{e^{-\beta\omega_m}}{1-e^{-\beta\omega_m}}+1\right)+\Omega[\nu(-1)_m]\frac{e^{-\beta\omega_m}}{1-e^{-\beta\omega_m}}\right] \\ &= \sum_m \frac{\mu_{m,\tau}\mu_{m,\eta}}{\sqrt{\lambda_m}}\left[\Omega[\nu(+1)_m]\frac{1}{1-e^{-\beta\omega_m}}+\Omega[\nu(-1)_m]\frac{e^{-\beta\omega_m}}{1-e^{-\beta\omega_m}}\right]\end{aligned} \tag{4.33}$$

Note that if we assume $\nu(+1)_m = -\nu(-1)_m$, the double-harmonic term becomes temperature-independent.
Finally, in the treatment of the partition function it is possible to account for the anharmonicity substituting the harmonic frequencies in the equations 4.29-4.32 with their anharmonic counterparts (see SPT in section 2.5). For example,

$$\frac{e^{-\beta\omega_m}}{(1-e^{-\beta\omega_m})} \quad \xrightarrow{\text{SPT}} \quad \frac{e^{-\beta\nu_m}}{(1-e^{-\beta\nu_m})} \tag{4.34}$$

where ν_m stands for $\nu(1)_m$.

Part II

Applications

Experience is a brutal teacher, but
you learn. My God, do you learn.

C.S. Lewis
1898-1963

In the previous chapters we have shown the equations of roto-vibrational energies and spectroscopic constants issuing from a perturbative treatment of the molecular Hamiltonian. This formulation can be used in three different ways.

On an experimental level, once we have an effective Hamiltonian for a given vibrational state (or for a polyad of such states), we can attempt to determine the values of the spectroscopic constants by fitting them to the experimental frequencies of transitions between the rotation-vibration states [2, 21]. Such fitting means that we try to obtain the values of the spectroscopic constants that provide the best agreement with the experimental data. On the other hand, we can attempt to evaluate the spectroscopic quantities from a fully quantum mechanical approach [3, 5]. To do this, we need a molecular equilibrium geometry together with a set of second, third and semi-diagonal fourth energy derivatives with respect to normal modes. The corresponding derivatives of properties (up to the third order) are needed for evaluating vibrationally averaged observables or intensities (dipole moment for infrared, polarizability for Raman, etc.). All these quantities can be computed by current electronic structure codes at different levels of sophistication.

Hartree-Fock (HF) [152], density functional theory (DFT) [153], and second-order Møller-Plesset theory (MP2) [154, 155] models will be employed in the present work, but also other post-HF models (e.g. multi-configurational self-Consistent field (MCSCF) [113, 156], coupled cluster (CC) [157, 158], etc.) could be used. In this frame, the expressions derived in the first sections can be used to reproduce and/or to predict the experimentally observed results. Finally, in the so-called semi-experimental (SE) approach the experimental data are handled with theoretical corrections to assess the physical quantities of interest.

In this work we will consider the latter two approaches. First, we will focus our attention to the problem of the determination of accurate molecular structures avoiding high-level expensive computations, with the aim of making feasible the

treatment of systems of increasing size and complexity. Then we will treat the vibrational energies and thermodynamic quantities of different molecules, validating our developments and pointing out the feasibility and the limitations of the VPT approach in reproducing the experimental results.

Chapter 5

Accurate equilibrium geometries

The last decades have seen many efforts to determine accurate molecular structures for systems of increasing size and complexity [6, 21, 159–170]. Detailed knowledge of the equilibrium structures of isolated molecular systems of chemical, biological or technological interest is indeed a prerequisite for a deeper understanding of other physical-chemical properties, ranging from a precise evaluation of the electronic structure to the understanding and analysis of the dynamical and environmental effects affecting the molecular structures and properties [2, 4–6, 159]. Moreover, the availability of reference molecular structures allows one to test the accuracy of different quantum mechanical (QM) approaches [6, 171–175], and it is essential for a correct development of accurate force fields either of general applicability (e.g. for systems of biological interest) [176–179] or specifically tailored for individual systems [180–183]. Furthermore, robust and reliable computational approaches are of primary importance for conformational analysis and modeling of drugs and biomolecules[171, 184], as well as for a deeper understanding of chemical reactivity in terms of transition state structures[185], which are not directly determinable from experiment. For a fruitful interplay of experiment and theory in the interpretation and quantification of molecular properties, and for validation purposes, it is hence desirable to have a large number of accurate equilibrium geometries at one's disposal.

Nowadays, an increasing number of experimental data is available thanks to the growing interest in the field, but the structural parameters derived from experiment often depend on the chosen technique and can be biased by vibration and/or environmental conditions [5, 6]. For example, the vibrationally averaged r_0 and substitution r_s structures are obtained from microwave and/or rotationally resolved infrared investigations through the analysis of the vibrational ground-state rotational constants for different isotopologues, but without an explicit consideration of vibrational effects [186]. The dependence of the results on experimental

conditions complicates both the comparison of structures obtained with different experimental techniques and the subsequent use of these empirical structures in the computation of molecular properties. In addition, all vibrationally averaged structures (r_0, r_s, $r_{\alpha,T}$, $r_{g,T}$, etc.) depend on the isotopic species considered [186, 187].

A way to avoid all these problems is to resort to equilibrium configuration structures (usually referred to as r_e) at the minimum of the PES in BO approximation. Although they are cumbersome to derive experimentally, and therefore generally available only for small molecules, these kind of structures are preferred as they exclude vibrational effects in a rigorous manner and are independent of the considered isotopic species. Moreover, depending solely on the electronic structure of the molecular system, r_e structures are directly comparable with the results from QM calculations.

Reference equilibrium structures can be obtained from high-level QM calculations, for instance making use of the CC singles and doubles approximation augmented by a perturbative treatment of triple excitations, CCSD(T) [158], which is able to provide accurate structures, rivaling the best experimental results, provided that extrapolation to the complete basis-set limit and core correlation are taken into proper account (see, for example, refs. [188–190]). However, for medium-sized molecular systems such computations are still very challenging, due to the unfavorable scaling of highly correlated levels of theory with the number of basis functions.

An important step forward in this field has been provided by the introduction of the so-called semi-experimental equilibrium geometry (hereafter r_e^{SE}), which is obtained by a least-squares fit of experimental rotational constants of different isotopologues corrected by computed vibrational contributions [6, 159, 191]. Introduced by Pulay *et al.*[191], this method is nowadays considered the best approach to determine accurate equilibrium structures for isolated molecules [192]. Such an interplay of theory and experiment paves the route toward the extension of accurate structural studies to systems larger than those treatable by experimental and QM methods separately.

From a computational point of view, the bottleneck of the SE protocol is the calculation of the cubic force field at a level of theory sufficiently accurate to give reliable vibrational corrections to rotational constants [192]. Actually, CCSD(T) is considered the gold standard for this kind of determination, but the computational cost restricts its applicability to systems of less than 10 atoms (see for example refs. [193–195]). Such a limitation needs to be overcome in order to set up a database of accurate molecular geometries to be used as references for benchmark QM calculations as well as for the validation of simpler models for larger systems, with special focus on biomolecule building blocks. Therefore, the setup and val-

idation of a SE approach able to combine high accuracy and low computational cost is of great interest.

In this view, we carried out a systematic study to demonstrate that the calculation of vibrational corrections from anharmonic force fields evaluated using the DFT permits to obtain r_e^{SE} structures that agree well with the best equilibrium geometries reported in the literature, but with a significantly reduced computational effort [196]. In previous studies, we showed that the B3LYP hybrid functional performs remarkably well for vibrational properties, when coupled to basis sets of at least polarized double-ζ quality including diffuse functions (in particular the SNSD basis set) [53, 197–199]. Moreover, despite the fact that the inclusion of a portion of the MP2 [154] energy leads to a significantly higher computational cost with respect to B3LYP computations, the double-hybrid B2PLYP functional [200], coupled with the cc-pVTZ basis set [201–204], has shown to provide very accurate harmonic frequencies and anharmonic corrections [190, 205]. On these grounds, all DFT computations have been performed at the B3LYP and B2PLYP levels.

After the presentation of the computational details, we dedicate a section to the validation study performed on 21 small molecules (hereafter the CCse set) for which a sufficient number of experimental rotational constants is available and cubic CCSD(T) force fields with at least triple-ζ basis sets were computationally feasible or already known. These reference values are next compared with those issuing from B3LYP, B2PLYP and MP2 cubic force fields. The remarkable accuracy of B2PLYP/VTZ and B3LYP/SNSD results allowed us to derive new SE equilibrium structures for an additional set of 27 medium-sized molecules characterized by the most representative bond patterns of organic systems, and including H, C, N, O, F, S and Cl atoms. The whole sets of 48 SE equilibrium structures (see Figure 5.1) determined using B2PLYP/VTZ and B3LYP/SNSD vibrational corrections (hereafter referred to as the B2se and B3se sets, respectively) represents two high quality benchmarks for structural studies and validation of computational models.

In addition to the rigorous SE approach, theoretical and experimental data can also be combined in cases for which the lack of experimental information for a sufficient number of isotopologues prevents the derivation of a complete SE equilibrium structure. In these cases, fixing some geometrical parameters to reliable and accurate estimates allows for the determination of the remaining structural parameters for systems otherwise nonentirely characterizable (see for example refs. [206–211]). To this end, in the last sections we present a new approach, denoted as the template approach, that exploits the accurate SE results obtained for reference molecules in order to derive SE equilibrium structures for similar systems by avoiding highly expensive CC computations.

5.1 Methodology and computational details

In the mixed experimental-theoretical approach, the r_e^{SE} structure is obtained by a LSF to the SE equilibrium rotational constants $(B_\tau^e)^{\mathrm{SE}}$, or their corresponding moments of inertia $(I_\tau^e)^{\mathrm{SE}}$, where the correlation between the latter and the geometrical parameters is given by eq. 1.30, and $(B_\tau^e)^{\mathrm{SE}}$ are calculated from $(B_\tau^0)^{\mathrm{EXP}}$ as,

$$(B_\tau^e)^{\mathrm{SE}} = (B_\tau^0)^{\mathrm{EXP}} - (\Delta B_\tau^0)^{\mathrm{QM}} \tag{5.1}$$

$(\Delta B_\tau^0)^{\mathrm{QM}}$ is explicitly given by,

$$\begin{aligned}(\Delta B_\tau^0)^{\mathrm{QM}} &= \frac{m_{\mathrm{e}}}{m_{\mathrm{p}}} g_{\tau\tau} B_\tau^e - \sum_i \frac{\alpha_{i,\tau} d_i}{2} \\ &= \Delta B_\tau^{\mathrm{el}} + \Delta B_\tau^{\mathrm{vib}}\end{aligned} \tag{5.2}$$

where $\Delta B_\tau^{\mathrm{vib}}$ is the vibrational contribution, given by eq. 3.11, and $\Delta B_\tau^{\mathrm{el}}$ is an electronic contribution, evaluated from the rotational **g** tensor and the ratio between electron (m_{e}) and proton (m_{p}) masses [32, 212, 213]. Although this term is often negligible, it will be systematically included in our computations for the sake of completeness.

In the present investigation, the cubic force fields required for the computation of the $\Delta B_\tau^{\mathrm{vib}}$ term have been evaluated at the CCSD(T) [157, 158], MP2 [154, 155] and DFT [153] levels. The correlation-consistent polarized cc-p(wC)VnZ basis sets [201–204] have mainly been used in CCSD(T) and MP2 calculations, with n = T, Q denoting the cardinal number of the corresponding basis set, shortly denoted as (wC)VnZ in the text. The frozen-core (fc) approximation has been adopted in conjunction with the VnZ sets, while all electrons (but 1s for second-row elements) have been correlated with wCVnZ.

The double-hybrid B2PLYP functional [200, 205, 214] has been used in conjunction with the cc-pVTZ basis set (VTZ) [201–204], and the hybrid B3LYP functional [215–217] with the SNSD basis set [198, 199, 218], which represents an excellent compromise between accuracy and computational cost for vibrational studies [197–199, 219].

The CFOUR program package [220] has been employed for MP2 and CCSD(T) computations, while DFT calculations have been performed with the GAUSSIAN suite of programs [221]. For all computational levels, the harmonic part has been obtained using analytic second derivatives, whereas the corresponding cubic force field has been determined in a normal-coordinate representation via numerical differentiation of the analytically computed harmonic force constants [47, 222–226]. At the DFT level, the force field calculations have been carried out using very-tight criteria for the SCF and geometry optimization convergence, together with an ultrafine grid for the numerical integration of the two-electron integrals

Figure 5.1: Sketch of the 39 asymmetric top molecules belonging to the B2se and B3se sets.

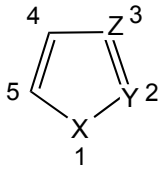

(a) (X,Y,Z)
(NH,CH,CH) pyrrole
(NH,N,CH) pyrazole
(NH,CH,N) imidazole
(O,CH,CH) furan
(S,CH,CH) thiophene

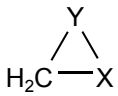

(b) (X,Y)
(NH,CH_2) aziridine
(O,CH_2) oxirane
(O,O) dioxirane

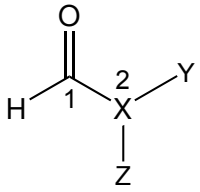

(c) (X,Y,Z)
(H,-,-) formaldehyde
(CH_2,OH,-) glycolaldehyde
(CH_2,CH_3,-) propanal
(C,CH_2,H) *cis*-acrolein
(C,H,CH_2) *trans*-acrolein
(O,H,-) *cis*-formic acid
(O,-,H) *trans*-formic acid
(O,OH,-) peroxyformic acid
(O,CH_3,-) *cis*-methyl formate

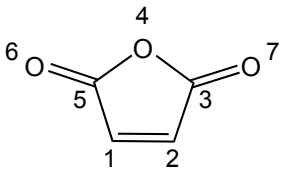

(d) maleic anhydride

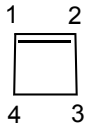

(e) cyclobutene

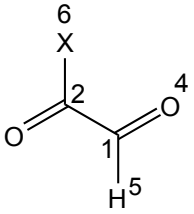

(f) X=H *trans*-glyoxal
X=OH glyoxylic acid
$X=CH_3$ pyruvic acid

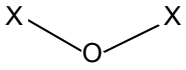

(g) X=H water
$X=CH_3$ dimethyl ether

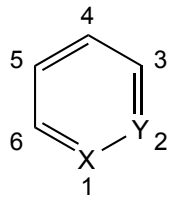

(h) (X,Y)
(N,CH) pyridine
(N,N) pyridazine

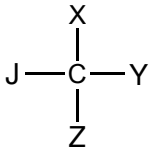

(i) (X,Y,Z,J)
(H,H,F,F) CH_2F_2
(Cl,Cl,F,F) CCl_2F_2
(H,H,Cl,Cl) CH_2Cl_2
(H,Cl,F,F) $CHClF_2$
(Cl,F,H,H) CH_2ClF

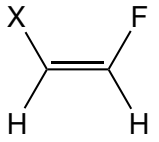

(j) X=H CH_2CHF
X=Cl *cis*-CHFCHCl

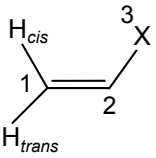

(k) X=H ethene
X=OH ethenol
$X=CH_3$ propene
$X=CHCH_2$ butadiene

and their derivatives. The numerical differentiations have been performed with the GAUSSIAN default step of 0.01 $\sqrt{\text{amu}}$ Å.
The $\Delta B_\tau^{\text{el}}$ contributions have been evaluated by calculating the $g_{\tau\tau}$ constants at the B3LYP/AVTZ level of theory.

To obtain accurate reference equilibrium structures for pyruvic acid, 2-fluoropyridine and 3-fluoropyridine, we have performed geometry optimizations at the CCSD(T) level accounting for basis-set truncation errors and core-valence correlation effects by means of a composite approach [188, 189]. The corresponding r_e is denoted as CCSD(T)/CBS+CV.

5.2 The performance of DFT force fields

A set of 21 molecules, including linear (HCN, HNC, HCO^+, $HNCCN^+$, HCCH, HCCCCH), symmetric-top (H_2CCCH_2, SH_3^+, NH_3) and asymmetric-top (H_2O, H_2CO, CH_2ClF, CH_2CHF, *cis*-CHFCHCl, oxirane, dioxirane, cyclobutene, *trans*-glyoxal, *cis* and *trans*-acrolein, pyridazine) molecules, has been selected to investigate the performance of the B2PLYP and B3LYP hybrid functionals in the computation of the vibrational contributions to experimental vibrational ground-state rotational constants $(B_\tau^0)^{\text{EXP}}$ subsequently used in the derivation of SE equilibrium geometries.

For all systems listed above, the experimental $(B_\tau^0)^{\text{EXP}}$ constants and the $\Delta B_\tau^{\text{vib}}$ contributions computed at the CCSD(T) and MP2 levels available in the literature have been collected. When not available, MP2 and/or CCSD(T) vibrational contributions have been calculated in this work (see Table 5.1 for details), together with the $\Delta B_\tau^{\text{vib}}$ contributions computed at the DFT level.

The $\Delta B_\tau^{\text{el}}$ contributions have also been taken into account. In particular, large $\Delta B_\tau^{\text{el}}$ values are found for H_2O (from about 7.6 to 0.7% of $(\Delta B_\tau^0)^{\text{QM}}$) and H_2CO (12.5-0.6%). Furthermore, the importance of taking into account the electronic contributions for *cis* and *trans*-acrolein and pyridazine is well known [227–229]. For both isomers of acrolein, ΔB_{el}^A, ΔB_{el}^B and ΔB_{el}^C are about 3.0-4.5%, 0.5-0.6% and 0.05-0.07% of $(\Delta B_\tau^0)^{\text{QM}}$. For pyridazine, ΔB_{el}^A and ΔB_{el}^B are about 0.7-1.2% of $(\Delta B_\tau^0)^{\text{QM}}$, while ΔB_{el}^C is about 0.3%.

The total $(\Delta B_\tau^0)^{\text{QM}}$ are rather small contributions. They vary from 2% to 3% of $(B_\tau^0)^{\text{EXP}}$, for systems like H_2O, to less than 1% in the case of $HNCCN^+$ and HCCCCH. Negative $(\Delta B_\tau^0)^{\text{QM}}$ corrections are obtained for all molecules except for $(B_0^A)^{\text{EXP}}$ of H_2O. The results obtained at the different levels of theory considered are in a good agreement to one another. By use of eq. 13 of ref. [192], it is possible to estimate that the resulting SE geometrical parameters differ by at most 0.25% from those obtained with vibrational contributions at the CCSD(T) level.

In the following, the SE equilibrium structures derived using vibrational con-

tributions from CCSD(T), MP2, B2PLYP/VTZ and B3LYP/SNSD force fields are referred to as CCSD(T) SE, MP2 SE, B2PLYP/VTZ SE and B3LYP/SNSD SE, respectively. The CCSD(T), B2PLYP/VTZ and B3LYP/SNSD SE equilibrium structures are explicitly reported in Table 5.1. The B3LYP/SNSD equilibrium structures are shown in order to be easily accessible in view of the template approach presented later in the text. The root mean square (RMS) of the residuals in terms of equilibrium rotational constants (hereafter simply referred to as residuals), and for planar molecules, the mean inertial defects $\Delta_e = I_C - I_B - I_A$ are also given in Table 5.1 as indicators of the quality of the fits. Indeed, small values of the RMS residuals and Δ_e indicate a good quality of the fits and that $(\Delta B_\tau^0)^{\mathrm{QM}}$ corrections lead to good SE equilibrium rotational constants, respectively.

The differences in the geometrical parameters of the MP2, B2PLYP/VTZ and B3LYP/SNSD SE equilibrium geometries with respect to the CCSD(T) SE equilibrium structures are graphically reported in Figure 5.2. It is noteworthy that for the whole set of bond lengths the deviation of MP2, B2PLYP and B3LYP results from the CCSD(T) references never exceeds 0.0026 Å. The deviations show a nearly Gaussian distribution with mean values close to zero and mean absolute errors (MAE) of 0.0004 Å, 0.0003 Å and 0.0007 Å for MP2, B2PLYP/VTZ and B3LYP/SNSD, respectively (see Table 5.2), thus pointing out the good accuracy of DFT vibrational contributions to rotational constants in evaluating SE equilibrium structures. The small standard deviations of MP2, B2PLYP/VTZ and B3LYP/SNSD can be considered fully satisfactory for geometrical parameter determinations. A larger MAE (0.0056 Å) is obtained for r_0 structures, obtained by a LSF of the molecular parameters to the pure experimental ground-state rotational constants, with a standard deviation of 0.0063 Å, a value significantly larger than the typical uncertainty affecting the SE methodology. The deviations for angles are also very small, with MAE of 0.03, 0.03, and 0.05 degrees for MP2, B2PLYP/VTZ and B3LYP/SNSD, respectively. Similarly to bond lengths, these values correspond to accuracies comparable with the intrinsic errors of the SE fitting procedure. Also for angles, the deviations of r_0 structures are an order of magnitude larger than that of the various r_e^{SE}'s.

A linear least-square fit of the CCSD(T) r_e^{SE} values, expressed as a function of the corresponding MP2 and DFT ones, gives the parameters reported in Table 5.3. It is noteworthy that in all cases the angular coefficient is very close to 1 and the intercept never exceeds, in absolute value, 0.0025 Å for bond lengths and 0.06 degrees for angles. This confirms that using B3LYP corrections in the SE approach leads to results that reproduce very well the best SE equilibrium structures. In addition, the analysis of R^2 and standard deviation values of the linear regression does not point out any significant deviation from linearity.

Table 5.1: r_e^{SE} and r_e geometries for the 21 molecules of the CCse set. Distances in Å, angles in degrees.

	r_e^{SE}[a]			r_e
	CCSD(T)	B2PLYP	B3LYP	B3LYP
– linear molecules –				
HCN[b]				
r(H-C)	1.0651(1)$^{\times,\dagger}$	1.0647(1)†	1.0645(1)†	1.0707
r(C-N)	1.1533(1)	1.1532	1.1536(1)	1.1551
Rms resid. [MHz]	0.0001	0.0001	0.0001	-
HNC[b]				
r(H-N)	0.9954(1)$^{\times,\dagger}$	0.9953(1)†	0.9946(1)†	1.0022
r(N-C)	1.1685(1)	1.1687(1)	1.1688(1)	1.1739
Rms resid. [MHz]	0.0001	0.0001	0.0001	-
HCO$^+$				
r(H-C)	1.0919(1)$^{\times,\dagger}$	1.0918(1)†	1.0916(1)†	1.0995
r(C-O)	1.1057(1)	1.1056(1)	1.1057(1)	1.1075
Rms resid. [MHz]	0.0001	0.0001	0.0001	-
HNCCN$^+$[c]				
r(H-N)	1.0133(1)$^{\asymp,\dagger}$	1.0136(1)†	1.0138(2)†	1.0191
r(N-C)	1.1406(1)	1.1399(2)	1.1392(4)	1.1455
r(C-C)	1.3724(1)	1.3730(2)	1.3735(4)	1.3686
r(C-N)	1.1634(1)	1.1621(1)	1.1607(3)	1.1628
Rms resid. [MHz]	0.0002	0.0003	0.0008	-
HCCH[d]				
r(C≡C)	1.2030(1)$^{+,\dagger}$	1.2030(1)†	1.2036(1)†	1.2060
r(C-H)	1.0617(1)	1.0613(1)	1.0611(1)	1.0676
Rms resid. [MHz]	0.0001	0.0001	0.0002	-
HCCCCH[e]				
r(C≡C)	1.2084(3)$^{\times,\dagger}$	1.2077(2)†	1.2070(4)†	1.2123
r(C-C)	1.3727(4)	1.3734(3)	1.3726(6)	1.3685
r(C-H)	1.0615(1)	1.0613(1)	1.0610(1)	1.0667
Rms resid. [MHz]	0.0008	0.0006	0.0012	-
– symmetric top molecules –				
SH$_3^+$[f]				
r(S-H)	1.3500(1)$^{+,\dagger}$	1.3502(1)†	1.3502(1)†	1.3683
a(H-S-H)	94.15(1)	94.13(1)	94.11(1)	94.30
Rms resid. [MHz]	0.0010	0.0007	0.0011	-
NH$_3$[b]				
r(N-H)	1.0110(2)$^{\times,\dagger}$	1.0111(1)†	1.0111(2)†	1.0176
a(H-N-H)	106.94(2)	106.93(2)	106.87(3)	106.59
Rms resid. [MHz]	0.0033	0.0032	0.0036	-
H$_2$CCCH$_2$				
r(C=C)	1.3066(1)$^{\div,\dagger}$	1.3069(2)†	1.3075(2)†	1.3077
r(C-H)	1.0807(1)	1.0805(5)	1.0800(4)	1.0874
a(H-C-H)	118.26(1)	118.32(6)	118.37(5)	117.41
Rms resid. [MHz]	0.0011	0.0092	0.0081	-
– asymmetric top molecules –				
H$_2$O[b]				
r(O-H)	0.9573(1)$^{\times,\dagger}$	0.9573(1)†	0.9572(1)†	0.9644
a(H-O-H)	104.53(1)	104.56(1)	104.47(1)	104.60
Rms resid. [MHz]	0.0004	0.0004	0.0004	-
Mean Δ_e [uÅ^2]	0.00506	0.00552	0.00603	-

H_2CO[b]				
r(C-O)	1.2047(1)$^{\times,\dagger}$	1.2048(1)†	1.2051(1)†	1.2052
r(C-H)	1.1003(1)	1.1004(1)	1.1002(1)	1.1099
a(H-C-O)	121.65(1)	121.63(1)	121.62(1)	121.84
Rms resid. [MHz]	0.0003	0.0003	0.0003	-
Mean Δ_e [uÅ^2]	0.00297	0.00308	0.00223	-
CH_2ClF[g]				
r(C-H)	1.0840(1)‡,†	1.0843(1)†	1.0842(1)†	1.0896
r(C-F)	1.3594(1)	1.3593(1)	1.3591(1)	1.3682
r(C-Cl)	1.7641(1)	1.7643(1)	1.7645(1)	1.7998
a(H-C-Cl)	107.96(1)	107.95(1)	107.93(1)	107.61
a(H-C-H)	112.57(1)	112.56(1)	112.55(1)	113.23
a(F-C-Cl)	110.02(1)	110.02(2)	110.02(2)	110.15
Rms resid. [MHz]	0.0001	0.0001	0.0001	-
CH_2CHF				
r(C1-F)	1.3424(2)$^{\div,\dagger}$	1.3422(2)†	1.3412(5)†	1.3528
r(C1-H)	1.0792(1)	1.0788(1)	1.0784(4)	1.0856
r(C1-C2)	1.3213(2)	1.3219(2)	1.3234(6)	1.3247
r(C2-H_{trans})	1.0772(1)	1.0773(1)	1.0768(4)	1.0839
r(C2-H_{cis})	1.0785(1)	1.0784(1)	1.0782(3)	1.0848
a(F-C1-H)	112.10(6)	112.23(7)	112.36(19)	111.62
a(F-C1-C2)	121.72(1)	121.70(1)	121.68(1)	121.90
a(C1-C2-H_{trans})	118.95(1)	118.93(1)	118.94(4)	119.25
a(C1-C2-H_{cis})	121.32(1)	121.31(1)	121.29(3)	121.72
Rms resid. [MHz]	0.0001	0.0001	0.0004	-
Mean Δ_e [uÅ^2]	0.00281	0.00164	0.00162	-
***cis*-CHFCHCl**[h]				
r(C1-Cl)	1.7129(2)$^{\div,\dagger}$	1.7126(7)†	1.7124(14)†	1.7404
r(C1-H)	1.0795(2)	1.0794(7)	1.0795(14)	1.0818
r(C1=C2)	1.3244(2)	1.3243(10)	1.3266(19)	1.3278
r(C2-F)	1.3313(2)	1.3318(8)	1.3306(16)	1.3416
r(C2-H)	1.0796(1)	1.0784(6)	1.0776(13)	1.0849
a(Cl-C1=C2)	123.08(1)	123.08(7)	123.08(13)	123.74
a(H-C1=C2)	121.08(2)	121.02(10)	121.06(19)	120.91
a(F-C2=C1)	122.56(2)	122.59(8)	122.47(15)	123.10
a(H-C2=C1)	123.49(2)	123.43(8)	123.33(16)	123.45
Rms resid. [MHz]	0.0002	0.0010	0.0020	-
Mean Δ_e [uÅ^2]	0.00712	0.01037	0.01604	-
oxirane[i]				
r(C-C)	1.4609(2)$^{\div,\dagger}$	1.4612(2)†	1.4615(2)†	1.4674
r(C-O)	1.4274(1)	1.4276(1)	1.4281(1)	1.4324
r(C-H)	1.0816(2)	1.0816(2)	1.0814(2)	1.0889
a(C-O-C)	61.56(1)	61.56(1)	61.55(1)	61.63
a(H-C-H)	116.25(2)	116.28(2)	116.33(2)	115.75
a(H-C-O)	114.87(3)	114.86(3)	114.82(3)	115.04
Rms resid. [MHz]	0.0015	0.0015	0.0015	-
dioxirane[j]				
r(C-O)	1.3846(5)$^{\div}$	1.3846(1)†	1.3850(1)†	1.3901
r(O-O)	1.5133(5)	1.5140(1)	1.5140(1)	1.5006
r(C-H)	1.0853(15)	1.0852(1)	1.0850(1)	1.0919
a(H-C-H)	117.03(20)	117.02(1)	117.06(1)	116.96
Rms resid. [MHz]	0.25	0.0005	0.0006	-

***trans*-glyoxal**[k]				
r(C=O)	1.2046(1)÷,†	1.2047(1)†	1.2051(1)†	1.2069
r(C-C)	1.5157(1)	1.5153(1)	1.5149(2)	1.5262
r(C-H)	1.1006(1)	1.1006(1)	1.1006(1)	1.1093
a(H-C-C)	115.23(1)	115.37(1)	115.37(1)	115.14
a(O=C-H)	123.60(1)	123.46(1)	123.45(1)	123.45
Rms resid. [MHz]	0.0001	0.0002	0.0002	-
Mean Δ_e [uÅ^2]	0.02157	0.01271	−0.02981	-
***cis*-acrolein**				
r(C1-C2)	1.4806(1)÷,†	1.4808(1)†	1.4809(3)†	1.4840
r(C2-C3)	1.3350(1)	1.3352(1)	1.3368(2)	1.3377
r(C1-O)	1.2108(1)	1.2111(1)	1.2102(2)	1.2145
r(C1-H)	1.1024(1)	1.1016(1)	1.1021(2)	1.1113
r(C2-H)	1.0824(1)	1.0818(1)	1.0807(2)	1.0885
r(C3-H$_{cis}$)	1.0808(1)	1.0814(1)	1.0800(3)	1.0868
r(C3-H$_{trans}$)	1.0797(1)	1.0792(1)	1.0786(2)	1.0857
a(C1-C2-C3)	121.21(1)	121.26(1)	121.33(2)	122.28
a(O-C1-C2)	123.96(1)	123.95(1)	123.88(2)	124.66
a(C2-C1-H)	115.83(1)	115.78(1)	115.81(2)	115.24
a(C3-C2-H)	121.57(1)	121.65(1)	121.63(2)	121.21
a(C2-C3-H$_{cis}$)	119.85(1)	119.79(1)	119.86(2)	120.35
a(C2-C3-H$_{trans}$)	121.61(1)	121.61(1)	121.66(4)	121.73
Rms resid. [MHz]	0.0001	0.0001	0.0003	-
Mean Δ_e [uÅ^2]	0.01311	−0.01911	0.01346	-
***trans*-acrolein**				
r(C1-C2)	1.4702(1)÷,†	1.4699(1)†	1.4703(1)†	1.4735
r(C2-C3)	1.3354(1)	1.3356(1)	1.3355(1)	1.3384
r(C1-O)	1.2103(1)	1.2108(1)	1.2109(1)	1.2142
r(C1-H)	1.1048(1)	1.1044(1)	1.1044(1)	1.1133
r(C2-H)	1.0814(1)	1.0814(1)	1.0817(1)	1.0876
r(C3-H$_{cis}$)	1.0825(1)	1.0827(1)	1.0826(1)	1.0883
r(C3-H$_{trans}$)	1.0795(1)	1.0794(1)	1.0792(1)	1.0856
a(C1-C2-C3)	120.18(1)	120.16(1)	120.21(1)	121.02
a(O-C1-C2)	124.02(1)	123.99(1)	123.97(1)	124.21
a(C2-C1-H)	115.08(1)	115.15(1)	115.11(1)	115.02
a(C3-C2-H)	122.78(1)	122.75(1)	122.85(1)	122.41
a(C2-C3-H$_{cis}$)	120.46(1)	120.45(1)	120.44(1)	120.89
a(C2-C3-H$_{trans}$)	122.10(1)	122.12(1)	122.07(1)	122.22
Rms resid. [MHz]	0.0001	0.0001	0.0001	-
Mean Δ_e [uÅ^2]	−0.00527	0.02043	−0.00845	-
cyclobutene				
r(C1=C2)	1.3406(1)÷,†	1.3406(1)†	1.3409(1)†	1.3420
r(C2-C3)	1.5141(1)	1.5145(1)	1.5149(1)	1.5193
r(C3-C4)	1.5639(1)	1.5639(2)	1.5646(2)	1.5736
r(C1-H)	1.0805(1)	1.0803(1)	1.0801(1)	1.0867
r(C3-H)	1.0894(1)	1.0895(1)	1.0892(1)	1.0961
a(C1-C2-C3)	94.23(1)	94.23(1)	94.23(1)	94.37
a(C1-C2-H)	133.42(1)	133.45(1)	133.47(1)	133.47
a(C4-C3-H)	114.64(1)	114.63(1)	114.60(1)	114.78
a(H-C3-H)	109.09(1)	109.14(1)	109.19(1)	108.59
Rms resid. [MHz]	0.0001	0.0001	0.0001	-

pyridazine[l]				
r(N2-C3)	1.3302(12)$^{\aleph 0,\dagger}$	1.3318(6)†	1.3324(24)†	1.3328
r(C3-C4)	1.3938(12)	1.3927(6)	1.3926(23)	1.3929
r(C4-C5)	1.3761(16)	1.3776(4)	1.3778(16)	1.3789
r(C4-H)	1.0802(4)	1.0798(1)	1.0791(5)	1.0780
r(C3-H)	1.0810(3)	1.0808(1)	1.0804(4)	1.0813
a(C3-C4-C5)	116.85(3)	116.85(1)	116.86(4)	116.87
a(N2-C3-C4)	123.86(4)	123.86(1)	123.87(5)	123.82
a(C4-C3-H)	121.35(6)	121.38(3)	121.39(11)	121.29
a(C5-C4-H)	122.37(4)	122.32(2)	122.32(7)	122.25
Rms resid. [MHz]	-	0.0003	0.0013	-
Mean Δ_e [uÅ^2]	-	−0.00214	−0.00103	-

All computations have been performed in this work except where otherwise indicated.
B2PLYP and B3LYP are used in conjunction with VTZ and SNSD basis sets, respectively.
a) Graphical symbols denote the basis sets used in the calculations of CCSD(T) $\Delta B_\tau^{\mathrm{vib}}$ contributions: ÷ VTZ; ‡ CVTZ; ≍ VQZ; × CVQZ; + wCVQZ, ℵ0 ANO0. † denotes the inclusion of $\Delta B_\tau^{\mathrm{el}}$. For all the structures calculated in this work, the uncertainties on the geometrical parameters are reported within parentheses, rounded to $1 \cdot 10^{-4}$ Å for lengths and $1 \cdot 10^{-2}$ degrees for angles also if smaller than these values. $\Delta_e = I_C - I_B - I_A$ is the inertial defect.
b) CCSD(T) $\Delta B_\tau^{\mathrm{vib}}$ from ref. [230].
c) CCSD(T) $\Delta B_\tau^{\mathrm{vib}}$ from ref. [231].
d) CCSD(T) $\Delta B_\tau^{\mathrm{vib}}$ from ref. [232].
e) CCSD(T) $\Delta B_\tau^{\mathrm{vib}}$ from ref. [233].
f) CCSD(T) $\Delta B_\tau^{\mathrm{vib}}$ from ref. [234].
g) CCSD(T) $\Delta B_\tau^{\mathrm{vib}}$ from ref. [235].
h) CCSD(T) $\Delta B_\tau^{\mathrm{vib}}$ from ref. [236].
i) CCSD(T) $\Delta B_\tau^{\mathrm{vib}}$ from ref. [237].
j) CCSD(T) r_e^{SE} from ref. [226].
k) CCSD(T) $\Delta B_\tau^{\mathrm{vib}}$ from ref. [238].
l) CCSD(T) r_e^{SE} from ref. [229].

Figure 5.2: Statistical distributions of the MP2, B2PLYP/VTZ and B3LYP/SNSD deviations from CCSD(T) SE equilibrium parameters for the molecules belonging to the CCse set (see Table 5.1).

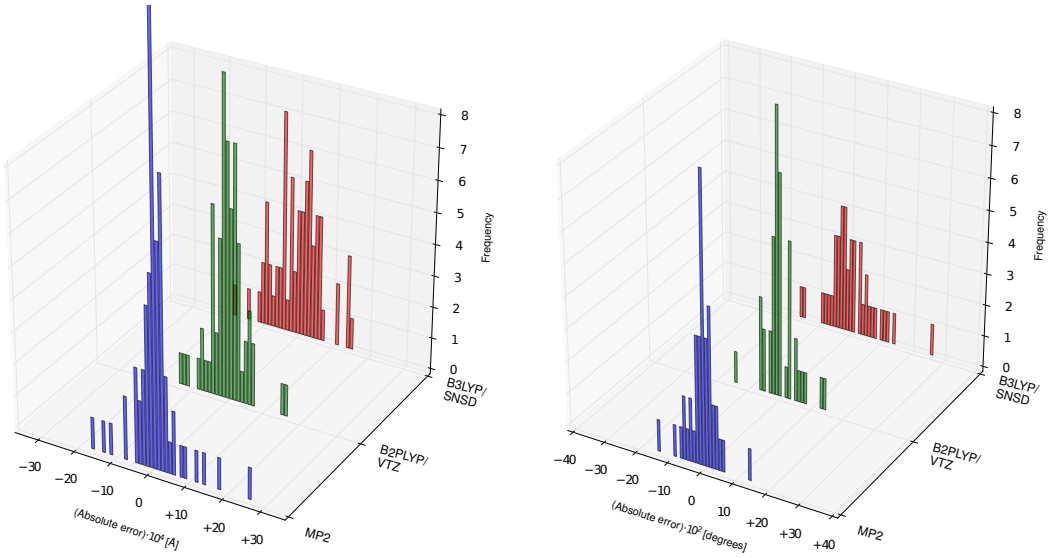

(a) all bonds

(b) all angles

Table 5.2: Mean, standard deviation, and mean absolute error (MAE) for the MP2, B2PLYP/VTZ and B3LYP/SNSD deviations from CCSD(T) SE equilibrium parameters for the molecules belonging to the CCse set (see Table 5.1).

	MP2[a]	B2PLYP	B3LYP
All bonds (68 items)			
Mean	+0.0001	+0.0000	−0.0001
St. Dev.	0.0006	0.0005	0.0009
MAE	0.0004	0.0003	0.0007
CH bonds (27 items)			
Mean	+0.0002	−0.0002	−0.0005
St. Dev.	0.0003	0.0003	0.0005
MAE	0.0002	0.0003	0.0005
CC bonds (18 items)			
Mean	+0.0001	0.0001	+0.0005
St. Dev.	0.0007	0.0006	0.0010
MAE	0.0005	0.0004	0.0009
CO bonds (7 items)			
Mean	+0.0001	0.0002	+0.0003
St. Dev.	0.0002	0.0002	0.0004
MAE	0.0001	0.0002	0.0005
All angles (42 items)			
Mean	+0.00	+0.00	+0.00
St. Dev.	0.04	0.05	0.08
MAE	0.03	0.03	0.05

For the different types of bonds, only the sets having at least 7 items have been considered. B3LYP and B2PLYP are used in conjunction with SNSD and VTZ basis sets, respectively.
a) all MP2 calculations have been performed with basis sets of at least triple-ζ quality.

Table 5.3: Parameters for linear regressions of the CCSD(T) r_e^{SE} parameters versus the MP2, B2PLYP/VTZ and B3LYP/SNSD r_e^{SE} ones for the molecules belonging to the CCse set (see Table 5.1).

	MP2[a]	B2PLYP/VTZ	B3LYP/SNSD
All bonds			
A	0.999740	1.000722	0.998132
B	0.000186	−0.000905	0.002348
R^2	0.999989	0.999991	0.999977
St. Dev.	0.000405	0.000361	0.000584
All angles			
A	1.000144	1.000389	1.000064
B	−0.012640	−0.047032	−0.009603
R^2	0.999985	0.999982	0.999956
St. Dev.	0.000609	0.000680	0.001043
$r_e^{\mathrm{SE}}(\mathrm{CCSD(T)}) = A \cdot r_e^{\mathrm{SE}}(\mathrm{MP2\ or\ DFT}) + B$			

a) all MP2 calculations have been performed with basis sets of at least triple-ζ quality.

5.3 From small to medium-large systems

In the previous section we demonstrated that the SE equilibrium structures derived from $\Delta B_\tau^{\mathrm{vib}}$ contributions calculated at the B2PLYP/VTZ and B3LYP/SNSD level have an accuracy comparable to that obtained when using CCSD(T) corrections. In view of these results, and aiming at increasing the number of geometrical patterns considered, in this section B2PLYP and B3LYP SE equilibrium structures are presented for 27 organic molecules containing H, C, N, O, F, S, and Cl atoms.

For the systems considered, to the best of our knowledge, SE equilibrium structures derived from CCSD(T) vibrational contributions are not available, but a sufficient number of isotopologues has been characterized experimentally to allow for a reliable determination of all geometrical parameters without any constraint and/or assumption. Focusing on the DFT quantum mechanical models, which permits keeping the computational costs low, the new SE equilibrium structures are compared with the most accurate determinations available in the literature. Together with the 21 molecules previously considered, two high-quality benchmark sets, including a total of 48 molecules (hereafter referred to as the B2se and B3se sets), have been set up for validating structural predictions from other experimental and/or computational approaches. The whole B2se and B3se sets, as well as the CCse set, are available in graphical interactive form on the Web site dreams.sns.it.[239].

The geometrical parameters for CH_2F_2, CCl_2F_2, CH_2Cl_2, $CHClF_2$, ethene,

ethenol, propene, butadiene, cyclopropane, aziridine, benzene, pyrrole, pyrazole, imidazole, furan, thiophene, maleic anhydride, pyridine, dimethyl ether, *cis* and *trans*-formic acid, *cis*-methyl formate, glycolaldehyde, and propanal are collected in Table 5.4 and compared with the best $r_e^{\rm SE}$ equilibrium structures available in the literature. In Table 5.5, we present the first SE equilibrium structures for three additional molecules (peroxyformic, glyoxylic and pyruvic acids), which are then compared with the best theoretical r_e structures available.

It is noteworthy that for most of the systems the RMS of the residuals for r_0 geometries is about one order of magnitude larger than the RMS of the residuals for SE equilibrium geometries. The small values for the latter, less than 7 kHz for all systems, demonstrate the good quality of the fits.

In analogy with the CCse set, equilibrium geometries obtained at the B3LYP/SNSD level are reported in Table 5.4 because of their subsequent use within the template approach presented in the next section.

Halomethanes

A systematic evaluation of the SE equilibrium structure for a series of chlorinated and fluorinated methanes has been carried out recently [240]. In this work, in addition to the SE equilibrium structure of CH_2ClF reported in the previous section, CH_2F_2, CCl_2F_2, CH_2Cl_2, and $CHClF_2$ have been considered as models to investigate the C-X bond pattern, where X is a halogen atom and the C hybridization is sp^3. CH_2F_2, CCl_2F_2 and CH_2Cl_2 have C_{2v} symmetry and are completely characterized by 5 geometrical parameters, while $CHClF_2$ belongs to the C_s symmetry group and has 6 unique structural parameters. In ref. [240], the $\Delta B_\tau^{\rm vib}$ contributions have been calculated at the MP2/VTZ (with the modified V(T+d)Z for the chlorine atom [241]) level of theory for the halomethanes considered, except for CCl_2F_2 (B3LYP/6-311+G(3df,2pd)). For all these systems, there is a good agreement between the SE equilibrium structures obtained employing DFT and MP2 vibrational contributions.

The C-F bond length shows the largest variation with the number of hydrogens bonded to the C atom, i.e. observing B3LYP results, it increases from 1.3286 Å for CCl_2F_2 (no H atoms) to 1.3363 Å for $CHClF_2$ (one H atom) and to 1.3533 Å/1.3594 Å for CH_2F_2/CH_2ClF (two H atoms). A similar trend is shown by the CCl bond length, which changes from 1.7641/1.7642 Å for CH_2ClF/CH_2Cl_2 to 1.7558 Å for $CHClF_2$ and to 1.7519 Å for CCl_2F_2. On the contrary, the CH bond length is only marginally affected by the number of halogen atoms bonded to the C atom (1.0810, 1.0840, 1.0849 and 1.0867 Å for CH_2Cl_2, CH_2ClF, $CHClF_2$, and CH_2F_2, respectively).

Substituted alkene compounds

Together with CH_2CHF and *cis*-CHFCHCl (presented in Table 5.1), ethene, ethenol, butadiene, and propene have been studied as representatives of the Y-C=C-X bond pattern for noncyclic molecules, where C is sp^2 hybridized and X and Y are either halogens or C atoms.

Ethene and ethenol (or vinyl alcohol) are the simplest alkene and enol compound, respectively. A $r_e^{\rm SE}$ structure for ethene, which is defined by 3 internal parameters (D_{2h} symmetry), is available in the literature [242]. It corresponds to a weighted average of different $r_e^{\rm SE}$ geometries calculated by use of $\Delta B_\tau^{\rm vib}$ at the MP2 and B3LYP levels, in conjunction with basis sets of at least triple-ζ quality, and where scaled quadratic force fields have been coupled with unscaled cubic force fields in the vibrational correction calculations. The uncertainties of 0.0010 Å and 0.10 degrees on the parameters of the structure of ref. [242] (see Table 5.4) include both the uncertainties related to the SE methodology and those estimated from the parameter differences found using the different QM models in the $\Delta B_\tau^{\rm vib}$ calculations. All the B2PLYP/VTZ and B3LYP/SNSD $r_e^{\rm SE}$ results, obtained by fitting the SE I_A^e and I_B^e moments of inertia, coincide with those of ref. [242] within the respective error bars.

The *syn* conformer of ethenol is fairly rigid and completely defined by 11 internal parameters (C_s symmetry). The SE equilibrium structure recently determined using $\Delta B_\tau^{\rm vib}$ computed at the MP2/VQZ level [243] is given in Table 5.4 together with the DFT $r_e^{\rm SE}$ results, obtained by fitting the SE I_A^e and I_C^e moments of inertia. The agreement is extremely good and the small RMS residual and uncertainties on the fitted parameters indicate that the B2PLYP/VTZ and B3LYP/SNSD SE equilibrium geometries are also accurate.

Propene is the simplest monomethyl internal rotor, and it has been largely studied by infrared and microwave spectroscopy (see refs. [244, 245] and references therein). As a consequence, experimental rotational constants are available for a large number of isotopologues (20). The molecular structure of propene (C_s symmetry with a synperplanar arrangement of the C1=C2-C3-H_{plane} moiety) is defined by 15 geometrical parameters, and has recently been evaluated by means of the SE approach using $\Delta B_\tau^{\rm vib}$ contributions at the MP2/VTZ(fc) level [245]. Some remarks on the fitting procedure need to be made. Due to large uncertainties affecting the $(B_A^0)^{\rm EXP}$ of some isotopologues [246] that lead to ill-conditioned results, the fits have been performed on the SE equilibrium moments of inertia corresponding to the $(B_B^0)^{\rm EXP}$ and $(B_C^0)^{\rm EXP}$ rotational constants. Moreover, CHD_{cis}=$CDCH_3$ and CH_2=$^{13}CHCH_3$ isotopologues have been excluded from the fit with B3LYP $\Delta B_\tau^{\rm vib}$ corrections, while CHD_{cis}=$CDCH_3$, CH_2=$^{13}CHCH_3$, CH_2=$CHCH_2D_{plane}$, CHD_{cis}=$CHCH_2D_{plane}$, and CHD_{cis}=$CHCH_2D_{out}$ isotopologues from the fit with B2PLYP $\Delta B_\tau^{\rm vib}$ corrections, because of the corresponding large residuals affecting

the equilibrium rotational constants.

In this framework, DFT vibrational contributions lead to residuals with very small RMS. Some fitted geometrical parameters defining the methyl hydrogen atoms lying outside the molecular C-C-C plane (in particular the C3-H_{out} bond length (1.0895 Å and 1.0817 Å for B3LYP and B2PLYP, respectively) and the C1=C2-C3-H_{out} dihedral angle (120.47 and 120.70 degrees)) are significantly smaller than the corresponding values obtained using MP2 vibrational contributions (1.0949 Å and 121.08 degrees), where the B2PLYP results are in a better agreement with the MP2 ones. It is noteworthy that, in contrast to the B3LYP trend, the MP2 SE C3-H_{out} bond length differs significantly from the other C-H bonds, which range between 1.0805 and 1.0862 Å.

Butadiene is a planar C_{2h} molecule, belonging to the class of polyenes, which are of great importance in biology and organic electronics due to a π-electron delocalization that increases as the C=C chain gets longer. In analogy with ethene, a r_e^{SE} structure for butadiene was obtained by Craig and co-workers from the average of different MP2 and B3LYP r_e^{SE} geometries. The B2PLYP/VTZ and B3LYP/SNSD r_e^{SE} parameters, obtained by fitting the SE I_A^e and I_C^e moments of inertia, agree with those of ref. [242] within the respective error bars.

Cyclic and heterocyclic compounds

Cyclic and heterocyclic compounds are important building blocks of organic and biological molecules. Together with cyclobutene reported in Table 5.1, which is one of the smallest cycloalkenes, we have studied cyclopropane and benzene (Table 5.4), which are among the simplest cycloalkanes and aromatic systems, and oxirane, dioxirane, pyridazine (Table 5.1), aziridine, pyrrole, pyrazole, imidazole, furan, thiophene, maleic anydride and pyridine (Table 5.4), as prototypical heterocyclic compounds.

Cyclopropane belongs to the D_{3h} symmetry group and it is completely defined by 3 geometrical parameters: the C-C and C-H distances and the HCH angle. The SE equilibrium structure has been previously determined by using a SDQ-MBPT(4)/VTZ cubic force field [247]. Though two rotational constants of the parent species (B_B^0 and B_C^0), B_B^0 of C_3D_6 and B_A^0, B_B^0, B_C^0 of $C_3H_4D_2$ have been experimentally determined, the inclusion of all of them in the fitting procedure leads to large residuals, as also noticed in ref. [247]. The geometries reported in Table 5.4 have been obtained by using the SE equilibrium moments of inertia of $C_3H_4D_2$, together with the SE I_B^e of the parent species. Thanks to its high symmetry (D_{6h}), the structure of benzene is defined by only 2 geometrical parameters: the C-H and C-C bond lengths. Its SE equilibrium structure has been determined for the first time by Stanton *et al.* [248] using vibrational contributions at the MP4(SDQ)/VTZ level. The DFT SE equilibrium structures of cyclopropane and

benzene show small uncertainties on the geometrical parameters and are in good agreement with the previous determinations.

Aziridine, also called ethylene imine, is one of the simplest nonaromatic N-heterocycles. Its equilibrium structure (C_s symmetry) is completely determined by 10 geometrical parameters, and is characterized by a high nitrogen inversion barrier. The rotational spectrum of aziridine has been studied in great detail because of its potential astrophysical interest [249–251]. Very recently, a SE equilibrium structure has been determined by combining the experimental ground-state rotational constants with $\Delta B_\tau^{\rm vib}$ contributions computed at the MP2/VTZ level [252]. The DFT SE equilibrium structures have been derived by fitting SE equilibrium inertia moments, all equally weighted. The resulting SE equilibrium structures show a very small RMS residual and good agreements with the MP2/VTZ one.

Pyrazole and imidazole are two five-membered heteroaromatic rings, with adjacent and nonadjacent nitrogen atoms, respectively. Both molecules are completely characterized by 15 geometrical parameters, and have C_s symmetry. Pyrazole is used in the synthesis of many medical/organic molecules, while imidazole is present in important biological building-blocks, such as histidine and the related hormone histamine. The B2PLYP/VTZ and B3LYP/SNSD $r_e^{\rm SE}$ geometries shown in Table 5.4 have been obtained by fitting the SE I_B^e and I_C^e moments of inertia for pyrazole, and I_A^e and I_C^e for imidazole, all equally weighted.

For imidazole, the experimental rotational constants used were taken from ref. [253] without applying any corrections, while in ref. [252] the experimental values were corrected by the contribution of theoretical quartic distortion constants within the predicated method. In spite of these methodological differences, the DFT $r_e^{\rm SE}$ parameters are in good agreement with the results of ref. [252].

Pyrrole, furan, and thiophene are three planar heterocyclic molecules belonging to the C_{2v} point group, whose structures are completely defined by 9, 8 and 8 parameters, respectively. For pyrrole and furan, the best SE equilibrium structures reported in the literature were determined by correcting the vibrational ground-state rotational constants with $\Delta B_\tau^{\rm vib}$ contributions calculated at the MP2/wCVTZ and MP2/VTZ levels, respectively [252, 254]. The best SE equilibrium geometry of thiophene was derived from a combined use of electron diffraction (ED), microwave spectroscopy (MW) and computed vibrational contributions at the B3LYP/6-311+G* level [255]. The DFT SE equilibrium geometries of pyrrole and furane are in good agreement with those already available. On the contrary, the B2PLYP/VTZ and B3LYP/SNSD SE equilibrium parameters of thiophene collected in Table 5.4 show relevant differences with respect to those previously determined, but a very good agreement one another. For example, the DFT SE value for r(CS) is about 0.0087 Å longer than that of ref. [255], while the DFT SE C=C bond length is about 0.0095 Å shorter than the corresponding

value of ref. [255].

It is interesting to note how the C-C bond lengths change when both the H atoms linked with the C atom in α-position with respect to the O atom of the ring are substituted with two O atoms, that is, when moving from furan to maleic anhydride. To the best of our knowledge, the most accurate SE equilibrium structure available for maleic anydride (C_{2v} symmetry) was derived using a MP2/VTZ cubic force field, also including the non negligible contribution due to $\Delta B_\tau^{\rm el}$ [256]. For example, the inclusion of the latter contributions reduces the RMS residual from 8.5 kHz to 0.4 kHz and the SE equilibrium inertial defect from a mean value of -0.01634 uÅ^2 to -0.00779 uÅ^2 in B3LYP calculations. For this molecule, the MP2 and DFT SE equilibrium structures agree very well one another. From Table 5.4 we note a significant decrease of the C3-C4 bond length when moving from furan to maleic anhydride (1.4344 Å in furan with respect to r(C1-C2)=1.3320 Å in maleic anhydride, see Figure 5.1 d) and a contemporary increase of the C2-C3 bond length (1.3542 Å in furan with respect to 1.4857 Å in maleic anhydride), and of the ring C-O distance (from 1.3598 Å in furan to 1.3848 Å in maleic anhydride).

Thanks to the large number of isotopologues experimentally investigated [257, 258] and to the limited number of independent geometrical parameters (10), it is possible to determine a full SE equilibrium structure for pyridine (C_{2v} symmetry). The $r_e^{\rm SE}$ structures given in Table 5.4 have been obtained by fitting the SE I_A^e and I_C^e moments of inertia derived from the experimental rotational constants corrected by $\Delta B_\tau^{\rm vib}$ contributions calculated at the B2PLYP/VTZ and B3LYP/SNSD levels. The I_A^e moment of inertia of the C4-deuterated isotopologue (see Figure 5.1) has been excluded from the fits because of the corresponding large residual affecting the equilibrium rotational constant. Even in this case, the inclusion of the $\Delta B_\tau^{\rm el}$ terms leads to a considerable improvement of the inertial defects. The B2PLYP and B3LYP SE equilibrium structures remarkably agree with one another and also with the $r_e^{\rm SE}$ determined in ref. [252] using B3LYP/6-311+G(3df,2pd) vibrational corrections and the so-called predicate approach.

Ethers, aldehydes, esters and carboxylic acids

In addition to *trans*-glyoxal, *cis*- and *trans*-acrolein (see Table 5.1), dimethyl ether, glycolaldehyde, propanal, formic acid and methyl formate (see Table 5.4), as well as peroxyformic, glyoxylic and pyruvic acids (see Table 5.5) have been investigated as models for the most significant oxygen-containing moieties.

Dimethyl ether, the simplest molecule with two internal rotors, has been studied in great detail as an interstellar molecule and because of the interest in its rotational-torsional spectrum [259–261]. Its equilibrium structure has C_{2v} symmetry (characterized by antiperiplanar arrangement of both the C-O-C-H_{plane} moieties) and is completely defined by 7 geometrical parameters. The SE equilib-

rium structures determined using DFT vibrational contributions are in remarkable agreement with that obtained in ref. [243] using an MP2/VTZ cubic force field (see Table 5.4).

Formic acid (C_s symmetry) can be considered the prototype of carboxylic acids and presents two rotamers, the *cis* and *trans* forms. The SE equilibrium structures of both forms have been previously obtained by combining the experimental ground-state rotational constants of several isotopologues (11 and 7 for the *cis* and *trans* forms, respectively) with $\Delta B_\tau^{\rm vib}$ calculated from a MP2/VTZ cubic force field [262]. As shown in Table 5.4, for both conformers, the SE equilibrium structures issuing from DFT vibrational contributions are in very good agreement with the reference SE results. There are just some discrepancies on HCO angles, where B2PLYP results (123.87 and 125.14 degrees) are more close to the MP2 ones (123.26 and 125.04 degrees) with respect to those given by B3LYP vibrational corrections (124.21 and 125.38 degrees).

cis-methyl formate is an important interstellar molecule and is considered the prototype system for studying the internal rotation of a methyl group [263]. At equilibrium, *cis*-methyl formate possesses a symmetry plane with one pair of equivalent out-of-plane hydrogen atoms (C_s symmetry) and d(C-O-C_m-H_{plane}) = 180.00 degrees, where H_{plane} is the methyl hydrogen on the symmetry plane. In ref. [263], $\Delta B_\tau^{\rm vib}$ contributions derived from a MP2/VTZ cubic force field were combined with the available experimental rotational constants. The agreement between the MP2 and DFT results is good for all parameters that are not related to the H_{plane} atom. In fact, quite large discrepancies are found for both the C_m-H_{plane} bond length (about 0.0052 Å) and the O-C_m-H_{plane} angles (about 0.69 Å). Note that the B2PLYP/VTZ and B3LYP/SNSD are in a very good agreement one another. As noted for propene, the DFT $r_e^{\rm SE}$ show a smaller difference between the C_m-H_{plane} and C_m-H_{out} bond lengths than the MP2 SE equilibrium structure.

Glycolaldehyde can be considered the simplest sugar. Only the *syn* conformer, which is stabilized by an intramolecular hydrogen bond, has been observed by microwave spectroscopy [264–268]. It has C_s symmetry and is completely defined by 12 geometrical parameters. Recently, a SE equilibrium structure was determined by combining the ground-state experimental rotational constants with $\Delta B_\tau^{\rm vib}$ contributions at the MP2/VTZ level [243]. The agreement with the new DFT SE equilibrium structures is generally good, except for some small discrepancies on r(O-H) (0.9618 Å and 0.9611 Åfor B3LYP and B2PLYP, respectively, versus 0.9593 Å for MP2), and a(C1-C2-H) (107.80 and 107.91 degrees versus 108.11 degrees). It is noteworthy that the B3LYP/SNSD $r_e^{\rm SE}$ is in remarkable agreement with the high level fully theoretical r_e (referred to as $r_e^{\rm BO}$ in Table 6 of ref. [243]): r(O-H)=0.9653 Å and a(C1-C2-H)=107.794 Å.

The *syn* conformer of propanal, or propionaldehyde, which is significantly more

stable than its *gauche* counterpart, has C_s symmetry (with d(C1-C2-C-H_{plane}) = 180.00) degrees) and is completely defined by 15 geometrical parameters. Once again, Table 5.4 shows that MP2/VTZ [243], B2PLYP/VTZ and B3LYP/SNSD cubic force fields lead to very similar SE equilibrium structures.

Finally, we report the first determination of the SE equilibrium structures of peroxyformic, glyoxylic and pyruvic acids (C_s symmetry) in Table 5.5, together with the B2PLYP/VTZ equilibrium geometries and the best r_e structures available for comparison purposes.

Peroxyformic acid is the simplest organic peroxyacid exhibiting internal hydrogen bonding. It presents a planar structure completely characterized by 9 geometrical parameters. The B2PLYP/VTZ and B3LYP/SNSD $r_e^{\rm SE}$ structures reported in Table 5.5 show a very good agreement for all parameters except the OH bond length, where the B3LYP result shows a quite large value (0.9770 Å) with respect to the B2PLYP counterpart (0.9720 Å). To the best of our knowledge, the most accurate r_e geometry presented in the literature has been optimized at MP2/AVTQZ level [269]. It is reported in Table 5.5, even if not enough accurate to allow a reliable quantitative comparison.

Glyoxylic acid is the simplest α-oxoacid (defined by 11 geometrical parameters), while pyruvic acid is the simplest of the alpha-keto acids, with a carboxylic acid and a ketone functional group (defined by 17 geometrical parameters). For the former, the DFT SE equilibrium structures have been obtained by fitting the SE I_B^e and I_C^e moments of inertia of 8 out of 9 experimentally observed isotopologues, where the $H^{13}COCOOH$ isotopologue has been excluded from the fits because of the large residuals shown by the fitted equilibrium rotational constants. The fit for the $r_e^{\rm SE}$ structures of pyruvic acid have been performed using SE I_A^e, I_B^e and I_C^e moments of inertia, with 3, 2 and 1 as weights respectively, of $CH_3COC^{18}OOH$, $CH_3COCO^{18}OH$ and $CH_3COCOOD$ isotopologues, and SE I_A^e and I_C, with 3 and 1 as weights respectively, of all other isotopologues. In Table 5.5, the SE equilibrium structures are compared with the theoretical r_e equilibrium geometries, optimized at the CCSD(T)/VQZ level for glyoxylic acid (from ref. [270]), and at the CCSD(T)/CBS+CV level for pyruvic acid (from this work).

Same discrepancies are found for the C1-C2 bonds, underestimated in the $r_e^{\rm SE}$ results (1.5211 Å and 1.5356 Å for glyoxylic and pyruvic acids, respectively) with respect to the B2PLYP $r_e^{\rm SE}$ (1.5244 Å and 1.5382 Å) and the CCSD(T) r_e (1.5256 Åand 1.5387 Å), and for the C=O bonds, where the largest differences are for r(C2=O) in pyruvic acid (1.2019 Å, 1.1980 Å and 1.1979 Å for B3LYP $r_e^{\rm SE}$, B2PLYP $r_e^{\rm SE}$ and CCSD(T) r_e, respectively). Differently from all systems considered above, for these last two molecules, the B3LYP and B2PLYP SE geometries then show differences that are relevant. The B2PLYP parameters are better in agreement with the fully theoretical results.

Table 5.4: r_e^{SE} and r_e geometries of CH_2F_2, CCl_2F_2, CH_2Cl_2, $CHClF_2$, ethene, ethenol, propene, butadiene, cyclopropane, aziridine, benzene, pyrrole, pyrazole, imidazole, furan, thiophene, maleic anhydride, pyridine, dimethyl ether, *cis* and *trans*-formic acid, *cis*-methyl formate, glycolaldehyde and propanal. Distances in Å, angles in degrees.

	r_e^{SE}[a]			r_e
	Literature	B2PLYP	B3LYP	B3LYP
		– halomethanes –		
CH_2F_2[b]				
r(C-F)	1.35323(1)†	1.3532(1)†	1.3533(1)†	1.3668
r(C-H)	1.08703(3)	1.0868(1)	1.0867(2)	1.0935
a(F-C-F)	108.282(2)	108.29(1)	108.29(1)	108.44
a(H-C-H)	113.442(9)	113.48(1)	113.48(2)	113.74
a(H-C-F)	108.750(2)	108.74(1)	108.74(1)	108.64
Rms resid. [MHz]	-	0.0005	0.0013	-
CCl_2F_2[c]				
r(C-F)	1.3287(8)†	1.3285(9)†	1.3286(7)†	1.3372
r(C-Cl)	1.7519(7)	1.7520(8)	1.7519(6)	1.7857
a(F-C-F)	107.75(9)	107.78(8)	107.77(6)	108.04
a(Cl-C-Cl)	111.62(7)	111.61(5)	111.61(4)	111.83
a(Cl-C-F)	109.35(1)	109.34(3)	109.34(3)	109.22
Rms resid. [MHz]	-	0.0010	0.0008	-
CH_2Cl_2[d]				
r(C-H)	1.0816(2)†	1.0816(8)†	1.0810(8)†	1.0862
r(C-Cl)	1.76425(3)	1.7640(2)	1.7642(2)	1.7956
a(H-C-H)	111.772(4)	111.77(9)	111.79(9)	112.48
a(Cl-C-Cl)	112.166(3)	112.18(2)	112.18(2)	112.85
a(Cl-C-H)	108.237(10)	108.23(3)	108.23(3)	107.90
Rms resid. [MHz]	-	0.0066	0.0069	-
$CHClF_2$[d]				
r(C-H)	1.0850(11)	1.0850(1)†	1.0849(2)†	1.0901
r(C-F)	1.3363(5)	1.3360(2)	1.3363(4)	1.3466
r(C-Cl)	1.7560(9)	1.7562(5)	1.7558(8)	1.7915
a(H-C-F)	109.97(4)	109.98(3)	110.02(4)	110.14
a(H-C-Cl)	109.60(6)	109.56(5)	109.45(9)	109.16
a(F-C-Cl)	109.62(4)	109.61(1)	109.63(2)	109.58
a(F-C-F)	108.06(6)	108.09(2)	108.06(3)	108.23
Rms resid. [MHz]	-	0.0004	0.0006	-
		– substituted alkene compounds –		
ethene[e]				
r(C=C)	1.3305(10)	1.3311(1)†	1.3317(1)†	1.3322
r(C-H)	1.0805(10)	1.0807(1)	1.0805(1)	1.0870
a(C=C-H)	121.45(10)	121.42(1)	121.40(1)	121.71
a(H-C-H)	117.10(10)	117.16(1)	117.19(1)	116.58
Rms resid. [MHz]	-	0.0003	0.0002	-
Mean Δ_e [uÅ^2]	-	0.00062	0.00119	-
ethenol[f]				
r(O-H)	0.9604(2)†	0.9603(1)†	0.9605(1)†	0.9668
r(C2-O)	1.3594(8)	1.3596(1)	1.3598(1)	1.3638

r(C2-H)	1.0794(4)	1.0790(1)	1.0789(1)	1.0860
r(C1=C2)	1.3312(9)	1.3313(1)	1.3316(1)	1.3344
r(C1-H_{cis})	1.0816(2)	1.0814(1)	1.0812(1)	1.0873
r(C1-H_{trans})	1.0772(4)	1.0772(1)	1.0770(1)	1.0831
a(C2-O-H)	108.81(4)	108.75(1)	108.70(1)	109.41
a(C1=C2-H)	122.65(32)	122.51(7)	122.58(8)	122.74
a(C1=C2-O)	126.297(5)	126.28(1)	126.26(1)	126.84
a(C2-C1-H_{cis})	121.90(4)	121.88(1)	121.87(1)	122.29
a(C2-C1-H_{trans})	119.59(2)	119.59(1)	119.58(1)	119.86
Rms resid. [MHz]	-	0.0001	0.0001	-
Mean Δ_e [uÅ^2]	−0.00424	−0.00381	−0.00206	-
propene[g]				
r(C1=C2)	1.3310(7)†	1.3315(4)†	1.3326(2)†	1.3340
r(C2-C3)	1.4956(7)	1.4958(4)	1.4956(2)	1.5004
r(C1-H_{cis})	1.0834(6)	1.0824(5)	1.0818(2)	1.0882
r(C1-H_{trans})	1.0805(12)	1.0800(5)	1.0804(2)	1.0862
r(C2-H)	1.0857(4)	1.0844(3)	1.0841(2)	1.0909
r(C3-H_{plane})	1.0862(8)	1.0873(9)	1.0880(4)	1.0947
r(C3-H_{out})	1.0949(9)	1.0917(16)	1.0895(7)	1.0976
a(C1=C2-C3)	124.47(2)	124.44(2)	124.43(1)	125.29
a(C2-C1-H_{cis})	121.08(5)	121.17(3)	121.13(2)	121.56
a(C2-C1-H_{trans})	121.55(14)	121.44(6)	121.31(3)	121.59
a(C1=C2-H)	118.75(13)	119.07(7)	118.84(4)	118.68
a(C2=C3-H_{plane})	111.10(4)	111.08(3)	111.07(2)	111.55
a(C2-C3-H_{out})	110.53(11)	110.85(16)	111.02(7)	111.03
d(C1=C2-C3-H_{out})	121.08(14)	120.70(18)	120.47(8)	120.80
Rms resid. [MHz]	-	0.0004	0.0002	-
butadiene[e]				
r(C1=C2)	1.3376(10)	1.3380(2)	1.3386(1)†	1.3411
r(C2-C3)	1.4539(10)	1.4547(2)	1.4543(2)	1.4561
r(C1-H_{cis})	1.0819(10)	1.0817(1)	1.0815(1)	1.0876
r(C1-H_{trans})	1.0793(10)	1.0796(1)	1.0793(1)	1.0854
r(C2-H)	1.0847(10)	1.0842(1)	1.0839(1)	1.0903
a(C1=C2-C3)	123.62(10)	123.54(1)	123.53(1)	124.29
a(C1=C2-H)	119.91(10)	119.81(2)	119.76(1)	119.34
a(C2=C1-H_{cis})	120.97(10)	120.96(1)	120.94(1)	121.41
a(C2=C1-H_{trans})	121.47(10)	121.45(1)	121.43(1)	121.63
Rms resid. [MHz]	-	0.0003	0.0002	-
Mean Δ_e [uÅ^2]	-	−0.00885	−0.00790	-
– cyclic and heterocyclic compounds –				
cyclopropane[h]				
r(C-C)	1.5030(10)	1.5024(1)	1.5031(1)†	1.5094
r(C-H)	1.0786(10)	1.0790(2)	1.0787(2)	1.0856
a(H-C-H)	114.97(10)	114.87(2)	114.94(2)	114.25
Rms resid. [MHz]	-	0.0020	0.0022	-
aziridine[i]				
r(C-N)	1.47013(6)†	1.4708(1)†	1.4714(1)†	1.4740
r(C-C)	1.47703(8)	1.4772(1)	1.4777(1)	1.4845
r(N-H)	1.01279(13)	1.0124(1)	1.0126(1)	1.0180
r(C-H_{cis})	1.08099(13)	1.0804(1)	1.0805(1)	1.0877
r(C-H_{trans})	1.07971(13)	1.0797(1)	1.0791(1)	1.0866

a(C-N-H)	109.376(9)	109.27(1)	109.16(1)	110.03
a(C-N-C)	60.311(6)	60.29(1)	60.28(1)	60.47
a(N-C-C)	59.845(3)	59.86(1)	59.86(1)	59.77
a(N-C-H_{cis})	118.28(2)	118.43(1)	118.19(1)	118.61
a(N-C-H_{trans})	114.46(2)	114.20(1)	114.38(1)	114.66
a(C-C-H_{cis})	117.829(14)	117.99(1)	117.81(1)	117.99
a(C-C-H_{trans})	119.538(14)	119.36(1)	119.49(1)	119.85
Rms resid. [MHz]	-	0.0002	0.0001	-
benzene[j]				
r(C-C)	1.3914(10)	1.3916(1)	1.3919(1)†	1.3961
r(C-H)	1.0802(20)	1.0799(1)	1.0795(1)	1.0865
Rms resid. [MHz]	-	0.0009	0.0016	-
Mean Δ_e [uÅ^2]	-	-	-	
pyrrole[k]				
r(C-N)	1.36940(17)†	1.3689(1)†	1.3694(1)†	1.3755
r(C2-C3)	1.3723(2)	1.3731(1)	1.3732(1)	1.3794
r(C3-C4)	1.4231(4)	1.4226(2)	1.4228(2)	1.4256
r(N-H)	1.00086(14)	1.0012(1)	1.0007(1)	1.0081
r(C2-H)	1.07532(13)	1.0746(1)	1.0744(1)	1.0801
r(C3-H)	1.07527(16)	1.0748(1)	1.0745(1)	1.0810
a(H-N-C2)	125.096(8)	125.08(1)	125.09(1)	125.08
a(C5-N-C2)	109.809(16)	109.84(1)	109.82(1)	109.85
a(N-C2-C3)	107.762(15)	107.75(1)	107.76(1)	107.66
a(C2-C3-C4)	107.334(12)	107.33(1)	107.33(1)	107.42
a(N-C2-H)	120.99(7)	121.23(2)	121.12(2)	121.16
a(C2-C3-H)	125.94(6)	125.88(2)	125.88(2)	125.70
Rms resid. [MHz]	-	0.0001	0.0001	-
Mean Δ_e [uÅ^2]	-	0.00236	0.00018	-
pyrazole[l]				
r(N1-N2)	1.3431(6)†	1.3438(1)	1.3441(1)†	1.3486
r(N2=C3)	1.3286(7)	1.3289(1)	1.3289(1)	1.3329
r(C3-C4)	1.4093(6)	1.4087(11)	1.4090(11)	1.4144
r(C4=C5)	1.3771(8)	1.3761(1)	1.3765(1)	1.3817
r(C5-N1)	1.3523(6)	1.3516(1)	1.3519(1)	1.3587
r(N1-H)	1.0014(4)	1.0016(1)	1.0014(1)	1.0092
r(C3-H)	1.0755(4)	1.0761(1)	1.0757(1)	1.0817
r(C4-H)	1.0736(4)	1.0741(1)	1.0739(1)	1.0797
r(C5-H)	1.0740(5)	1.0749(1)	1.0745(1)	1.0805
a(N1-N2-C3)	104.18(3)	104.11(1)	104.11(1)	104.23
a(N2-C3-C4)	111.90(5)	111.92(2)	111.93(2)	111.88
a(C3-C4-C5)	104.46(4)	104.47(2)	104.46(2)	104.53
a(C4-C5-N1)	106.23(4)	106.26(1)	106.26(1)	106.19
a(C5-N1-N2)	113.24(5)	113.24(3)	113.24(3)	113.18
a(N2-N1-H)	118.97(11)	118.87(2)	118.95(2)	119.06
a(N2-C3-H)	119.49(14)	119.42(3)	119.51(3)	119.49
a(C3-C4-H)	128.32(13)	128.20(3)	128.18(3)	128.22
a(N1-C5-H)	121.84(11)	121.70(2)	121.75(2)	121.82
Rms resid. [MHz]	-	0.0001	0.0001	-
Mean Δ_e [uÅ^2]	-	0.00021	0.00120	-

imidazole[m]				
r(N1-C2)	1.3612(9)†	1.3613(7)†	1.3616(7)†	1.3671
r(C2=N3)	1.3111(8)	1.3101(6)	1.3103(6)	1.3161
r(N3-C4)	1.3797(8)	1.3792(5)	1.3794(5)	1.3789
r(C4=C5)	1.3627(8)	1.3624(41)	1.3627(41)	1.3731
r(C5-N1)	1.3738(9)	1.3741(5)	1.3743(5)	1.3802
r(N1-H)	1.0008(5)	1.0016(3)	1.0011(3)	1.0096
r(C2-H)	1.0759(6)	1.0772(3)	1.0770(3)	1.0817
r(C4-H)	1.0747(6)	1.0755(4)	1.0752(4)	1.0809
r(C5-H)	1.0764(5)	1.0765(4)	1.0764(4)	1.0793
a(N1-C2-N3)	111.91(6)	111.92(4)	111.93(4)	111.56
a(C2-N3-C4)	105.02(5)	105.03(4)	105.03(4)	105.43
a(N3-C4-C5)	110.60(6)	110.62(8)	110.62(8)	110.61
a(C4-C5-N1)	105.45(6)	105.42(21)	105.43(21)	105.12
a(C5-N1-C2)	107.02(5)	107.01(16)	106.99(16)	107.29
a(C2-N1-H)	126.23(16)	126.20(11)	126.15(11)	126.41
a(N1-C2-H)	122.53(12)	122.34(9)	122.37(9)	122.43
a(N3-C4-H)	121.51(11)	121.48(9)	121.45(9)	121.40
a(N1-C5-H)	121.92(12)	121.94(9)	121.90(9)	122.22
Rms resid. [MHz]	-	0.0007	0.0006	-
Mean Δ_e [uÅ^2]	-	0.00097	0.00096	-
furan[n]				
r(C2-O)	1.3594(7)†	1.3598(1)†	1.3598(4)†	1.3647
r(C2=C3)	1.3552(8)	1.3551(2)	1.3542(4)	1.3611
r(C3-C4)	1.432(2)	1.4317(0)	1.4344(19)	1.4357
r(C2-H)	1.0735(7)	1.0731(2)	1.0739(3)	1.0790
r(C3-H)	1.0753(6)	1.0751(1)	1.0743(3)	1.0806
a(C2-O-C5)	106.63(6)	106.61(2)	106.50(3)	106.89
a(O-C2-C3)	110.66(9)	110.66(2)	110.79(4)	110.42
a(C2-C3-C4)	106.03(7)	106.04(3)	105.96(6)	106.14
a(H-C2-O)	115.88(6)	115.88(1)	115.82(3)	115.85
a(H-C3-C4)	127.66(5)	127.68(1)	127.61(3)	127.46
Rms resid. [MHz]	-	0.0003	0.0010	-
Mean Δ_e [uÅ^2]	-	−0.00097	0.00116	-
thiophene[o]				
r(S-C2)	1.704(2)	1.7126(5)†	1.7127(5)†	1.7404
r(C2=C3)	1.372(3)	1.3622(8)	1.3625(9)	1.3678
r(C3-C4)	1.421(4)	1.4233(21)	1.4233(21)	1.4289
r(C2-H)	1.085(5)	1.0771(5)	1.0772(5)	1.0811
r(C3-H)	1.088	1.0794(3)	1.0792(3)	1.0844
a(C2-S-C5)	92.4(2)	91.88(4)	91.88(4)	91.32
a(S-C2-C3)	111.6	111.66(3)	111.66(3)	111.53
a(C2=C3-C4)	112.2	112.40(7)	112.40(7)	112.81
a(H-C2-S)	119.9(3)	120.11(10)	120.06(10)	119.84
a(H-C3-C4)	124.4(4)	124.14(2)	124.14(3)	123.92
Rms resid. [MHz]	-	0.0009	0.0010	-
Mean Δ_e [uÅ^2]	-	0.00147	0.00340	-

maleic anhydride[p]				
r(C1=C2)	1.3324(5)†	1.3326(6)†	1.3320(10)†	1.3355
r(C2-C3)	1.4849(5)	1.4848(2)	1.4857(3)	1.4895
r(C3-O4)	1.3848(3)	1.3845(1)	1.3843(2)	1.3941
r(C3=O7)	1.1894(2)	1.1896(1)	1.1896(2)	1.1948
r(C1-H)	1.0765(2)	1.0760(1)	1.0761(1)	1.0822
a(C1=C2-C3)	107.96(1)	107.94(2)	107.94(3)	108.15
a(C2-C3=O7)	129.67(3)	129.65(1)	129.59(2)	129.85
a(C1=C2-H)	129.90(1)	129.86(1)	129.93(1)	129.84
a(C2-C3-O4)	107.78(2)	107.81(1)	107.79(2)	107.59
a(C3-O4-C5)	108.52(3)	108.51(1)	108.53(2)	108.53
a(O4-C5=O6)	122.55(4)	122.55(2)	122.61(3)	122.56
Rms resid. [MHz]	-	0.0003	0.0004	-
Mean Δ_e [uÅ^2]	−0.00057	−0.00499	−0.00779	-
pyridine[m]				
r(C2-C3)	1.3902(4)†	1.3907(2)†	1.3907(18)†	1.3954
r(C3-C4)	1.3890(4)	1.3885(2)	1.3888(13)	1.3930
r(N-C2)	1.3362(5)	1.3356(5)	1.3358(40)	1.3391
r(C2-H)	1.0816(4)	1.0821(2)	1.0818(12)	1.0887
r(C3-H)	1.0795(4)	1.0799(2)	1.0796(11)	1.0858
r(C4-H)	1.0803(4)	1.0806(2)	1.0802(13)	1.0865
a(C6-N-C2)	116.90(4)	116.95(2)	116.93(18)	117.19
a(N-C2-C3)	123.80(4)	123.77(3)	123.79(21)	123.64
a(C2-C3-C4)	118.54(4)	118.54(1)	118.53(11)	118.50
a(C3-C4-C5)	118.42(4)	118.43(1)	118.44(10)	118.54
a(N-C2-H)	115.90(5)	115.99(4)	115.97(28)	116.00
a(C3-C2-H)	120.30(6)	120.24(2)	120.25(18)	120.36
a(C2-C3-H)	120.11(6)	120.09(2)	120.10(18)	120.22
a(C3-C4-H)	120.71(2)	120.78(1)	120.78(7)	120.73
Rms resid. [MHz]	-	0.0004	0.0031	-
Mean Δ_e [uÅ^2]	-	−0.00232	0.00392	-
– ethers, aldehydes, esters and carboxylic acids –				
dimethyl ether[q]				
r(C-O)	1.40660(2)†	1.4071(1)†	1.4074(1)†	1.4139
r(C-H$_{plane}$)	1.0865(2)	1.0858(2)	1.0855(2)	1.0924
r(C-H$_{out}$)	1.09506(7)	1.0950(1)	1.0949(1)	1.1014
a(C-O-C)	111.100(3)	111.10(1)	111.06(1)	112.55
a(O-C-H$_{plane}$)	107.515(14)	107.50(1)	107.50(2)	107.34
a(O-C-H$_{out}$)	111.191(3)	111.14(1)	111.12(1)	111.40
d(C-O-C-H$_{out}$)	60.542(6)	60.52(1)	60.52(1)	60.67
Rms resid. [MHz]	-	0.0004	0.0005	-
***cis*-formic acid**[r]				
r(C-H)	1.0976(4)†	1.0981(1)†	1.0985(3)†	1.1063
r(C=O)	1.1920(4)	1.1911(1)	1.1910(3)	1.1960
r(C-O)	1.3472(4)	1.3482(1)	1.3485(3)	1.3540
r(O-H)	0.9610(4)	0.9612(1)	0.9619(2)	0.9680
a(H-C=O)	123.26(22)	123.87(3)	124.21(18)	123.99
a(O-C=O)	122.28(1)	122.28(1)	122.30(1)	122.41
a(C-O-H)	109.28(3)	109.18(1)	109.00(2)	109.71
Rms resid. [MHz]	-	0.0001	0.0003	-
Mean Δ_e [uÅ^2]	-	0.00008	−0.00067	-

***trans*-formic acid**[r]				
r(C-H)	1.0920(1)†	1.0918(2)†	1.0918(3)†	1.1000
r(C=O)	1.1980(1)	1.1976(3)	1.1973(5)	1.2026
r(C-O)	1.3406(1)	1.3411(3)	1.3417(5)	1.3469
r(O-H)	0.9662(1)	0.9660(2)	0.9656(4)	0.9729
a(H-C=O)	125.04(1)	125.14(15)	125.38(22)	125.15
a(O-C=O)	124.83(1)	124.81(1)	124.78(1)	125.05
a(C-O-H)	106.97(1)	106.81(2)	106.78(2)	107.37
Rms resid. [MHz]	-	0.0004	0.0005	-
Mean Δ_e [uÅ^2]	-	0.00005	0.00057	-
***cis*-methyl formate**[s]				
r(C_m-O)	1.4341(5)†	1.4347(13)†	1.4358(16)†	1.4440
r(C-O)	1.3345(4)	1.3346(13)	1.3343(15)	1.3411
r(C_m-H_{plane})	1.0793(10)	1.0848(25)	1.0845(30)	1.0893
r(C_m-H_{out})	1.0871(3)	1.0870(7)	1.0875(8)	1.0924
r(C-H)	1.0930(5)	1.0923(15)	1.0925(18)	1.1006
r(C=O)	1.2005(5)	1.2003(14)	1.2001(17)	1.2049
a(C_m-O-C)	114.32(4)	114.30(11)	114.26(13)	115.77
a(O-C_m-H_{plane})	106.05(16)	105.40(35)	105.35(42)	105.46
a(O-C_m-H_{out})	110.19(2)	110.15(5)	110.07(5)	110.24
a(O-C-H)	109.96(5)	109.58(14)	109.54(17)	109.24
a(O-C=O)	125.50(5)	125.47(14)	125.50(16)	125.81
d(H_{out}-C-O-C)	−60.28(3)	−60.37(7)	−60.36(8)	−60.37
Rms resid. [MHz]	-	0.0021	0.0025	-
glycolaldehyde[q]				
r(C1=O)	1.2086(4)†	1.2088(3)†	1.2083(5)†	1.2115
r(C1-H)	1.1015(3)	1.1010(2)	1.1011(4)	1.1096
r(C1-C2)	1.5003(3)	1.5006(2)	1.5014(4)	1.5065
r(C2-H)	1.0969(2)	1.0964(1)	1.0964(2)	1.1033
r(C2-O)	1.3962(3)	1.3965(2)	1.3970(4)	1.4014
r(O-H)	0.9593(5)	0.9611(3)	0.9618(6)	0.9721
a(C2-C1=O)	121.65[t]	121.65(2)	121.68(4)	122.05
a(C2-C1-H)	116.91[t]	116.90(3)	116.85(5)	116.47
a(C1-C2-H)	108.11(2)	107.91(1)	107.80(3)	107.79
a(C1-C2-O)	111.75(3)	111.78(2)	111.72(3)	112.63
a(C2-O-H)	106.28(2)	106.18(2)	106.14(3)	106.53
d(H-C2-C1=O)	122.35(2)	122.34(1)	122.27(2)	122.82
Rms resid. [MHz]	-	0.0003	0.0006	-
propanal[q]				
r(C1-C2)	1.5023(6)†	1.5022(4)†	1.5037(4)†	1.5087
r(C2-C3)	1.5164(4)	1.5162(5)	1.5165(4)	1.5260
r(C3-H_{plane})	1.0884(3)	1.0888(4)	1.0879(3)	1.0943
r(C3-H_{out})	1.0883(2)	1.0884(2)	1.0888(2)	1.0938
r(C2-H)	1.0949(2)	1.0950(2)	1.0946(2)	1.1012
r(C1=O)	1.2074(4)	1.2075(5)	1.2075(4)	1.2099
r(C1-H)	1.1056(3)	1.1057(4)	1.1040(3)	1.1145
a(C2-C3-H_{plane})	110.66(4)	110.61(6)	110.52(6)	110.62
a(C2-C3-H_{out})	110.72(2)	110.72(1)	110.68(1)	111.02

a(C1-C2-C3)	113.60(2)	113.61(4)	113.65(3)	114.84
a(C1-C2-H)	106.95(3)	106.95(3)	106.75(3)	106.63
a(C2-C1-O)	124.38(3)	124.37(4)	124.34(4)	124.98
a(C2-C1-H)	115.44(3)	115.45(5)	115.34(4)	114.91
d(O-C1-C2-H)	123.77(2)	123.79(3)	123.78(2)	124.39
d(C1-C2-C3-H_{out})	59.46(2)	59.46(2)	59.42(2)	59.64
Rms resid. [MHz]	-	0.0005	0.0004	-

B2PLYP and B3LYP are used in conjunction with VTZ and SNSD basis sets, respectively.
a) All fits have been performed on moments of inertia. For all structures evaluated in this work, the uncertainties on the geometrical parameters are reported within parentheses, rounded to $1{\cdot}10^{-4}$ Å for lengths and $1{\cdot}10^{-2}$ degrees for angles if smaller than these values. $\Delta_e = I_C - I_B - I_A$ is the inertial defect. † denotes the inclusion of $\Delta B_\tau^{\mathrm{el}}$.
b) MP2/VTZ r_e^{SE} from ref. [240].
c) B3LYP/6-311+G(3df,2pd) r_e^{SE} from ref. [240].
d) MP2/V(T+d)Z r_e^{SE} from ref. [240].
e) literature r_e^{SE} obtained as average of different MP2 and B3LYP r_e^{SE}, with basis sets of at least triple-ζ quality, where the $\Delta B_{\mathrm{vib}}^{\beta}$ are derived coupling scaled quadratic force fields with unscaled cubic force fields, from ref. [242].
f) MP2/VQZ r_e^{SE} from ref. [243].
g) MP2/VTZ r_e^{SE} from ref. [245].
h) SDQ-MBPT(4)/VTZ r_e^{SE} from ref. [247].
i) MP2/VTZ r_e^{SE} from ref. [252].
j) SDQ-MBPT(4)/VTZ r_e^{SE} from ref. [248].
k) MP2(AE)/wCVTZ r_e^{SE} from ref. [252].
l) B3LYP/6-311+G(3df,2pd) r_e^{SE} from ref. [252].
m) B3LYP/6-311+G(3df,2pd) r_e^{SE} from ref. [252], where the experimental ground-state rotational constants were corrected within the predicates method.
n) MP2/VTZ r_e^{SE} from ref. [254].
o) SE structure ED + MW + vibSP(B3LYP/6-311+G* force field), see ref. [255].
p) MP2/VTZ r_e^{SE} from ref. [256].
q) MP2/VTZ r_e^{SE} from ref. [243].
r) MP2/VTZ r_e^{SE} from ref. [262].
s) MP2/VTZ r_e^{SE} from ref. [263].
t) values calculated as $121.65 = 180.00 - 58.35$ and $116.91 = 180.00 - 63.09$, where 58.35 and 63.09 are taken from Table 6 of ref. [243].

Table 5.5: r_e^{SE} and r_e geometries for peroxyformic, glyoxylic and pyruvic acids. Distances in Å, angles in degrees.

	r_e^{SE}[a]		r_e		
	B3LYP	B2PLYP	B3LYP	B2PLYP	Best theo.
peroxyformic acid[b]					
r(C-H)	1.0900(2)†	1.0905(1)†	1.0987	1.0919	1.090
r(C=O)	1.2017(1)	1.2015(1)	1.2059	1.2042	1.205
r(C-O)	1.3379(2)	1.3368(1)	1.3432	1.3406	1.340
r(O-O)	1.4389(1)	1.4390(1)	1.4390	1.4414	1.432
r(O-H)	0.9770(2)	0.9720(3)	0.9852	0.9808	0.981
a(H-C=O)	127.01(1)	126.96(1)	127.18	127.05	127.3
a(H-C-O)	108.72(1)	108.72(1)	108.42	108.43	108.3
a(O=C-O)	124.27(2)	124.32(2)	124.40	124.52	124.4
a(C-O-O)	110.30(1)	110.31(1)	111.49	110.70	110.3
a(O-O-H)	100.51(1)	100.78(1)	101.27	100.42	100.5
Rms resid. [MHz]	0.0003	0.0002	-	-	-
glyoxylic acid[c]					
r(C1-C2)	1.5211(3)†	1.5244(3)†	1.5345	1.5276	1.5256
r(C1-H)	1.0964(3)	1.0966(3)	1.1045	1.0977	1.0963
r(C1=O)	1.2067(3)	1.2054(3)	1.2080	1.2081	1.2087
r(C2=O)	1.1994(3)	1.1967(3)	1.2034	1.2011	1.1977
r(C2-O)	1.3325(3)	1.3316(4)	1.3373	1.3356	1.3317
r(O-H)	0.9692(4)	0.9697(4)	0.9764	0.9727	0.9697
a(C2-C1-H)	115.59(2)	115.48(2)	115.13	115.13	115.41
a(C2-C1=O)	120.60(3)	120.69(3)	121.03	121.01	120.66
a(C1-C2=O)	121.95(3)	121.86(3)	121.74	121.97	121.90
a(C1-C2-O)	113.70(3)	113.48(3)	113.78	113.25	113.35
a(C-O-H)	106.84(2)	107.10(2)	107.67	106.95	106.74
Rms resid. [MHz]	0.0003	0.0003	-	-	-
Mean Δ_e [uÅ^2]	−0.01110	−0.01327	-	-	-
pyruvic acid[d]					
r(C1-C2)	1.5356(13)†	1.5382(8)†	1.5507	1.5434	1.5387
r(C1-C_m)	1.4877(12)	1.4898(7)	1.5042	1.4916	1.4893
r(C_m-H_p)	1.0812(9)	1.0819(5)	1.0904	1.0845	1.0845
r(C_m-H_o)	1.0909(3)	1.0902(2)	1.0955	1.0895	1.0893
r(C1=O)	1.2157(9)	1.2115(5)	1.2075	1.2153	1.2114
r(C2=O)	1.2019(9)	1.1980(5)	1.2091	1.2021	1.1979
r(C2-O)	1.3289(10)	1.3311(6)	1.3401	1.3346	1.3297
r(O-H)	0.9725(6)	0.9678(4)	0.9717	0.9746	0.9706
a(C1-C_m-H_p)	110.22(7)	110.19(4)	109.39	110.06	109.88
a(C1-C_m-H_o)	109.16(4)	109.26(2)	110.07	109.51	109.35

a(C2-C1-C_m)	117.27(12)	116.93(7)	114.95	116.98	116.91
a(C2-C1=O)	117.53(9)	117.75(5)	120.29	117.80	117.70
a(C1-C2=O)	122.71(9)	122.87(6)	122.84	123.10	122.80
a(C1-C2-O)	113.14(12)	112.81(7)	112.64	112.45	112.81
a(C2-O-H)	106.01(4)	106.39(3)	107.01	106.03	106.40
d(C2-C1-C_m-H_o)	57.77(6)	57.80(4)	58.36	58.01	58.07
Rms resid. [MHz]	0.0013	0.0008	-	-	-

B2PLYP and B3LYP are used in conjunction with VTZ and SNSD basis sets, respectively.
a) The uncertainties on the geometrical parameters are reported within parentheses, rounded to $1{\cdot}10^{-4}$ Å for lengths and $1{\cdot}10^{-2}$ degrees for angles if smaller than these values. $\Delta_e = I_C - I_B - I_A$ is the inertial defect. † denotes the inclusion of $\Delta B_\tau^{\rm el}$.
b) The fits have been performed using SE I_e^A, I_e^C moments of inertia. The best theo. r_e has been optimized at the MP2/AVQZ level, from ref. [269].
c) The fits have been performed using SE I_B^e and I_C^e moments of inertia. The best theo. r_e has been optimized at the CCSD(T)/VQZ level, from ref. [270].
d) The fits have been performed using SE I_A^e, I_B^e and I_C^e moments of inertia, with 3, 2 and 1 weight respectively, on $CH_3COC^{18}OOH$, $CH_3COCO^{18}OH$ and $CH_3COCOOD$ and SE I_A^e and I_C^e, with 3, 1 weight respectively, on all other isotopomers. The best theo. r_e has been optimized at the CCSD(T)/CBS+CV level [271].

Figure 5.3: Sketch of the 4 molecules determined within the template approach.

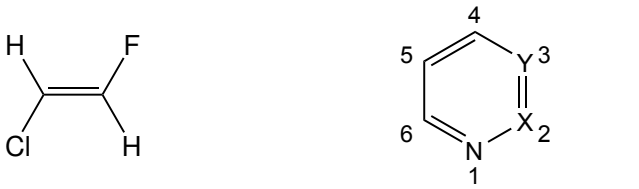

(a) *trans*-CHFCHCl

(b) (X,Y)
(CH, N) pyrimidine
(CF,CH) 2-fluoropyridine
(CH,CF) 3-fluoropyridine

5.4 Toward larger systems: the template approach

In all cases presented above, a large number of experimental data, coupled with a limited number of molecular parameters, permitted the complete determination of the molecular structure. This is often not possible when the molecular size and topological complexity increase because of the large number of isotopologues then required.

In these cases, the strategy widely adopted in the literature consists of fixing in the fitting procedure some parameters to the corresponding computed values [206, 208–210], or allowing some internal coordinates (called predicates) to vary from reference values within given uncertainties [272]. Although, as shown above, $\Delta B_\tau^{\rm vib}$

and $\Delta B_\tau^{\mathrm{el}}$ contributions calculated at the DFT level lead to very good r_e^{SE} results, the fixed parameters (or reference values within the predicated methodology) need to be estimated at much higher levels of theory to achieve good accuracy. An example is provided by the case of glycine Ip, for which the differences between the CCSD(T)/VTZ and CCSD(T)/CBS+CV equilibrium structures are significant [273]. Since CCSD(T)/CBS+CV calculations for large systems are computationally very expensive, they are not always feasible.

In the following, we present a new approach to deal with medium-large systems and a series of test cases that allow us to point out its reliability. When one is interested in the determination of the r_e^{SE} structure of a molecule for which high-level computations are too expensive, it is possible to use a similar molecule (e.g., an isomer or substituted system), for which an accurate r_e^{SE} structure is available, as a template for deriving the parameters to be fixed in the fitting procedure. These parameters can be obtained as,

$$r_e(\mathrm{fixed}) = r_e + \Delta\mathrm{TM} \tag{5.3}$$

where ΔTM is defined as

$$\Delta\mathrm{TM} = r_e^{\mathrm{SE}}(\mathrm{TM}) - r_e(\mathrm{TM}) \tag{5.4}$$

r_e is the geometrical parameter of interest calculated at the same level for both the molecule under consideration and that chosen as a reference, denoted as template-molecule (TM).

In the following, some examples of application of this new approach are given and the reachable accuracy is addressed. Due to its low computational cost, and showing the B3LYP/SNSD r_e^{SE} geometries accuracies comparable with those of the B2PLYP/VTZ r_e^{SE} ones, the B3LYP/SNSD level is considered as the preferred computational method in the next sections.

trans-1-chloro-2-fluoroethylene

The first system analyzed is *trans*-1-chloro-2-fluoroethylene, for which the lack of experimental rotational constants for the ^{13}C-containing isotopologues does not allow the determination of the C=C bond length. As discussed above, a possible solution is to fix this parameter at a value obtained at a very high level of theory, as done in ref. [236]. CCSD(T)/CBS+CV equilibrium geometries are available for both *cis* and *trans* isomers (see ref. [236] and Table 5.6) together with a complete r_e^{SE} equilibrium structure for the *cis* species (see Table 5.1). As a consequence, the *cis*-1-chloro-2-fluoroethylene can be used as a template for the estimation of the ΔTM correction for r(CC) of the *trans* isomer. According to eq. 5.4, the difference between the SE and theoretical values of r(CC) in *cis*-chlorofluoroethylene

Table 5.6: r_e equilibrium geometries of cis- and *trans*-1-chloro-2-fluoroethylene. Distances in Å, angles in degrees.

	***cis*-CHFCHCl**		***trans*-CHFCHCl**	
	CBS+CV[a]	B3LYP/SNSD	CBS+CV[a]	B3LYP/SNSD
r(C1-Cl)	1.7107	1.7404	1.7163	1.7495
r(C1-H)	1.0764	1.0818	1.0775	1.0825
r(C1=C2)	1.3249	1.3278	1.3240	1.3266
r(C2-F)	1.3310	1.3416	1.3376	1.3499
r(C2-H)	1.0787	1.0849	1.0785	1.0840
a(Cl-C1=C2)	123.10	123.74	120.63	121.11
a(H-C1-C2)	120.43	120.91	122.95	123.62
a(F-C2=C1)	122.53	123.10	120.14	120.10
a(H-C2=C1)	123.43	123.45	125.82	126.50

a) CCSD(T)/CBS+CV r_e equilibrium geometry from ref. [236].

Table 5.7: r_e^{SE} equilibrium geometries of *trans*-1-chloro-2-fluoroethylene. Distances in Å, angles in degrees.

	r_e^{SE}[a]			
	Fit 1[b]	Fit 2[c]	Fit 3[d]	Fit 4[e]
r(C1-Cl)	1.7188(9)	1.7190(9)	1.7178(9)	1.7179(9)
r(C1-H)	1.0775(21)	1.0774(21)	1.0780(21)	1.0779(21)
r(C1=C2)	1.3236$^{\surd}$	1.3233$^{\surd}$	1.3257$^{\surd}$	1.3254$^{\surd}$
r(C2-F)	1.3395(20)	1.3398(20)	1.3376(20)	1.3379(20)
r(C2-H)	1.0792(27)	1.0792(27)	1.0790(27)	1.0790(27)
a(Cl-C1=C2)	120.46(6)	120.45(6)	120.54(6)	120.53(6)
a(H-C1-C2)	122.60(15)	122.62(15)	122.47(15)	122.49(15)
a(F-C2=C1)	120.17(21)	120.16(21)	120.18(21)	120.18(21)
a(H-C2=C1)	125.86(5)	125.89(5)	125.69(5)	125.71(5)
Rms resid. [MHz]	0.0011	0.0011	0.0011	0.0011
Mean Δ_e [uÅ^2]	0.00308	0.00308	0.00308	0.00308

a) All fits have been performed on SE I_A^e and I_B^e moments of inertia, with 20 and 1 as weights, respectively, derived from $(B_\tau^0)^{\mathrm{exp}}$ constants corrected by B3LYP/SNSD $\Delta B_\tau^{\mathrm{vib}}$ and B3LYP/AVTZ $\Delta B_\tau^{\mathrm{el}}$ contributions. The digits within parentheses are the uncertainties on the geometrical parameters, while $\surd$ denotes the parameter kept fixed, obtained using *cis*-chlorofluoroethylene as TM (see text). $\Delta_e = I_C - I_B - I_A$ is the inertial defect.
b) r_e(fixed) = r_e(CBS+CV) + ΔTM; ΔTM = r_e^{SE}(CCSD(T)/VTZ) − r_e(CBS+CV).
c) r_e(fixed) = r_e(B3LYP/SNSD) + ΔTM; ΔTM = r_e^{SE}(CCSD(T)/VTZ) − r_e(B3LYP/SNSD).
d) r_e(fixed) = r_e(CBS+CV) + ΔTM; ΔTM = r_e^{SE}(B3LYP/SNSD) − r_e(CBS+CV).
e) r_e(fixed) = r_e(B3LYP/SNSD) + ΔTM; ΔTM = r_e^{SE}(B3LYP/SNSD) − r_e(B3LYP/SNSD).

has been employed to correct the theoretical value of the C=C bond length of *trans*-chlorofluoroethylene, obtained at the same level of theory. Subsequently, the corrected r(CC) has been kept fixed in the fits performed, with the corresponding results being reported in Table 5.7.

In all cases, the $\Delta B_\tau^{\rm vib}$ terms have been calculated at the B3LYP/SNSD level, and the B3LYP/AVTZ $\Delta B_\tau^{\rm el}$ contributions have also been included. The fits have been performed on the SE I_A^e and I_B^e moments of inertia, with 20 and 1 as relative weights, since I_B^e is about 20 times larger than I_A^e. The four fits differ for the level of theory used in the evaluation of $r_e^{\rm SE}$ of the template molecule and of r_e: $r_e^{\rm SE}$(C=C) has been taken from the SE equilibrium structure of *cis*-chlorofluoroethylene calculated with either CCSD(T)/VTZ $\Delta B_\tau^{\rm vib}$ contributions, fits 1 and 2, or B3LYP/SNSD $\Delta B_\tau^{\rm vib}$ contributions, fits 3 and 4, while the theoretical r_e(C=C) value at the CCSD(T)/CBS+CV level has been used for fits 1 and 3, and that at the B3LYP/SNSD level for fits 2 and 4. Table 5.7 shows that the results of fits 1 and 2 are similar to one another, and this is also the case for fits 3 and 4.

This suggests that the accuracy of the template approach is rather independent from the chosen theoretical method used in r_e estimation, and only limited by the accuracy of the template-molecule SE equilibrium structure considered. It is noteworthy that fit 4 allowed us to obtain a SE equilibrium structure completely independent from high-level (extremely expensive) computational results. This is particularly appealing in the treatment of medium-large systems, for which structural determinations at highly-correlated levels become computationally too expensive.

pyrimidine

Analogously to the case of *trans*-chlorofluoroethylene, the limited number of isotopologues experimentally investigated (7) makes the derivation of all geometrical parameters of pyrimidine not possible. In particular, no deutereted species have been studied experimentally, thus preventing the derivation of the C-H bond lengths and of the corresponding angles.

In Table 5.8, three different fits for the SE equilibrium structure of pyrimidine are reported, all obtained by correcting the experimental rotational constants with $\Delta B_\tau^{\rm vib}$ contributions at the B3LYP/SNSD level and fitting on the I_A^e and I_C^e moments of inertia, with the inclusion of $\Delta B_\tau^{\rm el}$ (see Table 5.8). To evaluate the nondeterminable parameters, pyridine has been used as TM (fit 1 in Table 5.8). The ΔTM corrections have been derived from the B3LYP/SNSD results of pyridine (Table 5.4). In particular, the N3-C4-H angle of pyrimidine has been estimated by using the ΔTM correction evaluated for the N-C2-H angle of pyridine; the ΔTM corrections for r(C2-H) and r(C4-H) have been based on the values for the C2-H

Table 5.8: r_e and r_e^{SE} equilibrium geometries for pyrimidine. Distances in Å, angles in degrees.

pyrimidine	r_e^{SE}[a]				r_e	
	Fit 1[b]	Fit 2[c]	Fit 3[d]	Literature[e]	Literature[f]	B3LYP/SNSD
r(C2-N3)	1.3334(1)	1.3334(1)	1.3334(1)	1.3331(3)	1.3339	1.3374
r(N3-C4)	1.3355(1)	1.3355(1)	1.3358(1)	1.3349(6)	1.3349	1.3385
r(C4-C5)	1.3868(4)	1.3867(3)	1.3866(4)	1.3874(4)	1.3874	1.3921
r(C2-H)	1.0814$^{\surd}$	1.0822$^{\surd}$	1.0816$^{\surd}$	1.0820(23)	1.0819	1.0883
r(C4-H)	1.0819$^{\surd}$	1.0826$^{\surd}$	1.0820$^{\surd}$	1.0843(17)	1.0824	1.0887
r(C5-H)	1.0789$^{\surd}$	1.0795$^{\surd}$	1.0784$^{\surd}$	1.0799(23)	1.0793	1.0851
a(C2-N3-C4)	115.69(1)	115.69(1)	115.68(1)	115.712(21)	115.656	115.91
a(N3-C4-C5)	122.27(2)	122.27(2)	122.27(2)	122.276(19)	122.332	122.25
a(C4-C5-C6)	116.72(1)	116.72(1)	116.72(2)	116.661(36)	116.632	116.61
a(N1-C2-H)	116.31(1)	116.31(1)	116.31(1)	116.318(19)	116.303	116.46
a(N3-C4-H)	116.45$^{\surd}$	116.37$^{\surd}$	116.32$^{\surd}$	116.48(20)	116.461	116.48
a(C4-C5-H)	121.64(1)	121.64(1)	121.64(1)	121.670(18)	121.684	121.70
Rms resid. [MHz]	0.0004	0.0003	0.0004	-	-	-
Mean Δ_e [uÅ^2]	−0.00133	−0.00133	−0.00133	-	-	-

a) All fits have been performed on SE I_A^e and I_C^e moments of inertia, derived from the $(B_\tau^0)^{\mathrm{EXP}}$ constants corrected by B3LYP/SNSD $\Delta B_\tau^{\mathrm{vib}}$ and B3LYP/AVTZ $\Delta B_\tau^{\mathrm{el}}$ contributions. The digits within parentheses are the uncertainties on the geometrical parameters, while $\surd$ denotes the parameters kept fixed. $\Delta_e = I_C - I_B - I_A$ is the inertial defect.
b) r_e(fixed) = r_e(B3LYP/SNSD) + ΔTM; ΔTM = r_e^{SE}(B3LYP/SNSD) − r_e(B3LYP/SNSD), with pyridine as TM: r(C2-H) and r(C4-H) from r(C2-H), r(C5-H) from r(C3-H), a(N3-C4-H) from a(N-C2-H), see text.
c) r_e(fixed) = r_e(B3LYP/SNSD) + ΔTM; ΔTM = r_e^{SE}(CCSD(T)/ANO0) − r_e(B3LYP/SNSD), with pyridazine as TM: r(C2-H) and r(C4-H) from r(C3-H), r(C5-H) from r(C4-H), a(N3-C4-H) from a(N2-C3-H), see text.
d) r_e(fixed) = r_e(B3LYP/SNSD) + ΔTM; ΔTM = r_e^{SE}(B3LYP/SNSD) − r_e(B3LYP/SNSD), with pyridazine as TM: r(C2-H) and r(C4-H) from r(C3-H), r(C5-H) from r(C4-H), a(N3-C4-H) from a(N2-C3-H), see text.
e) r_e^{SE} structure determined using B3LYP/6-311+G(3df,2pd) $\Delta B_{\mathrm{vib}}^{\beta}$ and the predicate approach, from ref. [252].
f) r_e^{BO}(II) in Table 9 of ref. [252].

distance of pyridine (these three parameters have in common the N-C-H pattern), while for the C5-H distance in pyrimidine the ΔTM correction has been calculated from r(C3-H) of pyridine (these two parameters share a N-CH-C-H pattern). For the SE equilibrium structure of pyrimidine obtained following this procedure (fit 1 in Table 5.8), we expect an accuracy similar to that of a full SE equilibrium structure obtained with B3LYP/SNSD $\Delta B_\tau^{\rm vib}$ contributions.

Fits 2 and 3 in Table 5.8 show that it is possible to obtain very similar results using pyridazine (see Table 5.1) as the TM instead of pyridine. This finding points out another interesting feature of the template approach, that is, the choice of TM is rather flexible: it is sufficient to find a molecule in which the parameter of interest, for example the C4-H bond length in pyrimidine, is present and involved in a similar bond pattern, a N-C-H bond chain for the case under consideration. The comparison of the results for fits 2 and 3 demonstrates that the SE equilibrium structure obtained with the TM approach does not change significantly if the $r_e^{\rm SE}$ (TM) parameter is taken from the best SE equilibrium structure available (CCSD(T)/ANO0 vibrational contributions in this case) or from the B3LYP/SNSD $r_e^{\rm SE}$.

A $r_e^{\rm SE}$ equilibrium structure of pyrimidine has been recently determined using a B3LYP/6-311+G(3df,2pd) cubic force field and the so-called predicate approach based on a CCSD(T) equilibrium geometry [252]. The remarkable agreement between the "template" and the "predicate" $r_e^{\rm SE}$ equilibrium geometries (see Table 5.8) gives further support to the template strategy, which has the advantage of avoiding any expensive CCSD(T) computation.

fluoropyridines

The first determinations of the SE equilibrium structure of 2- and 3-fluoropyridine are reported in Tables 5.9 and 5.10, respectively. Fluorine substitution reduces the molecular symmetry from C_{2v} to C_s, with the consequent increase of the number of unique internal parameters from 10 to 18. Because of the limited number of available experimental data, for these molecules it is not possible to evaluate all structural parameters. Therefore, some parameters have been fixed using the template approach.

Because of the lack of rotational data for deuterated species, only the parameters defining the C-C ring and the C-F bond length have been considered as free parameters for 2-fluoropyridine. On the other hand, for 3-fluoropyridine also the C-F bond length has been kept fixed in order to converge the fitting procedure.

Starting from the assumption that the substitution of a hydrogen atom with fluorine does not affect significantly the structure of the ring, we used pyridine as the TM for 2-fluoropyridine. The best results have been obtained by fitting the SE I_A^e and I_C^e moments of inertia. In fit 1, the ΔTM corrections have been

estimated by considering the CCSD(T)/CBS+CV level for r_e, while in fit 2, r_e has been calculated at the B3LYP/SNSD level. Even in this case, the values in Table 5.4 confirm that the resulting SE structures are negligibly affected by the level of theory chosen for r_e.

For 3-fluoropyridine, we proceeded analogously to 2-fluoropyridine for what concerns the C-H bonds, while, for the C-F distance and the corresponding C3-C2-F angle, 2-fluoropyridine has been employed as the TM. This is consistent with what was discussed above for pyrimidine, namely that the choice of the TM molecule is quite flexible, thus allowing the simultaneous use of more than one TM in the determination of the parameters to be fixed. As in 2-fluoropyridine, we have used the B3LYP/SNSD r_e^{SE} of pyridine combined with both CCSD(T)/CBS+CV (fit 1) and B3LYP/SNSD (fit 2) structures as r_e in the calculation of ΔTM.

Table 5.9: r_e and r_e^{SE} equilibrium geometries for 2-fluoropyridine. Distances in Å, angles in degrees.

2-fluoropyridine	$r_e^{\mathrm{SE}}{}^a$		r_e	
	Fit 1[b]	Fit 2[c]	CBS+CV	B3LYP/SNSD
r(N-C2)	1.3138(10)	1.3135(10)	1.3063	1.3120
r(N-C6)	1.3402(5)	1.3402(5)	1.3410	1.3438
r(C2-C3)	1.3838(14)	1.3840(14)	1.3898	1.3935
r(C3-C4)	1.3837(3)	1.3837(3)	1.3836	1.3898
r(C4-C5)	1.3949(4)	1.3948(4)	1.3933	1.3972
r(C5-C6)	1.3836(4)	1.3836(4)	1.3844	1.3909
r(C2-F)	1.3357(2)	1.3358(2)	1.3344	1.3483
r(C3-H)	1.0781$^{\surd}$	1.0775$^{\surd}$	1.0787	1.0839
r(C4-H)	1.0801$^{\surd}$	1.0796$^{\surd}$	1.0807	1.0860
r(C5-H)	1.0788$^{\surd}$	1.0783$^{\surd}$	1.0794	1.0848
r(C6-H)	1.0809$^{\surd}$	1.0811$^{\surd}$	1.0815	1.0876
a(C6-N-C2)	116.24(6)	116.24(6)	116.42	116.61
a(N-C2-C3)	126.17(7)	126.17(7)	126.17	126.08
a(C2-C3-C4)	116.73(3)	116.72(3)	116.59	116.53
a(C3-C4-C5)	119.06(1)	119.06(1)	119.09	119.21
a(C4-C5-C6)	118.37(0)	118.37(0)	118.39	118.33
a(C5-C6-N)	123.44(2)	123.44(2)	123.35	123.25
a(C3-C2-F)	118.43(12)	118.41(12)	117.87	117.98
a(C2-C3-H)	120.38$^{\surd}$	120.48$^{\surd}$	120.42	120.60
a(C3-C4-H)	120.33(1)	120.33(1)	120.34	120.10
a(C6-C5-H)	120.26$^{\surd}$	120.25$^{\surd}$	120.30	120.37
a(C5-C6-H)	120.86$^{\surd}$	120.86$^{\surd}$	120.91	120.97
Rms resid. [MHz]	0.0001	0.0001	-	-
Mean Δ_e [uÅ^2]	−0.00180	−0.00180	-	-

a) The fits have been performed on the SE I_A^e and I_C^e moments of inertia. The $(B_0^\beta)^{\mathrm{EXP}}$ constants have been corrected by B3LYP/SNSD $\Delta B_\tau^{\mathrm{vib}}$ and B3LYP/AVTZ $\Delta B_\tau^{\mathrm{el}}$ contributions. The digits within parentheses are the uncertainties on the geometrical parameters, while $\surd$ denotes the parameters kept fixed obtained using pyridine as TM, see text. $\Delta_e = I_C - I_B - I_A$ is the inertial defect.
b) r_e(fixed) = r_e(CBS+CV) + ΔTM; ΔTM = r_e^{SE}(B3LYP/SNSD) − r_e(CBS+CV).
c) r_e(fixed) = r_e(B3LYP/SNSD) + ΔTM; ΔTM = r_e^{SE}(B3LYP/SNSD) − r_e(B3LYP/SNSD).

Table 5.10: r_e and r_e^{SE} equilibrium geometries for 3-fluoropyridine. Distances in Å, angles in degrees.

3-fluoropyridine	$r_e^{\mathrm{SE}\,a}$		r_e	
	Fit 1[b]	Fit 2[c]	CBS+CV	B3LYP/SNSD
r(N-C2)	1.3346(9)	1.3352(9)	1.3323	1.3368
r(C2-C3)	1.3931(5)	1.3888(6)	1.3859	1.3904
r(C3-C4)	1.3714(6)	1.3757(6)	1.3786	1.3850
r(C4-C5)	1.3895(8)	1.3901(9)	1.3894	1.3933
r(C5-C6)	1.3940(5)	1.3926(5)	1.3888	1.3955
r(C6-N)	1.3314(9)	1.3326(10)	1.3337	1.3389
r(C2-H)	1.0811$^{\surd}$	1.0813$^{\surd}$	1.0817	1.0877
r(C3-F)	1.3406$^{\surd}$	1.3398$^{\surd}$	1.3393	1.3523
r(C4-H)	1.0791$^{\surd}$	1.0787$^{\surd}$	1.0797	1.0852
r(C5-H)	1.0794$^{\surd}$	1.0791$^{\surd}$	1.0800	1.0856
r(C6-H)	1.0808$^{\surd}$	1.0812$^{\surd}$	1.0814	1.0877
a(C6-N-C2)	117.68(6)	117.65(6)	117.73	117.88
a(N-C2-C3)	121.75(6)	121.85(6)	122.09	121.79
a(C2-C3-C4)	121.07(3)	121.07(3)	120.83	121.04
a(C3-C4-C5)	117.04(2)	116.94(2)	116.84	116.91
a(C4-C5-C6)	118.88(2)	118.91(2)	119.18	118.94
a(C5-C6-N)	123.58(5)	123.58(5)	123.33	123.43
a(C3-C2-H)	119.90$^{\surd}$	120.12$^{\surd}$	119.95	120.23
a(C4-C3-F)	120.59$^{\surd}$	120.19$^{\surd}$	119.14	119.76
a(C3-C4-H)	121.88(1)	121.97(1)	121.96	120.52
a(C6-C5-H)	120.24$^{\surd}$	120.25$^{\surd}$	120.28	120.37
a(C5-C6-H)	120.48$^{\surd}$	120.36$^{\surd}$	120.53	120.47
Rms resid. [MHz]	0.0004	0.0004	-	-
Mean Δ_e [uÅ^2]	−0.00180	−0.00180	-	-

a) The fits have been performed on the SE I_e^A and I_e^B moments of inertia. The $(B_0^\beta)^{\mathrm{EXP}}$ constants have been corrected by B3LYP/SNSD $\Delta B_\tau^{\mathrm{vib}}$ and B3LYP/AVTZ $\Delta B_\tau^{\mathrm{el}}$ contributions. The digits within parentheses are the uncertainties on the geometrical parameters, while $\surd$ denotes the parameters kept fixed obtained using pyridine and 2-fluoropyridine as TM, see text. $\Delta_e = I_C - I_B - I_A$ is the inertial defect.
b) r_e(fixed) = r_e(CBS+CV) + ΔTM; ΔTM = r_e^{SE}(B3LYP/SNSD) − r_e(CBS+CV).
c) r_e(fixed) = r_e(B3LYP/SNSD) + ΔTM; ΔTM = r_e^{SE}(B3LYP/SNSD) − r_e(B3LYP/SNSD).

Chapter 6

Vibrational energies and thermodynamics

The theoretical approach presented in the previous section has been included in a development version of the GAUSSIAN package [274]. The implementation can be used with any quantum mechanical procedure for which analytical second derivatives are available, among which HF, DFT, and MP2 [152–155]. Examples of applications with each model will be given in the next sections, with a particular attention to the computational strategies presented in the first part to overcome the problem of resonances. Moreover, in order to have an excellent compromise between accuracy and computational cost, the hybrid and reduced-dimensionality schemes will be presented and tested.

The first scheme is based on the observation that differences between anharmonic frequencies computed at two different levels of theory are largely due to the harmonic frequencies, which can be corrected by employing a higher level of theory. Then a hybrid CCSD(T)/DFT approach can be used to carry out VPT2 calculations [197, 275–277], where the harmonic frequencies are done at the CCSD(T) level and the anharmonic correction at the DFT level. From a practical point of view, this means that the CCSD(T) harmonic frequencies are inserted in eq. 2.2 in place of the DFT ones. It is noteworthy that, in order to get reliable results, the equilibrium geometries and the normal coordinates at the CCSD(T) and DFT levels must be consistent. This check has been automated in our procedure.

The second scheme is based on the consideration that the computations of cubic and quartic force constants is the more time demanding step when dealing with anharmonic calculations. It can be speed up by using a reduced-dimensionality scheme, in which the numerical differentiations are done along a subset of normal coordinates corresponding to the modes of interest to be treated anharmonically. In this case, the averaging done for K_{ijk} and K_{iijj} is applied over the number of elements actually calculated (1, 2 or 3 for K_{ijk} and 1 or 2 for K_{iijj}). Note that, if finite differentiation is performed along mode i, but not along modes j and k, the

force constants K_{jjj}, K_{kkk}, K_{jjk} and K_{jkk} can not be evaluated. The anharmonic corrections for fundamental and combination bands of ω_i will still be given by eq. 2.18 and eqs. 2.19-2.20, respectively, where χ_{ii} and g_{ii} terms are unchanged, whereas χ_{ij} terms differ from the fully-dimensionality ones for the absence of the elements (see eqs. 2.8-2.14),

$$\frac{K_{iij}K_{jjj}}{\lambda_j} \qquad \text{and} \qquad \frac{K_{iik}K_{jjk}}{\lambda_k} \tag{6.1}$$

More details on those schemes are available in refs. [199, 278], while an example of application will be given in the next sections.

6.1 Methodology and computational details

Within DFT, the standard B3LYP functional [215–217] has been used in conjunction with the SNSD basis set [218], that has been validated for vibrational studies [197, 198, 219, 279]. The double-hybrid functional B2PLYP [200, 214] and MP2 [154, 155] have been used in conjunction with the Dunning correlation-consistent valence aug-cc-pVTZ (AVTZ) and aug-cc-pVQZ (AVQZ) basis sets [201, 280].

For ferrocene, an organometallic compound taken as an example of medium-size systems, the B3LYP functional has been used in conjunction with the SNSD basis set for H and C atoms and the double-ζ ECP basis set of Hay and Wadt augmented with polarization functions (p type with exponent $\alpha = 0.1349150$) (aug-LANL2DZ) for Fe, with the LANL2DZ pseudo potential to describe core electrons [281]. The hybrid B3PW91 functional [216] has been also employed in conjunction with the m6-31G basis set, based on 6-31G and improved for first-row transition metals [282]. For triphenylamine, the B3LYP functional has been coupled with the valence double-ζ polarized basis set 6-31G* [283–286].

Frequency calculations have been systematically carried out at the equilibrium geometry obtained at the same level of theory, using respectively tight (10^{-8}) and very-tight (on force: 10^{-6} Hartree/Bohr, estimated displacement: $4 \cdot 10^{-6}$ Bohr) convergence criteria for the self-consistent field (SCF) and geometry optimization steps, respectively. For all DFT computations, an ultra-fine grid (199 radial points, 590 angular points) was used for the numerical integration of the two-electron integrals and their derivatives.

The third and semi-diagonal fourth derivatives of the PES have been obtained by numerical differentiation of the analytical second derivatives along the mass-weighted normal coordinates, with the default step $\delta Q_i = 0.01$ $\sqrt{\text{amu}}$ Å, as [47,

222],

$$K_{ijk} = \frac{1}{3}\left[\frac{K_{ij}(+\delta Q_k) - K_{ij}(-\delta Q_k)}{2\delta Q_k} + \frac{K_{ik}(+\delta Q_j) - K_{ik}(-\delta Q_j)}{2\delta Q_j} + \frac{K_{jk}(+\delta Q_i) - K_{jk}(-\delta Q_i)}{2\delta Q_i}\right] \tag{6.2}$$

$$K_{iijj} = \frac{1}{2}\left[\frac{K_{ii}(+\delta Q_j) + K_{ii}(-\delta Q_j) - 2K_{ii}(\boldsymbol{Q}_{\rm eq})}{\delta Q_j^2} + \frac{K_{jj}(+\delta Q_i) + K_{jj}(-\delta Q_i) - 2K_{jj}(\boldsymbol{Q}_{\rm eq})}{\delta Q_i^2}\right] \tag{6.3}$$

$$K_{iijk} = \frac{K_{jk}(+\delta Q_i) + K_{jk}(-\delta Q_i) - 2K_{jk}(\boldsymbol{Q}_{\rm eq})}{\delta Q_i^2} \tag{6.4}$$

To overcome the problem of 1-2 resonances in VPT2 calculations, the computational strategies presented in the previous sections have been employed. For the DVPT2 and GVPT2 approaches, a term has been identified as resonant if the absolute frequency difference in the denominator, Δ, is smaller than 200 cm^{-1} and Ξ in eq. 2.37 is larger than 1 cm^{-1}. The default parameters previously used for HDCPT2 ($\alpha = 1.0$, $\beta = 5.0 \times 10^5$ with ρ and Δ in cm^{-1}) have been used to compute Λ for both HDCPT2 and HDSPT2, see ref. [53].

Vibrational second-order 2-2 resonances are identified by two criteria: the absolute frequency difference between the two resonant states must be smaller than 10 cm^{-1}, and the off-diagonal term greater than 20 cm^{-1}.

For Coriolis resonances, the terms in eqs. 3.13-3.16 with an absolute frequency difference lower than 20 cm^{-1} are discarded.

6.2 Fully DFT and hybrid methods

A set of linear molecules, i.e. HCN, HNC, OCS, HCP, CO2, C_2H_2 and C_4H_2, have been selected to test the performance of full DFT and hybrid CCSD(T)/DFT methods to calculate the anharmonic corrections to the vibrational frequencies. On these molecules, all the schemes presented in the previous section to treat first-order resonances have been employed, and the results for the l-doubling interaction terms have been directly compared with the experimental data when present in the literature.

The VPT2 anharmonic corrections for the linear systems HCN, HNC, OCS and HCP, shown in Table 6.1, were calculated at the MP2, B3LYP and B2PLYP levels of theory, in conjunction with AVTZ and AVQZ, as well as SNSD for B3LYP, basis sets. In the Table, the best theoretical results, computed at the CCSD(T) level,

and experimental data are also reported for comparison purposes. For those systems, which are not affected by resonances, the anharmonic corrections calculated with the different methods are very close to one another. The main discrepancies with experimental results are found to be related to the harmonic part. More precisely, the corrections to the non-degenerate frequencies are very close to the observed values, while the corrections to the low-degenerate wavenumber show a greater sensitivity to the electronic methods and the size of the basis set. For HCN, OCS and HCP, B3LYP/SNSD gives very good result, while, for HNC, the large anharmonic correction for the degenerate wavenumber is due to its underestimation of the $K^{(I)}_{1111}$ quartic force constants.

CO_2 represents an interesting test to validate the DCPT2 and DSPT2 schemes in presence of resonances. It has been one of the first molecules used in infrared and Raman measurements and has served as a prototype for the study of resonances. Vibrational wavenumbers for fundamental, overtones and combination bands obtained at the B2PLYP/AVQZ level and with the hybrid scheme, where the CCSD(T)-F12a/AVTZ harmonic frequencies taken from ref. [287] are used in conjunction with the B2PLYP/AVQZ force field, are shown in Table 6.2. The states are grouped based on the polyads. The well-known type I Fermi resonance that affects this system is due to $2\omega_1 \approx \omega_2$, with normal modes 1 and 2 of Π and Σ symmetry, respectively. The lowest energy states $|\, n_i\, n_j, l_i\, l_j \,\rangle$ that are affected are collected in the following four polyads: $|\, 1_1 1_2, \pm 1_1 \,\rangle$ with $|\, 3_1, \pm 1_1 \,\rangle$, $|\, 2_2 \,\rangle$ with $|4_1, 0_1\rangle$ and $|2_1 1_2, 0_1\rangle$, $|1_2 1_3\rangle$ with $|2_1 1_3, 0_1\rangle$, and $|2_1, 0_1\rangle$ with $|1_2\rangle$. Note that the states $|\, 2_1, \pm 2_1 \,\rangle$ are not involved in the latter polyad since their interaction with $|\, 1_2 \,\rangle$ is symmetry forbidden. From a numerical point of view, this is due to the fact that only $K^{(I)}_{mss}$ is non-null for linear systems (see Tables 2.1 and A.2). The discrepancies of the GVPT2 frequencies at the B2PLYP/AVQZ level with respect to the experimental results are mostly due to the underestimation of the ω_2 harmonic frequency (1344 cm^{-1} versus 1351 cm^{-1}), as confirmed by the improvements obtained with the GVPT2 hybrid scheme, which leads to satisfactory agreements (the discrepancies never exceed 5 cm^{-1} and are on average 1-2 cm^{-1}).

DSPT2 and DCPT2 treatments of resonances deserve some considerations. DSPT2 results coincide with their GVPT2 counterparts for all the states that are not affected by resonances. Conversely, DCPT2 provides values equal to GVPT2 ones just for the states that do not contain excitations on degenerate normal modes 1 and 2 (i.e. $|\, 1_3 \,\rangle$ and $|\, 2_3 \,\rangle$), while the energies for the states $|\, 1_1, \pm 1 \,\rangle$, $|\, 2_2 \,\rangle$ and $|\, 2_1, \pm 2_1 \,\rangle$, which should also be unaffected by the resonance, are underestimated. In the perturbative treatment, these states do not involve resonant terms because those present in the elements of $\boldsymbol{\chi}$ are exactly erased by those in $\boldsymbol{g}$ when the summations in eq. 2.2 are performed. DSPT2 reproduces correctly this behavior, while the DCPT2 results are slightly different due to a non-complete cancellation of the

Table 6.1: Comparison of computed and experimental harmonic ω and anharmonic fundamental VPT2 wavenumbers ν for the linear molecules HCN, HNC, OCS, HCP (in cm^{-1}).

		MP2		B3LYP			B2PLYP		CCSD(T)	Exp.
		AVTZ	AVQZ	SNSD	AVTZ	AVQZ	AVTZ	AVQZ		
HCN[a]										
ω_1	Π	718	721	747	759	758	745	745	729	727
ω_2	Σ	2022	2034	2196	2200	2201	2125	2129	2125	2129
ω_3		3467	3466	3449	3444	3440	3460	3456	3435	3442
$\nu(1_1, \pm 1_1)$		715	718	729	745	744	733	733	717	[e]714
$\nu(1_2)$		1987	1999	2169	2173	2175	2094	2098	2096	[e]2097
$\nu(1_3)$		3334	3339	3317	3312	3312	3327	3328	3309	[e]3312
Δ_1		−3	−3	−18	−14	−13	−12	−12	−12	−13
Δ_2		−35	−35	−27	−26	−26	−31	−30	−29	−32
Δ_3		−133	−127	−132	−132	−128	−133	−128	−126	−130
HNC[b]										
ω_1	Π	485	488	477	468	467	467	467	471	490
ω_2	Σ	2016	2027	2097	2103	2104	2059	2063	2044	2067
ω_3		3818	3824	3801	3799	3801	3815	3818	3837	3842
$\nu(1_1, \pm 1_1)$		505	497	355	463	463	469	470	474	477
$\nu(1_2)$		1983	1993	2063	2069	2070	2023	2027	2008	2029
$\nu(1_3)$		3656	3661	3631	3634	3635	3650	3652	3666	3653
Δ_1		+20	+9	−122	−5	−4	+2	+3	+3	−13
Δ_2		−33	−34	−34	−34	−34	−36	−36	−36	−36
Δ_3		−162	−163	−170	−165	−165	−165	−165	−171	−189
OCS[c]										
ω_1	Π	506	524	518	527	527	523	523	524	524
ω_2	Σ	888	893	865	874	876	872	875	872	876
ω_3		2124	2092	2116	2108	2110	2079	2083	2095	2093
$\nu(1_1, \pm 1_1)$		502	520	514	523	524	519	520	520	521
$\nu(1_2)$		869	876	849	858	860	855	859	855	863
$\nu(1_3)$		2097	2064	2084	2078	2080	2048	2052	2064	2060
Δ_1		−4	−4	−4	−4	−3	−4	−3	−4	−3
Δ_2		−19	−17	−16	−16	−16	−16	−16	−17	−13
Δ_3		−27	−28	−32	−31	−30	−31	−31	−31	−33
HCP[d]										
ω_1	Π	677	689	697	712	720	699	707	689	688
ω_2	Σ	1245	1255	1322	1338	1342	1291	1297	1299	1298
ω_3		3355	3360	3345	3349	3348	3359	3359	3345	3346
$\nu(1_1, \pm 1_1)$		678	680	682	700	704	689	693	675	675
$\nu(1_2)$		1226	1236	1304	1319	1323	1272	1278	1281	1278
$\nu(1_3)$		3231	3233	3216	3219	3219	3231	3231	3213	3217
Δ_1		+1	−9	−15	−13	−16	−9	−14	−14	−13
Δ_2		−19	−19	−18	−19	−18	−19	−19	−18	−20
Δ_3		−124	−128	−129	−130	−129	−128	−129	−132	−129

Δ represents the anharmonic correction.
a) CCSD(T)/AVTZ and experimental values from ref. [287];
b) CCSD(T)/ANO1 and experimental values from ref. [288];
c) CCSD(T)/CVQZ and experimental values from ref. [289];
d) CCSD(T)/CV5Z and experimental values from ref. [290];
e) experimental values from ref. [68].

Table 6.2: Comparison of experimental and computed harmonic ω and anharmonic ν wavenumbers for CO_2 (in cm^{-1}).

State	B2PLYP[a]				HYBRID[b]				Best theo.		Exp.
	ω	ν_{GVPT2}	ν_{DCPT2}	ν_{DSPT2}	ω	ν_{GVPT2}	ν_{DCPT2}	ν_{DSPT2}	ω	ν	ν
$\vert\, 1_1, \pm 1_1 \,\rangle$	669	664	642	664	673	668	646	668	[g]673	[g]668	[defg]668
$\vert\, 1_2 \,\rangle$	1344	1275	1197	1285	1351	1284	1202	1293	[g]1351	[cg]1285	[cdefg]1285
$\vert\, 2_1, 0_1 \,\rangle$	1337	1382	1374	1374	1346	1390	1381	1381		[c]1388	[cdef]1388
$\vert\, 2_1, \pm 2_1 \,\rangle$	1337	1330	1286	1330	1346	1338	1293	1338		[d]1336	[def]1336
$\vert\, 3_1, \pm 1_1 \,\rangle$	2006	1918	1752	1934	2018	1931	1759	1947		[d]1933	[d]1934
$\vert\, 1_1 1_2, \pm 1_1 \,\rangle$	2013	2070	2061	2055	2024	2082	2072	2066		[d]2077	[df]2077
$\vert\, 1_3 \,\rangle$	2390	2345	2345	2345	2391	2347	2347	2347	[g]2391	[cg]2349	[cdefg]2349
$\vert\, 2_2 \,\rangle$	2688	2526	2220	2581	2702	2543	2227	2597		[c]2548	[c]2548
$\vert\, 4_1, 0_1 \,\rangle$	2674	2656	2660	2679	2691	2671	2673	2694		[c]2671	[c]2671
$\vert\, 2_1 1_2, 0_1 \,\rangle$	2681	2791	2742	2714	2696	2797	2757	2729		[c]2797	[c]2797
$\vert\, 2_3 \,\rangle$	4780	4666	4666	4666	4782	4670	4670	4670		[c]4673	[cf]4673
$\vert\, 1_1 1_3, \pm 1_1 \,\rangle$	3059	2997	2975	2997	3064	3003	2980	3003			[cf]3004
$\vert\, 1_2 1_3 \,\rangle$	3734	3600	3517	3605	3742	3610	3524	3615		[cde]3613	[cdef]3613
$\vert\, 2_1 1_3, 0_1 \,\rangle$	3727	3706	3701	3701	3737	3715	3710	3710		[cde]3715	[cdef]3714

The vibrational states $\vert\, n_i\, n_j, l_i\, l_j \,\rangle$ are grouped by polyads.
a) AVQZ basis set.
b) harmonic CCSD(T)-F12a/AVTZ, from ref. [287], and anharmonic B2PLYP/AVQZ force fields.
Refs.: c) [291], d) [292], e) [293], f) [294], g) [287].

transformed resonant terms.
DSPT2 reproduces well the energies of the states involved in 2-dimensional polyads, while the results are not satisfactory for energies involved in larger dimensionality polyads. This is due to the approximation of treating the interactions terms by simplified two-state interacting matrices, then losing in DSPT2 the simultaneous interactions between more than two states. Despite this, DSPT2 can be used to estimate the energies for the fundamental states, since the latter are usually involved in at most 2-dimensional polyads.

Shifting to longer chain linear systems, the results for acetylene and diacetylene are shown in Figure 6.1 and Table 6.3, respectively. Acetylene is a well-known system, for which fundamentals, first overtones, combination bands, and l-doublings have been largely studied in the literature. The results for the vibrational frequencies calculated at the MP2 and B2PLYP levels, with the AVTZ basis set, and B3LYP, with the SNSD basis set, are graphically reported in Figure 6.1, together with the results obtained with the hybrid CCSD(T)/B2PLYP scheme. For each wavenumber value, the series of five marks corresponds, from left to right side, to VPT2, DCPT2, HDCPT2 and DSPT2 and HDSPT2 results. In line with our previous comments, the deviations from experimental values are mainly due to the harmonic part. This error is strongly reduced with hybrid schemes, which yield very good results. The perturbative correction reproduces well the partial lifting of the zeroth-order degeneracy, as can be observed for $\nu(2_1, 0_1)$ and $\nu(2_1, \pm 2_1)$, as well as, for $\nu(2_2, 0_2)$ and $\nu(2_2, \pm 2_2)$. Moreover, the inclusion of l-doubling is necessary to lift the degeneracy between $\nu(1_1 1_2, +1_1 - 1_2)$ and $\nu(1_1 1_2, -1_1 + 1_2)$ and to obtain accurate energies for the combination energies involving degenerate normal modes. For all electronic methods, no first-order resonances are found with Martin's test. Therefore, the purely perturbative VPT2 approach gives good results, slightly improved with the DSPT2 and DCPT2 methods. This is due to the approximate inclusion of higher-order perturbative terms in the treatment of the possibly resonant terms.

High-resolution infrared and Raman spectra of C_2H_2 reported in the literature show the presence of fairly weak couplings between vibrational levels of the same symmetry due to second-order resonances[59, 296–299]. The 2-2 resonances between the two degenerate normal modes of acetylene were first reported by Huet and co-workers for $^{12}C_2D_2$[298]. In their work, the off-diagonal interaction energies between $|\, 2_1, 0_1 \,\rangle$ and $|\, 2_2, 0_2 \,\rangle$, and between $|\, 2_1, \pm 2_1 \,\rangle$ and $|\, 2_2, \pm 2_2 \,\rangle$, which involve respectively $\kappa_{12}^{(I)}$ and $\kappa_{12}^{(III+)}$, are expressed with the s_{45}^0 and $(r_{45}^0 + 2g_{45}^0)/2$ (see Table II in ref. [298]). It has been found that those resonances are particularly relevant for the isotopomers of acetylene, whose two bending vibrations are very close in energy. Furthermore, the need to account for these interactions appears crucial in the study of the highly excited trans-bend levels in $^{12}C_2H_2$, observed by Field and

Figure 6.1: Deviations of harmonic ω and anharmonic ν wavenumbers from experimental values (the origin of the y axis) for acetylene (in cm^{-1}).

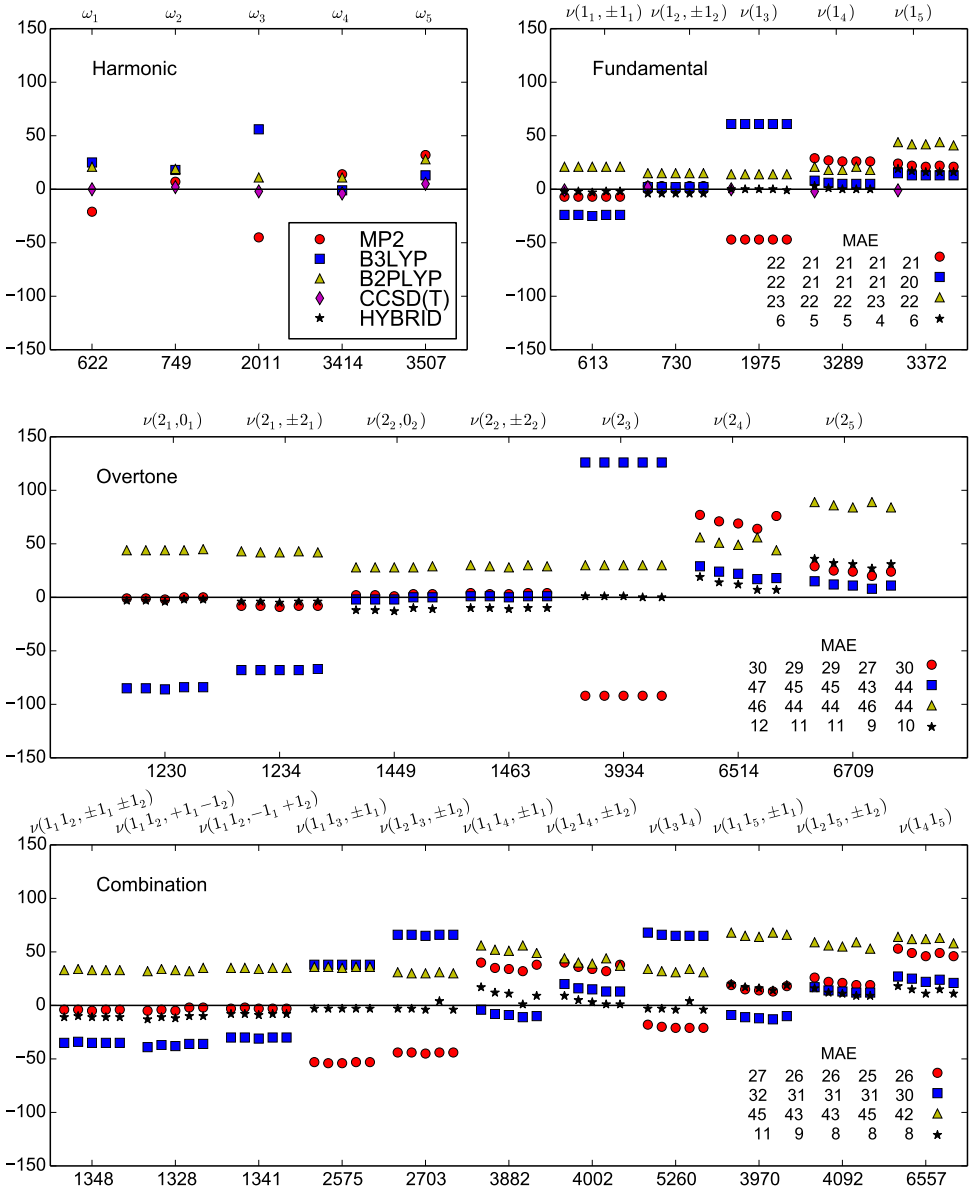

Experimental values are reported in the x axis at the bottom and the corresponding assignment at the top. The series of five values for each anharmonic frequency stands for, from left to right, VPT2, DCPT2, HDCPT2, DSPT2 and HDSPT2 treatments for possibly resonant terms.
Computational methods: MP2 and B2PLYP with AVTZ basis set and B3LYP with SNSD. CCSD(T)/A'CVQZ harmonic and anharmonic frequencies from Table V of ref. [295]. In the hybrid method, the harmonic frequencies are from CCSD(T)/A'CVQZ and the anharmonic force-field from B2PLYP/AVTZ calculations. Experimental values are taken from ref. [295] for fundamental frequencies, and from ref. [59] for overtones and combination bands.
MAE stands for mean absolute error.

Table 6.3: Experimental and computed harmonic ω and anharmonic ν fundamental wavenumbers for diacetylene (in cm^{-1}).

State	Symm.	B3LYP[a]		B2PLYP[b]		HYBRID[b]		Exp.
		ω	ν	ω	ν	ω	ν	ν
$\mid 1_1 \rangle$	Σ_g	3466	3343	3477	3352	3463	3338	3332
$\mid 1_2 \rangle$		2278	2238	2234	2189	2243	2197	2189
$\mid 1_3 \rangle$		915	901	908	890	894	872	872
$\mid 1_4 \rangle$	Σ_u	3467	3344	3478	3353	3465	3339	3334
$\mid 1_5 \rangle$		2111	2078	2064	2028	2064	2027	2022
$\mid 1_6, \pm 1_6 \rangle$	Π_g	659	647	645	638	636	627	626
$\mid 1_7, \pm 1_7 \rangle$		529	522	507	512	485	491	483
$\mid 1_8, \pm 1_8 \rangle$	Π_u	665	654	651	640	640	628	628
$\mid 1_9, \pm 1_9 \rangle$		237	237	231	232	221	222	220

The vibrational states are indicated as $\mid n_i, l_i \rangle$.
DFT calculations were done in conjunction of the AVTZ basis set.
Within the hybrid scheme, the harmonic wavenumbers, obtained at the AE-CCSD(T)/cc-pCVQZ level, were taken from ref. [61], and the anharmonic force-field calculated in this work at the B2PLYP/AVTZ level. The experimental values were taken from refs. [61] and [63].
a) VPT2 values, no Fermi resonances identified with Martin's test.
b) GVPT2 values, one weakly interaction between $\mid 1_3 \rangle$ and $\mid 2_9, 0_9 \rangle$ states.

Table 6.4: VPT2 second-order 2-2 interactions (Darling-Dennison) for $^{12}C_2H_2$ and $^{12}C_2D_2$ (in cm^{-1}).

	MP2[a]	B3LYP[b]	B2PLYP[a]	Exp.
$^{12}\mathbf{C_2H_2}$				
$\lvert 2\omega_4 - 2\omega_5 \rvert / 2$	102.0	98.8	100.7	–
$2\kappa_{45}/16$	−53.2	−50.0	−52.4	−49.0[c]
				−52.4[d]
				−51.5[e]
$^{12}\mathbf{C_2D_2}$				
$\lvert 2\omega_1 - 2\omega_2 \rvert / 2$	52.3	21.5	25.6	–
$4\kappa_{12}^{I}/16$	−6.2	−14.1	−8.2	−8.0[f]
$8\kappa_{12}^{III+}/64$	1.5	0.1	1.0	0.4[g]
$\lvert 2\omega_4 - 2\omega_5 \rvert / 2$	269.9	302.8	287.7	–
$2\kappa_{45}/16$	−25.7	−22.8	−25.0	−23.9[c]

Basis sets: a) AVTZ. b) SNSD.
c) $\kappa_{1133}/2$ in ref. [296]. d) $\kappa_{1133}/2$ in ref. [297]. e) $\kappa_{1133}/2$ in ref. [59]. f) s_{45}^0 in ref. [298]. g) $(r_{45}^0 + 2g_{45}^0)/2$ in ref. [298].

co-workers using the stimulated emission pumping (SEP) technique [300]. Our results obtained at the MP2/AVTZ, B3LYP/SNSD and B2PLYP/AVTZ levels show a very good agreement with those of Huet *et al.* (see Table 6.4). Another case of interacting states, between $|\, 2_4 \,\rangle$ and $|\, 2_5 \,\rangle$, was first considered by Mills [296]. In Mills' formalism, the interacting energy is reported in Table 1 of ref. [296] as $\kappa_{1133}/2$. This coupling ought to be considered in all symmetric isotopes of C_2H_2, in particular for $^{13}C_2H_2$. Even in this case, the agreement between our computational results and the observed values is remarkable.

Diacetylene has been extensively studied from both experimental and theoretical points of view, because of its prevalence in hydrocarbon combustion and pyrolysis and is known to be present in the interstellar medium and in the atmospheres of several planets and moons of our solar system[61, 63, 301]. The fundamental frequencies for diacetylene have been calculated at the B3LYP/AVTZ and B2PLYP/AVTZ levels, and with the hybrid scheme, where the harmonic frequencies obtained at the AE-CCSD(T)/cc-pCVQZ level [61] are coupled with the B2PLYP/AVTZ force-field. The results are reported in Table 6.3. For this system, Martin's test reveals a weak interaction due to $\omega_3 \approx 2\omega_9$ for B2PLYP and hybrid calculations, which is not found for B3LYP computations. The B2PLYP result for $\nu(1_3)$ (890 cm^{-1}), calculated with the GVPT2 approach, is in better agreement with the experimental data (872 cm^{-1}) than the B3LYP result (901 cm^{-1}), where the interaction term between the $|\, 1_3 \,\rangle$ and $|\, 2_9, 0_9 \,\rangle$ states is treated at the perturbative level (VPT2). As expected, the hybrid values show a very good agreement with the observed ones.

6.3 From medium to large symmetric top systems

The wavenumbers calculated at the B2PLYP/AVTZ level for the fundamental, first overtones and combination bands for cyclopropane, which is an oblate symmetric top belonging to the D_{3h} symmetry point group, are reported in Table 6.5. Also in this case, the states are ordered by polyads. Martin's test identifies for this system three weak Fermi resonances, related to the interaction between $|\, 1_1 \,\rangle$ and $|\, 2_2\rangle$, $|\, 1_2\rangle$ and $|2_{14}, 0_{14}\rangle$, $|\, 1_8, \pm 1_8\rangle$ and $|\, 1_9 1_2, \pm 1_9\rangle$, and one tight Fermi resonance, involving $|\, 1_9, \pm 1_9 \,\rangle$ and $|\, 2_{14}, \pm 2_{14} \,\rangle$ states. GVPT2, DCPT2 and DSPT2 results are reported in Table 6.5, together with the VPT2 values. HDCPT2 and HDSPT2 give results equal to DCPT2 and DSPT2, respectively, and are, therefore, omitted. The agreement with the experimental values is good for most of the energies, and both DCPT2 and DSPT2 show good results for the states not affected by resonances, as well as, for the states involving resonant interaction terms. Some discrepancies are found for $|\, 1_1 \,\rangle$, for which all methods slightly overestimate the experimental value, and $|\, 2_{11}, \pm 2_{11} \,\rangle$, that is underestimated by the theoretical

results with respect to the experimental one. VPT2 reproduces well the energy of $|\ 1_2\ \rangle$, but slightly overestimates $|\ 2_{14}, 0_{14}\ \rangle$. GVPT2, which treats variationally the interaction between the latter two states, overestimates the energy of $|\ 1_2\ \rangle$, whereas that of $|\ 2_{14}, 0_{14}\ \rangle$ is in agreement with the experimental value. For this case, DCPT2 and DSPT2 reproduce well the energy of $|1_2\rangle$, while for $|2_{14}, 0_{14}\rangle$ the overestimation is similar to that of VPT2. At variance, the results are very good for the combination states involving the excitations of the normal modes labeled as 10 and 14.

As shown above, the hybrid method allows to reduce the computational costs leading to satisfactory results. Table 6.6 shows the fundamental frequencies for benzene obtained with the hybrid model. Benzene is an oblate symmetric top (D_{6h} symmetry), which has been widely studied in the literature by both Raman and infrared spectroscopy[38, 303–306]. In the hybrid computation, the harmonic frequencies have been calculated at the CCSD(T)/ANO4321' level[307], and the anharmonic force field at the B3LYP/SNSD level. In Table 6.6, the fundamental frequencies at the B3LYP/SNSD level are also reported. B3LYP/SNSD calculations show a qualitatively good agreement with the experimental values for the majority of the frequencies. Martin's test identifies two weak type II Fermi resonances, the first affecting $|1_9, \pm 1_9\rangle$ and $|1_1 1_7, \pm 1_7\rangle$ states, the second $|1_{18}, \pm 1_{18}\rangle$ and $|1_9 1_{17}, \pm 1_9 \pm 1_{17}\rangle$, and a slightly stronger one, involving $|1_{13}\rangle$ and $|1_9 1_{17}, \pm 1_9 \pm 1_{17}\rangle$. The latter resonance leads to wrong VPT2 results for $\nu(1_{13})$ (3143 cm^{-1}), that shows a discrepancy of about 100 cm^{-1} with respect to the observed value (3057 cm^{-1}). At variance, the coupling between $|1_9, \pm 1_9\rangle$ and $|1_1 1_7, \pm 1_7\rangle$ is small, and the VPT2 result for $\nu(1_9, \pm 1_9)$ (1604 cm^{-1}) is closer to the observed value (1601 cm^{-1}) than the GVPT2 one (1588 cm^{-1}). The result of the DSPT2 and DCPT2 treatments (1599 cm^{-1}) is also very good. Some discrepancies are present also for $\nu(1_{18}, \pm 1_{18})$; VPT2, DSPT2 and DCPT2 ($\approx$ 3070 cm^{-1}) overestimate the reference value (3047 cm^{-1}), while the opposite is true for GVPT2 (3029 cm^{-1}). This frequency is close to the experimental value in the hybrid models, showing once again that the error is mainly due to the unsatisfactory treatment of the harmonic part. In the hybrid method, the two vibrational states $|\ (1_{13}\ \rangle$ and $|\ 1_{18}, \pm 1_{18}\ \rangle$ are still affected by resonance, showing similar results to those obtained by full DFT calculations. On the other hand, Martin's test does not identify the resonance affecting the $|1_9, \pm 1_9\rangle$ and $|1_1 1_7, \pm 1_7\rangle$ states in the hybrid case, because of the differences between the CCSD(T) and DFT harmonic frequencies. Moreover, two new weak couplings are identified, the first involving $|1_3\rangle$ and $|1_{19} 1_{20}, \pm 1_{19} \mp 1_{20}\rangle$, the second $|1_2\rangle$ and $|2_9, 0_9\rangle$. Consequently, $\nu(1_9, \pm 1_9)$ is not variationally treated and shows coincident values for all methods (1598 cm^{-1}), that is in good agreement with the observed one (1601 cm^{-1}), while $\nu(1_2)$ and $\nu(1_3)$ are very satisfactory in all VPT2, DSPT2, DCPT2 and GVPT2

Table 6.5: Harmonic ω, anharmonic ν wavenumbers for cyclopropane (in cm^{-1}).

State	Symm.	ω	ν_{VPT2}	ν_{DCPT2}	ν_{DSPT2}	ν_{GVPT2}	$\nu_{\mathrm{Exp.}}$
$\mid 1_1 \rangle$	A'_1	3163	3042	3040	3041	3046	3027
$\mid 2_2 \rangle$		3061	2993	2983	2982	2954	–
$\mid 1_2 \rangle$	A'_1	1531	1502	1497	1498	1515	1499
$\mid 2_{14}, 0_{14} \rangle$		1487	1471	1478	1475	1459	1461
$\mid 1_3 \rangle$	A'_1	1218	1191	1191	1191	1191	1189
$\mid 1_4 \rangle$	$A"_1$	1162	1129	1129	1129	1129	1127
$\mid 1_5 \rangle$	A'_2	1095	1072	1072	1072	1072	1067
$\mid 1_6 \rangle$	$A"_2$	3254	3108	3108	3108	3108	3102
$\mid 1_7 \rangle$	$A"_2$	863	860	860	860	860	854
$\mid 1_8, \pm 1_8 \rangle$	E'	3154	3006	3005	3005	3016	3019
$\mid 1_2 1_9, \pm 1_9 \rangle$		3016	2909	2924	2926	2907	–
$\mid 1_9, \pm 1_9 \rangle$	E'	1486	1422	1441	1441	1446	1440
$\mid 2_{14}, \pm 2_{14} \rangle$		1487	1515	1505	1495	1491	1480
$\mid 1_{10}, \pm 1_{10} \rangle$	E'	1056	1030	1030	1030	1030	1028
$\mid 1_{11}, \pm 1_{11} \rangle$	E'	887	854	854	854	854	868
$\mid 1_{12}, \pm 1_{12} \rangle$	$E"$	3233	3087	3087	3087	3087	3082
$\mid 1_{13}, \pm 1_{13} \rangle$	$E"$	1219	1194	1194	1194	1194	1191
$\mid 1_{14}, \pm 1_{14} \rangle$	$E"$	744	742	744	742	742	738
$\mid 2_{11}, 0_{11} \rangle$		1775	1714	1714	1714	1714	1727
$\mid 2_{11}, \pm 2_{11} \rangle$		1775	1690	1690	1690	1690	1734
$\mid 1_5 1_{10}, \pm 1_{10} \rangle$		2150	2097	2097	2097	2097	2090
$\mid 1_5 1_{14}, \pm 1_{14} \rangle$		1838	1814	1817	1814	1814	1805
$\mid 1_{10} 1_{14}, \pm 1_{10} \pm 1_{14} \rangle$		1799	1772	1775	1779	1772	1766
$\mid 1_{10} 1_{14}, +1_{10} - 1_{14} \rangle$		1799	1771	1774	1771	1771	1767
$\mid 1_{10} 1_{14}, -1_{10} + 1_{14} \rangle$		1799	1772	1775	1773	1772	–

The vibrational states are indicated as $\mid n_i\, n_j, l_i\, l_j \rangle$.
Computed values at the B2PLYP/AVTZ level. Observed values from ref. [302].
Note that the l-doubling between $\mid 1_{10} 1_{14}, +1_{10} - 1_{14} \rangle$ and $\mid 1_{10} 1_{14}, -1_{10} + 1_{14} \rangle$ has not been taken into account in the experimental observed values.

Table 6.6: Computed harmonic ω and experimental and calculated anharmonic fundamental wavenumbers ν for benzene (in cm^{-1}).

State	Symm.	B3LYP/SNSD					HYBRID					Exp.
		ω	ν_{VPT2}	ν_{DSPT2}	ν_{DCPT2}	ν_{GVPT2}	ω	ν_{VPT2}	ν_{DSPT2}	ν_{DCPT2}	ν_{GVPT2}	ν
$\mid 1_1 \rangle$	A_{1g}	1011	997	997	997	997	1003	989	989	989	989	993
$\mid 1_2 \rangle$		3195	3054	3055	3055	3054	*3210	3069	3070	3070	3073	3074
$\mid 1_3 \rangle$	A_{2g}	1375	1349	1349	1349	1349	*1380	1348	1351	1351	1350	(1350)
$\mid 1_4 \rangle$	B_{2g}	717	692	692	692	692	709	684	684	684	684	(707)
$\mid 1_5 \rangle$		1015	980	980	980	980	1009	974	974	974	974	(990)
$\mid 1_6, \pm 1_6 \rangle$	E_{1g}	864	842	842	842	842	865	843	843	843	843	847
$\mid 1_7, \pm 1_7 \rangle$	E_{2g}	616	612	612	612	612	611	607	607	607	607	608
$\mid 1_8, \pm 1_8 \rangle$		1193	1179	1179	1179	1179	1194	1179	1179	1179	1179	1178
$\mid 1_9, \pm 1_9 \rangle$		*1635	1604	1599	1599	1588	1637	1598	1598	1598	1598	1601
$\mid 1_{10}, \pm 1_{10} \rangle$		3169	3008	3008	3008	3008	3183	3023	3022	3022	3023	3057
$\mid 1_{11} \rangle$	A_{2u}	688	673	673	673	673	687	673	673	673	673	674
$\mid 1_{12} \rangle$	B_{1u}	1013	1009	1009	1009	1009	1020	1016	1016	1016	1016	(1010)
$\mid 1_{13} \rangle$		*3159	3143	3069	3069	2996	*3173	3105	3076	3076	3009	(3057)
$\mid 1_{14} \rangle$	B_{2u}	1169	1158	1158	1158	1158	1163	1152	1152	1152	1152	1150
$\mid 1_{15} \rangle$		1349	1323	1323	1323	1323	1326	1304	1302	1302	1304	1309
$\mid 1_{16}, \pm 1_{16} \rangle$	E_{1u}	1056	1038	1038	1038	1038	1056	1038	1038	1038	1038	1038
$\mid 1_{17}, \pm 1_{17} \rangle$		1509	1479	1479	1479	1479	1509	1479	1479	1479	1479	1484
$\mid 1_{18}, \pm 1_{18} \rangle$		*3185	3073	3067	3069	3029	*3200	3083	3080	3081	3040	3047
$\mid 1_{19}, \pm 1_{19} \rangle$	E_{2u}	411	402	402	402	402	406	397	397	397	397	398
$\mid 1_{20}, \pm 1_{20} \rangle$		987	968	968	968	968	985	966	966	966	966	976
MAE			13	9	9	12		10	9	9	9	

The vibrational states are indicated as $\mid n_i, l_i \rangle$.
In the hybrid method, the harmonic frequencies are calculated at the CCSD(T)/ANO4321' level, from Table 1 of ref. [307], and the anharmonic force field at the B3LYP/SNSD one. The experimental values are from ref. [38].
The values in parentheses have not been observed directly but have been deduced from combination bands. The frequencies treated as resonant (DVPT2/GVPT2) are indicated with a *. MAE stands for Mean Absolute Error.

approaches. These considerations show that a good description of the harmonic frequencies is also important to identify correctly the resonant terms affecting the system. In this case as well, HDCPT2 and HDSPT2 treatment of resonances have been omitted from Table 6.6 since they are equivalent to DCPT2 and DSPT2.

Following Amat's rule, $\langle\, n_s, l_s \mid \tilde{\mathcal{H}}_{40} \mid n_s, (l_s \pm 4)) \,\rangle$ and $\langle\, n_s n_t, l_s l_t \mid \tilde{\mathcal{H}}_{40} \mid n_s n_t, (l_s \pm 2)(l_t \mp 2) \,\rangle$ l-doublings are found to be non-null for benzene. The B3LYP/SNSD results for the R and S constants are shown in Table 6.7, together with the values calculated at the B3LYP/TZ2P level, taken as benchmark from ref. [304]. Note that in ref. [304], R and S are reported as $r = 4R$ and $s = 4S$. In both sets of results the resonances are treated at the DVPT2 level. The agreement between the two series of data is remarkable.

Table 6.7: R and S l-type doublings for C_6H_6, (in cm^{-1}).

Const.	Modes		This work	Lit.	Const.	Modes		This work	Lit.
S	7	6	0.10	–	S	18	8	0.60	0.64
S	8	6	0.19	0.27	S	18	9	−1.50	−1.56
R	8	7	0.18	–	S	18	10	−10.09	−10.26
S	9	6	−0.11	–	R	18	16	0.36	0.36
R	9	7	0.32	0.26*	R	18	17	−0.26	−0.39
R	9	8	−0.72	−0.78	S	19	6	1.51	1.92
S	10	6	0.61	0.71	R	19	7	0.03	−0.09
R	10	7	0.04	–	R	19	8	−0.60	−0.39
R	10	8	0.68	0.70	R	19	9	−0.21	−0.20
R	10	9	−1.66	−1.84	R	19	10	0.03	–
R	16	6	−0.01	–	S	19	16	0.69	0.68
S	16	7	−0.13	–	S	19	17	−0.33	−0.33
S	16	8	−0.53	−0.49	S	19	18	0.03	0.04
S	16	9	0.62	0.64	S	20	6	−0.71	−0.35
S	16	10	0.33	0.34	R	20	7	0.05	–
R	17	6	−0.09	–	R	20	8	−0.24	−0.21
S	17	7	0.05	–	R	20	9	−0.28	−0.30
S	17	8	−0.71	−0.68	R	20	10	0.75	0.85
S	17	9	0.13	0.10*	S	20	16	0.19	0.23
S	17	10	−0.44	−0.47	S	20	17	0.04	–
R	17	16	−0.40	−0.46	S	20	18	0.77	0.80
R	18	6	0.59	0.77	R	20	19	−0.50	−1.21
S	18	7	−0.02	–					

Calculation at the B3LYP/SNSD level. The resonances are treated at DVPT2 level.
The reference values are calculated at the B3LYP/TZ2P level, from Table VI of ref. [304]. Note that in the reference the values are reported as $r = 4R$ and $s = 4S$.
* indicates that the value corresponds with the one reported in parentheses in ref. [304]. For the numbering of the normal modes see Table 6.6.

Figure 6.2: Medium-sized symmetric top systems of interest.

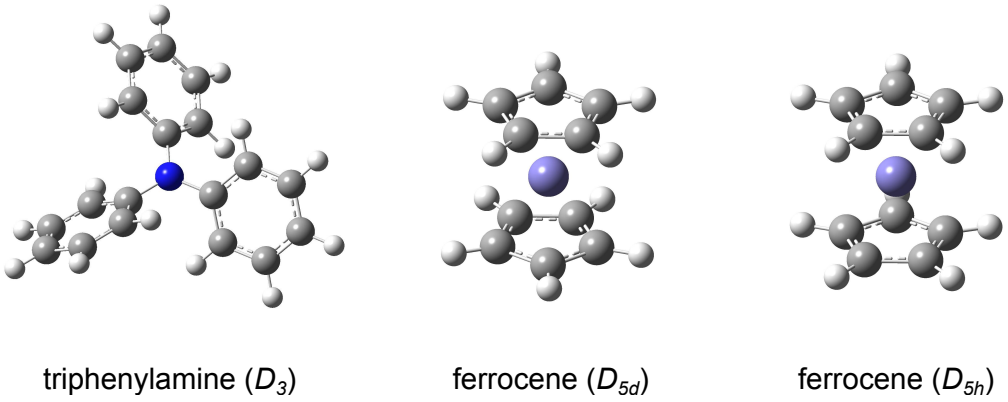

Table 6.8: Fundamental vibrational wavenumbers for triphenylamine (in cm^{-1}).

Symm.	B3LYP/6-31G*		Scaled	Exp.
	ω	ν^a	ν^b	ν^c
E	3182	3029	3127	3016
				3043
A_2	3190	3072	3135	3067
E	3190	3074	3135	
E	3205	3070	3150	
E	3217	3069	3159	
A_2	3214	3096	3158	3096
E	3214	3097	3157	3107

a) Anharmonic correction computed within the reduced dimensionality approach (see text), applying the DSPT2 method for resonances.
b) Harmonic values at the B3LYP/AVTZ level and scaled with a factor equal to 0.986, from ref. [308].
c) Observed values taken from ref. [308].

Table 6.9: Computed harmonic ω, GVPT2 anharmonic ν, and experimental wavenumbers for staggered D_{5d} and eclipsed D_{5h} ferrocene (in cm^{-1}).

Symm.	B3LYP[a]		B3PW91[b]		Symm.	B3LYP[a]		B3PW91[b]		Exp.[c]
D_{5h}	ω	ν	ω	ν	D_{5d}	ω	ν	ω	ν	ν
A_2"	453	440	488	475	A_{2u}	448	437	482	470	480
E_1'	466	457	501	492	E_{1u}	436	427	470	460	496
A_2"	828	815	830	829	A_{2u}	827	813	830	820	816
E_1'	845	837	857	840	E_{1u}	844	841	855	839	840
E_1'	1022	1000	1025	1006	E_{1u}	1021	1002	1026	1006	1012
A_2"	1130	1112	1142	1125	A_{2u}	1131	1113	1142	1126	1112
E_1'	1449	1415	1451	1418	E_{1u}	1450	1417	1451	1419	1416
E_1'	3239	3106	3245	3116	E_{1u}	3238	3107	3245	3115	3106
A_2"	3250	3116	3256	3126	A_{2u}	3249	3118	3256	3126	-

a) SNSD/aug-LANL2DZ basis set.
b) SNSD/m6-31G basis set.
c) Observed values from ref. [309].

Moving to larger systems, the importance of taking into account the anharmonicity appears clearly in Tables 6.8 and 6.9.

In the first Table, both the harmonic and anharmonic computational results for triphenylamine are compared with the observed frequencies. Triphenylamine has a D_3 three-bladed propeller structure, with a planar central NCCC moiety (see Figure 6.2), and has found applications in different fields, including for instance photoconductors and semiconductors [310–313]. With 96 vibrational normal modes, the determination of the complete anharmonic force field for this system is computationally very expensive even at the DFT level. However, within the reduced-dimensionality approach, it is possible to calculate the anharmonic corrections for a small selection of vibrational energies of interest. If the harmonic energy of the latter are well separated from the energies of the vibrations ignored in the anharmonic treatment, the cubic and quartic forces involving normal modes of both sets can be assumed to be negligible. In Table 6.8, the anharmonic corrections have been applied to fundamental vibrational states having harmonic wavenumbers larger than 3000 cm^{-1} which correspond to the CH stretchings region. The calculation has been done at the B3LYP/6-31G* level, and the resonances have been treated with the DSPT2 method. In Table 6.8, the empirical fundamental frequencies, obtained scaling the B3LYP/AVTZ harmonic frequencies by a factor of 0.986 (see ref. [308]), are also reported, together with the experimental results, measured by FTIR spectroscopy of triphenylamine monomers isolated in an argon matrix[308]. The inclusion of anharmonic effects leads to a significantly better agreement between the theoretical and experimental results with respect to the scaled values.

As a last example, we report the results for ferrocene, an organometallic compound of great interest in bio- and nano-technologies, with important applications of its derivatives in catalysis, molecular electronics, polymer chemistry, nonlinear optical and solar engineering [314–319]. Its geometry has been studied by several theoretical methods and shows a sandwich structure with the metal situated between two parallel cyclopentadienyl rings. A small energy barrier separates the staggered D_{5d} and eclipsed D_{5h} rotational orientation of the two rings (see Figures 6.2), with an energy difference of 0.9 kcal mol^{-1} from gas phase electron diffraction measurements [320–322]. In gas phases calculations, the eclipsed conformer is a global minimum, whereas the staggered conformer is a saddle point with an imaginary frequency. In a recent study, a quite good agreement was obtained between the harmonic vibrational frequencies of ferrocene calculated at the B3LYP/m6-31(d) level and the observed values [322]. A noticeable improvement in the theoretical results is obtained by taking into account the anharmonicity. From B3LYP calculations, with the hybrid SNSD/aug-LANL2DZ basis set as discussed in the computational details section, the anharmonic fundamental wavenumbers

show a quantitative agreement with the experimental ones, especially for the range above 800 cm^{-1}, where vibrations involving C and H atoms are excited. The lowest wavenumbers (480 and 496 cm^{-1}) are due to the excitations of vibrational modes involving the metal. The latter are better described by the B3PW91 functional, coupled with the SNSD/m6-31G basis set. It is noteworthy that B3PLYP and B3PW91 anharmonic corrections are not significantly different, showing that the discrepancies between the observed and B3LYP values are due again to deficitary description of the harmonic vibrations associated to Fe.

6.4 Thermodynamics

If the fundamental, overtone and combination energies have to be handled with care because of resonances, it has been shown in the theoretical section that the ZPVE is not affected. Both harmonic and anharmonic ZPVEs of linear (HCN, CO_2, C_2H_2), and symmetric top molecules (PH_3, $ClCH_3$, FCH_3) are shown in Table 6.10.

On overall, the mean anharmonic correction with respect to the harmonic ZPVE is about 0.4% for CO_2, 1% for HCN, 1.2% for C_2H_2, and 1.4% for the symmetric top systems. It is noteworthy that for all these molecules the magnitudes of the anharmonic corrections are little affected by the choice of the computational method and the basis set, at least in the present cases. From the ZPVE and the anharmonic fundamental energies, a comparison with the experimental thermodynamic data can be achieved by the SPT model [40, 53]. The calculated and experimental absolute entropies at 298.15 K and 1 atm are also reported in Table 6.10. Under those thermodynamic conditions, the absolute entropies calculated with all methods available to treat the resonances lead to very close results. Compared to accurate experimental values,the inclusion of anharmonic corrections in the calculated thermodynamic values improves the accuracy of the results by about $0.10 - 0.20$ J mol^{-1} K^{-1}.

Table 6.10: Comparison of computed and experimental harmonic (H) and anharmonic (A) ZPVE (in KJ mol^{-1}) and absolute entropies at 298.15 K and 1 atm (in J mol^{-1} K^{-1}), for linear and symmetric top molecules.

	MP2[a]		B3LYP[b]		B2PLYP[a]		Best th.	Exp.
	H	A	H	A	H	A		
HCN								
ZPVE	41.42	41.05	42.70	42.25	42.31	41.90	41.55[d]	41.61[d]
Δ		−0.37		−0.45		−0.41		
S	201.79	201.82	201.99	202.20	203.39	201.50	-	201.83[ce]
CO_2								
ZPVE	30.18	30.08	30.49	30.36	30.24	30.12	30.28[e]	-
Δ		−0.10		−0.13		−0.12		
S	213.88	213.95	213.74	213.78	213.72	213.79	-	213.69[ce]
C_2H_2								
ZPVE	69.65	68.93	70.73	69.58	70.59	69.85	68.61[e]	-
Δ		−0.72		−1.15		−0.74		
S	200.82	200.92	200.08	201.14	200.06	200.34	-	200.85[ce]
PH_3								
ZPVE	64.39	63.59	62.21	61.37	63.49	62.67	62.44[f]	-
Δ		−0.80		−0.84		−0.82		
S	209.90	209.98	210.25	210.33	209.97	210.05	-	210.13[ce]
$ClCH_3$								
ZPVE	100.75	99.36	98.73	97.34	99.79	98.43	-	-
Δ		−1.39		−1.39		−1.36		
S	233.77	233.92	234.42	234.58	233.06	234.22	-	234.26[ce]
FCH_3								
ZPVE	104.80	103.37	102.61	101.18	103.72	102.30	-	-
Δ		−1.43		−1.43		−1.42		
S	222.52	222.62	222.75	222.85	222.59	222.69	-	222.73[ce]

Δ's are the anharmonic corrections. Basis sets: a) AVTZ. b) SNSD.
c) The tabulated values have been lowered by 0.11 J mol^{-1} K^{-1}, to pass from the original 1 bar = 0.1 MPa values to 1 atm = 0.101325 MPa (see "reference part" in ref. [323]).
Refs.: c) [288]; d) [323]; e) [287]; f) [55].

Conclusions

The vibrational perturbation theory for roto-vibrational energies and thermodynamic functions for asymmetric, symmetric and linear top systems has been revised and fully generalized to allow for the treatment of both minima and first-order saddle points of the PES. A particular attention has been devoted to the treatments of off-diagonal elements of the Hamiltonian and the perturbative equations in the presence of resonances. Previous strategies for dealing with first-order resonances (i.e. GVPT2, DCPT2 and HDCPT2) have been generalized and a new treatment (i.e. DSPT2 and its hybrid counterpart HDSPT2), has been presented and validated. A versatile implementation has been included in the GAUSSIAN package.

Several case studies ranging from triatomic to large molecular systems have been explicitly treated by different quantum mechanical approaches to fully validate the computational tool. The results show that the perturbative developments are very effective and reasonably accurate, and can be applied easily to DFT and CCSD(T)/DFT hybrid levels in conjunction with medium sized basis sets, and with reduced-dimensionality schemes. The latter approximations are particular appealing when dealing with medium- to large-molecules, allowing the inclusion of anharmonicity also in the cases otherwise unpractical due to prohibitive computational cost.

Moreover, the use of roto-vibrational corrections to rotational constants within the semi-experimental approach for the determination of accurate equilibrium structures has been largely discussed. 21 small molecules for which accurate SE structures determined using CCSD(T) vibrational contributions are available have been selected (CCse set) and used to demonstrate that the $\Delta B_\tau^{\mathrm{vib}}$ contributions derived from cubic force fields at the DFT level lead to results with an accuracy comparable to that obtainable at higher levels of theory (MP2 and, especially, CCSD(T)). It has been shown that the B3LYP/SNSD and B2PLYP/VTZ models represent a very good compromise between accuracy and computational cost in the

calculation of $\Delta B_\tau^{\mathrm{vib}}$ contributions, thus avoiding the use of expensive CC calculations and making the accurate determination of molecular structures for medium and large systems feasible. Within this context, new SE equilibrium structures have been determined for a set of 27 molecules, mostly including building blocks of biomolecules. The latter, together with the SE equilibrium structures of the previous 21 molecules determined using B3LYP/SNSD and B2PLYP/VTZ vibrational contributions provide a set of 48 accurate equilibrium structures (referred to as the B3se and B2se sets, respectively) which can be recommended as reference data for the investigation of molecular properties, as well as for parameterisations and validation of QM models. Moreover, a new method, denoted template approach, has been proposed to deal with molecules for which there is a lack of experimental data and it is thus necessary to fix some geometrical parameters in the fitting procedure. This approach further extends the size of molecular systems amenable to highly accurate molecular structure determinations.

Finally, new equations for the pure vibrational term of polarizability, and the square modulus of electric dipole transition moment, have been generalized for excitations from any vibrational quantum numbers in the specific case of asymmetric top systems. It is noteworthy that future implementations of the latter equations are of particular interest for the calculations of temperature-dependent polarizabilities and IR spectra.

Part III

Appendices

Appendix A

Force constants classification

The force constants involving degenerate modes can be related to one another based on symmetry considerations. This chapter gathers those relations for cubic and quartic force constants, used to define the proper terms to be employed in the vibrational Hamiltonian. The symmetry relations for the cubic and quartic force constants involving degenerate modes are reported in Tables A.2-A.8. In the latter, the molecular point group symmetries are labeled with the notation presented in Table A.1.

Table A.1: Symmetry groups labels.

I	Ia:	C_{Nv}, D_N, D_{Nh} (any N); D_{Nd} (N odd);
	Ib:	$D_{(N/2)d}$ ($N/2$ even);
II	IIa:	C_N, C_{Nh} (any N); S_{2N} (N odd);
	IIb:	S_N ($N/2$ even).

I and II are non-abelian and abelian, respectively.

Table A.2: Non-vanishing cubic energy derivatives with respect to Q_{i_σ} and their symmetry relations[121].

Symmetry	$\mathcal{H}^{(1)}_{vib}$ w.r.t. $Q_{i\sigma}Q_{j_\nu}Q_{k_\tau}$	Q_m	c_s c_t c_u	Group	N
$K_{ms_1s_1}= K_{ms_2s_2}$	$K^{(I)}_{mss}$ $Q_m(Q^2_{s_1}+Q^2_{s_2})/2$	A_1	any c_s	I, II	$N\geqslant 3,\infty$
$K_{ms_1s_1}=-K_{ms_2s_2}$	$K^{(III)}_{mss}$ $Q_m(Q^2_{s_1}-Q^2_{s_2})/2$	B_1	$4c_s=N$	I, II	$N=4,8,4p,\ldots$
$K_{ms_1s_2}$	$K^{(IV)}_{mss}$ $Q_mQ_{s_1}Q_{t_2}$	B_2	$4c_s=N$	I, II	$N=4,8,4p,\ldots$
$K_{ms_1t_1}= K_{ms_2t_2}$	$K^{(I)}_{mst}$ $Q_m(Q_{s_1}Q_{t_1}+Q_{s_2}Q_{t_2})$	A_1	$c_s=c_t$	I, II	$N\geqslant 3,\infty$
$K_{ms_1t_2}=-K_{ms_2t_1}$	$K^{(II)}_{mst}$ $Q_m(Q_{s_1}Q_{t_2}-Q_{s_2}Q_{t_1})$	A_2	$c_s=c_t$	I, II	$N\geqslant 3$
$K_{ms_1t_1}=-K_{ms_2t_2}$	$K^{(III)}_{mst}$ $Q_m(Q_{s_1}Q_{t_1}-Q_{s_2}Q_{t_2})$	B_1	$c_s+c_t=N/2$	I, II	$N=4,6,2p,\ldots$
$K_{ms_1t_2}= K_{ms_2t_1}$	$K^{(IV)}_{mst}$ $Q_m(Q_{s_1}Q_{t_2}+Q_{s_2}Q_{t_1})$	B_2	$c_s+c_t=N/2$	I, II	$N=4,6,2p,\ldots$
$K_{s_1s_1s_1}=-K_{s_1s_2s_2}$	$K^{(I)}_{sss}$ $(Q^3_{s_1}-3Q_{s_1}Q^2_{s_2})/6$		$3c_s=N$	I, II	$N=3,6,3p,\ldots$
$K_{s_2s_2s_2}=-K_{s_1s_1s_2}$	$K^{(II)}_{sss}$ $(Q^3_{s_2}-3Q^2_{s_1}Q_{s_2})/6$		$3c_s=N$	II	$N=3,6,3p,\ldots$
$K_{s_1s_1t_1}=-K_{s_2s_2t_1}$ $=-K_{s_1s_2t_2}$	$K^{(I)}_{sst}$ $(Q^2_{s_1}Q_{t_1}-Q^2_{s_2}Q_{t_2}-2Q_{s_1}Q_{s_2}Q_{t_2})/2$		$2c_s+c_t=N$	I, II	$N=3,\geqslant 5$
$K_{s_1s_1t_2}=-K_{s_2s_2t_2}$ $= K_{s_1s_2t_1}$	$K^{(II)}_{sst}$ $(Q^2_{s_1}Q_{t_2}-Q^2_{s_2}Q_{t_2}+2Q_{s_1}Q_{s_2}Q_{t_1})/2$		$2c_s+c_t=N$	II	$N=3,\geqslant 5$
$K_{s_1s_1t_1}=-K_{s_2s_2t_1}$ $= K_{s_1s_2t_2}$	$K^{(III)}_{sst}$ $(Q^2_{s_1}Q_{t_1}-Q^2_{s_2}Q_{t_2}+2Q_{s_1}Q_{s_2}Q_{t_2})/2$		$c_t=2c_s$	I, II	$N\geqslant 5$
$K_{s_1s_1t_2}=-K_{s_2s_2t_2}$ $=-K_{s_1s_2t_1}$	$K^{(IV)}_{sst}$ $(Q^2_{s_1}Q_{t_2}-Q^2_{s_2}Q_{t_2}-2Q_{s_1}Q_{s_2}Q_{t_1})/2$		$c_t=2c_s$	II	$N\geqslant 5$
$K_{s_1t_1u_1}=-K_{s_2t_2u_1}$ $=-K_{s_1t_2u_2}$ $=-K_{s_2t_1u_2}$	$K^{(I)}_{stu}$ $(Q_{s_1}Q_{t_1}Q_{u_1}-Q_{s_2}Q_{t_2}Q_{u_1}-Q_{s_1}Q_{t_2}Q_{u_2}-Q_{s_2}Q_{t_1}Q_{u_2})$		$c_s+c_t+c_u=N$	I, II	$N=3,\geqslant 5$
$K_{s_1t_1u_2}=-K_{s_2t_2u_2}$ $= K_{s_1t_2u_1}$ $= K_{s_2t_1u_1}$	$K^{(II)}_{stu}$ $(Q_{s_1}Q_{t_1}Q_{u_2}-Q_{s_2}Q_{t_2}Q_{u_2}+Q_{s_1}Q_{t_2}Q_{u_1}+Q_{s_2}Q_{t_1}Q_{u_1})$		$c_s+c_t+c_u=N$	II	$N=3,\geqslant 5$
$K_{s_1t_1u_1}=-K_{s_2t_2u_1}$ $= K_{s_1t_2u_2}$ $= K_{s_2t_1u_2}$	$K^{(III)}_{stu}$ $(Q_{s_1}Q_{t_1}Q_{u_1}-Q_{s_2}Q_{t_2}Q_{u_1}+Q_{s_1}Q_{t_2}Q_{u_2}+Q_{s_2}Q_{t_1}Q_{u_2})$		$c_u=c_s+c_t$	I, II	$N\geqslant 5$
$K_{s_1t_1u_2}=-K_{s_2t_2u_2}$ $=-K_{s_1t_2u_1}$ $=-K_{s_2t_1u_1}$	$K^{(IV)}_{stu}$ $(Q_{s_1}Q_{t_1}Q_{u_2}-Q_{s_2}Q_{t_2}Q_{u_2}-Q_{s_1}Q_{t_2}Q_{u_1}-Q_{s_2}Q_{t_1}Q_{u_1})$		$c_u=c_s+c_t$	II	$N\geqslant 5$

c_i is the subscript labelling the degenerate representation of mode i, for example $c_i=1$ for E or E_1, $c_i=2$ for E_2, etc.
p is a non zero integer number and N indicates the order of the principal symmetry axis. For I and II Group classification see Table A.1.

Table A.3: Non-vanishing quartic energy derivatives K_{mmss}, K_{mnss} and K_{mnst} with respect to Q_{i_σ} and their symmetry relations[60].

Symmetry	$\mathcal{H}^{(2)}_{vib}$ w.r.t. $Q_{i\sigma}Q_{j\nu}Q_{k\tau}Q_{l\epsilon}$	Q_m	Q_n	c_s c_t	Group	N
$K_{mms_1s_1}=K_{mms_2s_2}$	$K_{mmss}\ Q_m^2(Q_{s_1}^2+Q_{s_2}^2)/4$	A_1 or A_2		any c_s	I, II	$N\geqslant 3,\infty$
		B_1 or B_2		any c_s	I, II	$N=4,6,2p,\ldots$
$K_{mms_1t_1}=K_{mms_2t_2}$	$K^{(I)}_{mmst}\ Q_m^2(Q_{s_1}Q_{t_1}+Q_{s_2}Q_{t_2})/2$	A_1 or A_2		$c_s=c_t$	I, II	$N\geqslant 3,\infty$
		B_1 or B_2		$c_s=c_t$	I, II	$N=4,6,2p,\ldots$
$K_{mms_1t_2}=-K_{mms_2t_1}$	$K^{(II)}_{mmst}\ Q_m^2(Q_{s_1}Q_{t_2}-Q_{s_2}Q_{t_1})/2$	A_1 or A_2		$c_s=c_t$	II	$N\geqslant 3,\infty$
		B_1 or B_2		$c_s=c_t$	II	$N=4,6,2p,\ldots$
$K_{mns_1s_1}=K_{mns_2s_2}$	$K^{(I)}_{mnss}\ Q_mQ_n(Q_{s_1}^2+Q_{s_2}^2)/2$	A_1	A_1	any c_s	I, II	$N\geqslant 3,\infty$
		A_2	A_2			
		B_1	B_1	any c_s	I, II	$N=4,6,2p,\ldots$
		B_2	B_2			
$K_{mns_1s_1}=-K_{mns_2s_2}$	$K^{(II)}_{mnss}\ Q_mQ_n(Q_{s_1}^2-Q_{s_2}^2)/2$	A_1	B_1	$c_s=N/4$	I, II	$N=4,8,4p,\ldots$
		A_2	B_2			
$K_{mns_1s_2}$	$K^{(III)}_{mnss}\ Q_mQ_nQ_{s_1}Q_{s_2}$	A_1	B_2	$c_s=N/4$	I, II	$N=4,8,4p,\ldots$
		A_2	B_1			
$K_{mns_1t_1}=K_{mns_2t_2}$	$K^{(I)}_{mnst}\ Q_mQ_n(Q_{s_1}Q_{t_1}+Q_{s_2}Q_{t_2})$	A_1	A_1	$c_s=c_t$	I, II	$N\geqslant 3,\infty$
		A_2	A_2			
		B_1	B_1	$c_s=c_t$	I, II	$N=4,6,2p,\ldots$
		B_2	B_2			
$K_{mns_1t_1}=-K_{mns_2t_2}$	$K^{(II)}_{mnst}\ Q_mQ_n(Q_{s_1}Q_{t_1}-Q_{s_2}Q_{t_2})$	A_1	B_1	$c_s+c_t=N/2$	I, II	$N=4,6,2p,\ldots$
		A_2	B_2			
$K_{mns_1t_2}=K_{mns_2t_1}$	$K^{(III)}_{mnst}\ Q_mQ_n(Q_{s_1}Q_{t_2}+Q_{s_2}Q_{t_1})$	A_1	A_2	$c_s=c_t$	I, II	$N\geqslant 3,\infty$
		A_2	A_1			
		B_1	B_2	$c_s=c_t$	I, II	$N=4,6,2p,\ldots$
		B_2	B_1			
$K_{mns_1t_2}=-K_{mns_2t_1}$	$K^{(IV)}_{mnst}\ Q_mQ_n(Q_{s_1}Q_{t_2}-Q_{s_2}Q_{t_1})$	A_1	B_2	$c_s+c_t=N/2$	I, II	$N=4,6,2p,\ldots$
		A_2	B_1			

c_i is the subscript labelling the degenerate representation of mode i, for example $c_i=1$ for E or E_1, $c_i=2$ for E_2, etc.
p is a non zero integer number and N indicates the order of the principal symmetry axis. For I and II Group classification see Table A.1.

Table A.4: Non-vanishing quartic energy derivatives K_{msss}, K_{msst} and K_{mstu} with respect to Q_{i_σ} and their symmetry relations[60].

Symmetry	$\mathcal{H}^{(2)}_{vib}$ w.r.t. $Q_{i\sigma}Q_{j\nu}Q_{k\tau}Q_{l\epsilon}$	Q_m	c_s c_t c_u	Group	N
$K_{ms_1s_1s_1}=-K_{ms_1s_2s_2}$	$K^{(I)}_{msss}\ Q_m(Q^3_{s_1}-3Q_{s_1}Q^2_{s_2})/6$	A_1	$3c_s=N$	I, II	$N=3,6,3p,\dots$
		B_1	$3c_s=N/2$	I, II	$N=6,12,6p,\dots$
$K_{ms_2s_2s_2}=-K_{ms_1s_1s_2}$	$K^{(II)}_{msss}\ Q_m(Q^3_{s_2}-3Q^2_{s_1}Q_{s_2})/6$	A_2	$3c_s=N$	I, II	$N=3,6,3p,\dots$
		B_2	$3c_s=N/2$	I, II	$N=6,12,6p,\dots$
$K_{ms_1s_1t_1}=-K_{ms_2s_2t_1}$	$K^{(I)}_{msst}\ Q_m(Q^2_{s_1}Q_{t_1}-Q^2_{s_2}Q_{t_1}+2Q_{s_1}Q_{s_2}Q_{t_2})/2$	A_1	$c_t=2c_s$	I, II	$N\geqslant 5$
$=K_{ms_1s_2t_2}$		B_1	$c_t=2c_s-N/2$	I, II	$N=6,8,2p,\dots$
$K_{ms_1s_1t_1}=-K_{ms_2s_2t_1}$	$K^{(II)}_{msst}\ Q_m(Q^2_{s_1}Q_{t_1}-Q^2_{s_2}Q_{t_1}-2Q_{s_1}Q_{s_2}Q_{t_2})/2$	A_1	$2c_s+c_t=N$	I, II	$N=3,\geqslant 5$
$=-K_{ms_1s_2t_2}$		B_1	$2c_s+c_t=N/2$	I, II	$N=6,8,2p,\dots$
$K_{ms_1s_1t_2}=-K_{ms_2s_2t_2}$	$K^{(III)}_{msst}\ Q_m(Q^2_{s_1}Q_{t_2}-Q^2_{s_2}Q_{t_2}-2Q_{s_1}Q_{s_2}Q_{t_1})/2$	A_2	$c_t=2c_s$	I, II	$N\geqslant 5$
$=-K_{ms_1s_2t_1}$		B_2	$c_t=2c_s-N/2$	I, II	$N=6,8,2p,\dots$
$K_{ms_1s_1t_2}=-K_{ms_2s_2t_2}$	$K^{(IV)}_{msst}\ Q_m(Q^2_{s_1}Q_{t_2}-Q^2_{s_2}Q_{t_2}+2Q_{s_1}Q_{s_2}Q_{t_1})/2$	A_2	$2c_s+c_t=N$	I, II	$N=3,\geqslant 5$
$=K_{ms_1s_2t_1}$		B_2	$2c_s+c_t=N/2$	I, II	$N=6,8,2p,\dots$
$K_{ms_1t_1u_1}=-K_{ms_2t_2u_1}$	$K^{(I)}_{mstu}Q_m(Q_{s_1}Q_{t_1}Q_{t_1}-Q_{s_2}Q_{t_2}Q_{t_1}$	A_1	$c_u=c_s+c_t$	I, II	$N=\geqslant 5$
$=K_{ms_1t_2u_2}$	$+Q_{s_1}Q_{t_2}Q_{t_2}+Q_{s_2}Q_{t_1}Q_{t_2})$	B_1	$c_u=c_s+c_t-N/2$	I, II	$N=6,8,2p,\dots$
$=K_{ms_2t_1u_2}$					
$K_{ms_1t_1u_1}=-K_{ms_2t_2u_1}$	$K^{(II)}_{mstu}Q_m(Q_{s_1}Q_{t_1}Q_{t_1}-Q_{s_2}Q_{t_2}Q_{t_1}$	A_1	$c_s+c_t+c_u=N$	I, II	$N=3,\geqslant 5$
$=-K_{ms_1t_2u_2}$	$-Q_{s_1}Q_{t_2}Q_{t_2}-Q_{s_2}Q_{t_1}Q_{t_2})$	B_1	$c_s+c_t+c_u=N/2$	I, II	$N=6,8,2p,\dots$
$=-K_{ms_2t_1u_2}$					
$K_{ms_1t_1u_2}=-K_{ms_2t_2u_2}$	$K^{(III)}_{mstu}Q_m(Q_{s_1}Q_{t_1}Q_{t_2}-Q_{s_2}Q_{t_2}Q_{t_2}$	A_2	$c_u=c_s+c_t$	I, II	$N=\geqslant 5$
$=-K_{ms_1t_2u_1}$	$-Q_{s_1}Q_{t_2}Q_{t_1}-Q_{s_2}Q_{t_1}Q_{t_1})$	B_2	$c_u=c_s+c_t-N/2$	I, II	$N=6,8,2p,\dots$
$=-K_{ms_2t_1u_1}$					
$K_{ms_1t_1u_2}=-K_{ms_2t_2u_2}$	$K^{(IV)}_{mstu}Q_m(Q_{s_1}Q_{t_1}Q_{t_2}-Q_{s_2}Q_{t_2}Q_{t_2}$	A_2	$c_s+c_t+c_u=N$	I, II	$N=3,\geqslant 5$
$=K_{ms_1t_2u_1}$	$+Q_{s_1}Q_{t_2}Q_{t_1}+Q_{s_2}Q_{t_1}Q_{t_1})$	B_2	$c_s+c_t+c_u=N/2$	I, II	$N=6,8,2p,\dots$
$=K_{ms_2t_1u_1}$					

c_i is the subscript labelling the degenerate representation of mode i, for example $c_i=1$ for E or E_1, $c_i=2$ for E_2, etc.
p is a non zero integer number and N indicates the order of the principal symmetry axis. For I and II Group classification see Table A.1.

Table A.5: Non-vanishing quartic energy derivatives K_{ssss} and K_{sstt} with respect to Q_{i_σ} and their symmetry relations[60].

Symmetry	$\mathcal{H}^{(2)}_{vib}$ w.r.t. $Q_{i\sigma}Q_{j\nu}Q_{k\tau}Q_{l\epsilon}$	c_s c_t	Group	N
$K_{s_1s_1s_1s_1}= K_{s_2s_2s_2s_2}$ $=3K_{s_1s_1s_2s_2}$	$K^{(I)}_{ssss}(Q^4_{s_1}+Q^4_{s_2}+2Q^2_{s_1}Q^2_{s_2})/24$	$c_s \neq N/4$	I, II	$N=3,\geqslant 5,\infty$
$K_{s_1s_1s_1s_1}= K_{s_2s_2s_2s_2}$ $K_{s_1s_1s_2s_2}$	$K^{(II)}_{ssss}(Q^4_{s_1}+Q^4_{s_2})/24$ $K^{(III)}_{ssss}Q^2_{s_1}Q^2_{s_2}/4$	$c_s = N/4$	I, II	$N=4,8,4p,\ldots$
$K_{s_1s_1s_1s_2}=-K_{s_1s_2s_2s_2}$	$K^{(IV)}_{ssss}(Q^3_{s_1}Q_{s_2}-Q_{s_1}Q^3_{s_2})/6$	$c_s = N/4$	II	$N=4,8,4p,\ldots$
$K_{s_1s_1t_1t_1}= K_{s_2s_2t_2t_2}$ $= K_{s_1s_1t_2t_2}$ $= K_{s_2s_2t_1t_1}$	$K^{(I)}_{sstt}(Q^2_{s_1}Q^2_{t_1}+Q^2_{s_2}Q^2_{t_2}+Q^2_{s_1}Q^2_{t_2}+Q^2_{s_2}Q^2_{t_1})/4$	$c_t+c_s \neq N/2$ $c_t \neq c_s$	I, II	$N\geqslant 5$
$K_{s_1s_1t_1t_1}= K_{s_2s_2t_2t_2}$ $K_{s_1s_1t_2t_2}= K_{s_2s_2t_1t_1}$ $K_{s_1s_2t_1t_2}=(K_{s_1s_1t_1t_1}-K_{s_1s_1t_2t_2})/2$	$K^{(II)}_{sstt}(Q^2_{s_1}Q^2_{t_1}+Q^2_{s_2}Q^2_{t_2}+2Q_{s_1}Q_{s_2}Q_{t_1}Q_{t_2})/4$ $K^{(III)}_{sstt}(Q^2_{s_1}Q^2_{t_2}+Q^2_{s_2}Q^2_{t_1}-2Q_{s_1}Q_{s_2}Q_{t_1}Q_{t_2})/4$	$c_t = c_s \neq N/4$	I, II	$N=3,\geqslant 5,\infty$
$K_{s_1s_1t_1t_1}= K_{s_2s_2t_2t_2}$ $K_{s_1s_1t_2t_2}= K_{s_2s_2t_1t_1}$ $K_{s_1s_2t_1t_2}=(K_{s_1s_1t_2t_2}-K_{s_1s_1t_1t_1})/2$	$K^{(IV)}_{sstt}(Q^2_{s_1}Q^2_{t_1}+Q^2_{s_2}Q^2_{t_2}-2Q_{s_1}Q_{s_2}Q_{t_1}Q_{t_2})/4$ $K^{(V)}_{sstt}(Q^2_{s_1}Q^2_{t_2}+Q^2_{s_2}Q^2_{t_1}+2Q_{s_1}Q_{s_2}Q_{t_1}Q_{t_2})/4$	$c_t+c_s = N/2$ $c_t \neq c_s$	I, II	$N=6,8,2p,\ldots$
$K_{s_1s_1t_1t_1}= K_{s_2s_2t_2t_2}$ $K_{s_1s_1t_2t_2}= K_{s_2s_2t_1t_1}$ $K_{s_1s_2t_1t_2}$	$K^{(VI)}_{sstt}(Q^2_{s_1}Q^2_{t_1}+Q^2_{s_2}Q^2_{t_2})/4$ $K^{(VII)}_{sstt}(Q^2_{s_1}Q^2_{t_2}+Q^2_{s_2}Q^2_{t_1})/4$ $K^{(VIII)}_{sstt}Q_{s_1}Q_{s_2}Q_{t_1}Q_{t_2}$	$c_t = c_s = N/4$	I, II	$N=4,8,4p,\ldots$
$K_{s_1s_1t_1t_2}=-K_{s_2s_2t_1t_2}$ $= K_{s_1s_2t_1t_1}$ $=-K_{s_1s_2t_2t_2}$	$K^{(IX)}_{sstt}(Q^2_{s_1}Q_{t_1}Q_{t_2}-Q^2_{s_2}Q_{t_1}Q_{t_2}$ $+Q_{s_1}Q_{s_2}Q^2_{t_1}-Q_{s_1}Q_{s_2}Q^2_{t_2})/2$	$c_t+c_s = N/2$ $c_t \neq c_s$	II	$N=6,8,2p,\ldots$
$K_{s_1s_1t_1t_2}=-K_{s_2s_2t_1t_2}$ $=-K_{s_1s_2t_1t_1}$ $= K_{s_1s_2t_2t_2}$	$K^{(X)}_{sstt}(Q^2_{s_1}Q_{t_1}Q_{t_2}-Q^2_{s_2}Q_{t_1}Q_{t_2}$ $-Q_{s_1}Q_{s_2}Q^2_{t_1}+Q_{s_1}Q_{s_2}Q^2_{t_2})/2$	$c_t = c_s \neq N/4$	II	$N=3,\geqslant 5,\infty$
$K_{s_1s_1t_1t_2}=-K_{s_2s_2t_1t_2}$ $K_{s_1s_2t_1t_1}=-K_{s_1s_2t_2t_2}$	$K^{(XI)}_{sstt}(Q^2_{s_1}Q_{t_1}Q_{t_2}-Q^2_{s_2}Q_{t_1}Q_{t_2})/2$ $K^{(XII)}_{sstt}(Q_{s_1}Q_{s_2}Q^2_{t_1}-Q_{s_1}Q_{s_2}Q^2_{t_2})/2$	$c_t = c_s = N/4$	II	$N=4,8,4p,\ldots$

c_i is the subscript labelling the degenerate representation of mode i, for example $c_i = 1$ for E or E_1, $c_i = 2$ for E_2, etc.
p is a non zero integer number and N indicates the order of the principal symmetry axis. For I and II Group classification see Table A.1.

Table A.6: Non-vanishing quartic energy derivatives K_{ssst} with respect to Q_{i_σ} and their symmetry relations[60].

Symmetry	$\mathcal{H}^{(2)}_{vib}$ w.r.t. $Q_{i\sigma}Q_{j\nu}Q_{k\tau}Q_{l\epsilon}$	c_s c_t	Group	N
$K_{s_1s_1s_1t_1}$ = $-K_{s_2s_2s_2t_2}$	$K^{(I)}_{ssst}(Q^3_{s_1}Q_{t_1} - Q^3_{s_2}Q_{t_2}$	$c_t = 3c_s$	I, II	$N \geqslant 7$
$= K_{s_1s_1s_2t_2}$	$+3Q^2_{s_1}Q_{s_2}Q_{t_2} - 3Q_{s_1}Q^2_{s_2}Q_{t_1})/6$	$c_t = 3c_s - N$	I, II	$N = 5, \geqslant 7$
$= -K_{s_1s_2s_2t_1}$				
$K_{s_1s_1s_1t_1} = K_{s_2s_2s_2t_2}$	$K^{(II)}_{ssst}(Q^3_{s_1}Q_{t_1} + Q^3_{s_2}Q_{t_2}$			
$= -K_{s_1s_1s_2t_2}$	$-3Q^2_{s_1}Q_{s_2}Q_{t_2} - 3Q_{s_1}Q^2_{s_2}Q_{t_1})/6$	$3c_s + c_t = N$	I, II	$N \geqslant 5$
$= -K_{s_1s_2s_2t_1}$				
$K_{s_1s_1s_1t_1} = K_{s_2s_2s_2t_2}$	$K^{(III)}_{ssst}(Q^3_{s_1}Q_{t_1} + Q^3_{s_2}Q_{t_2}$			
$= 3K_{s_1s_1s_2t_2}$	$+9Q^2_{s_1}Q_{s_2}Q_{t_2} + 9Q_{s_1}Q^2_{s_2}Q_{t_1})/6$	$c_s = c_t \neq N/4$	I, II	$N = 3, \geqslant 5, \infty$
$= 3K_{s_1s_2s_2t_1}$				
$K_{s_1s_1s_1t_1} = K_{s_2s_2s_2t_2}$	$K^{(IV)}_{ssst}(Q^3_{s_1}Q_{t_1} + Q^3_{s_2}Q_{t_2})/6$	$c_s = c_t = N/4$	I, II	$N = 4, 8, 4p, \ldots$
$K_{s_1s_1s_2t_2} = K_{s_1s_2s_2t_1}$	$K^{(V)}_{ssst}(Q^2_{s_1}Q_{s_2}Q_{t_2} + Q_{s_1}Q^2_{s_2}Q_{t_1})/2$			
$K_{s_1s_1s_1t_2} = K_{s_2s_2s_2t_1}$	$K^{(VI)}_{ssst}(Q^3_{s_1}Q_{t_2} + Q^3_{s_2}Q_{t_1}$	$c_t = 3c_s$	II	$N \geqslant 7$
$= -K_{s_1s_1s_2t_1}$	$-3Q^2_{s_1}Q_{s_2}Q_{t_1} - 3Q_{s_1}Q^2_{s_2}Q_{t_2})/6$	$c_t = 3c_s - N$	II	$N = 5, \geqslant 7$
$= -K_{s_1s_2s_2t_2}$				
$K_{s_1s_1s_1t_2} = -K_{s_2s_2s_2t_1}$	$K^{(VII)}_{ssst}(Q^3_{s_1}Q_{t_2} - Q^3_{s_2}Q_{t_1}$			
$= K_{s_1s_1s_2t_1}$	$+3Q^2_{s_1}Q_{s_2}Q_{t_1} - 3Q_{s_1}Q^2_{s_2}Q_{t_2})/6$	$3c_s + c_t = N$	II	$N \geqslant 5$
$= -K_{s_1s_2s_2t_2}$				
$K_{s_1s_1s_1t_2} = -K_{s_2s_2s_2t_1}$	$K^{(VIII)}_{ssst}(Q^3_{s_1}Q_{t_2} - Q^3_{s_2}Q_{t_1}$			
$= -3K_{s_1s_1s_2t_1}$	$-9Q^2_{s_1}Q_{s_2}Q_{t_1} + 9Q_{s_1}Q^2_{s_2}Q_{t_2})/6$	$c_s = c_t \neq N/4$	II	$N = 3, \geqslant 5, \infty$
$= 3K_{s_1s_2s_2t_2}$				
$K_{s_1s_1s_1t_2} = -K_{s_2s_2s_2t_1}$	$K^{(IX)}_{ssst}(Q^3_{s_1}Q_{t_2} - Q^3_{s_2}Q_{t_1})/6$	$c_s = c_t = N/4$	II	$N = 4, 8, 4p, \ldots$
$K_{s_1s_1s_2t_1} = -K_{s_1s_2s_2t_2}$	$K^{(X)}_{ssst}(Q^2_{s_1}Q_{s_2}Q_{t_1} - Q_{s_1}Q^2_{s_2}Q_{t_2})/2$			

c_i is the subscript labelling the degenerate representation of mode i, for example $c_i = 1$ for E or E_1, $c_i = 2$ for E_2, etc.
p is a non zero integer number and N indicates the order of the principal symmetry axis. For I and II Group classification see Table A.1.

Table A.7: Non-vanishing quartic energy derivatives K_{sstu} with respect to Q_{i_σ} and their symmetry relations[60].

Symmetry	$\mathcal{H}^{(2)}_{vib}$ w.r.t. $Q_{i\sigma}Q_{j\nu}Q_{k\tau}Q_{l\epsilon}$	c_s c_t c_u	Group	N
$K_{s_1s_1t_1u_1}=-K_{s_2s_2t_2u_2}$ $=K_{s_1s_1t_2u_2}$ $=-K_{s_2s_2t_1u_1}$ $=K_{s_1s_2t_1u_2}$ $=-K_{s_1s_2t_2u_1}$	$K^{(I)}_{sstu}(Q^2_{s_1}Q_{t_1}Q_{u_1}-Q^2_{s_2}Q_{t_2}Q_{u_2}+Q^2_{s_1}Q_{t_2}Q_{u_2}$ $-Q^2_{s_2}Q_{t_1}Q_{u_1}+2Q_{s_1}Q_{s_2}Q_{t_1}Q_{u_2}-2Q_{s_1}Q_{s_2}Q_{t_2}Q_{u_1})/2$	$c_u=2c_s+c_t$	I, II	$N\geqslant 7$
		$c_u=2c_s+c_t-N$	I, II	$N=5,\geqslant 7$
$K_{s_1s_1t_1u_1}=K_{s_2s_2t_2u_2}$ $=-K_{s_1s_1t_2u_2}$ $=-K_{s_2s_2t_1u_1}$ $=-K_{s_1s_2t_1u_2}$ $=-K_{s_1s_2t_2u_1}$	$K^{(II)}_{sstu}(Q^2_{s_1}Q_{t_1}Q_{u_1}+Q^2_{s_2}Q_{t_2}Q_{u_2}-Q^2_{s_1}Q_{t_2}Q_{u_2}$ $-Q^2_{s_2}Q_{t_1}Q_{u_1}-2Q_{s_1}Q_{s_2}Q_{t_1}Q_{u_2}-2Q_{s_1}Q_{s_2}Q_{t_2}Q_{u_1})/2$	$2c_s+c_t+c_u=N$ $c_s\neq N/4, c_s+c_t\neq N/2$	I, II	$N\geqslant 5$
$K_{s_1s_1t_1u_1}=K_{s_2s_2t_2u_2}$ $=-K_{s_1s_1t_2u_2}$ $=-K_{s_2s_2t_1u_1}$ $=K_{s_1s_2t_1u_2}$ $=K_{s_1s_2t_2u_1}$	$K^{(III)}_{sstu}(Q^2_{s_1}Q_{t_1}Q_{u_1}+Q^2_{s_2}Q_{t_2}Q_{u_2}-Q^2_{s_1}Q_{t_2}Q_{u_2}$ $-Q^2_{s_2}Q_{t_1}Q_{u_1}+2Q_{s_1}Q_{s_2}Q_{t_1}Q_{u_2}+2Q_{s_1}Q_{s_2}Q_{t_2}Q_{u_1})/2$	$c_t+c_u=2c_s\neq N/2$ $c_t\neq c_u$	I, II	$N\geqslant 7$
$K_{s_1s_1t_1u_1}=K_{s_2s_2t_2u_2}$ $=-K_{s_1s_1t_2u_2}$ $=-K_{s_2s_2t_1u_1}$	$K^{(IV)}_{sstu}(Q^2_{s_1}Q_{t_1}Q_{u_1}+Q^2_{s_2}Q_{t_2}Q_{u_2}-Q^2_{s_1}Q_{t_2}Q_{u_2}-Q^2_{s_2}Q_{t_1}Q_{u_1})/2$	$c_t+c_u=N/2$ $c_t\neq c_u$	I, II	$N=8,12,4p,\ldots$
$K_{s_1s_2t_1u_2}=K_{s_1s_2t_2u_1}$	$K^{(V)}_{sstu}(Q_{s_1}Q_{s_2}Q_{t_1}Q_{u_2}+Q_{s_1}Q_{s_2}Q_{t_2}Q_{u_1})$	$c_s=N/4$	I, II	$N=8,12,4p,\ldots$
$K_{s_1s_1t_1u_1}=K_{s_2s_2t_2u_2}$ $=K_{s_1s_1t_2u_2}$ $=K_{s_2s_2t_1u_1}$	$K^{(VI)}_{sstu}(Q^2_{s_1}Q_{t_1}Q_{u_1}+Q^2_{s_2}Q_{t_2}Q_{u_2}+Q^2_{s_1}Q_{t_2}Q_{u_2}+Q^2_{s_2}Q_{t_1}Q_{u_1})/2$	$c_s\neq c_t=c_u$ $c_s+c_t\neq N/2$	I, II	$N\geqslant 3$
$K_{s_1s_1t_1u_1}=K_{s_2s_2t_2u_2}$ $K_{s_1s_1t_2u_2}=K_{s_2s_2t_1u_1}$ $K_{s_1s_2t_1u_2}=K_{s_1s_2t_2u_1}$ $=(K_{s_1s_1t_2u_2}-K_{s_1s_1t_1u_1})/2$	$K^{(VII)}_{sstu}(Q^2_{s_1}Q_{t_1}Q_{u_1}+Q^2_{s_2}Q_{t_2}Q_{u_2}-Q_{s_1}Q_{s_2}Q_{t_1}Q_{u_2}-Q_{s_1}Q_{s_2}Q_{t_2}Q_{u_1})/2$ $K^{(VIII)}_{sstu}(Q^2_{s_1}Q_{t_2}Q_{u_2}+Q^2_{s_2}Q_{t_1}Q_{u_1}+Q_{s_1}Q_{s_2}Q_{t_1}Q_{u_2}+Q_{s_1}Q_{s_2}Q_{t_2}Q_{u_1})/2$	$c_s\neq c_t=c_u$ $c_s+c_t\neq N/2$	I, II	$N=6,8,2p,\ldots$
$K_{s_1s_1t_1u_1}=K_{s_2s_2t_2u_2}$ $K_{s_1s_1t_2u_2}=K_{s_2s_2t_1u_1}$ $K_{s_1s_2t_1u_2}=K_{s_1s_2t_2u_1}$ $=(K_{s_1s_1t_1u_1}-K_{s_1s_1t_2u_2})/2$	$K^{(IX)}_{sstu}(Q^2_{s_1}Q_{t_1}Q_{u_1}+Q^2_{s_2}Q_{t_2}Q_{u_2}+Q_{s_1}Q_{s_2}Q_{t_1}Q_{u_2}+Q_{s_1}Q_{s_2}Q_{t_2}Q_{u_1})/2$ $K^{(X)}_{sstu}(Q^2_{s_1}Q_{t_2}Q_{u_2}+Q^2_{s_2}Q_{t_1}Q_{u_1}-Q_{s_1}Q_{s_2}Q_{t_1}Q_{u_2}-Q_{s_1}Q_{s_2}Q_{t_2}Q_{u_1})/2$	$c_s=c_t=c_u\neq N/4$	I, II	$N=3,\geqslant 5,\infty$
$K_{s_1s_1t_1u_1}=K_{s_2s_2t_2u_2}$ $K_{s_1s_1t_2u_2}=K_{s_2s_2t_1u_1}$ $K_{s_1s_2t_1u_2}=K_{s_1s_2t_2u_1}$	$K^{(XI)}_{sstu}(Q^2_{s_1}Q_{t_1}Q_{u_1}+Q^2_{s_2}Q_{t_2}Q_{u_2})/2$ $K^{(XII)}_{sstu}(Q^2_{s_1}Q_{t_2}Q_{u_2}+Q^2_{s_2}Q_{t_1}Q_{u_1})/2$ $K^{(XIII)}_{sstu}(Q_{s_1}Q_{s_2}Q_{t_1}Q_{u_2}+Q_{s_1}Q_{s_2}Q_{t_2}Q_{u_1})$	$c_s=c_t=c_u=N/4$	I, II	$N=4,8,4p,\ldots$

c_i is the subscript labelling the degenerate representation of mode i, for example $c_i=1$ for E or E_1, $c_i=2$ for E_2, etc.
p is a non zero integer number and N indicates the order of the principal symmetry axis. For I and II Group classification see Table A.1.

— Table A.7 continued —

Symmetry	$\mathcal{H}^{(2)}_{vib}$ w.r.t. $Q_{i\sigma}Q_{j_\nu}Q_{k_\tau}Q_{l_\epsilon}$	$c_s \quad c_t \quad c_u$	Group	N
$K_{s_1s_1t_1u_2}= \quad K_{s_2s_2t_2u_1}$ $=-K_{s_1s_1t_2u_1}$ $=-K_{s_2s_2t_1u_2}$ $=-K_{s_1s_2t_1u_1}$ $=-K_{s_1s_2t_2u_2}$	$K^{(XIV)}_{sstu}(Q^2_{s_1}Q_{t_1}Q_{u_2}+Q^2_{s_2}Q_{t_2}Q_{u_1}-Q^2_{s_1}Q_{t_2}Q_{u_1}$ $-Q^2_{s_2}Q_{t_1}Q_{u_2}-2Q_{s_1}Q_{s_2}Q_{t_1}Q_{u_1}-2Q_{s_1}Q_{s_2}Q_{t_2}Q_{u_2})/2$	$c_u = 2c_s + c_t$	II	$N \geqslant 7$
		$c_u = 2c_s + c_t - N$	II	$N = 5, \geqslant 7$
$K_{s_1s_1t_1u_2}=-K_{s_2s_2t_2u_1}$ $= \quad K_{s_1s_1t_2u_1}$ $=-K_{s_2s_2t_1u_2}$ $= \quad K_{s_1s_2t_1u_1}$ $=-K_{s_1s_2t_2u_2}$	$K^{(XV)}_{sstu}(Q^2_{s_1}Q_{t_1}Q_{u_2}-Q^2_{s_2}Q_{t_2}Q_{u_1}+Q^2_{s_1}Q_{t_2}Q_{u_1}$ $-Q^2_{s_2}Q_{t_1}Q_{u_2}+2Q_{s_1}Q_{s_2}Q_{t_1}Q_{u_1}-2Q_{s_1}Q_{s_2}Q_{t_2}Q_{u_2})/2$	$2c_s + c_t + c_u = N$ $c_s \neq N/4, c_s + c_t \neq N/2$	II	$N \geqslant 5$
$K_{s_1s_1t_1u_2}=-K_{s_2s_2t_2u_1}$ $= \quad K_{s_1s_1t_2u_1}$ $=-K_{s_2s_2t_1u_2}$ $=-K_{s_1s_2t_1u_1}$ $= \quad K_{s_1s_2t_2u_2}$	$K^{(XVI)}_{sstu}(Q^2_{s_1}Q_{t_1}Q_{u_2}-Q^2_{s_2}Q_{t_2}Q_{u_1}+Q^2_{s_1}Q_{t_2}Q_{u_1}$ $-Q^2_{s_2}Q_{t_1}Q_{u_2}-2Q_{s_1}Q_{s_2}Q_{t_1}Q_{u_1}+2Q_{s_1}Q_{s_2}Q_{t_2}Q_{u_2})/2$	$c_t + c_u = 2c_s \neq N/2$ $c_t \neq c_u$	II	$N \geqslant 7$
$K_{s_1s_1t_1u_2}=-K_{s_2s_2t_2u_1}$ $= \quad K_{s_1s_1t_2u_1}$ $=-K_{s_2s_2t_1u_2}$	$K^{(XVII)}_{sstu}(Q^2_{s_1}Q_{t_1}Q_{u_2}-Q^2_{s_2}Q_{t_2}Q_{u_1}+Q^2_{s_1}Q_{t_2}Q_{u_1}-Q^2_{s_2}Q_{t_1}Q_{u_2})/2$	$c_t + c_u = N/2$ $c_t \neq c_u$	II	$N = 8, 12, 4p, \ldots$
$K_{s_1s_2t_1u_1}=-K_{s_1s_2t_2u_2}$	$K^{(XVIII)}_{sstu}(Q_{s_1}Q_{s_2}Q_{t_1}Q_{u_1}-Q_{s_1}Q_{s_2}Q_{t_2}Q_{u_2})$	$c_s = N/4$	II	$N = 8, 12, 4p, \ldots$
$K_{s_1s_1t_1u_2}=-K_{s_2s_2t_2u_1}$ $= \quad K_{s_1s_1t_2u_1}$ $=-K_{s_2s_2t_1u_2}$	$K^{(XIX)}_{sstu}(Q^2_{s_1}Q_{t_1}Q_{u_2}-Q^2_{s_2}Q_{t_2}Q_{u_1}+Q^2_{s_1}Q_{t_2}Q_{u_1}-Q^2_{s_2}Q_{t_1}Q_{u_2})/2$	$c_s \neq c_t = c_u$ $c_s + c_t \neq N/2$	II	$N \geqslant 3$
$K_{s_1s_1t_1u_2}=-K_{s_2s_2t_2u_1}$ $K_{s_1s_1t_2u_1}=-K_{s_2s_2t_1u_2}$ $K_{s_1s_2t_1u_1}=-K_{s_1s_2t_2u_2}$ $= \quad (K_{s_1s_1t_1u_2}+K_{s_1s_1t_2u_1})/2$	$K^{(XX)}_{sstu}(Q^2_{s_1}Q_{t_1}Q_{u_2}-Q^2_{s_2}Q_{t_2}Q_{u_1}+Q_{s_1}Q_{s_2}Q_{t_1}Q_{u_1}-Q_{s_1}Q_{s_2}Q_{t_2}Q_{u_2})/2$ $K^{(XXI)}_{sstu}(Q^2_{s_1}Q_{t_2}Q_{u_1}-Q^2_{s_2}Q_{t_1}Q_{u_2}+Q_{s_1}Q_{s_2}Q_{t_1}Q_{u_1}-Q_{s_1}Q_{s_2}Q_{t_2}Q_{u_2})/2$	$c_s \neq c_t = c_u$ $c_s + c_t \neq N/2$	II	$N = 6, 8, 2p, \ldots$
$K_{s_1s_1t_1u_2}=-K_{s_2s_2t_2u_1}$ $K_{s_1s_1t_2u_1}=-K_{s_2s_2t_1u_2}$ $K_{s_1s_2t_1u_1}=-K_{s_1s_2t_2u_2}$ $= \quad -(K_{s_1s_1t_1u_2}+K_{s_2s_2t_2u_1})/2$	$K^{(XXII)}_{sstu}(Q^2_{s_1}Q_{t_1}Q_{u_2}-Q^2_{s_2}Q_{t_2}Q_{u_1}-Q_{s_1}Q_{s_2}Q_{t_1}Q_{u_1}+Q_{s_1}Q_{s_2}Q_{t_2}Q_{u_2})/2$ $K^{(XXIII)}_{sstu}(Q^2_{s_1}Q_{t_2}Q_{u_1}-Q^2_{s_2}Q_{t_1}Q_{u_2}-Q_{s_1}Q_{s_2}Q_{t_1}Q_{u_1}+Q_{s_1}Q_{s_2}Q_{t_2}Q_{u_2})/2$	$c_s = c_t = c_u \neq N/4$	II	$N = 3, \geqslant 5, \infty$
$K_{s_1s_1t_1u_2}=-K_{s_2s_2t_2u_1}$ $K_{s_1s_1t_2u_1}=-K_{s_2s_2t_1u_2}$ $K_{s_1s_2t_1u_1}=-K_{s_1s_2t_2u_2}$	$K^{(XXIV)}_{sstu}(Q^2_{s_1}Q_{t_1}Q_{u_2}-Q^2_{s_2}Q_{t_2}Q_{u_1})/2$ $K^{(XXV)}_{sstu}(Q^2_{s_1}Q_{t_2}Q_{u_1}-Q^2_{s_2}Q_{t_1}Q_{u_2})/2$ $K^{(XXVI)}_{sstu}(Q_{s_1}Q_{s_2}Q_{t_1}Q_{u_1}-Q_{s_1}Q_{s_2}Q_{t_2}Q_{u_2})$	$c_s = c_t = c_u = N/4$	II	$N = 4, 8, 4p, \ldots$

c_i is the subscript labelling the degenerate representation of mode i, for example $c_i = 1$ for E or E_1, $c_i = 2$ for E_2, etc.
p is a non zero integer number and N indicates the order of the principal symmetry axis. For I and II Group classification see Table A.1.

Table A.8: Non-vanishing quartic energy derivatives K_{stuv} with respect to Q_{i_σ} and their symmetry relations[60].

Symmetry	$\mathcal{H}^{(2)}_{vib}$ w.r.t. $Q_{i\sigma}Q_{j\nu}Q_{k_\tau}Q_{l_\epsilon}$	c_s c_t c_u c_v	Group	N
$K_{s_1t_1u_1v_1}=-K_{s_2t_2u_2v_2}$	$K^{(I)}_{stuv}(Q_{s_1}Q_{s_1}Q_{t_1}Q_{u_1}-Q_{s_2}Q_{s_2}Q_{t_2}Q_{u_2}+Q_{s_1}Q_{s_1}Q_{t_2}Q_{u_2}-Q_{s_2}Q_{s_2}Q_{t_1}Q_{u_1}$			
$=K_{s_1t_1u_2v_2}$	$+Q_{s_1}Q_{s_2}Q_{t_1}Q_{u_2}-Q_{s_2}Q_{s_1}Q_{t_2}Q_{u_1}-Q_{s_1}Q_{s_2}Q_{t_2}Q_{u_1}+Q_{s_2}Q_{s_1}Q_{t_1}Q_{u_2})$	$c_v=c_s+c_t+c_u$	I, II	$N\geqslant 7$
$=-K_{s_2t_2u_1v_1}$				
$=K_{s_1t_2u_1v_2}$				
$=-K_{s_2t_1u_2v_1}$		$c_v=c_s+c_t+c_u-N$	I, II	$N=5,\geqslant 7$
$=-K_{s_1t_2u_2v_1}$				
$=K_{s_2t_1u_1v_2}$				
$K_{s_1t_1u_1v_1}=K_{s_2t_2u_2v_2}$	$K^{(II)}_{stuv}(Q_{s_1}Q_{s_1}Q_{t_1}Q_{u_1}+Q_{s_2}Q_{s_2}Q_{t_2}Q_{u_2}-Q_{s_1}Q_{s_1}Q_{t_2}Q_{u_2}-Q_{s_2}Q_{s_2}Q_{t_1}Q_{u_1}$			
$=-K_{s_1t_1u_2v_2}$	$-Q_{s_1}Q_{s_2}Q_{t_1}Q_{u_2}-Q_{s_2}Q_{s_1}Q_{t_2}Q_{u_1}-Q_{s_1}Q_{s_2}Q_{t_2}Q_{u_1}-Q_{s_2}Q_{s_1}Q_{t_1}Q_{u_2})$	$c_s+c_t+c_u+c_v=N$	I, II	$N\geqslant 5$
$=-K_{s_2t_2u_1v_1}$		$c_s+c_t\neq N/2$		
$=-K_{s_1t_2u_1v_2}$		$c_s+c_u\neq N/2$,		
$=-K_{s_2t_1u_2v_1}$		$c_s+c_v\neq N/2$		
$=-K_{s_1t_2u_2v_1}$				
$=-K_{s_2t_1u_1v_2}$				
$K_{s_1t_1u_1v_1}=K_{s_2t_2u_2v_2}$	$K^{(III)}_{stuv}(Q_{s_1}Q_{s_1}Q_{t_1}Q_{u_1}+Q_{s_2}Q_{s_2}Q_{t_2}Q_{u_2}+Q_{s_1}Q_{s_1}Q_{t_2}Q_{u_2}+Q_{s_2}Q_{s_2}Q_{t_1}Q_{u_1}$			
$=K_{s_1t_1u_2v_2}$	$+Q_{s_1}Q_{s_2}Q_{t_1}Q_{u_2}+Q_{s_2}Q_{s_1}Q_{t_2}Q_{u_1}-Q_{s_1}Q_{s_2}Q_{t_2}Q_{u_1}-Q_{s_2}Q_{s_1}Q_{t_1}Q_{u_2})$			
$=K_{s_2t_2u_1v_1}$		$c_s+c_v=c_t+c_u\neq N/2$	I, II	$N\geqslant 7$
$=K_{s_1t_2u_1v_2}$		$c_s<c_t<c_u<c_v$		
$=K_{s_2t_1u_2v_1}$				
$=-K_{s_1t_2u_2v_1}$				
$=-K_{s_2t_1u_1v_2}$				
$K_{s_1t_1u_2v_2}=K_{s_2t_2u_1v_1}$	$K^{(IV)}_{stuv}(Q_{s_1}Q_{s_1}Q_{t_1}Q_{u_1}+Q_{s_2}Q_{s_2}Q_{t_2}Q_{u_2}-Q_{s_1}Q_{s_2}Q_{t_2}Q_{u_1}-Q_{s_2}Q_{s_1}Q_{t_1}Q_{u_2})$			
$=K_{s_1t_2u_1v_2}$	$K^{(V)}_{stuv}(Q_{s_1}Q_{s_1}Q_{t_2}Q_{u_2}+Q_{s_2}Q_{s_2}Q_{t_1}Q_{u_1}+Q_{s_1}Q_{s_2}Q_{t_1}Q_{u_2}+Q_{s_2}Q_{s_1}Q_{t_2}Q_{u_1})$			
$=K_{s_2t_1u_2v_1}$		$c_s+c_v=c_t+c_u=N/2$	I, II	$N=8,10,2p,\ldots$
$K_{s_1t_1u_1v_1}=K_{s_2t_2u_2v_2}$		$c_s<c_t<c_u<c_v$		
$=-K_{s_1t_2u_2v_1}$				
$=-K_{s_2t_1u_1v_2}$				
$K_{s_1t_1u_1v_1}=K_{s_2t_2u_2v_2}$	$K^{(VI)}_{stuv}(Q_{s_1}Q_{s_1}Q_{t_1}Q_{u_1}+Q_{s_2}Q_{s_2}Q_{t_2}Q_{u_2}+Q_{s_1}Q_{s_1}Q_{t_2}Q_{u_2}+Q_{s_2}Q_{s_2}Q_{t_1}Q_{u_1})$			
$=K_{s_1t_1u_2v_2}$	$K^{(VII)}_{stuv}(Q_{s_1}Q_{s_2}Q_{t_1}Q_{u_2}+Q_{s_2}Q_{s_1}Q_{t_2}Q_{u_1}-Q_{s_1}Q_{s_2}Q_{t_2}Q_{u_1}-Q_{s_2}Q_{s_1}Q_{t_1}Q_{u_2})$			
$=K_{s_2t_2u_1v_1}$		$c_s=c_t<c_u=c_v$	I, II	$N\geqslant 5$
$K_{s_1t_2u_1v_2}=K_{s_2t_1u_2v_1}$		$c_s+c_u\neq N/2$		
$=-K_{s_1t_2u_2v_1}$				
$=-K_{s_2t_1u_1v_2}$				

— Table A.8 continued —

Symmetry	$\mathcal{H}^{(2)}_{vib}$ w.r.t. $Q_{i\sigma}Q_{j_\nu}Q_{k_\tau}Q_{l_\epsilon}$	$c_s \quad c_t \quad c_u \quad c_v$	Group	N
$K_{s_1t_1u_1v_1} = K_{s_2t_2u_2v_2}$	$K^{(VIII)}_{stuv}(Q_{s_1}Q_{s_1}Q_{t_1}Q_{u_1} + Q_{s_2}Q_{s_2}Q_{t_2}Q_{u_2} - Q_{s_1}Q_{s_2}Q_{t_2}Q_{u_1} - Q_{s_2}Q_{s_1}Q_{t_1}Q_{u_2})$			
$K_{s_1t_1u_2v_2} = K_{s_2t_2u_1v_1}$	$K^{(IX)}_{stuv}(Q_{s_1}Q_{s_1}Q_{t_2}Q_{u_2} + Q_{s_2}Q_{s_2}Q_{t_1}Q_{u_1} + Q_{s_1}Q_{s_2}Q_{t_2}Q_{u_1} + Q_{s_2}Q_{s_1}Q_{t_1}Q_{u_2})$	$c_s = c_t \neq c_u = c_v$	I, II	$N = 6, 8, 2p, \ldots$
$K_{s_1t_2u_1v_2} = K_{s_2t_1u_2v_1}$	$K^{(X)}_{stuv}(Q_{s_1}Q_{s_2}Q_{t_1}Q_{u_2} + Q_{s_2}Q_{s_1}Q_{t_2}Q_{u_1} - Q_{s_1}Q_{s_2}Q_{t_2}Q_{u_1} - Q_{s_2}Q_{s_1}Q_{t_1}Q_{u_2})$	$c_s + c_u = N/2$		
$K_{s_1t_2u_2v_1} = K_{s_2t_1u_1v_2}$				
$= (K_{s_1t_1u_1v_1} - K_{s_1t_1u_2v_2} + K_{s_1t_2u_1v_2})$				
$K_{s_1t_1u_1v_1} = K_{s_2t_2u_2v_2}$	$K^{(XI)}_{stuv}(Q_{s_1}Q_{s_1}Q_{t_1}Q_{u_1} + Q_{s_2}Q_{s_2}Q_{t_2}Q_{u_2} + Q_{s_1}Q_{s_2}Q_{t_2}Q_{u_1} + Q_{s_2}Q_{s_1}Q_{t_1}Q_{u_2})$			
$K_{s_1t_1u_2v_2} = K_{s_2t_2u_1v_1}$	$K^{(XII)}_{stuv}(Q_{s_1}Q_{s_1}Q_{t_2}Q_{u_2} + Q_{s_2}Q_{s_2}Q_{t_1}Q_{u_1} + Q_{s_1}Q_{s_2}Q_{t_2}Q_{u_1} + Q_{s_2}Q_{s_1}Q_{t_1}Q_{u_2})$			
$K_{s_1t_2u_1v_2} = K_{s_2t_1u_2v_1}$	$K^{(XIII)}_{stuv}(Q_{s_1}Q_{s_2}Q_{t_1}Q_{u_2} + Q_{s_2}Q_{s_1}Q_{t_2}Q_{u_1} - Q_{s_1}Q_{s_2}Q_{t_2}Q_{u_1} - Q_{s_2}Q_{s_1}Q_{t_1}Q_{u_2})$	$c_s = c_t = c_u = c_v = N/4$	I, II	$N = 3, \geqslant 5, \infty$
$K_{s_1t_2u_2v_1} = K_{s_2t_1u_1v_2}$				
$= (K_{s_1t_1u_1v_1} + K_{s_1t_1u_2v_2} - K_{s_1t_2u_1v_2})$				
$K_{s_1t_1u_1v_1} = K_{s_2t_2u_2v_2}$	$K^{(XIV)}_{stuv}(Q_{s_1}Q_{s_1}Q_{t_1}Q_{u_1} + Q_{s_2}Q_{s_2}Q_{t_2}Q_{u_2})$			
$K_{s_1t_1u_2v_2} = K_{s_2t_2u_1v_1}$	$K^{(XV)}_{stuv}(Q_{s_1}Q_{s_1}Q_{t_2}Q_{u_2} + Q_{s_2}Q_{s_2}Q_{t_1}Q_{u_1})$			
$K_{s_1t_2u_1v_2} = K_{s_2t_1u_2v_1}$	$K^{(XVI)}_{stuv}(Q_{s_1}Q_{s_2}Q_{t_1}Q_{u_2} + Q_{s_2}Q_{s_1}Q_{t_2}Q_{u_1})$	$c_s = c_t = c_u = c_v = N/4$	I, II	$N = 4, 8, 4p, \ldots$
$K_{s_1t_2u_2v_1} = K_{s_2t_1u_1v_2}$	$K^{(XVII)}_{stuv}(Q_{s_1}Q_{s_2}Q_{t_2}Q_{u_1} + Q_{s_2}Q_{s_1}Q_{t_1}Q_{u_2})$			
$K_{s_1t_1u_1v_2} = K_{s_2t_2u_2v_1}$	$K^{(XVIII)}_{stuv}(Q_{s_1}Q_{s_1}Q_{t_1}Q_{u_2} + Q_{s_2}Q_{s_2}Q_{t_2}Q_{u_1} - Q_{s_1}Q_{s_1}Q_{t_2}Q_{u_1} - Q_{s_2}Q_{s_2}Q_{t_1}Q_{u_2}$			
$= -K_{s_1t_1u_2v_1}$	$-Q_{s_1}Q_{s_2}Q_{t_1}Q_{u_1} - Q_{s_2}Q_{s_1}Q_{t_2}Q_{u_2} - Q_{s_1}Q_{s_2}Q_{t_2}Q_{u_2} - Q_{s_2}Q_{s_1}Q_{t_1}Q_{u_1})$	$c_v = c_s + c_t + c_u$	II	$N \geqslant 7$
$= -K_{s_2t_2u_1v_2}$				
$= -K_{s_1t_2u_1v_1}$				
$= -K_{s_2t_1u_2v_2}$		$c_v = c_s + c_t + c_u - N$	II	$N = 5, \geqslant 7$
$= -K_{s_1t_2u_2v_2}$				
$= -K_{s_2t_1u_1v_1}$				
$K_{s_1t_1u_1v_2} = -K_{s_2t_2u_2v_1}$	$K^{(XIX)}_{stuv}(Q_{s_1}Q_{s_1}Q_{t_1}Q_{u_2} - Q_{s_2}Q_{s_2}Q_{t_2}Q_{u_1} + Q_{s_1}Q_{s_1}Q_{t_2}Q_{u_1} - Q_{s_2}Q_{s_2}Q_{t_1}Q_{u_2}$			
$= K_{s_1t_1u_2v_1}$	$+Q_{s_1}Q_{s_2}Q_{t_1}Q_{u_1} - Q_{s_2}Q_{s_1}Q_{t_2}Q_{u_2} - Q_{s_1}Q_{s_2}Q_{t_2}Q_{u_2} + Q_{s_2}Q_{s_1}Q_{t_1}Q_{u_1})$	$c_s + c_t + c_u + c_v = N$	II	$N \geqslant 5$
$= -K_{s_2t_2u_1v_2}$		$c_s + c_t \neq N/2$		
$= K_{s_1t_2u_1v_1}$		$c_s + c_u \neq N/2$		
$= -K_{s_2t_1u_2v_2}$		$c_s + c_v \neq N/2$		
$= -K_{s_1t_2u_2v_2}$				
$= K_{s_2t_1u_1v_1}$				
$K_{s_1t_1u_1v_2} = -K_{s_2t_2u_2v_1}$	$K^{(XX)}_{stuv}(Q_{s_1}Q_{s_1}Q_{t_1}Q_{u_2} - Q_{s_2}Q_{s_2}Q_{t_2}Q_{u_1} - Q_{s_1}Q_{s_1}Q_{t_2}Q_{u_1} + Q_{s_2}Q_{s_2}Q_{t_1}Q_{u_2}$			
$= -K_{s_1t_1u_2v_1}$	$-Q_{s_1}Q_{s_2}Q_{t_1}Q_{u_1} + Q_{s_2}Q_{s_1}Q_{t_2}Q_{u_2} - Q_{s_1}Q_{s_2}Q_{t_2}Q_{u_2} + Q_{s_2}Q_{s_1}Q_{t_1}Q_{u_1})$			
$= K_{s_2t_2u_1v_2}$		$c_s + c_v = c_t + c_u \neq N/2$	II	$N \geqslant 7$
$= -K_{s_1t_2u_1v_1}$		$c_s < c_t < c_u < c_v$		
$= K_{s_2t_1u_2v_2}$				
$= -K_{s_1t_2u_2v_2}$				
$= K_{s_2t_1u_1v_1}$				

— Table A.8 continued —

Symmetry	$\mathcal{H}^{(2)}_{vib}$ w.r.t. $Q_{i\sigma}Q_{j\nu}Q_{k\tau}Q_{l\epsilon}$	$c_s \quad c_t \quad c_u \quad c_v$	Group	N
$K_{s_1t_1u_2v_1}=-K_{s_2t_2u_1v_2}$	$K^{(XXI)}_{stuv}(Q_{s_1}Q_{s_1}Q_{t_1}Q_{u_2}-Q_{s_2}Q_{s_2}Q_{t_2}Q_{u_1}-Q_{s_1}Q_{s_2}Q_{t_2}Q_{u_2}+Q_{s_2}Q_{s_1}Q_{t_1}Q_{u_1})$			
$= \ K_{s_1t_2u_1v_1}$	$K^{(XXII)}_{stuv}(Q_{s_1}Q_{s_1}Q_{t_2}Q_{u_1}-Q_{s_2}Q_{s_2}Q_{t_1}Q_{u_2}+Q_{s_1}Q_{s_2}Q_{t_1}Q_{u_1}-Q_{s_2}Q_{s_1}Q_{t_2}Q_{u_2})$			
$=-K_{s_2t_1u_2v_2}$		$c_s+c_v=c_t+c_u=N/2$	II	$N=8,10,2p,\ldots$
$K_{s_1t_1u_1v_2}=-K_{s_2t_2u_2v_1}$		$c_s<c_t<c_u<c_v$		
$=-K_{s_1t_2u_2v_2}$				
$= \ K_{s_2t_1u_1v_1}$				
$K_{s_1t_1u_1v_2}=-K_{s_2t_2u_2v_1}$	$K^{(XXIII)}_{stuv}(Q_{s_1}Q_{s_1}Q_{t_1}Q_{u_2}-Q_{s_2}Q_{s_2}Q_{t_2}Q_{u_1}-Q_{s_1}Q_{s_1}Q_{t_2}Q_{u_1}+Q_{s_2}Q_{s_2}Q_{t_1}Q_{u_2})$			
$=-K_{s_1t_1u_2v_1}$	$K^{(XXIV)}_{stuv}(Q_{s_1}Q_{s_2}Q_{t_1}Q_{u_1}-Q_{s_2}Q_{s_1}Q_{t_2}Q_{u_2}+Q_{s_1}Q_{s_2}Q_{t_2}Q_{u_2}-Q_{s_2}Q_{s_1}Q_{t_1}Q_{u_1})$			
$= \ K_{s_2t_2u_1v_2}$		$c_s=c_t<c_u=c_v$	II	$N\geqslant 5$
$K_{s_1t_2u_1v_1}=-K_{s_2t_1u_2v_2}$		$c_s+c_u\neq N/2$		
$= \ K_{s_1t_2u_2v_2}$				
$=-K_{s_2t_1u_1v_1}$				
$K_{s_1t_1u_1v_2}=-K_{s_2t_2u_2v_1}$	$K^{(XXV)}_{stuv}(Q_{s_1}Q_{s_1}Q_{t_1}Q_{u_2}-Q_{s_2}Q_{s_2}Q_{t_2}Q_{u_1}-Q_{s_1}Q_{s_2}Q_{t_2}Q_{u_2}+Q_{s_2}Q_{s_1}Q_{t_1}Q_{u_1})$			
$K_{s_1t_1u_2v_1}=-K_{s_2t_2u_1v_2}$	$K^{(XXVI)}_{stuv}(Q_{s_1}Q_{s_1}Q_{t_2}Q_{u_1}-Q_{s_2}Q_{s_2}Q_{t_1}Q_{u_2}-Q_{s_1}Q_{s_2}Q_{t_2}Q_{u_2}+Q_{s_2}Q_{s_1}Q_{t_1}Q_{u_1})$	$c_s=c_t\neq c_u=c_v$	II	$N=6,8,2p,\ldots$
$K_{s_1t_2u_1v_1}=-K_{s_2t_1u_2v_2}$	$K^{(XXVII)}_{stuv}(Q_{s_1}Q_{s_2}Q_{t_1}Q_{u_1}-Q_{s_2}Q_{s_1}Q_{t_2}Q_{u_2}+Q_{s_1}Q_{s_2}Q_{t_2}Q_{u_2}-Q_{s_2}Q_{s_1}Q_{t_1}Q_{u_1})$	$c_s+c_u=N/2$		
$K_{s_1t_2u_2v_2}=-K_{s_2t_1u_1v_1}$				
$= \ (K_{s_1t_2u_1v_1}-K_{s_1t_1u_1v_2}-K_{s_1t_1u_2v_1})$				
$K_{s_1t_1u_1v_2}=-K_{s_2t_2u_2v_1}$	$K^{(XXVIII)}_{stuv}(Q_{s_1}Q_{s_1}Q_{t_1}Q_{u_2}-Q_{s_2}Q_{s_2}Q_{t_2}Q_{u_1}+Q_{s_1}Q_{s_2}Q_{t_2}Q_{u_2}-Q_{s_2}Q_{s_1}Q_{t_1}Q_{u_1})$			
$K_{s_1t_1u_2v_1}=-K_{s_2t_2u_1v_2}$	$K^{(XXIX)}_{stuv}(Q_{s_1}Q_{s_1}Q_{t_2}Q_{u_1}-Q_{s_2}Q_{s_2}Q_{t_1}Q_{u_2}+Q_{s_1}Q_{s_2}Q_{t_2}Q_{u_2}-Q_{s_2}Q_{s_1}Q_{t_1}Q_{u_1})$			
$K_{s_1t_2u_1v_1}=-K_{s_2t_1u_2v_2}$	$K^{(XXX)}_{stuv}(Q_{s_1}Q_{s_2}Q_{t_1}Q_{u_1}-Q_{s_2}Q_{s_1}Q_{t_2}Q_{u_2}+Q_{s_1}Q_{s_2}Q_{t_2}Q_{u_2}-Q_{s_2}Q_{s_1}Q_{t_1}Q_{u_1})$	$c_s=c_t=c_u=c_v=N/4$	II	$N=3,\geqslant 5,\infty$
$K_{s_1t_2u_2v_2}= \ K_{s_2t_1u_1v_1}$				
$= \ (K_{s_1t_1u_1v_2}+K_{s_1t_1u_2v_1}+K_{s_1t_2u_1v_1})$				
$K_{s_1t_1u_1v_2}=-K_{s_2t_2u_2v_1}$	$K^{(XXXI)}_{stuv}(Q_{s_1}Q_{s_1}Q_{t_1}Q_{u_2}-Q_{s_2}Q_{s_2}Q_{t_2}Q_{u_1})$			
$K_{s_1t_1u_2v_1}=-K_{s_2t_2u_1v_2}$	$K^{(XXXII)}_{stuv}(Q_{s_1}Q_{s_1}Q_{t_2}Q_{u_1}-Q_{s_2}Q_{s_2}Q_{t_1}Q_{u_2})$			
$K_{s_1t_2u_1v_1}=-K_{s_2t_1u_2v_2}$	$K^{(XXXIII)}_{stuv}(Q_{s_1}Q_{s_2}Q_{t_1}Q_{u_1}-Q_{s_2}Q_{s_1}Q_{t_2}Q_{u_2})$	$c_s=c_t=c_u=c_v=N/4$	II	$N=4,8,4p,\ldots$
$K_{s_1t_2u_2v_2}=-K_{s_2t_1u_1v_1}$	$K^{(XXXIV)}_{stuv}(Q_{s_1}Q_{s_2}Q_{t_2}Q_{u_2}-Q_{s_2}Q_{s_1}Q_{t_1}Q_{u_1})$			

c_i is the subscript labelling the degenerate representation of mode i, for example $c_i=1$ for E or E_1, $c_i=2$ for E_2, etc.
p is a non zero integer number and N indicates the order of the principal symmetry axis. For I and II Group classification see Table A.1.

Appendix B

χ_0 vibrational contribution

The explicit form of χ_0 term is given by,

$$\begin{aligned}
\chi_0 =& \frac{1}{64}\sum_m \frac{K_{mmmm}}{\lambda_m} + \frac{1}{48}\sum_s \sum_{\sigma\leq III} \frac{\delta_\sigma K^{(\sigma)}_{ssss}}{\lambda_s} - \frac{7}{576}\sum_m \frac{{K_{mmm}}^2}{\lambda_m^2} \\
&+ \frac{11}{144}\sum_s\sum_\sigma \frac{\left\{K^{(\sigma)}_{sss}\right\}^2}{\lambda_s^2} + \frac{3}{64}\sum_m\sum_{n\neq m}\frac{K^2_{mnn}}{\lambda_n(4\lambda_n-\lambda_m)} \\
&+ \frac{1}{16}\sum_s\sum_{t\neq s}\sum_\sigma \frac{\left\{K^{(\sigma)}_{sst}\right\}^2(8\lambda_s+\lambda_t)}{\lambda_s\lambda_t(4\lambda_s-\lambda_t)} - \frac{1}{4}\sum_m\sum_{n>m}\sum_{o>n}\frac{{K_{mno}}^2}{\Delta_{mno}} \\
&+ \frac{1}{32}\sum_m\sum_s\left[\frac{2\left\{K^{(I)}_{mss}\right\}^2}{\lambda_s(4\lambda_s-\lambda_m)} + \frac{\left[\left\{K^{(III)}_{mss}\right\}^2+\left\{K^{(IV)}_{mss}\right\}^2\right](\lambda_s+\lambda_m)}{\lambda_m\lambda_s(4\lambda_s-\lambda_m)}\right] \\
&- \frac{1}{2}\sum_m\sum_s\sum_{t>s}\sum_\sigma\frac{\left\{K^{(\sigma)}_{mst}\right\}^2}{\Delta_{mst}} - \sum_s\sum_{t>s}\sum_{u>t}\sum_\sigma\frac{\left\{K^{(\sigma)}_{stu}\right\}^2}{\Delta_{stu}} - \frac{\Gamma}{4}\sum_\tau B^e_\tau \\
&- \frac{1}{2}\sum_\tau B^e_\tau\sum_m\sum_{n>m}\left\{\zeta_{mn,\tau}\right\}^2 - B^e_x\sum_m\sum_s\left[\left\{\zeta_{ms_1,x}\right\}^2+\left\{\zeta_{ms_1,y}\right\}^2\right] \\
&- \sum_s\sum_{t>s}\left(B^e_z\left[\left\{\zeta_{s_1t_1,z}\right\}^2+\left\{\zeta_{s_1t_2,z}\right\}^2\right] + 2B^e_x\left[\left\{\zeta_{s_1t_1,x}\right\}^2+\left\{\zeta_{s_1t_1,y}\right\}^2\right]\right)
\end{aligned} \tag{B.1}$$

In the orientation chosen in this work for the degenerate normal modes (see Section 1.4 and refs. [70, 71]), $\zeta_{s_1s_2,z} = 1$ and $\zeta_{ms_1,y} = \zeta_{ms_2,x}$ are the only Coriolis terms that are non-null for linear molecules. For symmetric top systems, $\zeta_{mn,x}$, $\zeta_{mn,y}$, $\zeta_{ms_1,z}$ and $\zeta_{ms_2,z}$ are always zero, and we have used the following relations

to simplify the last terms in the above equation:

$$\left\{\zeta_{ms_1,x}\right\}^2 = \left\{\zeta_{ms_2,y}\right\}^2 \tag{B.2}$$

$$\left\{\zeta_{ms_2,x}\right\}^2 = \left\{\zeta_{ms_1,y}\right\}^2 \tag{B.3}$$

and,

$$\left\{\zeta_{s_1t_1,x}\right\}^2 = \left\{\zeta_{s_2t_2,x}\right\}^2 = \left\{\zeta_{s_1t_2,y}\right\}^2 = \left\{\zeta_{s_2t_1,y}\right\}^2 \tag{B.4}$$

$$\left\{\zeta_{s_1t_1,y}\right\}^2 = \left\{\zeta_{s_2t_2,y}\right\}^2 = \left\{\zeta_{s_1t_2,x}\right\}^2 = \left\{\zeta_{s_2t_1,x}\right\}^2 \tag{B.5}$$

$$\left\{\zeta_{s_1t_1,z}\right\}^2 = \left\{\zeta_{s_2t_2,z}\right\}^2 \tag{B.6}$$

$$\left\{\zeta_{s_1t_2,z}\right\}^2 = \left\{\zeta_{s_2t_1,z}\right\}^2 \tag{B.7}$$

Appendix C

Vibrational l-doubling constants

The off-diagonal elements $\langle\, \phi^{(0)}_{A_a} \mid \tilde{\mathcal{H}}^{(2)} \mid \phi^{(0)}_{B_b} \,\rangle$ presented in eqs. 2.31-2.33 are all composed by a quantum numbers dependent part and a constant one. In the notation adopted in this paper, the explicit form of the latter is given by the following expressions,

$$\begin{aligned} D_s U_s^{\pm} = & \left(K^{(II)}_{ssss} - 3K^{(III)}_{ssss} \pm 4iK^{(IV)}_{ssss}\right) \\ & - 2\sum_m \left[\left\{K^{(III)}_{mss}\right\}^2 - \left\{K^{(IV)}_{mss}\right\}^2\right] \frac{8\lambda_s - 3\lambda_m}{\lambda_m(4\lambda_s - \lambda_m)} \end{aligned} \tag{C.1}$$

$$\begin{aligned} E_{st} R_{st}^{\pm} = & 2\left[K^{(II)}_{sstt} - K^{(III)}_{sstt} + K^{(VIII)}_{sstt}\right] + \left[K^{(VI)}_{sstt} - K^{(VII)}_{sstt}\right] \\ & - \frac{4K^{(I)}_{sss}K^{(I)}_{stt} - 4K^{(II)}_{sss}K^{(II)}_{stt}}{\lambda_s} - \frac{4K^{(I)}_{ttt}K^{(I)}_{sst} - 4K^{(II)}_{ttt}K^{(II)}_{sst}}{\lambda_t} \\ & - \sum_m \left[2\sum_{\sigma\neq I} \frac{K^{(\sigma)}_{mss}K^{(\sigma)}_{mtt}}{\lambda_m} + \frac{4\left[\left\{K^{(I)}_{mst}\right\}^2 - \left\{K^{(II)}_{mst}\right\}^2\right](\lambda_m - \lambda_s - \lambda_t)}{\Delta_{mst}}\right] \\ & - 4\sum_{u\neq s,t} \frac{K^{(I)}_{ssu}K^{(I)}_{ttu} + K^{(II)}_{ssu}K^{(II)}_{ttu} + K^{(III)}_{ssu}K^{(III)}_{ttu} + K^{(IV)}_{ssu}K^{(IV)}_{ttu}}{\lambda_u} \\ & + \frac{8B_z^e}{\hbar^2}\left[{\zeta_{s_1t_1,z}}^2 - {\zeta_{s_1t_2,z}}^2\right](\lambda_s + \lambda_t) \end{aligned}$$

$$
\begin{aligned}
&\mp 2i\Bigg\{\left[2K^{(X)}_{sstt}+K^{(XI)}_{sstt}-K^{(XII)}_{sstt}\right]\\
&\quad-\frac{2K^{(I)}_{sss}K^{(II)}_{stt}+2K^{(II)}_{sss}K^{(I)}_{stt}}{\lambda_s}+\frac{2K^{(I)}_{ttt}K^{(II)}_{sst}+2K^{(II)}_{ttt}K^{(I)}_{sst}}{\lambda_t}\\
&\quad-2\sum_{u\neq s,t}\frac{K^{(I)}_{ssu}K^{(II)}_{ttu}-K^{(II)}_{ssu}K^{(I)}_{ttu}-K^{(III)}_{ssu}K^{(IV)}_{ttu}+K^{(IV)}_{ssu}K^{(III)}_{ttu}}{\lambda_u}\\
&\quad+\frac{8B^e_z}{\hbar^2}\zeta_{s_1t_1,z}\zeta_{s_1t_2,z}(\lambda_s+\lambda_t)\Bigg\}
\end{aligned}
\tag{C.2}
$$

$$
\begin{aligned}
E_{st}S^{\pm}_{st}=&2\left[K^{(IV)}_{sstt}-K^{(V)}_{sstt}-K^{(VIII)}_{sstt}\right]+\left[K^{(VI)}_{sstt}-K^{(VII)}_{sstt}\right]\\
&-\frac{4K^{(I)}_{sss}K^{(III)}_{stt}-4K^{(II)}_{sss}K^{(IV)}_{stt}}{\lambda_s}-\frac{4K^{(I)}_{ttt}K^{(III)}_{sst}-4K^{(II)}_{ttt}K^{(IV)}_{sst}}{\lambda_t}\\
&-\sum_m\Bigg[\frac{2\left(K^{(III)}_{mss}K^{(III)}_{mtt}-K^{(IV)}_{mss}K^{(IV)}_{mtt}\right)}{\lambda_m}\\
&\quad+\frac{4\left[\left\{K^{(III)}_{mst}\right\}^2-\left\{K^{(IV)}_{mst}\right\}^2\right](\lambda_m-\lambda_s-\lambda_t)}{\Delta_{mst}}\Bigg]\\
&-4\sum_{u\neq s,t}\frac{K^{(I)}_{ssu}K^{(III)}_{ttu}+K^{(II)}_{ssu}K^{(IV)}_{ttu}+K^{(III)}_{ssu}K^{(I)}_{ttu}+K^{(IV)}_{ssu}K^{(II)}_{ttu}}{\lambda_u}\\
&\pm 2i\Bigg\{\left[2K^{(IX)}_{sstt}+K^{(XI)}_{sstt}+K^{(XII)}_{sstt}\right]\\
&\quad+\frac{2K^{(I)}_{sss}K^{(IV)}_{stt}+2K^{(II)}_{sss}K^{(III)}_{stt}}{\lambda_s}+\frac{2K^{(I)}_{ttt}K^{(IV)}_{sst}+2K^{(II)}_{ttt}K^{(III)}_{sst}}{\lambda_t}\\
&\quad+2\sum_{u\neq s,t}\frac{K^{(I)}_{ssu}K^{(IV)}_{ttu}-K^{(II)}_{ssu}K^{(III)}_{ttu}-K^{(III)}_{ssu}K^{(II)}_{ttu}+K^{(IV)}_{ssu}K^{(I)}_{ttu}}{\lambda_u}\Bigg\}
\end{aligned}
\tag{C.3}
$$

$$
\Delta_{ijk}=\lambda_i{}^2+\lambda_j{}^2+\lambda_k{}^2-2(\lambda_i\lambda_j+\lambda_i\lambda_k+\lambda_j\lambda_k) \tag{C.4}
$$

where $D_i=128\lambda_s/\hbar^2$, $E_{ij}=32\sqrt{\lambda_i\lambda_j}/\hbar^2$.

Appendix D

Deperturbed treatment of resonances

The possibly resonant terms present in χ_0, $\boldsymbol{\chi}$, $\boldsymbol{g}$ (see eqs. B.1-2.14), and U, R, S (see eqs. C.1–C.3) equations can be found rewriting the fraction expressions as sums of terms with minimal denominators,

$$\frac{1}{\omega_i\omega_j(4\lambda_i-\lambda_j)} = \frac{1}{4\lambda_i\omega_j}\left(\frac{1}{2\omega_i+\omega_j}+\frac{1}{2\omega_i-\omega_j}\right) \tag{D.1}$$

$$\frac{1}{\lambda_i(4\lambda_i-\lambda_j)} = -\frac{1}{2\lambda_i\omega_j}\left(\frac{1}{2\omega_i+\omega_j}-\frac{1}{2\omega_i-\omega_j}\right) \tag{D.2}$$

$$\frac{(8\lambda_i-3\lambda_j)}{\omega_j(4\lambda_i-\lambda_j)} = \frac{1}{2}\left(\frac{4}{\omega_j}+\frac{1}{2\omega_i+\omega_j}-\frac{1}{2\omega_i-\omega_j}\right) \tag{D.3}$$

$$\frac{(8\lambda_i-\lambda_j)}{\omega_j(4\lambda_i-\lambda_j)} = \frac{1}{2}\left(\frac{4}{\omega_j}-\frac{1}{2\omega_i+\omega_j}+\frac{1}{2\omega_i-\omega_j}\right) \tag{D.4}$$

$$\frac{(8\lambda_i+\lambda_j)}{\omega_j(4\lambda_i-\lambda_j)} = \frac{1}{2}\left(\frac{4}{\omega_j}-\frac{3}{2\omega_i+\omega_j}+\frac{3}{2\omega_i-\omega_j}\right) \tag{D.5}$$

$$\frac{(\lambda_i-\lambda_j-\lambda_k)}{\Delta_{ijk}} = \frac{1}{4\omega_i}\left(\frac{1}{\omega_i+\omega_j+\omega_k}+\frac{1}{\omega_i+\omega_j-\omega_k}+\frac{1}{\omega_i-\omega_j+\omega_k}+\frac{1}{\omega_i-\omega_j-\omega_k}\right) \tag{D.6}$$

$$\frac{1}{\Delta_{ijk}} = \frac{1}{8\omega_i\omega_j\omega_k}\left(\frac{1}{\omega_i+\omega_j+\omega_k}-\frac{1}{\omega_i+\omega_j-\omega_k}-\frac{1}{\omega_i-\omega_j+\omega_k}+\frac{1}{\omega_i-\omega_j-\omega_k}\right) \tag{D.7}$$

If a resonance of the type $2\omega_j \approx \omega_i$ or $\omega_i \approx \omega_j + \omega_k$ occurs, the last term in the right-hand side of the equations presented above is discarded.

Concerning the vibrational correction to rotational constants, the possibly res-

onant terms in $\alpha_{i,\tau}$ equations (eqs. 3.12-3.16) are,

$$\frac{3\lambda_i + \lambda_j}{\lambda_i - \lambda_j} = \frac{2\omega_i}{\omega_i + \omega_j} - 1 + \frac{2\omega_i}{\omega_i - \omega_j} \tag{D.8}$$

If $\omega_i \approx \omega_j$, the last term in the right-hand side of the above equation is removed.

Appendix E

2-2 second-order resonances constants

The constant terms present in the off-diagonal elements $\langle\, \phi^{(0)}_{A_a} \mid \tilde{\mathcal{H}}^{(2)} \mid \phi^{(0)}_{B_b} \,\rangle$ involved in 2-2 second-order resonances (eqs. 2.60-2.64) are given by,

$$\begin{aligned} F_{mn}\kappa_{mn} =& K_{mmnn} - \sum_o \Bigg[\frac{K_{mmo}K_{nno}}{4\omega_o} \left(\frac{1}{2\omega_m + \omega_o} - \frac{1}{2\omega_m - \omega_o} + \frac{1}{2\omega_n + \omega_o} \right. \\ & \left. - \frac{1}{2\omega_n - \omega_o} \right) + \frac{{K_{mno}}^2}{\omega_o} \left(\frac{1}{\omega_m - \omega_n + \omega_o} - \frac{1}{\omega_m - \omega_n - \omega_o} \right) \Bigg] \\ & - \frac{4}{\hbar^2} \sum_\tau B^e_\tau {\zeta_{mn,\tau}}^2 (\omega_m + \omega_n)^2 \end{aligned} \tag{E.1}$$

$$\begin{aligned} F_{ms}\kappa_{ms} =& - K_{mmss} + \sum_\sigma \frac{\{K^{(\sigma)}_{mss}\}^2}{\omega_s} \left(\frac{1}{\omega_m} + \frac{1}{2\omega_s - \omega_m} \right) \\ & + \frac{1}{4} \sum_n \frac{K_{mmn}K^{(I)}_{nss}}{\omega_n} \left(\frac{1}{2\omega_m + \omega_n} - \frac{1}{2\omega_m - \omega_n} + \frac{1}{2\omega_s + \omega_n} - \frac{1}{2\omega_s - \omega_n} \right) \\ & + \sum_{t \neq s} \sum_\sigma \frac{\left\{K^{(\sigma)}_{mst}\right\}^2}{\omega_t} \left(\frac{1}{\omega_m - \omega_s + \omega_t} - \frac{1}{\omega_m - \omega_s - \omega_t} \right) \\ & + \frac{4}{\hbar^2} B^e_x \left({\zeta_{ms_1,x}}^2 + {\zeta_{ms_1,y}}^2 \right) \left(\omega_m + \omega_s \right)^2 \end{aligned} \tag{E.2}$$

$$
\begin{aligned}
F_{st}\kappa_{st}^{(I)} = & \sum_{\sigma \leq VII} \beta_\sigma K_{sstt}^{(\sigma)} \\
& - \sum_{\sigma} \frac{\left\{K_{sst}^{(\sigma)}\right\}^2}{\omega_s} \left(\frac{1}{\omega_t} + \frac{1}{2\omega_s + \omega_t} \right) - \sum_{\sigma} \frac{\left\{K_{stt}^{(\sigma)}\right\}^2}{\omega_t} \left(\frac{1}{\omega_s} + \frac{1}{2\omega_t + \omega_s} \right) \\
& - \sum_{m} \left[\frac{K_{mss}^{(I)} K_{mtt}^{(I)}}{4\omega_m} \left(\frac{1}{2\omega_s + \omega_m} - \frac{1}{2\omega_s - \omega_m} + \frac{1}{2\omega_t + \omega_m} - \frac{1}{2\omega_t - \omega_m} \right) \right. \\
& \qquad \left. + \sum_{\sigma} \frac{\left\{K_{mst}^{(\sigma)}\right\}^2}{2\omega_m} \left(\frac{1}{\omega_m + \omega_s - \omega_t} + \frac{1}{\omega_m - \omega_s + \omega_t} \right) \right] \\
& - \sum_{u \neq s,t} \sum_{\sigma} \frac{\left\{K_{stu}^{(\sigma)}\right\}^2}{\omega_u} \left(\frac{1}{\omega_s - \omega_t + \omega_u} - \frac{1}{\omega_s - \omega_t - \omega_u} \right) \\
& - \frac{2}{\hbar^2} \left[2B_x^e \left({\zeta_{s_1 t_1, x}}^2 + {\zeta_{s_1 t_1, y}}^2 \right) + B_z^e \left({\zeta_{s_1 t_1, z}}^2 + {\zeta_{s_1 t_2, z}}^2 \right) \right] \left(\omega_s + \omega_t \right)^2
\end{aligned}
\tag{E.3}
$$

$$
\begin{aligned}
F_{st}\kappa_{st}^{\pm(II)} = & \left[K_{sstt}^{(IV)} - K_{sstt}^{(V)} + \frac{1}{2} \left(K_{sstt}^{(VI)} - K_{sstt}^{(VII)} \right) - K_{sstt}^{(VIII)} \right. \\
& \left. \pm i \left(2K_{sstt}^{(IX)} + K_{sstt}^{(XI)} + K_{sstt}^{(XII)} \right) \right] \\
& + \frac{1}{6\omega_s} \left[K_{sss}^{(I)} K_{stt}^{(III)} - K_{sss}^{(II)} K_{stt}^{(IV)} \mp i \left(K_{sss}^{(II)} K_{stt}^{(III)} + K_{sss}^{(I)} K_{stt}^{(IV)} \right) \right] \\
& \qquad \times \left(\frac{2}{\omega_s} - \frac{3}{2\omega_t + \omega_s} + \frac{3}{2\omega_t - \omega_s} \right) \\
& + \frac{1}{6\omega_t} \left[K_{sst}^{(III)} K_{ttt}^{(I)} - K_{sst}^{(IV)} K_{ttt}^{(II)} \mp i \left(K_{sst}^{(III)} K_{ttt}^{(II)} + K_{sst}^{(IV)} K_{ttt}^{(I)} \right) \right] \\
& \qquad \times \left(\frac{2}{\omega_t} - \frac{3}{2\omega_s + \omega_t} + \frac{3}{2\omega_s - \omega_t} \right) \\
& - \frac{1}{4\omega_m} \sum_{m} \left\{ 4 \left(\left\{K_{mst}^{(III)}\right\}^2 - \left\{K_{mst}^{(IV)}\right\}^2 \right) \right. \\
& \qquad \times \left(\frac{1}{\omega_m + \omega_s - \omega_t} + \frac{1}{\omega_m - \omega_s + \omega_t} \right) \\
& \qquad - \left(K_{mss}^{(III)} K_{mtt}^{(III)} - K_{mss}^{(IV)} K_{mtt}^{(IV)} \right) \\
& \qquad \left. \times \left(\frac{1}{2\omega_s + \omega_m} - \frac{1}{2\omega_s - \omega_m} + \frac{1}{2\omega_t + \omega_m} - \frac{1}{2\omega_t - \omega_m} \right) \right\}
\end{aligned}
$$

$$
\begin{aligned}
&- \frac{1}{2\omega_u} \sum_{u \neq s,t} \Bigg\{ \Bigg[K^{(I)}_{ssu} K^{(III)}_{ttu} + K^{(III)}_{ssu} K^{(I)}_{ttu} + K^{(IV)}_{ssu} K^{(II)}_{ttu} + K^{(II)}_{ssu} K^{(IV)}_{ttu} \\
&\qquad \pm i \left(K^{(II)}_{ssu} K^{(III)}_{ttu} + K^{(III)}_{ssu} K^{(II)}_{ttu} - K^{(I)}_{ssu} K^{(IV)}_{ttu} - K^{(IV)}_{ssu} K^{(I)}_{ttu} \right) \Bigg] \\
&\qquad \times \left(\frac{1}{2\omega_s + \omega_u} - \frac{1}{2\omega_s - \omega_u} + \frac{1}{2\omega_t + \omega_u} - \frac{1}{2\omega_t - \omega_u} \right) \Bigg\}
\end{aligned}
\tag{E.4}
$$

$$
\begin{aligned}
F_{st}\kappa^{\pm(III)}_{st} = &\Bigg[K^{(II)}_{sstt} - K^{(III)}_{sstt} + \frac{1}{2} \left(K^{(VI)}_{sstt} - K^{(VII)}_{sstt} \right) + K^{(VIII)}_{sstt} \\
&\pm i \left(-2K^{(X)}_{sstt} - K^{(XI)}_{sstt} + K^{(XII)}_{sstt} \right) \Bigg] \\
&+ \frac{1}{6\omega_s} \left[K^{(I)}_{sss} K^{(I)}_{stt} - K^{(II)}_{sss} K^{(II)}_{stt} \mp i \left(K^{(II)}_{sss} K^{(I)}_{stt} + K^{(I)}_{sss} K^{(II)}_{stt} \right) \right] \\
&\quad \times \left(\frac{2}{\omega_s} - \frac{3}{2\omega_t + \omega_s} + \frac{3}{2\omega_t - \omega_s} \right) \\
&+ \frac{1}{6\omega_t} \left[K^{(I)}_{sst} K^{(I)}_{ttt} - K^{(II)}_{sst} K^{(II)}_{ttt} \pm i \left(K^{(II)}_{sst} K^{(I)}_{ttt} + K^{(I)}_{sst} K^{(II)}_{ttt} \right) \right] \\
&\quad \times \left(\frac{2}{\omega_t} - \frac{3}{2\omega_s + \omega_t} + \frac{3}{2\omega_s - \omega_t} \right) \\
&- \frac{1}{4\omega_m} \sum_m \Bigg\{ 4 \left(\left\{ K^{(I)}_{mst} \right\}^2 - \left\{ K^{(II)}_{mst} \right\}^2 \right) \\
&\qquad \times \left(\frac{1}{\omega_m + \omega_s - \omega_t} + \frac{1}{\omega_m - \omega_s + \omega_t} \right) \\
&\qquad - \left(K^{(III)}_{mss} K^{(III)}_{mtt} - K^{(IV)}_{mss} K^{(IV)}_{mtt} \right) \\
&\qquad \times \left(\frac{1}{2\omega_s + \omega_m} - \frac{1}{2\omega_s - \omega_m} + \frac{1}{2\omega_t + \omega_m} - \frac{1}{2\omega_t - \omega_m} \right) \Bigg\}
\end{aligned}
$$

$$
\begin{aligned}
&- \frac{1}{2\omega_u} \sum_{u \neq s,t} \Bigg\{ \Bigg[K^{(I)}_{ssu} K^{(I)}_{ttu} + K^{(II)}_{ssu} K^{(II)}_{ttu} + K^{(III)}_{ssu} K^{(III)}_{ttu} + K^{(IV)}_{ssu} K^{(IV)}_{ttu} \\
&\qquad \mp i \left(K^{(I)}_{ssu} K^{(II)}_{ttu} - K^{(II)}_{ssu} K^{(I)}_{ttu} - K^{(III)}_{ssu} K^{(IV)}_{ttu} + K^{(IV)}_{ssu} K^{(III)}_{ttu} \right) \Bigg] \\
&\qquad \times \left(\frac{1}{2\omega_s + \omega_u} - \frac{1}{2\omega_s - \omega_u} + \frac{1}{2\omega_t + \omega_u} - \frac{1}{2\omega_t - \omega_u} \right) \Bigg\} \\
&- \frac{4}{\hbar} B^z_e \left[{\zeta_{s_1 t_1, z}}^2 - {\zeta_{s_1 t_2, z}}^2 \right] \left(\omega_s + \omega_t \right)^2 \pm \frac{8i}{\hbar^2} B^z_e \zeta_{s_1 t_1, z} \zeta_{s_1 t_2, z} \left(\omega_s + \omega_t \right)^2
\end{aligned}
\tag{E.5}
$$

where $F_{ij} = \omega_i \omega_j / \hbar^2$, $\beta_1 = 1, \beta_j = 1/2$ $(j > 1)$ and all the contributions are expressed in partial fractions with ω constants to easily identify the possible first-order resonant terms. When a first-order resonance occurs, the relative term is removed from $\mathcal{S}^{(1)}$ in eq. 1.45 and then from both the diagonal and off-diagonal elements of $\tilde{\mathcal{H}}^{(2)}$.

Appendix F

CT vs RS developments for properties

In this section we want to point out the differences between the CT and the RS developments when dealing with the molecular properties. Generalizing to both the transition integral ($|\,\psi_{A_a}\,\rangle \neq |\,\psi_{B_b}\,\rangle$) and the expectation value ($|\,\psi_{A_a}\,\rangle = |\,\phi_{B_b}\rangle$) of a property $\boldsymbol{M}$,

$$\langle\, \boldsymbol{M} \,\rangle_{A_a B_b} = \frac{\langle\, \psi_{A_a} \mid \boldsymbol{M} \mid \psi_{B_b} \,\rangle}{\sqrt{\langle\, \psi_{A_a} \mid \psi_{A_a} \,\rangle \langle\, \psi_{B_b} \mid \psi_{B_b} \,\rangle}} \tag{F.1}$$

in CT theory, $\phi = e^{i\mathcal{S}}\psi$ (see eqs. 1.41) is applied to the previous expression with the choice $\phi \equiv \phi^{(0)}$, where $\phi^{(0)}$ are the eigenfunctions of $\mathcal{H}^{(0)}$. Under the contact transformation eq. F.1 becomes,

$$\begin{aligned} {}^{\mathrm{CT}}\langle\, \boldsymbol{M} \,\rangle_{A_a B_b} &= \frac{\langle\, \phi^{(0)}_{A_a} \mid \tilde{\boldsymbol{M}} \mid \phi^{(0)}_{B_b} \,\rangle}{\sqrt{\langle\, \phi^{(0)}_{A_a} \mid \phi^{(0)}_{A_a} \,\rangle \langle\, \phi^{(0)}_{B_b} \mid \phi^{(0)}_{B_b} \,\rangle}} \\ &= \langle\, \phi^{(0)}_{A_a} \mid \tilde{\boldsymbol{M}} \mid \phi^{(0)}_{B_b} \,\rangle \end{aligned} \tag{F.2}$$

where $\tilde{\boldsymbol{M}} = e^{i\mathcal{S}} \boldsymbol{M} e^{-i\mathcal{S}}$ is the effective property and $\langle\, \phi^{(0)}_{A_a} \mid \phi^{(0)}_{A_a} \,\rangle = 1$.
On the other hand, in RS perturbation theory, eq. F.1 is developed expanding the wavefunction in perturbation orders,

$$|\,\psi_{A_a}\,\rangle = |\,\phi^{(0)}_{A_a}\,\rangle + \lambda|\,\phi^{(1)}_{A_a}\,\rangle + \lambda^2|\,\phi^{(2)}_{A_a}\,\rangle + \ldots \tag{F.3}$$

where $\phi^{(0)}$ are again the eigenfunctions of $\mathcal{H}^{(0)}$.

Up to the first perturbative order, the CT effective property is given by,

$$\begin{aligned} {}^{\mathrm{CT}}\langle\, \boldsymbol{M} \,\rangle^{(1)}_{A_a B_b} &= \langle\, \phi^{(0)}_{A_a} \mid \tilde{\boldsymbol{M}}^{(1)} \mid \phi^{(0)}_{B_b} \,\rangle \\ &= \langle\, \phi^{(0)}_{A_a} \mid \boldsymbol{M}^{(1)} \mid \phi^{(0)}_{B_b} \,\rangle + i\langle\, \phi^{(0)}_{A_a} \mid [\mathcal{S}^{(1)}, \boldsymbol{M}^{(0)}] \mid \phi^{(0)}_{B_b} \,\rangle \end{aligned} \tag{F.4}$$

Using hereafter the short notation $X_{A_aB_b} \equiv \langle \phi^{(0)}_{A_a} \mid X \mid \phi^{(0)}_{B_b} \rangle$ and $E_{AB} \equiv E^{(0)}_A - E^{(0)}_B$, the latter term in the above equation can be written as,

$$\begin{aligned} i\langle \phi^{(0)}_{A_a} \mid [\boldsymbol{\mathcal{S}}^{(1)}, \boldsymbol{M}^{(0)}] \mid \phi^{(0)}_{B_b} \rangle & \\ &= i\langle \phi^{(0)}_{A_a} \mid \boldsymbol{\mathcal{S}}^{(1)}\boldsymbol{M}^{(0)} - \boldsymbol{M}^{(0)}\boldsymbol{\mathcal{S}}^{(1)} \mid \phi^{(0)}_{B_b} \rangle \\ &= i\sum_C \sum_c \mathcal{S}^{(1)}_{A_aC_c} \boldsymbol{M}^{(0)}_{C_cB_b} - i\sum_D \sum_d \boldsymbol{M}^{(0)}_{A_aD_d} \mathcal{S}^{(1)}_{D_dB_b} \\ &= i\sum_{C\neq A}^{*} \sum_c \frac{(-i)\mathcal{H}^{(1)}_{A_aC_c}}{E_{AC}} \boldsymbol{M}^{(0)}_{C_cB_b} - i\sum_{D\neq B}^{*} \sum_d \boldsymbol{M}^{(0)}_{A_aD_d} \frac{(-i)\mathcal{H}^{(1)}_{D_dB_b}}{E_{DB}} \\ &= \sum_{C\neq A}^{*} \sum_c \frac{\mathcal{H}^{(1)}_{A_aC_c}}{E_{AC}} \boldsymbol{M}^{(0)}_{C_cB_b} - \sum_{D\neq B}^{*} \sum_d \boldsymbol{M}^{(0)}_{A_aD_d} \frac{\mathcal{H}^{(1)}_{D_dB_b}}{E_{DB}} \end{aligned} \tag{F.5}$$

where the following relations have been used,

$$\sum_A \sum_a \mid \phi^{(0)}_{A_a} \rangle\langle \phi^{(0)}_{A_a} \mid = 1, \qquad \mathcal{S}^{(1)}_{A_aB_b} = \frac{(-i)\mathcal{H}^{(1)}_{A_aB_b}}{E_{A_aB_b}} \qquad \text{and} \qquad \mathcal{S}^{(1)}_{A_aA_b} = 0 \tag{F.6}$$

Substituting eq. F.5 in eq. F.4,

$${}^{\mathrm{CT}}\langle \boldsymbol{M} \rangle^{(1)}_{A_aB_b} = \boldsymbol{M}^{(1)}_{A_aB_b} + \sum_{C\neq A}^{*} \sum_c \frac{\mathcal{H}^{(1)}_{A_aC_c}}{E_{AC}} \boldsymbol{M}^{(0)}_{C_cB_b} - \sum_{D\neq B}^{*} \sum_d \boldsymbol{M}^{(0)}_{A_aD_d} \frac{\mathcal{H}^{(1)}_{D_dB_b}}{E_{DB}} \tag{F.7}$$

In RS theory,

$${}^{\mathrm{RS}}\langle \boldsymbol{M} \rangle^{(1)}_{A_aB_b} = \langle \phi^{(0)}_{A_a} \mid \boldsymbol{M}^{(1)} \mid \phi^{(0)}_{B_b} \rangle + \langle \phi^{(1)}_{A_a} \mid \boldsymbol{M}^{(0)} \mid \phi^{(0)}_{B_b} \rangle + \langle \phi^{(0)}_{A_a} \mid \boldsymbol{M}^{(0)} \mid \phi^{(1)}_{B_b} \rangle \tag{F.8}$$

where,

$$\mid \phi^{(1)}_{A_a} \rangle = -\sum_{B\neq A}^{*} \sum_b \mid \phi^{(0)}_{B_b} \rangle \frac{\mathcal{H}^{(1)}_{B_bA_a}}{E_{BA}} \tag{F.9}$$

It is easy to see that the equation resulting from the replacement of eq. F.9 in eq. F.8 is exactly eq. F.7, then ${}^{\mathrm{CT}}\langle \boldsymbol{M} \rangle^{(1)}_{A_aB_b} = {}^{\mathrm{RS}}\langle \boldsymbol{M} \rangle^{(1)}_{A_aB_b}$.
Up to second perturbative order, the CT effective property is given by,

$$\begin{aligned} {}^{\mathrm{CT}}\langle \boldsymbol{M} \rangle^{(2)}_{A_aB_b} =& \langle \phi^{(0)}_{A_a} \mid \tilde{\boldsymbol{M}}^{(2)} \mid \phi^{(0)}_{B_b} \rangle \\ =& \langle \phi^{(0)}_{A_a} \mid \boldsymbol{M}^{(2)} \mid \phi^{(0)}_{B_b} \rangle + i\langle \phi^{(0)}_{A_a} \mid [\boldsymbol{\mathcal{S}}^{(1)}, \boldsymbol{M}^{(1)}] \mid \phi^{(0)}_{B_b} \rangle \\ & - \frac{1}{2}\langle \phi^{(0)}_{A_a} \mid [\boldsymbol{\mathcal{S}}^{(1)}, [\boldsymbol{\mathcal{S}}^{(1)}, \boldsymbol{M}^{(0)}]] \mid \phi^{(0)}_{B_b} \rangle + i\langle \phi^{(0)}_{A_a} \mid [\boldsymbol{\mathcal{S}}^{(2)}, \boldsymbol{M}^{(0)}] \mid \phi^{(0)}_{B_b} \rangle \end{aligned} \tag{F.10}$$

The second term in the left-hand side of the last equality in the previous expression is,

$$
\begin{aligned}
& i\langle\, \phi^{(0)}_{A_a} \mid [\mathcal{S}^{(1)}, \boldsymbol{M}^{(1)}] \mid \phi^{(0)}_{B_b} \,\rangle \\
& \qquad = i\langle\, \phi^{(0)}_{A_a} \mid \mathcal{S}^{(1)}\boldsymbol{M}^{(1)} - \boldsymbol{M}^{(1)}\mathcal{S}^{(1)} \mid \phi^{(0)}_{B_b} \,\rangle \\
& \qquad = \sum_{C\neq A}^{*}\sum_{c} \frac{\mathcal{H}^{(1)}_{A_aC_c}}{E_{AC}} \boldsymbol{M}^{(1)}_{C_cB_b} - \sum_{D\neq B}^{*}\sum_{d} \boldsymbol{M}^{(1)}_{A_aD_d}\frac{\mathcal{H}^{(1)}_{D_dB_b}}{E_{DB}}
\end{aligned}
\tag{F.11}
$$

while the third one,

$$
\begin{aligned}
& -\frac{1}{2}\langle\, \phi^{(0)}_{A_a} \mid [\mathcal{S}^{(1)}, [\mathcal{S}^{(1)}, \boldsymbol{M}^{(0)}]] \mid \phi^{(0)}_{B_b} \,\rangle \\
& \qquad = -\frac{1}{2}\langle\, \phi^{(0)}_{A_a} \mid \mathcal{S}^{(1)}\mathcal{S}^{(1)}\boldsymbol{M}^{(0)} + \boldsymbol{M}^{(0)}\mathcal{S}^{(1)}\mathcal{S}^{(1)} - 2\mathcal{S}^{(1)}\boldsymbol{M}^{(0)}\mathcal{S}^{(1)} \mid \phi^{(0)}_{B_b} \,\rangle \\
& \qquad = -\frac{1}{2}\sum_{C,D}\sum_{c,d} \mathcal{S}^{(1)}_{A_aD_d}\mathcal{S}^{(1)}_{D_dC_c}\boldsymbol{M}^{(0)}_{C_cB_b} - \frac{1}{2}\sum_{C,D}\sum_{c,d} \boldsymbol{M}^{(0)}_{A_aC_c}\mathcal{S}^{(1)}_{C_cD_d}\mathcal{S}^{(1)}_{D_dB_b} \\
& \qquad\qquad + \sum_{C,D}\sum_{c,d} \mathcal{S}^{(1)}_{A_aC_c}\boldsymbol{M}^{(0)}_{C_cD_d}\mathcal{S}^{(1)}_{D_dB_b} \\
& \qquad = \frac{1}{2}\sum_{D\neq A}^{*}\sum_{C\neq D}^{*}\sum_{c,d} \frac{\mathcal{H}^{(1)}_{A_aD_c}}{E_{AD}}\frac{\mathcal{H}^{(1)}_{D_dC_c}}{E_{DC}}\boldsymbol{M}^{(0)}_{C_cB_b} + \frac{1}{2}\sum_{D\neq B}^{*}\sum_{C\neq D}^{*}\sum_{c,d} \boldsymbol{M}^{(0)}_{A_aC_c}\frac{\mathcal{H}^{(1)}_{C_cD_d}}{E_{CD}}\frac{\mathcal{H}^{(1)}_{D_dB_b}}{E_{DB}} \\
& \qquad\qquad - \sum_{C\neq A}^{*}\sum_{D\neq B}^{*}\sum_{c,d} \frac{\mathcal{H}^{(1)}_{A_aC_c}}{E_{AC}}\boldsymbol{M}^{(0)}_{C_cD_d}\frac{\mathcal{H}^{(1)}_{D_dB_b}}{E_{DB}}
\end{aligned}
\tag{F.12}
$$

Remembering that,

$$
\mathcal{S}^{(2)}_{A_aB_b} = \frac{(-i)}{E_{AB}}\left[\mathcal{H}^{(2)}_{A_aB_b} - \frac{1}{2}\sum_{C\neq A}^{*}\sum_{c} \frac{\mathcal{H}^{(1)}_{A_aC_c}\mathcal{H}^{(1)}_{C_cB_b}}{E_{CA}} - \frac{1}{2}\sum_{C\neq B}^{*}\sum_{c} \frac{\mathcal{H}^{(1)}_{A_aC_c}\mathcal{H}^{(1)}_{C_cB_b}}{E_{CB}}\right]
\tag{F.13}
$$

the last term in eq. F.10 is given by,

$$
\begin{aligned}
& i\langle\, \phi^{(0)}_{A_a} \mid [\mathcal{S}^{(2)}, \boldsymbol{M}^{(0)}] \mid \phi^{(0)}_{B_b} \,\rangle \\
&\quad = i\langle\, \phi^{(0)}_{A_a} \mid \mathcal{S}^{(2)}\boldsymbol{M}^{(0)} - \boldsymbol{M}^{(0)}\mathcal{S}^{(2)} \mid \phi^{(0)}_{B_b} \,\rangle \\
&\quad = i\sum_{C}\sum_{c} \mathcal{S}^{(2)}_{A_aC_c}\boldsymbol{M}^{(0)}_{C_cB_b} - i\sum_{C}\sum_{c} \boldsymbol{M}^{(0)}_{A_aC_c}\mathcal{S}^{(2)}_{C_cB_b} \\
&\quad = \sum_{C\neq A}\sum_{c} \frac{\mathcal{H}^{(2)}_{A_aC_c}}{E_{AC}}\boldsymbol{M}^{(0)}_{C_cB_b} - \sum_{C\neq B}\sum_{c} \boldsymbol{M}^{(0)}_{A_aC_c}\frac{\mathcal{H}^{(2)}_{C_cB_b}}{E_{CB}} \\
&\qquad - \frac{1}{2}\sum_{C\neq A}^{*}\sum_{D\neq A}^{*}\sum_{c,d} \frac{\mathcal{H}^{(1)}_{A_aD_d}\mathcal{H}^{(1)}_{D_dC_c}}{E_{AC}E_{DA}}\boldsymbol{M}^{(0)}_{C_cB_b} - \frac{1}{2}\sum_{C\neq A}^{*}\sum_{D\neq C}^{*}\sum_{c,d} \frac{\mathcal{H}^{(1)}_{A_aD_d}\mathcal{H}^{(1)}_{D_dC_c}}{E_{AC}E_{DC}}\boldsymbol{M}^{(0)}_{C_cB_b} \\
&\qquad + \frac{1}{2}\sum_{C\neq B}^{*}\sum_{D\neq C}^{*}\sum_{c,d} \boldsymbol{M}^{(0)}_{A_aC_c}\frac{\mathcal{H}^{(1)}_{C_cD_d}\mathcal{H}^{(1)}_{D_dB_b}}{E_{CB}E_{DC}} + \frac{1}{2}\sum_{C\neq B}^{*}\sum_{D\neq B}^{*}\sum_{c,d} \boldsymbol{M}^{(0)}_{A_aC_c}\frac{\mathcal{H}^{(1)}_{C_cD_d}\mathcal{H}^{(1)}_{D_dB_b}}{E_{CB}E_{DB}}
\end{aligned}
\tag{F.14}
$$

Some simplifications can be done observing that the second term in the last equality of eq. F.12 can be rewritten as (with a similar consideration for the first one),

$$
\begin{aligned}
\frac{1}{2}\sum_{D\neq B}^{*}\sum_{C\neq D}^{*}\sum_{c,d} \boldsymbol{M}^{(0)}_{A_aC_c}\frac{\mathcal{H}^{(1)}_{C_cD_d}}{E_{CD}}\frac{\mathcal{H}^{(1)}_{D_dB_b}}{E_{DB}} =& \frac{1}{2}\sum_{D\neq B}^{*}\sum_{C\neq D,B}^{*}\sum_{c,d} \boldsymbol{M}^{(0)}_{A_aC_c}\frac{\mathcal{H}^{(1)}_{C_cD_d}}{E_{CD}}\frac{\mathcal{H}^{(1)}_{D_dB_b}}{E_{DB}} \\
& - \frac{1}{2}\sum_{C\neq B}^{*}\sum_{c} \boldsymbol{M}^{(0)}_{A_aB_b}\frac{\mathcal{H}^{(1)}_{B_bC_c}\mathcal{H}^{(1)}_{C_cB_b}}{{E_{BC}}^2}
\end{aligned}
\tag{F.15}
$$

and the last two terms in eq. F.14 as (with similar considerations for the third and fourth ones),

$$
\begin{aligned}
\frac{1}{2}\sum_{C\neq B}^{*}\sum_{D\neq C}^{*}\sum_{c,d} \boldsymbol{M}^{(0)}_{A_aC_c}\frac{\mathcal{H}^{(1)}_{C_cD_d}}{E_{CB}}\frac{\mathcal{H}^{(1)}_{D_dB_b}}{E_{DC}} =& \frac{1}{2}\sum_{C\neq B}^{*}\sum_{D\neq B,C}^{*}\sum_{c,d} \boldsymbol{M}^{(0)}_{A_aC_c}\frac{\mathcal{H}^{(1)}_{C_cD_d}}{E_{CB}}\frac{\mathcal{H}^{(1)}_{D_dB_b}}{E_{DC}} \\
& - \frac{1}{2}\sum_{C\neq B}^{*}\sum_{c} \boldsymbol{M}^{(0)}_{A_aC_c}\frac{\mathcal{H}^{(1)}_{C_cB_b}\mathcal{H}^{(1)}_{B_bB_b}}{{E_{BC}}^2}
\end{aligned}
\tag{F.16}
$$

$$
\begin{aligned}
\frac{1}{2}\sum_{C\neq B}^{*}\sum_{D\neq B}^{*}\sum_{c,d} \boldsymbol{M}^{(0)}_{A_aC_c}\frac{\mathcal{H}^{(1)}_{C_cD_d}\mathcal{H}^{(1)}_{D_dB_b}}{E_{CB}E_{DB}} =& \frac{1}{2}\sum_{C\neq B}^{*}\sum_{D\neq B,C}^{*}\sum_{c,d} \boldsymbol{M}^{(0)}_{A_aC_c}\frac{\mathcal{H}^{(1)}_{C_cD_d}\mathcal{H}^{(1)}_{D_dB_b}}{E_{CB}E_{DB}} \\
& + \frac{1}{2}\sum_{C\neq B}^{*}\sum_{c} \boldsymbol{M}^{(0)}_{A_aC_c}\frac{\mathcal{H}^{(1)}_{C_cC_c}\mathcal{H}^{(1)}_{C_cB_b}}{{E_{CB}}^2}
\end{aligned}
\tag{F.17}
$$

The first terms in the right-hand side of eqs. F.15-F.17 can be summed,

$$\frac{1}{2}\sum_{D\neq B}^{*}\sum_{C\neq D,B}^{*}\sum_{c,d}\boldsymbol{M}^{(0)}_{A_aC_c}\frac{\mathcal{H}^{(1)}_{C_cD_d}}{E_{CD}}\frac{\mathcal{H}^{(1)}_{D_dB_b}}{E_{DB}}+\frac{1}{2}\sum_{C\neq B}^{*}\sum_{D\neq B,C}^{*}\sum_{c,d}\boldsymbol{M}^{(0)}_{A_aC_c}\frac{\mathcal{H}^{(1)}_{C_cD_d}}{E_{CB}}\frac{\mathcal{H}^{(1)}_{D_dB_b}}{E_{DC}}$$
$$+\frac{1}{2}\sum_{C\neq B}^{*}\sum_{D\neq B,C}^{*}\sum_{c,d}\boldsymbol{M}^{(0)}_{A_aC_c}\frac{\mathcal{H}^{(1)}_{C_cD_d}\mathcal{H}^{(1)}_{D_dB_b}}{E_{CB}E_{DB}}=\sum_{C\neq B}^{*}\sum_{D\neq B,C}^{*}\sum_{c,d}\boldsymbol{M}^{(0)}_{A_aC_c}\frac{\mathcal{H}^{(1)}_{C_cD_d}\mathcal{H}^{(1)}_{D_dB_b}}{E_{BC}E_{BD}} \tag{F.18}$$

Then collecting all terms eq. F.10 becomes,

$$\begin{aligned}
{}^{\mathrm{CT}}\langle\,\boldsymbol{M}\,\rangle^{(2)}_{A_aB_b} =&\boldsymbol{M}^{(2)}_{A_aB_b}+\sum_{C\neq A}^{*}\sum_{c}\frac{\mathcal{H}^{(1)}_{A_aC_c}}{E_{AC}}\boldsymbol{M}^{(1)}_{C_cB_b}-\sum_{D\neq B}^{*}\sum_{d}\boldsymbol{M}^{(1)}_{A_aD_d}\frac{\mathcal{H}^{(1)}_{D_dB_b}}{E_{DB}}\\
&+\sum_{C\neq A}\sum_{c}\frac{\mathcal{H}^{(2)}_{A_aC_c}}{E_{AC}}\boldsymbol{M}^{(0)}_{C_cB_b}-\sum_{C\neq B}\sum_{c}\boldsymbol{M}^{(0)}_{A_aC_c}\frac{\mathcal{H}^{(2)}_{C_cB_b}}{E_{CB}}\\
&-\sum_{C\neq A}^{*}\sum_{D\neq B}^{*}\sum_{c,d}\frac{\mathcal{H}^{(1)}_{A_aC_c}}{E_{AC}}\boldsymbol{M}^{(0)}_{C_cD_d}\frac{\mathcal{H}^{(1)}_{D_dB_b}}{E_{DB}}\\
&+\sum_{C\neq A}^{*}\sum_{D\neq A,C}^{*}\sum_{c,d}\frac{\mathcal{H}^{(1)}_{A_aD_c}}{E_{AC}}\frac{\mathcal{H}^{(1)}_{D_dC_c}}{E_{AD}}\boldsymbol{M}^{(0)}_{C_cB_b}+\sum_{C\neq B}^{*}\sum_{D\neq B,C}^{*}\sum_{c,d}\boldsymbol{M}^{(0)}_{A_aC_c}\frac{\mathcal{H}^{(1)}_{C_cD_d}}{E_{BC}}\frac{\mathcal{H}^{(1)}_{D_dB_b}}{E_{BD}}\\
&-\frac{1}{2}\sum_{C\neq A}^{*}\sum_{c}\frac{\mathcal{H}^{(1)}_{A_aC_c}\mathcal{H}^{(1)}_{C_cA_a}}{{E_{AC}}^2}\boldsymbol{M}^{(0)}_{A_aB_b}-\frac{1}{2}\sum_{C\neq B}^{*}\sum_{c}\boldsymbol{M}^{(0)}_{A_aB_b}\frac{\mathcal{H}^{(1)}_{B_bC_c}\mathcal{H}^{(1)}_{C_cB_b}}{{E_{BC}}^2}\\
&+\frac{1}{2}\sum_{C\neq A}^{*}\sum_{c}\frac{\mathcal{H}^{(1)}_{A_aC_c}\mathcal{H}^{(1)}_{C_cC_c}}{{E_{AC}}^2}\boldsymbol{M}^{(0)}_{C_cB_b}-\frac{1}{2}\sum_{C\neq B}^{*}\sum_{c}\boldsymbol{M}^{(0)}_{A_aC_c}\frac{\mathcal{H}^{(1)}_{C_cB_b}\mathcal{H}^{(1)}_{B_bB_b}}{{E_{BC}}^2}\\
&-\frac{1}{2}\sum_{C\neq A}^{*}\sum_{c}\frac{\mathcal{H}^{(1)}_{A_aA_a}\mathcal{H}^{(1)}_{A_aC_c}}{{E_{AC}}^2}\boldsymbol{M}^{(0)}_{C_cB_b}+\frac{1}{2}\sum_{C\neq B}^{*}\sum_{c}\boldsymbol{M}^{(0)}_{A_aC_c}\frac{\mathcal{H}^{(1)}_{C_cC_c}\mathcal{H}^{(1)}_{C_cB_b}}{{E_{BC}}^2}
\end{aligned} \tag{F.19}$$

In RS theory the second-order correction to the property is given by,

$$\begin{aligned}
{}^{\mathrm{RS}}\langle\,\boldsymbol{M}\,\rangle^{(2)}_{A_aB_b} =&\langle\,\phi^{(2)}_{A_a}\mid\boldsymbol{M}^{(0)}\mid\phi^{(0)}_{B_b}\,\rangle+\langle\,\phi^{(0)}_{A_a}\mid\boldsymbol{M}^{(2)}\mid\phi^{(0)}_{B_b}\,\rangle+\langle\,\phi^{(0)}_{A_a}\mid\boldsymbol{M}^{(0)}\mid\phi^{(2)}_{B_b}\,\rangle\\
&+\langle\,\phi^{(1)}_{A_a}\mid\boldsymbol{M}^{(1)}\mid\phi^{(0)}_{B_b}\,\rangle+\langle\,\phi^{(1)}_{A_a}\mid\boldsymbol{M}^{(0)}\mid\phi^{(1)}_{B_b}\,\rangle+\langle\,\phi^{(0)}_{A_a}\mid\boldsymbol{M}^{(1)}\mid\phi^{(1)}_{B_b}\,\rangle
\end{aligned} \tag{F.20}$$

where $|\,\phi^{(1)}_{B_b}\,\rangle$ is given by eq. F.9 and,

$$|\,\phi^{(2)}_{B_b}\,\rangle = -\sum_{C\neq B}^{*}\sum_{c}|\,\phi^{(0)}_{C_c}\,\rangle\frac{\mathcal{H}^{(2)}_{C_cB_b}}{E_{CB}} + \sum_{C\neq B}^{*}\sum_{D\neq B}^{*}\sum_{c,d}|\,\phi^{(0)}_{C_c}\,\rangle\frac{\mathcal{H}^{(1)}_{C_cD_d}\mathcal{H}^{(1)}_{D_dB_b}}{E_{BC}E_{BD}} - \sum_{C\neq B}^{*}\sum_{c}|\,\phi^{(0)}_{C_c}\,\rangle\frac{\mathcal{H}^{(1)}_{C_cB_b}\mathcal{H}^{(1)}_{B_bB_b}}{{E_{BC}}^2} - \frac{1}{2}\sum_{C\neq B}^{*}\sum_{c}|\,\phi^{(0)}_{B_b}\,\rangle\frac{\mathcal{H}^{(1)}_{B_bC_c}\mathcal{H}^{(1)}_{C_cB_b}}{{E_{BC}}^2} \quad \text{(F.21)}$$

Substituting eq. F.21 in F.20 and pointing out that,

$$\sum_{C\neq B}^{*}\sum_{D\neq B}^{*}\sum_{c,d}|\,\phi^{(0)}_{C_c}\,\rangle\frac{\mathcal{H}^{(1)}_{C_cD_d}\mathcal{H}^{(1)}_{D_dB_b}}{E_{BC}E_{BD}} = \sum_{C\neq B}^{*}\sum_{D\neq B,C}^{*}\sum_{c,d}|\,\phi^{(0)}_{C_c}\,\rangle\frac{\mathcal{H}^{(1)}_{C_cD_d}\mathcal{H}^{(1)}_{D_dB_b}}{E_{BC}E_{BD}} + \sum_{C\neq B}^{*}\sum_{c}|\,\phi^{(0)}_{C_c}\,\rangle\frac{\mathcal{H}^{(1)}_{C_cC_c}\mathcal{H}^{(1)}_{C_cB_b}}{{E_{BC}}^2} \quad \text{(F.22)}$$

we obtain,

$$\begin{aligned}
{}^{\mathrm{RS}}\langle\,\boldsymbol{M}\,\rangle^{(2)}_{A_aB_b} =& \boldsymbol{M}^{(2)}_{A_aB_b} + \sum_{C\neq A}^{*}\sum_{c}\frac{\mathcal{H}^{(1)}_{A_aC_c}}{E_{AC}}\boldsymbol{M}^{(1)}_{C_cB_b} - \sum_{D\neq B}^{*}\sum_{d}\boldsymbol{M}^{(1)}_{A_aD_d}\frac{\mathcal{H}^{(1)}_{D_dB_b}}{E_{DB}} \\
&+ \sum_{C\neq A}\sum_{c}\frac{\mathcal{H}^{(2)}_{A_aC_c}}{E_{AC}}\boldsymbol{M}^{(0)}_{C_cB_b} - \sum_{C\neq B}\sum_{c}\boldsymbol{M}^{(0)}_{A_aC_c}\frac{\mathcal{H}^{(2)}_{C_cB_b}}{E_{CB}} \\
&- \sum_{C\neq A}^{*}\sum_{D\neq B}^{*}\sum_{c,d}\frac{\mathcal{H}^{(1)}_{A_aC_c}}{E_{AC}}\boldsymbol{M}^{(0)}_{C_cD_d}\frac{\mathcal{H}^{(1)}_{D_dB_b}}{E_{DB}} \\
&+ \sum_{C\neq A}^{*}\sum_{D\neq A,C}^{*}\sum_{c,d}\frac{\mathcal{H}^{(1)}_{A_aD_c}}{E_{AC}}\frac{\mathcal{H}^{(1)}_{D_dC_c}}{E_{AD}}\boldsymbol{M}^{(0)}_{C_cB_b} + \sum_{C\neq B}^{*}\sum_{D\neq B,C}^{*}\sum_{c,d}\boldsymbol{M}^{(0)}_{A_aC_c}\frac{\mathcal{H}^{(1)}_{C_cD_d}}{E_{BC}}\frac{\mathcal{H}^{(1)}_{D_dB_b}}{E_{BD}} \\
&- \frac{1}{2}\sum_{C\neq A}^{*}\sum_{c}\frac{\mathcal{H}^{(1)}_{A_aC_c}\mathcal{H}^{(1)}_{C_cA_a}}{{E_{AC}}^2}\boldsymbol{M}^{(0)}_{A_aB_b} - \frac{1}{2}\sum_{C\neq B}^{*}\sum_{c}\boldsymbol{M}^{(0)}_{A_aB_b}\frac{\mathcal{H}^{(1)}_{B_bC_c}\mathcal{H}^{(1)}_{C_cB_b}}{{E_{BC}}^2} \\
&+ \sum_{C\neq A}^{*}\sum_{c}\frac{\mathcal{H}^{(1)}_{A_aC_c}\mathcal{H}^{(1)}_{C_cC_c}}{{E_{AC}}^2}\boldsymbol{M}^{(0)}_{C_cB_b} - \sum_{C\neq B}^{*}\sum_{c}\boldsymbol{M}^{(0)}_{A_aC_c}\frac{\mathcal{H}^{(1)}_{C_cB_b}\mathcal{H}^{(1)}_{B_bB_b}}{{E_{BC}}^2} \\
&- \sum_{C\neq A}^{*}\sum_{c}\frac{\mathcal{H}^{(1)}_{A_aA_a}\mathcal{H}^{(1)}_{A_aC_c}}{{E_{AC}}^2}\boldsymbol{M}^{(0)}_{C_cB_b} + \sum_{C\neq B}^{*}\sum_{c}\boldsymbol{M}^{(0)}_{A_aC_c}\frac{\mathcal{H}^{(1)}_{C_cC_c}\mathcal{H}^{(1)}_{C_cB_b}}{{E_{BC}}^2}
\end{aligned} \quad \text{(F.23)}$$

that differs from eq. F.19 just for the factor 1/2 in the last four terms. It is noteworthy that the last terms are all null if all diagonal elements of $\mathcal{H}^{(1)}$ are null, such as for the case $\mathcal{H}^{(1)} = \mathcal{H}_{30}$.

In the calculation of vibrationally averaged properties (see section 4.1), the non null terms in the right-hand side of eq. F.23 are the first three and the sixth, the ninth and the tenth one, but the last three sum to zero.

Bibliography

1. *Frontiers of Molecular Spectroscopy* (ed Laane, J.) (Elsevier, 2008).
2. *Handbook of high-resolution spectroscopy* (eds Quack, M. & Merkt, F.) 2182 (John Wiley & Sons, Inc., Weinheim, Germany, 2011).
3. Jensen, P. & Bunker, P. *Computational molecular spectroscopy* (Wiley, New York, 2000).
4. *Computational spectroscopy: methods, experiments and applications* (ed Grunenberg, J.) (Wiley-VCH Verlag GmbH & Co. KGaA, Weinheim, Germany, 2010).
5. *Computational strategies for spectroscopy: from small molecules to nano systems* (ed Barone, V.) (Wiley & Sons, Inc., Hoboken, New Jersey, 2011).
6. *Equilibrium molecular structures: from spectroscopy to quantum chemistry* (eds Demaison, J., Boggs, J. & Császár, A.) (CRC Press, Boca Raton, FL, 2011).
7. Carter, S. & Handy, N. *Comput. Phys. Rep.* **5,** 115 (1986).
8. Bowman, J. *Acc. Chem. Res.* **19,** 202 (1986).
9. Jung, J. & Gerber, R. *J. Chem. Phys.* **105,** 10332 (1996).
10. Carter, S., Culik, S. & Bowman, J. *J. Chem. Phys.* **107,** 10458 (1997).
11. Chaban, G., Jung, J. & Gerber, R. *J. Chem. Phys.* **111,** 1823 (1999).
12. Wright, N. & Gerber, R. *J. Chem. Phys.* **112,** 2598 (2000).
13. Koput, J., Carter, S. & Handy, N. *J. Chem. Phys.* **115,** 8345 (2001).
14. Cassam-Chenai, P. & Lievin, J. *Int. J. Quantum Chem.* **93,** 245 (2003).
15. Yagi, K., Hirao, K., Taketsugu, T., Schmidt, M. & Gordon, M. *J. Chem. Phys.* **121,** 1383 (2004).

16. Bowman, J. M., Carrington, T. & Meyer, H.-D. *Mol. Phys.* **106,** 2145–2182 (2008).
17. Pesonen, J. & Halonen, L. in *Adv. Chem. Phys.* 269–349 (John Wiley & Sons, Inc., 2003).
18. Császár, A. G. *et al. Phys. Chem. Chem. Phys.* **14,** 1085–1106 (2012).
19. Carrington, T. & Wang, X.-G. *WIREs Comput. Mol. Sci.* **1,** 952–963 (2011).
20. Tennyson, J. *WIREs Comput. Mol. Sci.* **2,** 698–715 (2012).
21. Puzzarini, C., Stanton, J. F. & Gauss, J. *Int. Rev. Phys. Chem.* **29,** 273 (2010).
22. Ruud, K., Åstrand, P.-O. & Taylor, P. R. *J. Chem. Phys.* **112,** 2668–2683 (2000).
23. Neugebauer, J. & Hess, B. A. *J. Chem. Phys.* **118,** 7215–7225 (2003).
24. Christiansen, O. *Phys. Chem. Chem. Phys.* **9,** 2942–2953 (2007).
25. Christiansen, O. *Phys. Chem. Chem. Phys.* **14,** 6672–6687 (19 2012).
26. Roy, T. K. & Gerber, R. B. *Phys. Chem. Chem. Phys.* **15,** 9468–9492 (2013).
27. Bowman, J. M., Carter, S. & Huang, X. *Int. Rev. Phys. Chem.* **22,** 533–549 (2003).
28. Carter, S., Culik, S. J. & Bowman, J. M. *J. Chem. Phys.* **107,** 10548–10469 (1997).
29. Nielsen, H. H. *Rev. Mod. Phys.* **23,** 90–136 (2 1951).
30. Mills, I. M. in *Molecular spectroscopy: modern research* 115–140 (K.N. Rao and C.W. Mathews, 1972).
31. Willetts, A., Handy, N. C., Green, W. H. & Jayatilaka, D. *J. Phys. Chem.* **94,** 5608–5616 (1990).
32. Papoušek, D. & Aliev, M. *Molecular vibrational-rotational spectra* (Elsevier, New York, 1982).
33. Califano, S. *Vibrational States* (John Wiley & Sons Ltd, 1976).
34. Truhlar, D. G., Olson, R. W., Jeannotte, A. C. & Overend, J. *J. Am. Chem. Soc.* **98,** 2373–2379 (1976).
35. Isaacson, A. D., Truhlar, D. G., Scanlon, K. & Overend, J. *J. Chem. Phys.* **75,** 3017 (1981).
36. Isaacson, A. D. & Hung, S.-C. *J. Chem. Phys.* **101,** 3928–3935 (1994).
37. Clabo Jr., D. A., Allen, W. D., Remington, R. B., Yamaguchi, Y. & Schaefer III, H. F. *Chem. Phys.* **123,** 187–239 (1988).

38. Maslen, P., Handy, N., Amos, D. & Jayatilaka, D. *J. Chem. Phys.* **97,** 4233 (1992).
39. Zhang, Q., Day, P. & Truhlar, D. *J. Chem. Phys.* **98,** 4948 (1993).
40. Barone, V. *J. Chem. Phys.* **120,** 3059–3065 (2004).
41. Bloino, J., Biczysko, M., Crescenzi, O. & Barone, V. *J. Chem. Phys.* **128,** 244105 (2008).
42. Vázquez, J. & Stanton, J. *Mol. Phys.* **104,** 377–388 (2006).
43. Vázquez, J. & Stanton, J. F. *Mol. Phys.* **105,** 101–109 (2007).
44. Kemble, E. C. *The Fundamental Principles of Quantum Mechanics* (Dover Publications, 2005).
45. Schiff, L. I. *Quantum mechanics* (McGraw-Hill Education, 1968).
46. Ruden, T., Taylor, P. & Helgaker, T. *J. Chem. Phys.* **119,** 1951–1960 (2003).
47. Barone, V. *J. Chem. Phys.* **122,** 014108 (2005).
48. Carbonnière, P., Dargelos, A. & Pouchan, C. *Theor. Chem. Acc.* **125,** 543–554 (2010).
49. Krasnoshchekov, S. V., Isayeva, E. V. & Stepanov, N. F. *J. Phys. Chem. A* **116,** 3691–3709 (2012).
50. Gaw, F., Willetts, A., Handy, N. & Green, W. in *Advances in Molecular Vibrations and Collision Dynamics* (ed Bowman, J. M.) 169–185 (JAI Press, 1991).
51. Dressler, S. & Thiel, W. *Chem. Phys. Lett.* **273,** 71–78 (1997).
52. Bloino, J., Guido, C., Lipparini, F. & Barone, V. *Chem. Phys. Lett.* **496,** 157 (2010).
53. Bloino, J., Biczysko, M. & Barone, V. *J. Chem. Theory Comput.* **8,** 1015 (2012).
54. Hermes, M. R. & Hirata, S. *J. Chem. Phys.* **139,** 034111 (2013).
55. Wang, D., Qiang, S. & Zhu, A. *J. Chem. Phys.* **112,** 9624 (2000).
56. Bunker, P. R., Kraemer, W. P. & Spirko, V. *Can. J. Phys.* **62,** 1801 (1984).
57. Mattioda, A. L., Ricca, A., Tucker, J., Bauschlicher Jr, C. W. & Allamandola, L. J. *Astron. J.* **137,** 4054 (2009).
58. Zhang, Z., Shen, Z., Ren, Y & Bian, W. *Chem. Phys.* **400,** 1 (2012).
59. Temsamani, M. & Herman, M. *J. Chem. Phys.* **102,** 6371 (1995).
60. Henry, L. & Amat, G. *J. Mol. Spectrosc.* **15,** 168–179 (1965).

61. Simmonett, A., Schaefer, H. & Allen, W. *J. Chem. Phys.* **130,** 44301 (2009).

62. McNaughton, D. & Bruget, D. *J. Mol. Spectrosc.* **150,** 620 (1991).

63. McNaughton, D. & Bruget, D. *J. Mol. Struct.* **273,** 11 (1992).

64. Shindo, F., Chaquin, P., J.C., G., Jolly, A. & Fr., R. *J. Mol. Spectrosc.* **210,** 191 (2001).

65. Gronowki, M. & Kolos, R. *Chem. Phys. Lett.* **428,** 245 (2006).

66. Janoschek, R. *J. Mol. Struct.* **232,** 147 (1991).

67. Wang, H., Szczepanski, J., Cooke, A., Brucat, P. & Vala, M. *Int. J. Quantum Chem.* **102,** 806 (2005).

68. Mellau, G. *J. Chem. Phys.* **134,** 234303 (2011).

69. Schulze, G., Koja, O., Winnewisser, B. & M., W. *J. Mol. Struct.* **517,** 307 (2000).

70. Henry, L. & Amat, G. *Cahiers Phys.* **95,** 273 (1958).

71. Henry, L. & Amat, G. *Cahiers Phys.* **118,** 230 (1960).

72. Lounila, J., Wasser, R. & Diehl, P. *Mol. Phys.* **62,** 19–31 (1987).

73. Vaara, J., Lounila, J., Ruud, K. & Helgaker, T. *J. Chem. Phys.* **109,** 8388–8397 (1998).

74. Åstrand, P.-O., Ruud, K. & Taylor, P. R. *J. Chem. Phys.* **112,** 2655–2667 (2000).

75. Barone, V., Carbonniere, P. & Pouchan, C. *J. Chem. Phys.* **122,** 224308 (2005).

76. Mort, B. C. & Autschbach, J. *J. Phys. Chem. A* **110,** 11381–11383 (2006).

77. Draucínský, M., Kaminský, J. & Bouř, P. *J. Chem. Phys.* **130,** 094106 (2009).

78. Marcott, C., Golden, W. & Overend, J. *Spectrochim. Acta A* **34,** 661–665 (1978).

79. Faulkner, T. R., Marcott, C., Moscowitz, A. & Overend, J. *J. Am. Chem. Soc.* **99,** 8160–8168 (1977).

80. Hanson, H. M. & Nielsen, H. H. *J. Mol. Spectrosc.* **4,** 468–476 (1960).

81. Hanson, H. M. & Cook, A. R. *J. Mol. Spectrosc.* **16,** 130–134 (1965).

82. Di Lauro, C. & Mills, I. *J. Mol. Spectrosc.* **21,** 386–413 (1966).

83. Cartwright, G. J. & Mills, I. M. *J. Mol. Spectrosc.* **34,** 415–439 (1970).

84. Secroun, C., Barbe, A. & Jouve, P. *J. Mol. Spectrosc.* **45,** 1–9 (1973).

85. Kwan, Y. Y. *J. Mol. Spectrosc.* **49,** 27–47 (1974).
86. Kwan, Y. Y. *J. Mol. Spectrosc.* **51,** 151–159 (1974).
87. Polavarapu, P. L. *Mol. Phys.* **89,** 1503–1510 (1996).
88. Bour, P. *J. Phys. Chem.* **98,** 8862–8865 (1994).
89. Bishop, D. M. & Kirtman, B. *J. Chem. Phys.* **95,** 2646–2658 (1991).
90. Bishop, D. M. & Kirtman, B. *J. Chem. Phys.* **97,** 5255–5256 (1992).
91. Bludský, O., Bak, K. L., Jørgensen, P. & Špirko, V. *J. Chem. Phys.* **103,** 10110–10115 (1995).
92. Bak, K. L., Bludský, O. & Jørgensen, P. *J. Chem. Phys.* **103,** 10548–10555 (1995).
93. Luis, J. M., Duran, M. & Andrés, J. L. *J. Chem. Phys.* **107,** 1501–1512 (1997).
94. Kirtman, B., Luis, J. M. & Bishop, D. M. *J. Chem. Phys.* **108,** 10008–10012 (1998).
95. Bishop, D. M., Luis, J. M. & Kirtman, B. *J. Chem. Phys.* **108,** 10013–10017 (1998).
96. Helgaker, T. *et al. Chem. Rev.* **112,** 543–631 (2012).
97. Bloino, J. & Barone, V. *J. Chem. Phys.* **136,** 124108 (2012).
98. Bloino, J. *J. Phys. Chem. A,* 10.1021/jp509985u (2015).
99. Plíva, J. *J. Mol. Spectrosc.* **139,** 278 (1990).
100. Willetts, A. & Handy, N. *Chem. Phys. Lett.* **235,** 286 (1995).
101. Barchewitz, M. *Spectroscopie Infrarouge* (Gauthier-Villars, 1961).
102. Bunker, P. & Jensen, F. *Molecular symmetry and spectroscopy* (NRC Research Press National Research Council of Canada, 1998).
103. Born, M. & Oppenheimer, R. *Ann. Phys. (Berlin, Ger.)* **389,** 457–484 (1927).
104. Jensen, P. & Bunker, P. in *Computational molecular spectroscopy* (eds Jensen, P. & Bunker, P.) 3–12 (Wiley, New York, 2000).
105. Eckart, C. *Phys. Rev.* **47,** 552–558 (7 1935).
106. Sayvetz, A. *J. Chem. Phys.* **7,** 383–389 (1939).
107. Watson, J. K. G. *Mol. Phys.* **15,** 479–490 (1968).
108. Aliev, M. & Watson, J. K. G. in *Molecular spectroscopy: modern research* (ed Rao, K. N.) 1–67 (Academic Press, Ohio, 1985).

109. Barone, V. & Minichino, C. *J. Mol. Struct.-Theochem* **330,** 365–376 (1995).

110. Isaacson, A. D. & Zhang, X.-G. *Theo. Chem. Acta* **74,** 493–511 (1988).

111. Isaacson, A. D. *J. Chem. Phys.* **108,** 9978–9986 (1998).

112. Landau, L. D. & Lifshitz, E. *Quantum Mechanics: Non-Relativistic Theory* (Pergamon, Oxford, 1965).

113. Jensen, F. *Introduction to Computational Chemistry* (Wiley, 2006).

114. Messiah, A. *Quantum Mechanics* (Dover Publications, 1999).

115. Sakurai, J. *Modern Quantum Mechanics* (Wesley, 1967).

116. Rosnik, A. M. & Polik, W. F. *Mol. Phys.* **112,** 261 (2014).

117. Lehmann, K. *Mol. Phys.* **66,** 1129 (1989).

118. Borro, A., Mills, I. & Venuti, E. *J. Chem. Phys.* **102,** 3938 (1995).

119. Martin, J. & Taylor, P. *Spectrochim. Acta A* **53,** 1039 (1997).

120. Wolfram Research, I. *Mathematica Edition: Version 8* Wolfram Research, Inc. 2010.

121. Henry, L. & Amat, G. *J. Mol. Spectrosc.* **5,** 319–325 (1961).

122. Miller, W., Hernandez, R., Handy, N., Jayatilaka, D. & Willets, A. *Chem. Phys. Lett.* **172,** 62 (1990).

123. Nguyen, T. L., Stanton, J. F. & Barker, J. R. *Chem. Phys. Lett.* **499,** 9–15 (2010).

124. Amat, G. *Compt. Rend.* **250,** 1439 (1960).

125. Grenier-Bresson, M. *J. Phys. Radium* **21,** 555 (1960).

126. Grenier-Besson, M. *J. Phys.-Paris* **25,** 757 (1964).

127. Krasnoshchekov, S. V., Isayeva, E. V. & Stepanov, N. F. *J. Chem. Phys.* **141,** 234114 (2014).

128. Martin, J., Lee, T., Taylor, P. & Francois, J. *J. Chem. Phys.* **103,** 2589 (1995).

129. Szabo, A. *Modern Quantum Chemistry: Introduction to Advanced Electronic Structure Theory* (Courier Dover Publications, 1996).

130. Kuhler, K. & Truhlar, D. *J. Chem. Phys.* **104,** 4664 (1996).

131. Darling, B. & Dennison, D. *Phys. Rev.* **57,** 128 (1940).

132. McQuarrie, D. A. *Statistical Mechanics* (University Science Books, 2000).

133. Truhlar, D. G. & Isaacson, A. D. *J. Chem. Phys.* **94,** 357 (1991).

134. Watson, J. in *Vibrational spectra and structure* 1–89 (Elsevier, 1977).
135. Kivelson, D. & Wilson, B. *J. Chem. Phys.* **20,** 1575 (1920).
136. Watson, J. K. G. *J. Chem. Phys.* **45,** 1360 (1966).
137. Watson, J. *J. Chem. Phys.* **46,** 1935 (1967).
138. Watson, J. *J. Chem. Phys.* **48,** 4517 (1968).
139. Aliev, M. & Watson, J. K. G. *J. Mol. Spectrosc.* **61,** 29 (1976).
140. Wilson, E. B. *J. Chem. Phys.* **4,** 526–528 (1936).
141. Wilson, E. B. *J. Chem. Phys.* **5,** 617–620 (1937).
142. Chung, K. T. & Parker, P. M. *J. Chem. Phys.* **43,** 3865–3868 (1965).
143. Chung, K. T. & Parker, P. M. *J. Chem. Phys.* **43,** 3869–3874 (1965).
144. Watson, J. *J. Chem. Phys.* **48,** 181 (1966).
145. Zare, R. *Angular Momentum* (Wiley, 1988).
146. Winnewisser, G. *J. Chem. Phys.* **56,** 2944–2954 (1972).
147. Van Eijck, B. *J. Mol. Spectrosc.* **53,** 246–249 (1974).
148. Watson, J. K. G. *Mol. Phys.* **19,** 465–487 (1970).
149. Martí, J. & Bishop, D. M. *J. Chem. Phys.* **99,** 3860–3864 (1993).
150. Bishop, D. M. & Norman, P. in *Handbook of Advanced Electronic and Photonic Materials and Devices* (ed Nalwa, H. S.) 1–62 (Academic Press, Burlington, 2001). ISBN: 978-0-12-513745-4.
151. Egidi, F. *et al. J. Chem. Theory Comput.* **10,** 2456–2464 (2014).
152. Pople, J. A., Krishnan, R., Schlegel, H. B. & Binkley, J. S. *Int. J. Quantum Chem.* **16,** 225 (1979).
153. Stratmann, R. E., Burant, J. C., Scuseria, G. E. & Frisch, M. J. *J. Chem. Phys.* **106,** 10175–10183 (1997).
154. Møller, C. & Plesset, M. S. *Phys. Rev.* **46,** 618–622 (1934).
155. Harrison, R. J., Fitzgerald, G. B., Laidig, W. D. & Barteltt, R. J. *Chem. Phys. Lett.* **124,** 291 (1986).
156. Helgaker, T., Jørgensen, P. & Olsen, J. *Electronic-Structure Theory* (Wiley, Chichester, 2000).
157. Shavitt, I. & Bartlett, R. *Many-body methods in chemistry and physics* (Cambridge University Press, New York, 2009).
158. Raghavachari, K., Trucks, G. W., Pople, J. A. & Head-Gordon, M. *Chem. Phys. Lett.* **157,** 479 (1989).

159. *Accurate molecular structures. Their determination and importance* (eds Domenicano, A. & Hargittai, I.) (Oxford University Press, New York, 1992).

160. Bak, K. L. *et al. J. Chem. Phys.* **114,** 6548 (2001).

161. Demaison, J. *Mol. Phys.* **105,** 3109 (2007).

162. Puzzarini, C. & Biczysko, M. in *Structure elucidation in organic chemistry* (ed Cid, M.-M.) 27–64 (Wiley-VCH Verlag GmbH & Co. KGaA, Weinheim, Germany, 2015).

163. Pérez, C. *et al. Science* **336,** 897–901 (2012).

164. Melandri, S., Sanz, M. E., Caminati, W., Favero, P. G. & Kisiel, Z. *J. Am. Chem. Soc.* **120,** 11504–11509 (1998).

165. Caminati, W. *Angew. Chem., Int. Ed.* **48,** 9030–9033. ISSN: 1521-3773 (2009).

166. Lovas, F. J. *et al. J. Am. Chem. Soc.* **127,** 4345–4349 (2005).

167. Pietraperzia, G. *et al. J. Phys. Chem. A* **113,** 14343–14351 (2009).

168. Blanco, S., Lesarri, A., López, J. C. & Alonso, J. L. *J. Am. Chem. Soc.* **126,** 11675–11683 (2004).

169. Peña, I. *et al. J. Phys. Chem. Lett.* **4,** 65–69 (2013).

170. Puzzarini, C. *et al. J. Phys. Chem. Lett.* **5,** 534–540 (2014).

171. Grimme, S. & Steinmetz, M. *Phys. Chem. Chem. Phys.* **15,** 16031–16042 (2013).

172. Jurecka, P., Sponer, J., Cerny, J. & Hobza, P. *Phys. Chem. Chem. Phys.* **8,** 1985–1993 (17 2006).

173. Zhao, Y. & Truhlar, D. G. *J. Chem. Theory Comput.* **3,** 289–300 (2007).

174. Barone, V., Biczysko, M. & Pavone, M. *Chem. Phys.* **346,** 247–256 (2008).

175. Barone, V., Biczysko, M., Bloino, J. & Puzzarini, C. *J. Chem. Phys.* **141,** 034107 (2014).

176. Senn, H. M. & Thiel, W. *Angew. Chem., Int. Ed.* **48,** 1198–1229. ISSN: 1521-3773 (2009).

177. Brooks, B. R. *et al. J. Comput. Chem.* **30,** 1545–1614. ISSN: 1096-987X (2009).

178. Pronk, S. *et al. Bioinformatics* **29,** 845–854 (2013).

179. Grubisic, S., Brancato, G., Pedone, A. & Barone, V. *Phys. Chem. Chem. Phys.* **14,** 15308–15320 (44 2012).

180. Maple, J. R., Dinur, U. & Hagler, A. T. *Proc. Natl. Acad. Sci. U.S.A.* **85,** 5350–5354 (1988).

181. Dasgupta, S., Yamasaki, T. & Goddard, W. A. *J. Chem. Phys.* **104,** 2898–2920 (1996).

182. Biczysko, M. *et al. Theor. Chem. Acc.* **131,** 1201 (2012).

183. Barone, V. *et al. Phys. Chem. Chem. Phys.* **15,** 3736–3751 (11 2013).

184. Risthaus, T., Steinmetz, M. & Grimme, S. *J. Comput. Chem.* **35,** 1509–1516. ISSN: 1096-987X (2014).

185. Cramer, C. *Essentials of computational chemistry: theories and models* (John Wiley & Sons Ltd., Chichester, U.K., 2005).

186. Császár, A. in *Equilibrium molecular structures: from spectroscopy to quantum chemistry* (eds Demaison, J., Boggs, J. & Császár, A.) 233–261 (CRC Press, Boca Raton, FL, 2011).

187. Kuchitsu, K. in *Accurate molecular structures. Their determination and importance* (eds Domenicano, A. & Hargittai, I.) 14 (Oxford University Press, New York, 1992).

188. Heckert, M., Kállay, M. & Gauss, J. *Mol. Phys.* **103,** 2109 (2005).

189. Heckert, M., Kállay, M., Tew, D. P., Klopper, W. & Gauss, J. *J. Chem. Phys.* **125,** 044108 (2006).

190. Barone, V., Biczysko, M., Bloino, J. & Puzzarini, C. *Phys. Chem. Chem. Phys.* **15,** 10094–10111 (2013).

191. Pulay, P., Meyer, W. & Boggs, J. E. *J. Chem. Phys.* **68,** 5077 (1978).

192. Pawłowski, F. *et al. J. Chem. Phys.* **116,** 6482 (2002).

193. Senent, M. L., Puzzarini, C., Domínguez-Gómez, R., Carvajal, M. & Hochlaf, M. *J. Chem. Phys.* **140,** 124302 (2014).

194. Ormond, T. K. *et al. J. Phys. Chem. A* **118,** 708–718 (2014).

195. Wang, X., Huang, X., Bowman, J. M. & Lee, T. J. *J. Chem. Phys.* **139,** 224302 (2013).

196. Piccardo, M., Penocchio, E., Puzzarini, C., Biczysko, M. & Barone, V. *J. Phys. Chem. A* **119,** 2058–2082 (2015).

197. Puzzarini, C., Biczysko, M. & Barone, V. *J. Chem. Theory Comput.* **6,** 828 (2010).

198. Carnimeo, I. *et al. J. Chem. Phys.* **139,** 074310 (2013).

199. Barone, V., Biczysko, M. & Bloino, J. *Phys. Chem. Chem. Phys.* **16,** 1759–1787 (2014).

200. Grimme, S. *J. Chem. Phys.* **124,** 034108 (2006).

201. Dunning Jr., T. H. *J. Chem. Phys.* **90,** 1007–1023 (1989).

202. Woon, D. E. & Dunning Jr., T. H. *J. Chem. Phys.* **98,** 1358–1371 (1993).

203. Woon, D. E. & Dunning Jr., T. H. *J. Chem. Phys.* **103,** 4572–4585 (1995).

204. Peterson, K. A. & Dunning Jr., T. H. *J. Chem. Phys.* **117,** 10548–10560 (2002).

205. Biczysko, M., Panek, P., Scalmani, G., Bloino, J. & Barone, V. *J. Chem. Theory Comput.* **6,** 2115–2125 (2010).

206. Demaison, J. F. & Craig, N. C. *J. Phys. Chem. A* **115,** 8049 (2011).

207. Puzzarini, C. & Barone, V. *Phys. Chem. Chem. Phys.* **13,** 7189 (2011).

208. Demaison, J. *et al. J. Phys. Chem. A* **116,** 8684–8692 (2012).

209. Demaison, J., Craig, N. C., Conrad, A. R., Tubergen, M. J. & Rudolph, H. D. *J. Phys. Chem. A* **116,** 9116–9122 (2012).

210. Demaison, J. *et al. J. Phys. Chem. A* **117,** 2278–2284 (2013).

211. Barone, V., Biczysko, M., Bloino, J., Egidi, F. & Puzzarini, C. *J. Chem. Phys.* **138,** 234303 (2013).

212. Gauss, J., Ruud, K. & Helgaker, T. *J. Chem. Phys.* **105,** 2804–2812 (1996).

213. Flygare, W. *Chem. Rev.* **74,** 653–687 (1976).

214. Neese, F., Schwabe, T. & Grimme, S. *The Journal of Chemical Physics* **126,** 124115 (2007).

215. Lee, C., Yang, W. & Parr, R. G. *Phys. Rev. B* **37,** 785 (1988).

216. Becke, A. D. *J. Chem. Phys.* **98,** 5648–5652 (1993).

217. Stephens, P. J., Devlin, F. J., Chabalowski, C. F. & Frisch, M. J. *J. Phys. Chem.* **98,** 11623 (1994).

218. *The SNSD basis set is available in Download section (accessed October 2014)* <`http://dreamslab.sns.it`>.

219. Barone, V., Bloino, J. & Biczysko, M. *Phys. Chem. Chem. Phys.* **12,** 1092 (5 2010).

220. Stanton, J. *et al. CFOUR, Coupled-Cluster techniques for Computational Chemistry, a quantum-chemical program package* 2010. <`http://www.cfour.de/`>.

221. Frisch, M. J. *et al. Gaussian Development Version, Revision H.32* Gaussian Inc. Wallingford CT 2013.

222. Schneider, W. & Thiel, W. *Chem. Phys. Lett.* **157,** 367 (1989).

223. Stanton, J. F. & Gauss, J. *Int. Rev. Phys. Chem.* **19,** 61–95 (2000).

224. Thiel, W., Scuseria, G., Schaefer, H. F. S. & Allen, W. D. *J. Chem. Phys.* **89,** 4965–4975 (1988).

225. Barone, V. *J. Chem. Phys.* **101,** 10666–10676 (1994).

226. Stanton, J. F., Lopreore, C. L. & Gauss, J. *J. Chem. Phys.* **108,** 7190–7196 (1998).

227. Benson, R. C. & Flygare, W. H. *J. Chem. Phys.* **58,** 2366–2372 (1973).

228. Blom, C. E., Grassi, G. & Bauder, A. *J. Am. Chem. Soc.* **106,** 7427–7431 (1984).

229. Esselman, B. J. *et al. J. Chem. Phys.* **139,** 224304 (2013).

230. Puzzarini, C., Heckert, M. & Gauss, J. *J. Chem. Phys.* **128,** 194108 (2008).

231. Puzzarini, C. & Cazzoli, G. *J. Mol. Spectrosc.* **256,** 53 (2009).

232. Liévin, J., Demaison, J., Herman, M., Fayt, A. & Puzzarini, C. *J. Chem. Phys.* **134,** 064119 (2011).

233. Thorwirth, S., Harding, M. E., Muders, D. & Gauss, J. *J. Mol. Spectrosc.* **251,** 220–223 (2008).

234. Puzzarini, C. *J. Mol. Spectrosc.* **242,** 70–75 (2007).

235. Pietropolli-Charmet, A. *et al. J. Chem. Phys.* **139,** 164302 (2013).

236. Puzzarini, C., Cazzoli, G., Gambi, A. & Gauss, J. *J. Chem. Phys.* **125,** 054307 (2006).

237. Puzzarini, C., Biczysko, M., Bloino, J. & Barone, V. *Astrophys. J.* **785,** 107 (2014).

238. Larsen, R. W. *et al. Phys. Chem. Chem. Phys.* **5,** 5031–5037 (2003).

239. *The CCse, B3se and B2se sets are available in Download section (accessed February 2015)* <`http://dreamslab.sns.it`>.

240. Vogt, N., Demaison, J. & Rudolph, H. D. *Mol. Phys.* **112,** 2873–2883 (2014).

241. Dunning Jr., T. H., Peterson, K. A. & Wilson, A. K. *J. Chem. Phys.* **114,** 9244–9253 (2001).

242. Craig, N. C., Groner, P. & McKean, D. C. *J. Phys. Chem. A* **110,** 7461–7469 (2006).

243. Vogt, N., Demaison, J., Vogt, J. & Rudolph, H. D. *J. Comput. Chem.* **35,** 2333–2342. ISSN: 1096-987X (2014).

244. Lide, D. R. & Mann, D. E. *J. Chem. Phys.* **27,** 868–873 (1957).

245. Demaison, J. & Rudolph, H. *J. Mol. Spectrosc.* **248,** 66–76 (2008).

246. Lide, D. R. & Christensen, D. *J. Chem. Phys.* **35,** 1374–1378 (1961).

247. Gauss, J., Cremer, D. & Stanton, J. F. *J. Phys. Chem. A* **104,** 1319–1324 (2000).

248. Gauss, J. & Stanton, J. F. *J. Phys. Chem. A* **104,** 2865–2868 (2000).

249. Thorwirth, S., Müller, H. S. P. & Winnewisser, G. *J. Mol. Spectrosc.* **199,** 116–123 (2000).

250. Thorwirth, S., Gendriesch, R., Müller, H. S. P., Lewen, F. & Winnewisser, G. *J. Mol. Spectrosc.* **201,** 323–325 (2000).

251. Bak, B. & Skaarup, S. *J. Mol. Struct.* **10,** 385–391 (1971).

252. Császár, A. G., Demaison, J. & Rudolph, H. D. *J. Phys. Chem. A* **119,** 1731–1746 (2015).

253. Christen, D., Griffiths, J. H. & Sheridan, J. *Z. Naturforsch.* **37a,** 1378 (1982).

254. Demaison, J., Császár, A. G., Margulès, L. D. & Rudolph, H. D. *J. Phys. Chem. A* **115,** 14078–14091 (2011).

255. Kochikov, I. V. *et al. J. Mol. Struct.* **567,** 29–40 (2001).

256. Vogt, N., Demaison, J. & Rudolph, H. *Struct. Chem.* **22,** 337–343 (2011).

257. Mata, F., Quintana, M. J. & Sørensen, G. O. *J. Mol. Struct.* **42,** 1–5 (1977).

258. Sørensen, G. O., Mahler, L. & Rastrup-Andersen, N. *J. Mol. Struct.* **20,** 119–126 (1974).

259. Blukis, U., Kasai, P. H. & Myers, R. J. *J. Chem. Phys.* **38,** 2753–2760 (1963).

260. Groner, P., Albert, S., Herbst, E. & De Lucia, F. C. *Astrophys. J.* **500,** 1059 (1998).

261. Niide, Y. & Hayashi, M. *J. Mol. Spectrosc.* **220,** 65–79. ISSN: 0022-2852 (2003).

262. Demaison, J., Herman, M. & Liévin, J. *J. Chem. Phys.* **126,** 164305 (2007).

263. Demaison, J., Margulès, L., Kleiner, I. & Császár, A. *J. Mol. Spectrosc.* **259,** 70 (2010).

264. Marstokk, K. M. & Møllendal, H. *J. Mol. Spectrosc.* **5,** 205–213 (1970).

265. Bouchez, A. *et al. Astron. Astrophys.* **540,** A51 (2012).

266. Haykal, I., Motiyenko, R. A., Margulès, L. & Huet, T. R. *Astron. Astrophys.* **549,** A96 (2013).

267. Carroll, P. B., Drouin, B. J. & Widicus Weaver, S. L. *Astrophys. J.* **723,** 845 (2010).

268. Carroll, P. B. *et al. J. Mol. Spectrosc.* **284,** 21–28 (2013).

269. Hazra, M. K. & Sinha, A. *J. Phys. Chem. A* **115,** 5294–5306 (2011).

270. Bakri, B., Demaison, J., Margulès, L. & Møllendal, H. *J. Mol. Spectrosc.* **208,** 92–100. ISSN: 0022-2852 (2001).

271. Puzzarini, C. *private communication.*

272. Demaison, J. in *Equilibrium molecular structures: from spectroscopy to quantum chemistry* (eds Demaison, J., Boggs, J. & Császár, A.) 29–52 (CRC Press, Boca Raton, FL, 2011).

273. Barone, V., Biczysko, M., Bloino, J. & Puzzarini, C. *J. Chem. Theory Comput.* **9,** 1533 (2013).

274. Frisch, M. J. *et al. Gaussian Development Version, Revision H.36* Gaussian Inc. Wallingford CT 2013.

275. Carbonniere, P., Lucca, T., Pouchan, C., Rega, N. & Barone, V. *J. Comput. Chem.* **26,** 384 (2005).

276. Begue, D., Carbonniere, P. & Pouchan, C. *J. Phys. Chem. A* **109,** 4611–4616 (2005).

277. Puzzarini, C., Biczysko, M. & Barone, V. *J. Chem. Theory Comput.* **7,** 3702–3710 (2011).

278. Barone, V. *et al. Int. J. Quantum Chem.* **112,** 2185–2200 (2012).

279. Barone, V., Cimino, P. & Stendardo, E. *J. Chem. Theory Comput.* **4,** 751 (2008).

280. Kendall, R. A., Dunning Jr., T. H. & Harrison, R. J. *J. Chem. Phys.* **96,** 6796 (1992).

281. Hay, P. & Wadt, W. *J. Chem. Phys.* **82,** 299 (1985).

282. Mitin, A., Baker, J. & Pulay, P. *J. Chem. Phys.* **118,** 7775 (2003).

283. Ditchfield, R., Hehre, W. & Pople, J. *J. Chem. Phys.* **54,** 724 (1971).

284. Hehre, W., Ditchfield, R. & Pople, J. *J. Chem. Phys.* **56,** 2257 (1972).

285. Hariharan, P. & Pople, J. *Theor. Chem. Acc.* **28,** 213 (1973).

286. Francl, M. *et al. J. Chem. Phys.* **77,** 3654 (1982).

287. Rauhut, G., Knizia, G. & Werner, H.-J. *J. Chem. Phys.* **130,** 054105 (2009).

288. Timothy, J., Christopher, E., Gazdy, B. & Bowman, J. *J. Phys. Chem.* **97,** 8937 (1993).

289. Pak, Y. & Woods, R. *J. Chem. Phys.* **107,** 5094 (1997).

290. Koput, J. & Carter, S. *Spectrochim. Acta A* **53,** 1091 (1997).

291. Requena, A., Bastida, A. & Zuniga, J. *Chem. Phys.* **175,** 255 (1993).

292. Adel, A. & Dennison, M. *Phys. Rev.* **43,** 716 (1933).

293. Suzuki, I. *J. Mol. Spectrosc.* **25,** 479 (1968).

294. Miller, C. & Brown, L. *J. Mol. Spectrosc.* **228,** 329 (2004).

295. Martin, J., Lee, T. & Taylor, P. *J. Chem. Phys.* **108,** 676 (1998).

296. Mills, I. & Robiette, A. *Mol. Phys.* **56,** 743 (1985).

297. Smith, B. & Winn, J. *J. Chem. Phys.* **89,** 4638 (1988).

298. Huet, T. R., Herman, M. & Johns, J. W. C. *J. Chem. Phys.* **94,** 3407–3414 (1991).

299. Plíva, J. *J. Mol. Spectrosc.* **44,** 165 (1972).

300. Jonas, D. M. *et al. J. Chem. Phys.* **99,** 7350–7370 (1993).

301. Coustenis, A., Bézard, B. & Gautier, D. *Icarus* **80,** 54 (1981).

302. Maisello, T., Maki, A. & Blake, T. *J. Mol. Spectrosc.* **255,** 45 (2009).

303. Handy, N. & Willetts, A. *Spectrochim. Acta A* **53,** 1169 (1997).

304. Miani, A., E., C., Palmieri, P., Trombetti, A. & Handy, N. *J. Chem. Phys.* **112,** 248 (1999).

305. Goodman, L., Ozkabak, A. G. & Thakur, S. N. *J. Phys. Chem.* **95,** 9044 (1991).

306. Henry, B. R. & Siebrand, W. *J. Chem. Phys.* **49,** 5369 (1968).

307. Martin, J., Taylor, P. & Lee, T. *Chem. Phys. Lett.* **275,** 414 (1997).

308. Reva, I., Lapinski, L., Chattopadhyay, N. & Fausto, R. *Phys. Chem. Chem. Phys.* **5,** 3844 (2003).

309. Lippincott, E. & Nelson, R. *Spectrochim. Acta* **10,** 307 (1957).

310. Yasuda, Y., Kamiyama, T. & Shirota, Y. *Electrochim. Acta* **45,** 1537 (2000).

311. Ostrauskaite, J., Karickal, H., Leopold, A, Haarerb, D. & Thelakkat, M. *J. Mater. Chem.* **12,** 58 (2002).

312. Steiger, J., Schmechel, R. & von Seggern, H. *Synth. Met.* **129,** 1 (2002).

313. Janic, I. & Kakas, M. *J. Mol. Struct.* **114,** 249 (1984).

314. Rulkens, R. *et al. J. Am. Chem. Soc.* **118,** 12683–12695 (1996).

315. Sarhan, A.-W., Nouchi, Y. & Izumi, T. *Tetrahedron* **59,** 6353 (2003).

316. Paquet, C., Cyr, P., Kumacheva, E. & Manners, I. *Chem. Commun.* **2,** 234 (2004).

317. Van Staveren, D. R. & Metzler-Nolte, N. *Chem. Rev.* **104,** 5931–5986 (2004).

318. Nagaral, R., Lee, J. & Shin, W. *Electrochim. Acta* **54,** 6508 (2009).

319. Cooper, D., Yennie, C., Morin, J., Delaney, S. & Suggs, J. *J. Organomet. Chem.* **696,** 3058 (2011).

320. Haaland, A. & Nilsson, J. *Acta Chem. Scand.* **22,** 2653 (1968).

321. Berces, A., Ziegler, T. & Fan, L. *J. Phys. Chem.* **98,** 1584 (1994).

322. Mohammadi, N., Ganesan, A., Chantler, C. & Wang, F. *J. Organomet. Chem.* **713,** 51 (2012).

323. Chase, t. e. M. NIST-JANAF Thermochemical Table. *J. Phys. Chem. Ref. Data* **9,** 1 (1998).

Acronyms

BO Born-Oppenheimer.

CC coupled cluster.

CT contact transformation.

DCPT2 degeneracy-corrected vibrational second-order perturbation theory.

DFT density functional theory.

DSPT2 degeneracy smeared vibrational second-order perturbation theory.

DVPT2 deperturbed vibrational second-order perturbation theory.

GVPT generalized vibrational perturbation theory.

GVPT2 generalized vibrational second-order perturbation theory.

HDCPT2 hybrid DCPT2-VPT2 scheme.

HDSPT2 hybrid DSPT2-VPT2 scheme.

HF Hartree-Fock.

MP2 second-order Møller-Plesset theory.

PES potential energy surface.

QM quantum mechanical.

RS Rayleigh-Schrödinger.

SE semi-experimental.

TM template-molecule.

TS transition state.

VPT vibrational perturbation theory.

VPT2 vibrational second-order perturbation theory.

ZPVE zero-point vibrational energy.

Acknowledgements

My deepest gratitude to all people who were involved in this work in many different ways. First, I thank Prof. Vincenzo Barone for the scientific support and Julien Bloino for his suggestions and helps for the coding. My sincere thanks to Malgorzata Biczysko for dedicating her time and providing me many useful suggestions, and to Emanuele Penocchio, with whom I had many pleasing moments, full of interesting scientific discussions.

I thank all my friends especially Danilo Calderini, Serena Manti, Daniele Licari, Danilo Di Maio, Bala Chandramouli, Giordano Mancini, Elisa Bertolucci, Franco Egidi, Nicola De Mitri, Ivan Carnimeo, Michele Visciarelli, Luciano Carta, Livia Vallini, Mireia Segado, Teresa Fornaro, Marta Giani, Valentina Ruggiero, Marta Davila and Andrea Pallottini, for their encouragements and motivations during my years of the Ph.D., and with whom I spent many good times.

Last but not the least, my deepest gratitude to my parents and family, Manuela, Mauro, Marco, Giacomo e Giovanni, for their intense love, support and encouragements.